Host protein phosphorylation during *Shigella flexneri* infection

—

A phosphoproteomic based systems biology approach

Inauguraldissertation

zur
Erlangung der Würde eines Doktors der Philosophie
vorgelegt der
Philosophisch-Naturwissenschaftlichen Fakultät
der Universität Basel

von
Christoph Schmutz
aus Basel BS

BASEL, 2015

Genehmigt von der Philosophisch-Naturwissenschaftlichen Fakultät

auf Antrag von:

Prof. Dr. Cécile Arrieumerlou
Dissertationsleiterin
Prof. Dr. Christoph Dehio
Korreferent

Basel, den 22.04.2014

Prof. Dr. Jörg Schibler
Dekan

Abstract

The enteroinvasive bacterium *Shigella flexneri* triggers its uptake into epithelial cells by injecting several effector proteins via its type three secretion system (TTSS) and interferes with various host cell processes at later stages of infection. In this study, we systematically addressed the impact of *S. flexneri* infection on the host signaling network by quantitative phosphoproteomics. We were able to identify several hundreds of proteins undergoing a change in their phosphorylation state during the first two hours of infection. Using bioinformatic tools, we could demonstrate that many phosphoproteins are related to the cytoskeleton, signal transduction, cell cycle, and transcription regulation. The temporal phosphorylation patterns were addressed by fuzzy c-means clustering, revealing six temporally distinct phosphorylation profiles as well as kinases potentially responsible for these phosphorylations. In particular, we found a cluster of ataxia telangiectasia mutated (ATM) substrates, related to genotoxic stress, that became phosphorylated at a late stage of infection. We identified mTOR as the most overrepresented signaling pathway and could demonstrate that both, mTORC1 and mTORC2, become activated during *S. flexneri* infection. To identify phosphoproteins commonly regulated during bacterial infection, we compared our dataset to a published phosphoproteome of cells infected with *Salmonella typhimurium*. This analysis revealed a large subset of co-regulated phosphoproteins, indicating that both pathogens interfere with similar cellular signaling cascades. Furthermore, we addressed the impact of the *S. flexneri* effector protein OspF on the host phosphorylation network. OspF is known to inactivate the MAPKs p38 and ERK. The phosphorylation of several hundred proteins was affected in an OspF-dependent manner, demonstrating the massive impact a single bacterial effector can have on the host signaling network.

In a second project we addressed the activation mechanism of AKT and mTOR during *S. flexneri* infection by studying the effector IpgD. IpgD is a phosphoinositide 4-phosphatase generating PI5P from PI(4,5)P2 leading to activation of AKT. We could demonstrate that the effector protein IpgD is sufficient to induce mTOR activation by the use of a protein delivery tool based on the TTSS of *Yersinia enterocolitica*. Interestingly, AKT activation was independent of canonical PI3K activity shortly after IpgD translocation, whereas at later timepoints AKT activation was PI3K-dependent. These data suggest two distinct IpgD-dependent AKT activation mechanisms. Finally, we could show that the Inositol polyphosphate multikinase IPMK contributes to AKT phosphorylation during infection.

Thesis statement

The work presented here was performed in the group of Prof. Cécile Arrieumerlou in the Focal Area of Infection Biology at the Biozentrum of the University of Basel, Switzerland. My PhD was supervised by a thesis committee consisting of:

Prof. Cécile Arrieumerlou
Prof. Christoph Dehio
Prof. Mike Hall
Prof. Matthias Wymann

The present thesis is written in cumulative format. The first chapter introduces the major topics related to my work, whereas the following chapters illustrate the results of my research consisting of a published article and related additional unpublished results. In addition, results from a second project, written as manuscript in preparation, will be presented. Finally, the major aspects of my thesis are discussed and future project directions are provided. For reasons of readability, not all abbreviations are written out in full, but instead a comprehensive glossary of abbreviations can be found at the end of the thesis.

Contents

List of figures

List of tables

Chapter I

Introduction

1 Shigellosis

1.1 Discovery of a dysentery causing bacillus

In 1896, the first *Shigella* species was discovered by Kiyoshi Shiga[195]. In this last decade of the 19th century, dysentery epidemics affecting tens of thousands of people occurred frequently in Japan, accompanied by a high mortality rate of more than 20%[195]. Shiga isolated and biochemically described a bacillus from stool. When sub-cultured and fed to dogs, the bacillus caused diarrhea. By the use of an agglutination technique, he could further show that the organism coalesced when exposed to serum of convalescent dysentery patients[195]. Later on, he also described the production of toxic factors by the organism and thus discovered the prominent Shiga toxin. The pathogen, initially termed *Bacillus dysenterie* was renamed to *Shigella* in 1930, in honor of its discoverer Kiyoshi Shiga.

1.2 Shigellosis

Shigella is the causative agent of shigellosis, a disease also known as dysentery. *Shigella* is an important cause for morbidity and mortality predominantly affecting children under the age of 5 years in developing countries. In 1999, it has been estimated that approximately 165 million cases of shigellosis occur annually from which 1.1 million have a fatal outcome[143]. However, more recent research implied a similar incidence of shigellosis but the death estimate is 98% lower as previously reported[17]. The reduction in fatal outcome in the absence of *Shigella spp.* specific interventions may be due to an overall improvement in nutrition, rehydration therapy and better availability of antibiotics. However, the emergence of multi-drug resistant *Shigella* and the continuous high incidence indicate that shigellosis is still an unsolved global health problem[239]. *Shigella* are transmitted via the feco-oral route mainly by consumption of contaminated water or food. It has been shown that the pathogen is highly contagious as already 10-100 bacteria can cause the disease[61]. This is a reason why *Shigella* can easily disseminate in settings characterized by overcrowding, limited access to water, compromised personal hygiene and inadequate sanitation[18]. Shigellosis is an acute intestinal infection, with symptoms ranging from mild watery diarrhea to severe bacillary dysentery accompanied by abdominal cramps, tenesmus, fever and stool containing blood and mucus. The disease is usually self-limiting and treatment mainly consists of replacing fluids and salts lost by diarrhea, as well as antibiotic treatment. *Shigella* strains have progressively become resistant to most of the

widely used and inexpensive antibiotics over the last decades, resulting in treatment failure[195]. Nalidixic acid is an example of a first-line drug, used against shigellosis, whose wide application in many countries led to emergence of resistant strains[96]. In addition, also resistance against ciprofloxacin, a highly effective alternative, is increasingly common[264]. The increasing prevalence of antibiotic resistance gives more pressure toward the need for a vaccine. However, to date there is still no vaccine available although different strategies have been explored. These include live or attenuated strains of *Shigella*, lipopolysaccharide (LPS) protein conjugates, mixtures of TTSS subunit components as well as recombinant proteins[18].

1.3 Cellular pathogenesis of shigellosis

Shigella spp. are transmitted via the feco-oral route and are taken up upon ingestion of contaminated water or food[250]. *Shigella* are highly contagious also due to their pronounced acid resistance allowing them to pass the acidic environment of the stomach[92]. After *Shigella* passed the stomach and the small intestine it reaches the large intestine where it overcomes the epithelial barrier and initiates the infection. On a cellular level the infection is a multistep process, because *Shigella* is not able to directly infect polarized epithelial cells from the apical side oriented towards the gut lumen[182]. Therefore *Shigella* first has to cross the epithelium which is a physical barrier against infection of commensal or pathogenic bacteria (Figure 1.2.1). Microfold cells (m-cells) are located on specific areas of the large intestine named peyers patches, and continuously transport particles and microorganisms from the gut lumen to the underlying lymphoid tissue by a process termed transcytosis[166]. M-cells therefore have an important role in the intestinal immunity by presenting antigens from the gut lumen to resident dendritic or T-cells in the sub-mucosa. *Shigella* takes advantage of this system and passes the epithelial barrier by transcytosis through m-cells[240] [284]. However, more recent research also revealed filopodial capture of *Shigella* by epithelial cells, allowing also apical infection[232].

Once released in the intra-epithelial pocket, *Shigella* becomes phagocytosed by residential macrophages. *Shigella* rapidly escapes the phagocytic vacuole and subsequently induces pyroptosis of the macrophage by use of its type three secretion system (TTSS)[305] [306] [253]. Macrophage cell death is leading to the release of the pro-inflammatory cytokines IL-1β and IL-18. Both cytokines induce a massive inflammatory response which is a hallmark of the disease[262]. IL-1β triggers a strong inflammatory response subsequently leading to the recruitment of PMNs. IL-18 on the other hand attracts natural killer (NK) cells and promotes the production of interferon γ (INF-γ), thus further enhancing the inflammatory response[241] [246]. Once *Shigella* is released from the dying macrophage, it has access to the basolateral side of the epithelium and can invade its replicative niche,

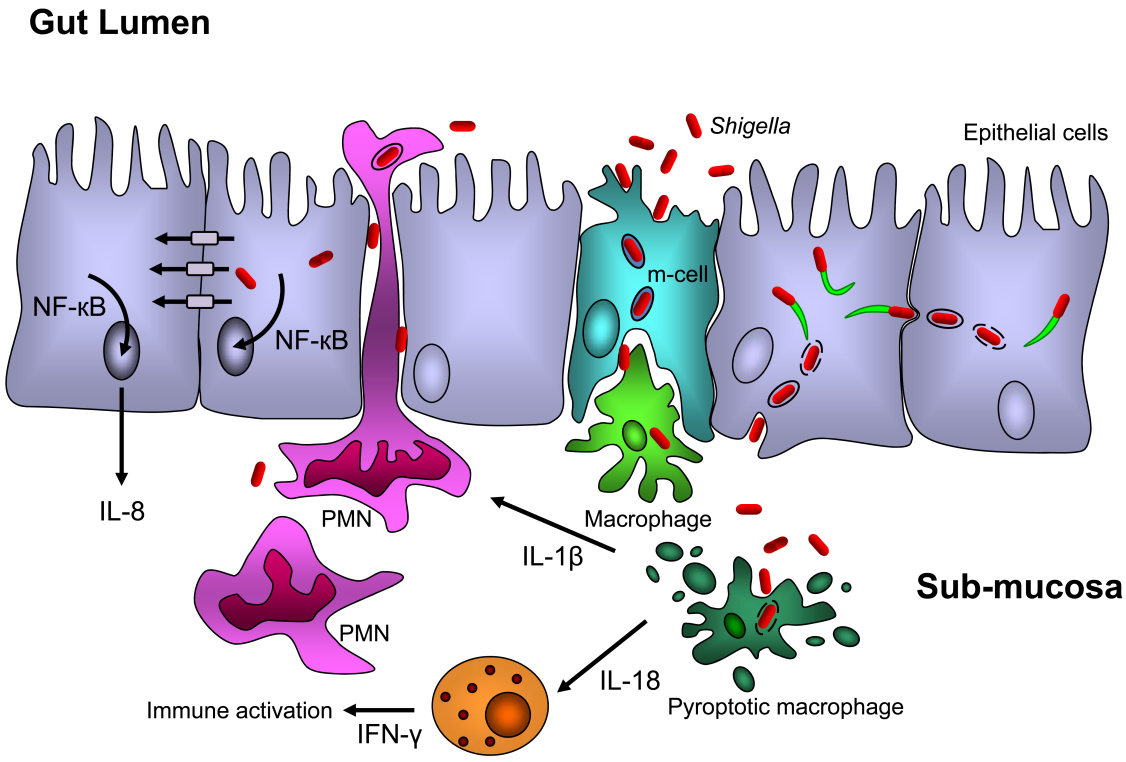

Figure 1.2.1 Schematic representation of cellular *Shigella* pathogenesis. *Shigella* crosses the colonic epithelial layer by transcytosis through microfold cells (m-cells) and subsequently becomes phagocytosed by resident macrophages. Infected macrophages rapidly undergo pyroptosis, thereby releasing interleukin 1β (IL-1β) and interleukin 18 (IL-18). Once *Shigella* is released from the dying macrophage, it invades epithelial cells from the baso-lateral side through the induction of macropinocytosis. *Shigella* rapidly lyses the vacuole and replicates within the host cell cytoplasm and spreads to neighbouring cells by actin-based motility (ABM). Intracellular *Shigella* are detected by pathogen recognition receptors and an innate immune response is initiated in cooperation with uninfected neighboring cells, leading o the release of interleukin-8 (IL-8) and the attraction of polymorphonuclear cells (PMN)s to the site of infection. In addition, PMNs transmigrate through the epithelial layer and thereby facilitate further bacterial invasion. Ultimately, PMNs phagocytose the invading pathogen and contribute to the clearance oft the infection. For more details, refer to the manuscript. *Adapted with modifications from Schroeder and Hilbi*[250].

intestinal epithelial cells. *Shigella* promotes its invasion into the host cells by the use of its TTSS. Several bacterial effector molecules are delivered into the host cell and induce massive cytoskeletal rearrangements, leading to the engulfment of the bacteria and their uptake by macropinocytosis[250]. Once inside the epithelial cell, *Shigella* lyses the vacuole and is released into the cytoplasm where it can replicate[238].

In the cytoplasm, *Shigella* is recognized by the intracellular pattern recognition receptor Nod1 leading to the induction of a pro-inflammatory response resulting in the release of IL-8, triggered through activation of NF-κB and the MAPK signaling pathway[86] [209] [215]. Secreted IL-8 potentiates the host inflammatory response by attracting further PMN cells[243]. Although it was assumed that infected cells recognizing intracellular *Shigella* secrete IL-8, recent research from our laboratory revealed that indeed uninfected bystander cells are responsible for the production of IL-8. Infected cells, unable to produce IL-8 due to the countermeasures of the bacteria, propagate danger signals to neighboring cells in a gap junction-dependent manner, and therefore potentiate the inflammatory response[128].

1.4 Determinants of *Shigella* virulence

Organisms from the genus *Shigella* belong to the phylum of *Escherichia* from the *Enterobacteriacea* family and are thus closely related to non-pathogenic *E. coli*[250]. *Shigella* are small, uncapsulated and non-motile gram-negative, nosporulating, facultative anaerobic bacteria. Four different species of *Shigella* have been described based on serological, biochemical or clinical phenotypes[288]: *S. dysenteriae* (serogroup A, consisting of 13 serotypes), *S. flexneri* (serogroup B, consisting of 15 serotypes), *S. boydii* (serogroup C, consisting of 18 serotypes) and *S. sonnei* (serogroup D, consisting of one serotype). The serotype classification is based on the O-antigen component of the LPS present on the outer membrane of the cell wall. *S. flexneri*, *S. sonnei* and *S. boydii* have been associated with endemic disease, whereas *S. dysenteriae*, harboring the Shiga toxin, is the major cause of epidemic outbreaks and the most severe form of dysentery, causing the majority of fatal shigellosis cases[195] [143]. The prevalence of different serotypes varies geographically and can also change during an outbreak. Because immune responses are predominantly serotype specific, reinfections by *Shigella* bearing different O-antigens are possible[142]. Recently, comparative genomic studies revealed that *Shigella spp.* belong to the species *E. coli* rather than forming a separate genus[250] [82] [231]. There is only about 1.5% sequence divergence between *S. flexneri* and *E. coli* K-12 which is marginal compared to the divergence of 15% between *Salmonella enterica* and *E. coli*[250] [150].

During evolution, acquisition of genes through horizontal gene transfer, such as virulence associated genes termed pathogenicity islands (PAI), as well as loss of genes through

deletion or gene inactivation, shaped the specific genotypes of *Shigella*. The loss of gene function is best exemplified by comparing *E. coli* K12 to *Shigella* where an average of 726 genes are missing and more than 200 pseudogenes are found per *Shigella* strain [292] [213]. The genetic information associated with virulence is encoded on the bacterial chromosome and on a large virulence plasmid. The dynamics of these genetic rearrangements are reflected by a high number of insertion sequences (IS) found on the chromosome and on the virulence plasmid [33]. In addition to PAI found on the virulence plasmid, *Shigella* pathogenicity islands (SHI) were identified on the chromosome. These include the SHI-1 encoded virulence factors immunoglobulin A-like cytotoxic protease SigA as well as the enterotoxin ShET1 that were both found to induce intestinal fluid accumulation [250] [72]. SHI-O is a another important SHI, because it encodes for proteins modifying the structure of the bacterial LPS O-antigens which are a major virulence factor and responsible for the large variety of *Shigella* serotypes [192]. Furthermore, acquisition of the chromosomal PAI *Shigella* resistance locus (SRL) mediates resistance against streptomycin, ampicillin, chloramphenicol and tetracycline [276].

As already introduced, *Shigella* infection is a complex multistep process that requires the action of a large repertoire of bacterial virulence factors. The essential parts of those factors are encoded on the *S. flexneri* large virulence plasmid which was shown to be essential for macrophage killing and invasion of epithelial cells [250] [244] [170]. Sequencing of virulence plasmids from different *Shigella* strains revealed that these plasmids of approximately 200 kb contain a mosaic of around 100 genes and a comparable number of IS [33]. The plasmid encodes the molecular machinery required for bacterial invasion and subsequent intracellular survival. The core of the plasmid contains the conserved 31kb entry region, encoding genes for the assembly and function of the TTSS system needle complex as well as corresponding early effectors, translocators and chaperones [250]. More precisely, the entry region can be subdivided into different groups based on the function of the corresponding genes. TTSS effector molecules that manipulate host cell processes in favor of the bacteria belong to the first group. Among them are the dominant immunogenic antigens of *S. flexneri*, IpaA to IpaD. IpaB, IpaC and IpaD are translocator proteins that form a pore in the eukaryotic cell allowing the translocation of further effector molecules [26]. In addition, some of them are necessary for macrophage killing and the induction of cytoskeleton rearrangements promoting the uptake of the bacteria. Another group contains the two transcriptional activators VirB and MxiE that regulate TTSS related genes located in the entry region as well as some chromosomal IpaH effector proteins [2] [250] [28]. Virulence gene expression is tightly controlled and not permanently active. The major trigger for virulence gene expression are environmental changes upon uptake by the host. These include changes in pH, osmolarity, iron concentration and most importantly a temperature shift to 37°C [270] [250]. This shift is responsible for induction of the transcriptional

activator VirF, which in turn activates the second virulence plasmid regulator VirB as well as the actin nucleator protein IcsA (VirG) [2] [271] [250]. VirB promotes the expression of the entry region genes and of some Osp effector molecules, scattered on the virulence plasmid, equipping the bacteria with the TTSS and a first set of early effector molecules required for host cell invasion [84]. The secretion of this early set of effectors in turn increases the transcription of already induced proteins and an additional set of TTSS effectors. The transcriptional activator MxiE controls the expression of this "second set" TTSS of effectors. MxiE activity is blocked by an antiactivator complex built up by OspD1 and the chaperone Spa15 [208]. When TTSS secretion is induced, the early effector OspD1 as well as other substrates including IpaB and IpaC are translocated into the host cell and IpgC, the cognate chaperone of IpaB and IpaC, becomes released. IpgC subsequently associates with MxiE inducing the transcription of the second set of effectors which are then secreted by intracellular bacteria to modulate post-invasion aspects of the infection [171]. The activity of the TTSS was recently investigated during the course of infection. The TTSS is activated upon bacterial entry, but down-regulated after 60 minutes when bacteria gain access to the cytoplasm. It is proposed that contact with the plasma membrane is important for TTSS activity and rupture of the membrane leads to inactivation of the TTSS. The inactivation of the TTSS may allow the replenishment of the bacterial TTS substrate store for subsequent infection of neighboring cells. This is in line with the observation that the TTSS becomes reactivated during cell-to-cell spread [35].

1.5 The Mxi-Spa type three secretion system (TTSS)

More than half of the genes from the entry region encode proteins required for the secretion of Ipa proteins as well as other effectors. These genes are named membrane expression of ipa (*mxi*) and surface presentation of ipa (*spa*) antigens. Thus, the *mxi-spa* locus encodes all components needed for the assembly and function of a TTSS that is required to directly translocate bacterial effector proteins from the bacterial cytoplasm into the host cell. A requirement for this is a molecular device allowing the one step shuttle of proteins through totally three membranes: the bacterial inner- and outer membrane as well as the host cell membrane [46]. More than 24 different bacterial species interacting with animal or plant hosts harbor a TTSS, including *Shigella spp.*, *Salmonella spp.*, *Yersinia spp.*, enteropathogenic *Escherichia coli* (EPEC), enterohaemorrhagic *Escherichia coli* (EHEC), or *Pseudomonas spp* [180]. Although the TTSS architecture varies between the different species, it shares a conserved main structure, related to the flagellar TTSS [46]. Therby, the TTSS can be distinguished from the type 4 secretion system found in many gram-negative bacteria like *Brucella spp.*, *Legionella spp.* or *Bartonella spp.*, which also allows translocation of effector molecules from the bacterial cytoplasm into the host cell but is

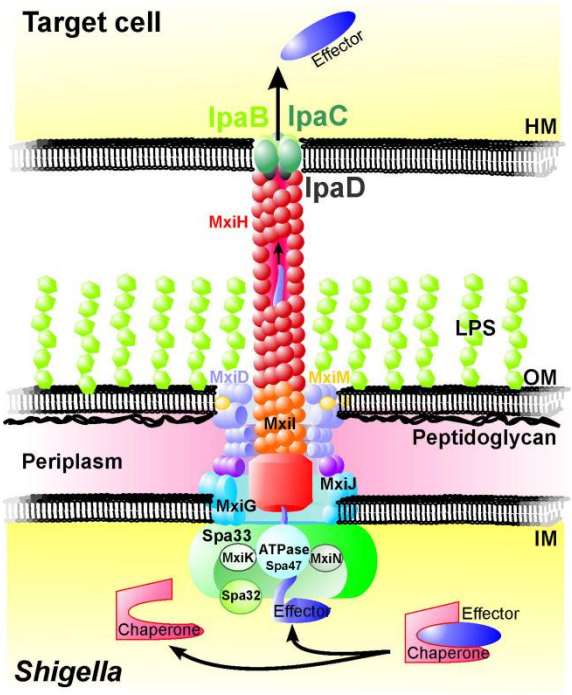

Figure 1.5.1 Architecture of the *S. flexneri* Mxi-Spa TTSS. Four main parts build the *S. flexneri* TTSS. In the bacterial cytoplasm is the C ring located which is compromised of proteins energizing and recognizing the transport of substrates, the release of chaperones and substrate unfolding. The basal body, consisting of seven rings, spans the bacterial IM, the periplasm and the OM. The needle protrudes from the basal body and the bacterial surface. Host cell membrane contact triggers the IpaD guided membrane insertion of the IpaB-IpaC translocon at the tip of the needle. *From Schroeder and Hilbi*[250].

derived from bacterial DNA conjugation systems[55] [78].

The architecture of the TTSS is characterized by a syringe like device with a total length between 77 and 92 nm, consisting of a seven ring basal body with a length of 32nm and a protruding needle with a length of 45 to 60nm and a 2-3 nm wide channel, allowing the transport of largely unfolded proteins[250] [4]. The *S. flexneri* Mxi-Spa TTSS is built by more than 25 different proteins, all encoded in the entry region of the large virulence plasmid[46] (Figure 1.5.1). The needle complex consisting of the C-ring, basal body and needle is sufficient to secrete proteins into the extracellular space but the translocator proteins IpaB, IpaC and IpaD are required on the tip of the TTSS needle for successful translocation of effector proteins into the host cell[174] [282]. These translocator proteins are stored in the cytoplasm and premature association of IpaB and IpaC is prevented by binding to the chaperone IpgC, whereas IpaD has self-chaperoning activity[125]. Although it is not entirely understood how the mechanism of secretion is controlled, it is assumed that IpaD is localized on the tip of the needle and blocks secretion through interactions with IpaB[67] [237]. Upon host cell contact, the TTSS becomes activated, presumably by induction of conformational changes of IpaD leading to repositioning of IpaB and its subsequent passage and membrane insertion together with IpaC forming the translocation pore[26] [67] [282]. Once the translocation pore is formed, the needle is in an open conformational state and additional effector proteins can be translocated through the TTSS channel into the host cell.

1.6 Adherence to the host cell

The initial contact of *Shigella* and the epithelial host cell occurs on cholesterol rich microdomains of the plasma membrane, the lipid rafts [149]. Lipid rafts contain more cholesterol and sphingolipids than the surrounding plasma membrane and are usually highly enriched in saturated fatty acids, allowing close package. As a consequence of this, lipid rafts are more ordered and less fluid than the surrounding membrane [256]. Many signaling proteins are not randomly distributed over the whole cell membrane but are rather enriched in lipid rafts, like G proteins, growth factor receptors, src family kinases or protein kinase C (PKC), creating an asymmetric distribution of these signaling clusters. Therefore, lipid rafts function as signaling platform by bringing proteins spatially together and facilitating their interaction [257].

Lipid rafts are attractive targets for different pathogens including bacteria, viruses and parasites [227] [106] [90]. It has been shown, that already purified lipid rafts, devoid of proteins but otherwise mimicking the lipid composition, are sufficient to trigger effector secretion by the TTSS [279]. In addition, cholesterol was shown to be important for both, binding and entry of *Shigella* and that the initial interaction occurs at lipid rafts. More precisely, The TTSS translocator protein IpaB and its *Salmonella* homologue SipB are cholesterol binding proteins and subsequent secretion of other effectors is dependent on cholesterol in the plasma membrane [103].

Shigella further adheres to the target cell by binding the two host cell receptors CD44 and $\alpha5\beta1$ integrin which can both be found in lipid rafts and accumulate at the site of entry. Binding to CD44 occurs through IpaB whereas $\alpha5\beta1$ integrin is bound by the IpaBCD complex [285] [258]. Binding to either one of the receptors induces actin cytoskeleton rearrangements and promotes *Shigella* invasion [285] [149]. Entry via lipid rafts may also be important for the determination of the faith of the intracellular bacteria. It has been demonstrated that uptake via lipid rafts protects some bacteria, including *Mycobacterium spp.* from lysosomal degradation [75] [53]. These findings are in line with the observation that cholesterol depletion in macrophages inhibits macrophage cell death and the activation of caspase-1 upon *Shigella* infection [249].

Alternatively, it has been demonstrated, that prior to contact with the main cell body, the bacteria are captured by pre-existing filopodial extensions [232]. Once *Shigella* is captured by these filopodia, they retract towards the cell body and promote bacterial-host contact and subsequent engulfment. The filopdial capture was further shown to be dependent on the TTSS in particular on the needle tip complex proteins IpaB and IpaD.

Table 1.1 *S. flexneri* TTSS translocated effector proteins encoded on the large virulence plasmid

Effector	Biochemical activity	Host cell target(s)	Virulence function and/or phenotype	Reference
IpaA	Vinculin activation	Vinculin, beta1-integrins, Rho signaling	Efficient invasion, actin cytoskeleton rearrangements, disassembly of cell-matrix adherence	[57] [99] [121] [272]
IpaB	Membrane fusion	Cholesterol, CD44, caspase-1	Control of type three secretion, translocon formation, phagosome escape, macrophage apoptosis	[26] [39] [106] [111] [115] [172]
IpaC	Actin polymerization	Actin, β-catenin	Translocon formation, filopodium formation, phagosome escape, disruption of EC tight junctions	[26] [103] [173] [273]
IpaD			Control of type three secretion, membrane insertion of translocon	[67] [172] [282]
IpaH7.8			Efficient phagosome escape	[74]
IpaH9.8	E3 ubiquitin ligase	Splicing factor U2AF, MAPK kinase, NEMO/IKKγ, ABIN-1, NF-κB pathway	Host cell transcriptome modulation, reduction of inflammation	[202] [230] [11]
IpaH0722	E3 ubiquitin ligase	TRAF2	Inhibition of NF-κB activation, dampening of inflammatory response	[12]
IpaJ	Cysteine protease	ARF1	Inhibition of Golgi cargo transport, Golgi fragmentation	[34]
IcsB		Atg5	Camouflage of IcsA for autophagic evasion	[5] [199] [200] [129]
IpgB1	RhoG mimicry	ELMO protein	Induction of Rac1-dependent membrane ruffling , regulation of inflammation	[187] [100] [201] [97]
IpgB2	RhoA mimicry	RhoA ligands	Induction of actin stress fiber-dependent membrane ruffling	[187] [97] [137]
IpgD	Phosphoinositide 4-phosphatase	Phosphatidylinositol 4,5-bisphosphate	Facilitation of entry, promotion of host cell survival, prevents termination of EGFR signaling, down-regulates inflammation by preventing ATP secretion	[194] [193] [212] [222] [219]
OspB		Retinoblastoma Protein, GEF-H1, NF-κB pathway	Reduction of inflammation	[304] [80]
OspC1		Nucleus and cytoplasm	Induction of PMN migration	[302]
OspC3	Caspase-4 binding, prevents p19/p10 heterodimerization	Caspase-4	Reduction of cell death, increased bacterial replication	[139]
OspD1			TTSS substrate, unknown function in host cells, antiactivator of MxiE	[208]
OspE1/2		ILK, Focal contacts	Maintenance of host cell morphology, stabilization of focal adhesion	[175] [71] [134]
OspF	Phosphothreonine lyase	MAPKs ERK and p38	Inhibition of histone phosphorylation and NF-κB-dependent gene expression, reduction of PMN recruitment	[9] [156] [302]

Table 1.1 – *Continued on next page*

Table 1.1 – *Continued from previous page*

Effector	Biochemical activity	Host cell target(s)	Virulence function and/or phenotype	Reference
OspG	Protein kinase, ubiquitination inhibitor	Ubiquitin-conjugating enzymes	Downregulation of NF-κB activation, reduction of inflammation	[132]
OspZ		NF-κB	blockage of NF-κB subunit p65 nuclear translocation, downregulation of IL-8 expression, reduces PMN transepithelial migration	[303] [190]
VirA	Cysteine protease	a-Tubulin	Facilitation of entry and intracellular motility by degradation of microtubules, Golgi fragmentation Calpain activation, cell death	[294] [22] [34]

1.7 *Shigella* entry

Shigella invasion into epithelial cells requires complex rearrangements of the membrane and the actin cytoskeleton. These processes are orchestrated in time and space by a multitude of bacterial and host factors. In particular, several bacterial TTSS effectors are translocated into the host cell, activating tyrosine kinases and Rho GTPase signaling[110] [29]. Thus, at the site of entry, *Shigella* induces massive rearrangements of the actin cytoskeleton leading to the formation of cellular protrusions building a macropinocytic pocket that encloses the bacteria[250]. Beside its function as a translocator protein, IpaC induces the recruitment and activation of the tyrosine kinase Src leading to actin polymerization[181]. Src was initially discovered as a proto-oncogene in chicken, sharing high similarity to the *v-src* gene of the sarcoma virus[260]. Src was the first tyrosine kinase discovered and plays an important role in various cancers. The activity of Src is regulated by phosphorylation of tyrosine 530 leading to rearrangement of SH domains and subsequent activation or deactivation of the kinase function. Substrates of Src are transcription factors, adaptor proteins or focal adhesion proteins[25]. Dehio and colleagues revealed that cortactin becomes tyrosine phosphorylated upon *Shigella* infection and is recruited to *Shigella* entry foci[56]. Furthermore, they could show that Src is responsible for cortactin phosphorylation upon *Shigella* infection and is as well recruited to the entry structure. Two other TTSS effectors, IpgB1 and IpgB2 belonging to the WXXXE effector family that has been associated with mimicking Rho GTPase signaling, are also injected by *Shigella*. In line with this, it was found that IpgB1 mimics active RhoG, a Rho GTPase regulating actin dynamics, by ELMO binding and recruitment of DOCK180 which is a GTP exchange factor (GEF) for Rac[100] [32]. *In vitro* assays demonstrated in addition, that IpgB1 acts a GEF for for Cdc42 and Rac[114]. IpgB2 was shown to mimic the GTP-bound form of RhoA and expression of the effector in eukaryotic cells induced the formation of actin stress fibers as well as membrane ruffling[187]. More recently, IpgB2 was

shown to have GEF activity towards RhoA[137]. The effector protein VirA is a cysteine protease that destabilizes the microtubule network subsequently leading to activation of Rac1[295]. As exemplified in section 2.4, the *Shigella* effector IpgD has been implicated in invasion by loosening the connection between cortical actin and the membrane through its phosphoinositide 4-phosphatase activity[193]. This facilitates the remodeling of actin and thus affects membrane ruffling[193]. Although phenotypic changes towards the actin cytoskeleton are observed, the contribution of IpgD to the invasiveness of *Shigella* seems to be negligible[193]. Further, the translocated effector IpaA plays an important role in the entry process by binding of Vinculin. Vinculin is a focal adhesion protein and is involved in the anchoring of the actin cytoskeleton to integrin receptors. Three different Vinculin binding sites on IpaA have been identified which act in different ways. One binding site acts a mimicry of the focal adhesion protein talin and induces vinculin activation. The second binding site stabilizes the IpaA interaction while the third binding site may allow the formation of IpaA-vinculin scaffolds[206]. Through vinculin binding and activation, IpaA induces actin plolymerization arrest which is needed for bacterial anchorage at the site of entry[121,99].

1.8 Phagosome escape and autophagy evasion

Once *Shigella* has invaded the epithelial cell, it is captured in the phagosome. In contrast to *Salmonella Typhimurium*, which modifies the phagosome towards the creation of a replication permissive vacuole, *S. flexneri* lyses the surrounding membranes within 15 minutes and escapes into the cytoplasm, which represents its main replicative niche[204]. Membrane lysis depends on the Mxi-Spa TTSS and the translocator proteins IpaB, IpaC and IpaD[250]. The vacuolar membrane remnants associated proteins subsequently undergo polyubiquitination and the autophagy markers LC3 and p62 become recruited and are targeted to autophagy[62]. At the same time, ubiquitination of membrane associated host proteins leads to the induction of a pro-inflammatory cascade. The E3 ubiquitin ligase TNF receptor-associated factor 6 (TRAF6) itself becomes ubiquitinated at vacuolar membranes and thus affects NF-κB signaling. *S. flexneri* developed a strategy to prevent its autophagy (a process termed xenophagy[266]) by the use of the bacterial effector IcsB[200]. IcsB interacts with IcsA (VirG), a protein mediating intra- and inter-cellular movement of *S. flexneri* as elucidated in section 2.1[14]. IcsB competitively binds to IcsA, thus camouflaging IcsA from recognition by the autophagic protein ATG5 and enables the bacteria to evade autophagic recognition[179] [200].

2 Cellular processes affected by *Shigella* infection of epithelial cells

As described in the previous section, *Shigella* makes us of its TTSS to induce cell death in macrophages and for the subsequent invasion of epithelial cells. *Shigella* utilizes a set of effector proteins that are directly translocated into the non-phagocytic host cell inducing actin cytoskeleton rearrangements that are promoting the uptake of the bacteria. Besides reaching the replicative niche, it is of equal importance to maintain the niche for a sufficient amount of time allowing replication and consecutive spread into the environment. To counteract the defense mechanisms of the host, *Shigella* evolved a second set of effector molecules for post-invasion purposes. These effector molecules are secreted inside the host cell and interfere with various cellular processes in favor of the bacteria. *Shigella* prevents a loss of the replicative niche by interfering with the host cell cycle and decelerating the renewal of the epithelium. In addition, *Shigella* developed several strategies to prevent or at least delay host cell death. Finally, several effector molecules adjust signaling pathways that induce a pro-inflammatory response to reduce the inflammation of the tissue to a level that is beneficial for the preservation of *Shigella* infection. On overview of cellular processes affected by *S.flexneri* effectors is depicted in the figures 2.3.1 and 3.6.1.

2.1 Intra- and intercellular movement by actin based motility as a major virulence factor

After invasion of the epithelial host cell and lysis of the vacuole, *Shigella* is released into its replicative niche, the cytoplasm. *Shigella* and other intracellular bacteria including *Listeria monocytogenes*, *Rickettsia spp.*, *Mycobacterium marinum* and *Burkholderia pseudomallei* as well as the vaccinia virus have developed sophisticated systems to hijack the actin polymerization machinery of the host, allowing them to move intra or inter-cellularly by a mechanism termed actin-based motility (ABM) [89] [93] [98] [118]. This mechanism allows the pathogen to actively spread in the human tissue and is a major virulence factor.

Research in animal models of *Shigella* infection revealed that ABM and spread between intestinal epithelial cells is crucial for disease [242]. The molecular mechanisms of *Shigella* ABM have been studied extensively [118]. ABM by *Shigella* is induced by the bacterial surface protein intracellular spread (IcsA), also known as VirG [23]. Interestingly, IcsA is not related to the *Listeria* ABM inducing surface protein ActA and both proteins pro-

mote actin polymerization through distinct mechanisms[118]. *Shigella* IcsA is localized at one pole of the bacterium. Apyrase encoded by *phoN2* and cleavage of IcsA by the serine protease SopA are essential for IcsA unipolar distribution[58] [64] [247]. IcsA stimulates actin polymerization using several host proteins including Wiskott-Aldrich syndrome protein (N-WASP) and the Arp2/3 complex[263] [93]. The unipolar recruited host proteins work as actin nucleators and catalyze a directed elongation of actin that propels *Shigella* through the cytoplasm. The Arp2/3 complex stimulates polymerization from the side of a pre-existing filament leading to a Y shaped branched actin structure. For efficient actin polymerization the Arp2/3 complex has to become activated through nucleation-promoting factors like N-WASP[118]. N-WASP itself has to become activated by the protein Toca-1, which in addition has been shown to be associated with intracellular bacteria and necessary for ABM[155]. Other host proteins that were shown to be involved in ABM are septins. Septins are components of the cytoskeleton and were shown to organize as a ring in the bud neck of yeast and are assembled into non-polar filaments, thus regarded as unconventional cytoskeletal components[179]. It has been demonstrated that intracellular *S. flexneri* can either become compartmentalized in septin-cage like structures or form actin comet tails. Septin cages serve to counteract ABM and thus restrict the dissemination of invasive pathogens[179]. However, there is also a role for septin cages in autophagy as autophagy markers like p62 and LC3 are recruited to septin cages[179]. Thus, septins play a dual role in the infection process, by inhibiting ABM and beeing involved in autophagy.

While the described molecular mechanisms of intracellular motility have been extensively studied, less is known about the subsequent steps of membrane protrusion formation and engulfment, leading to dissemination of bacteria to adjacent cells. Although specific bacterial factors important for the induction of *Shigella* containing protrusions have not yet been identified, the TTSS is crucial for cell-cell spread[198]. Host factors promoting *Shigella* protrusions include the motor protein myosin X which is important for the elongation of protrusions. Furthermore, a switch from Arp2/3 to formin mediated actin polymerization in protrusions has been reported[107]. The adherens junction molecule E-cadherin was shown to be involved in the generation of protrusions and internalization of the protrusion by the neighboring cell[245]. In addition to adherens junctions also gap junction or tight junction proteins have been implicated in the intercellular dissemination of *Shigella*. It is noteworthy that *Shigella* dissemination predominantly takes place at contacts of tricellular tight junctions, areas in cell monolayers where three different cells form contact with each other[81]. Subsequently, *Shigella* containing protrusions are engulfed by neighboring cells via an endocytic pathway. The lysis of the surrounding double membrane in cells newly infected by cell to cell spread, is dependent on the TTSS and the translocator proteins IpaB, IpaC and IpaD[118]. Once *Shigella* is freed into the cytoplasm

a new cycle of replication and dissemination to neighboring cells can start [250].

2.2 *Shigella* is interfering with the host cell cycle

There is a growing number of pathogenic bacteria identified that actively interfere with the host cell cycle. The term cyclomodulin has been proposed to describe bacterial toxins or effector proteins that manipulate the eukaryotic cell cycle [197]. Cyclomodulins inhibiting cellular proliferation of the intestinal epithelium can be an important virulence factor, because they prevent renewal of the epithelium and therefore alter the integrity of the epithelial layer which can facilitate extra-intestinal invasion or prolong bacterial colonization by inhibition of cell shedding [197]. In 2007, it has been reported that *S. flexneri* interferes with the cell cycle of epithelial cells via delivery of the effector IpaB [120]. A yeast-two hybrid screen revealed interaction of IpaB with Mad2L2, an inhibitor of the anaphase promoting complex (APC) [120]. The APC is a multi-subunit complex, harboring E3 ubiquitin ligase activity, which targets substrates, like Cyclin A or Cyclin B1 for degradation by the proteasome during mitosis, allowing mitotic progression. IpaB leads to unscheduled APC activation and subsequent Cyclin B1 degradation leads to cell cycle arrest [73]. Cell cycle progression by modulation of APC ubiquitin ligase activity was shown to slow down upon delivery of IpaB by *S. flexneri* into host cells where it targets Mad2L2 [120]. In a rabbit ileal loop infection model it has been shown that *S. flexneri* infection reduces the abundance of epithelial progenitors in an IpaB-dependent manner. In addition, IpaB delivery increased the colonization rate of the loops, compared to an IpaB mutant which still functions as a TTSS translocator but has decreased binding activity towards Mad2L2. Rapid turnover of epithelial cells limits bacterial colonization by shedding of infected cells. Therefore, this represents a possible strategy to prolong the availability of *S. flexneri* replicative niche. In addition, as a consequence of cell cycle inhibition, the integrity of the epithelial layer is impaired. This might contribute to further infection of the intestinal epithelium because bacteria can get access to the baso-lateral surface of the cells without the need to cross the epithelial layer by transcytosis through m-cells.

2.3 *Shigella* maintains host cell adhesion

Besides preventing the renewal of the epithelium by interfering with the cell cycle, *Shigella* also enhances host cell adhesion to colonize the intestinal epithelium. The TTSS effector OspE binds to integrin-like kinase (ILK) leading to an increase in cell surface level of β1-integrin and suppressed phosphorylation of focal adhesion kinase (FAK) and paxillin. Thereby, OspE reduces adhesion turnover and suppresses the detachment of infected cells from the basement membrane, important for the promotion of bacterial colonization [134]. Because OspE orthologues are found in other enteropathogens such as EPEC or *Salmonella*

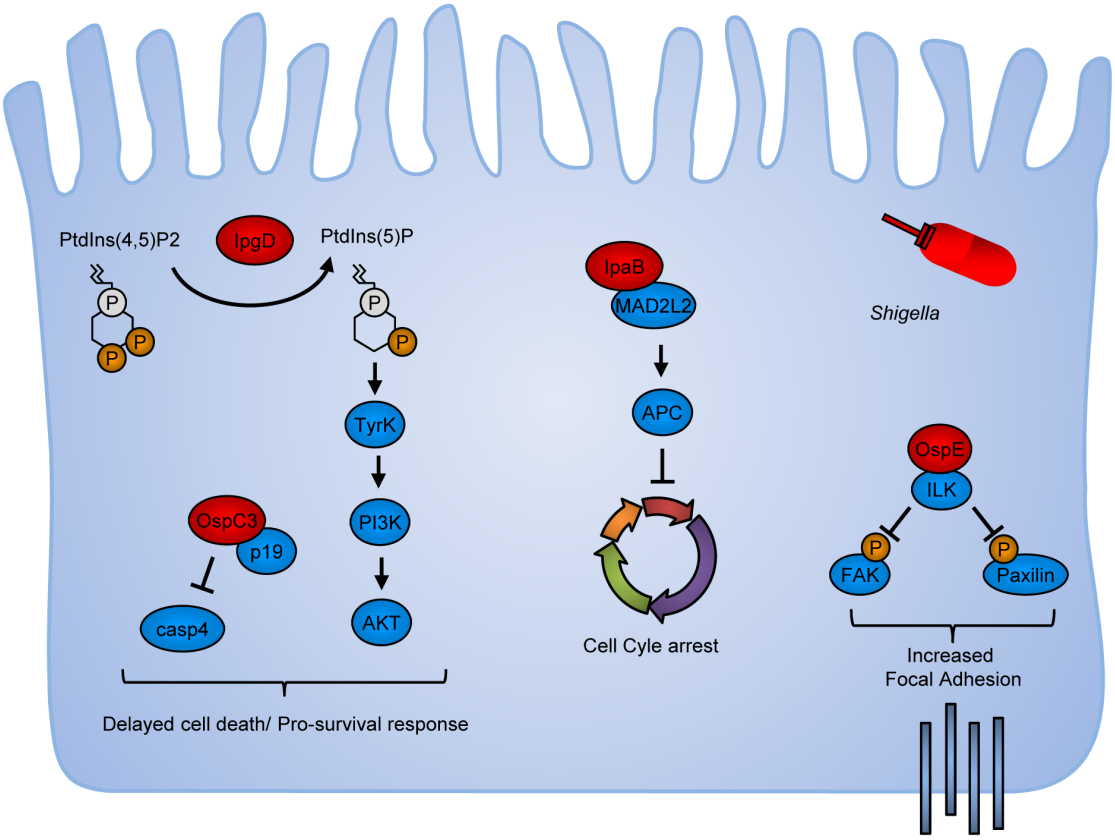

Figure 2.3.1 *Shigella* effectors modulate several cellular processes. Several effector proteins are secreted by intracellular *Shigella* and interfere with host signaling cascades in order to promote host cell survival, cell cycle arrest and increased cellular focal adhesion. For more details, refer to the manuscript.

spp., maintenance of cell adhesion appears as a widespread strategy for bacteria that interact with the intestinal epithelium [275].

2.4 *Shigella* is manipulating apoptotic and pro-survival signals

Programmed cell death is a tightly regulated process that can either be activated by intrinsic factors through intracellular pathways involving the endoplasmatic reticulum and mitochondria or in an extrinsic way involving extracellular stimuli. Both result in a cleavage-dependent caspase activation and subsequently apoptotic symptoms like cell shrinkage, chromatin condensation, membrane blebbing and formation of apoptotic bodies. Many pathogens including *Shigella* have evolved tools to manipulate the survival pathways of the host. *Shigella* has evolved active strategies to expand the lifespan of its epithelial reproductive niche, mostly by preventing or at least delaying apoptotic and necrotic cell death. *Shigella* is equipped with at least two distinct effectors that promote

survival of the epithelial host cell, namely VirA and IpgD. *Shigella* infection of epithelial cells induces a genotoxic response and subsequently activation of the apoptosis inducer p53 within the first two hours of infection[22]. However, the *Shigella* effector VirA, which was already known to promote early cytoskeletal processes and to promote the uptake into epithelial cells, can also activate calpain proteases in a calcium-dependent manner. Calpains degrade p53, a protein important in the DNA repair response and also for the induction of apoptosis. While degradation of p53 delays apoptosis, the impairment of a DNA repair response will ultimately lead to necrotic cell death of the host cells at later stages of infection[22]. It has been demonstrated that *Shigella* can rescue cells from staurosporine induced apoptosis but not if the transcriptional regulator *mxiE* is deleted[43]. Clark and colleagues screened for all MxiE regulated effector proteins but could not identify a mutant that lacked the ability to rescue cells from staurosporine induced apoptosis[69]. Therefore, they looked for proteins associated with MxiE and were able to identify the TTSS chaperone Spa15 which also gets translocated into the host cell[70]. Upon deletion of *spa15*, *Shigella* was no longer able to protect cells from staurosporine induced apoptosis. They conclude that Spa15 contributes to intracellular survival of *Shigella* by preventing apoptosis of infected host cells, although the molecular mechanism is not known.

IpgD is another *Shigella* effector protein delivered into epithelial cells by the TTSS and was shown to modulate the survival pathways of the host cell[212]. IpgD is a phosphoinositide 4-phosphatase generating phosphatidylinositol 5-phosphate (PI5P) from phosphatidylinositol 4,5-bisphosphate (PI(4,5)P2). An overview of phosphatidylinositol signaling is shown in figure 2.5.1. IpgD is rapidly secreted into the host cell already by extracellular bacteria[193]. Because IpgD is early delivered during the infection process, it was assumed to play a role in the entry process. Although the Δ*ipgD* mutant elicited entry structures with a highly altered morphology, bacteria were still able to invade the host cells[193]. Later on, it has been demonstrated that PI5P is rapidly produced at the site of *Shigella* entry and co-localizes with the kinase AKT phosphorylated on Ser473, which is crucial for its activation. Subsequently, it has been shown that AKT phosphorylation on Ser473 is dependent on IpgD[212]. AKT is a serine/threonine specific protein kinase and plays a major role in many physiological processes such as metabolism, apoptosis, survival, growth and protein synthesis. AKT is one of the most frequently activated kinases in cancer[6]. Therefore it is of great interest, that *Shigella* has evolved a tool to actively activate this kinase to prolong survival of the infected cell. Downstream of IpgD induced AKT signaling phosphorylation of GSK3A, FKHR and p70S6K was observed although the detailed functions of these proteins in the context of infection remain unclear[212]. Moreover, the exact mechanism of IpgD-dependent AKT activation is yet unknown, although it has been proposed that PI5P leads to the activation of tyrosine kinases and subsequently Class I PI3Ks which produce phosphatidylinositol (3,4,5)-trisphosphate (PI(3,4,5)P3) promoting

AKT activation[212].

EGFR is a tyrosine kinase that has been assigned to play a role in the PI3K-AKT activation pathway upon *Shigella* infection[222]. It was demonstrated that EGFR is required for PI5P-dependent AKT activation in *S. flexneri* infected epithelial cells or in cells overexpressing IpgD. Cells treated with PI5P are enriched for EGFR in early endosomes preventing its lysosomal degradation. Thus, IpgD is modulating the trafficking of the host cell by impairing the maturation and transport of endosomes to lysosomes, which extends the duration of survival signals by protecting EGFR from degradation[222].

Altogether, the research described in this section shows that *Shigella* developed multiple strategies to circumvent or delay host cell death and subsequently the loss of its replicative niche. These mechanisms can be viewed as a major virulence factor because they expand the timespan in which the pathogen can replicate and disseminate either within the tissue or to the environment.

2.5 The endocytic and secretory pathways are modulated by *Shigella*

Burnaevskiy and colleagues found that *Shigella* inhibits the cargo transport through the Golgi apparatus and that the Golgi apparatus itself becomes fragmented upon *Shigella* infection[34]. This effect was shown to be TTSS-dependent and a subsequent screen for the responsible components revealed the effector proteins VirA and IpaJ to induce Golgi fragmentation and to inhibit hormone trafficking through the secretory pathway. Deletion of either VirA or IpaJ in a mouse model of mucosal infection strongly affected the replication of the bacteria compared to wild-type, showing the importance of these effectors for *in vivo* virulence. It was demonstrated that IpaJ cleaves the N-myristoylated glycine from ARF1 by its cysteine protease activity. In addition, IpaJ demyristoylated a large portion of N-myristoylated proteins found in mammalian cells. The myristoyl group is sequestered in GDP-inactive ARF1 and liberated for membrane binding upon GTP exchange. IpaJ can therefore distinguish the activation state of its substrate and only cleaves GTP bound active ARF1, leading to the release of activated ARF1 from the Golgi upon *Shigella* infection[34].

2.6 Metabolic adaptations to an intracellular lifestyle

The epithelial cell reflects the main replicative niche of *Shigella*. Understanding the bacterial replication process in the host cell is very important because intracellular growth is key for virulence. It is noteworthy, that the pathogen faces different environments at the different stages of infection until it reaches the cytoplasm of epithelial cells. Therefore, *Shigella* has to be highly adaptive and regulate transcription and protein expression according to current demands. It is not surprising that more than 900 genes are differ-

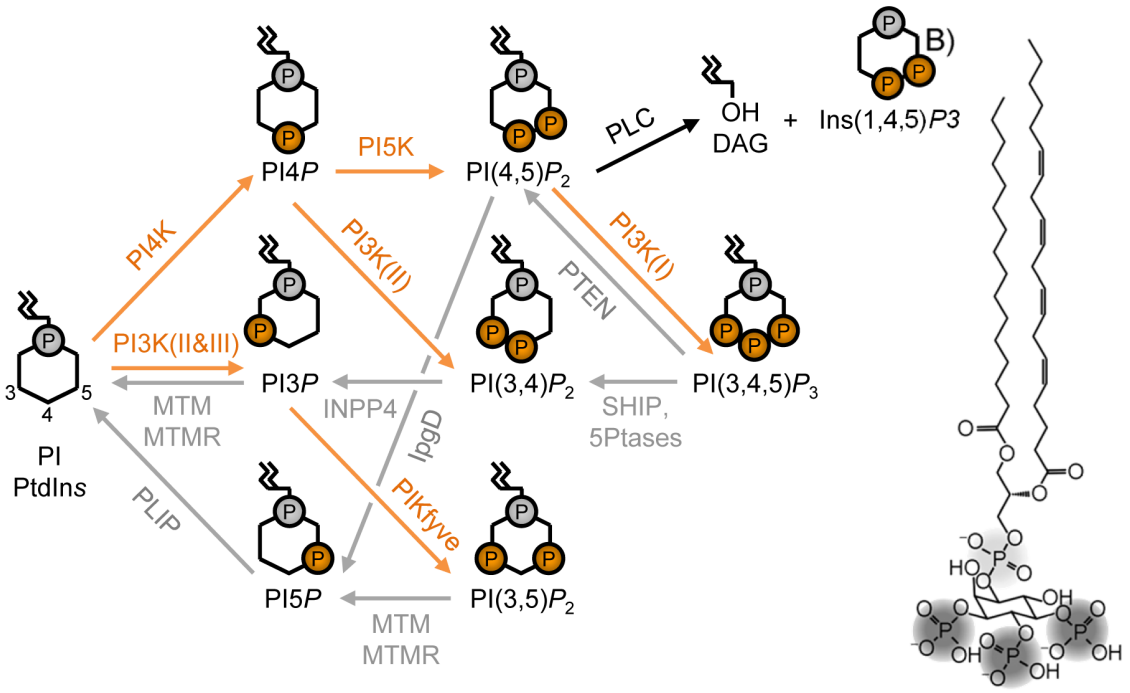

Figure 2.5.1 The main enzymes involved in Biosynthesis and metabolism of phosphoinositides. Left: Lipid kinases (orange) and lipid phosphatases (grey) mediate the conversion of phosphatidylinositol (PI) to PI(3,4,5)P3 and the corresponding interstages that all have important functions in phosphoinositol signaling. PI becomes phosphorylated by phosphatidylinositol 4-kinase (PI4K) to phosphatidylinositol 4-phosphate (PI4P) which itself gets further phosphorylated by phosphatidylinositol 5-kinase (PI5K) to PI(4,5)P2. phospholipase C (PLC) can produce diacylglycerol (DAG) and Inositol-1,4,5-trisphosphate (Ins(1,4,5)P3) from PI(4,5)P2. PI(4,5)P2 can be converted to PI(3,4,5)P3 by class I PI3K a process that can be reversed by the action of the 3 lipid phosphatase phosphatase and tensin homolog (PTEN). PI(3,4,5)P3 can be also be dephosphorylated by phosphatidylinositol 3,4,5-trisphosphate 5-phosphatase (SHIP) yielding in phosphatidylinositol 3,4-bisphosphate (PI(3,4)P2) which can also be produced by class II PI3K from PI4P. PI(3,4)P2 becomes degraded by inositol polyphosphate 4-phosphatase type I (INPP4) to phosphatidylinositol 3-phosphate (PI3P) which can also be formed by phosphorylation of PI by class II and III PI3K (Vps34). PI3P can be converted to phosphatidylinositol 3,5-bisphosphate (PI(3,5)P2) by the phosphatase PIKfyve. myotubularin (MTM) and myotubularin-related protein (MTMR) are a family of lipid phosphatases that can dephosphorylate both, PI3P and PI(3,5)P2 to PI and PI5P respectively. PI5P can also be generated from PI(4,5)P2 by the phosphatidylinositol 4,5-bisphosphate 4-phosphatase IpgD which is an effector secreted by *S. flexneri*. PI5P can be converted to PI by PTEN-like phosphatase (PLIP) activity. Right: Structure of PI(3,4,5)P3. PI(3,4,5)P3 consists of a polar inositol ring that is phosphorylated on position 3, 4 and 5 and coupled by a further phosphate group and a glycerol backbone to two non polar fatty acid tails, usually stearic acid and arachidonic acid. *adapted with modifications from Wymann and Schultz*[291].

entially regulated when comparing *Shigella* growth in HeLa cells to growth in broth[163]. Interestingly, the key virulence genes as the *ipa-mxi-spa* locus and *icsA* were drastically down-regulated during intracellular growth, indicating that these genes are not crucial for growth once the bacteria are inside the cell. At the same time, bacteria have to compete for iron, magnesium and phosphate indicated by up-regulation of the *sitABCD* iron transport system, the magnesium transporter gene *mgtA*, and genes of the *phoBR* regulon that includes *phoA* gene, encoding periplasmic phosphatase, and the *pstS* and *phnC* genes, encoding ABC phosphate transporters. A recent study also aimed to find differences between *in vivo* and *in vitro* gene expression[177]. Nine genes that are transcriptionally altered during growth within epithelial cells and are specific to *S. flexneri* species were found. Deletion of the transcriptional regulator *intracellular growth regulator (icgR)*, described in this study, had no effect on growth *in vitro* but resulted in increased intracellular multiplication in HCT-8 cells. The TonB-dependent iron transport system was previously shown to be important for *Shigella dysenteriae* intracellular growth. A *tonB* mutant was invasive but had a reduced rate of multiplication. Interestingly this was also observed in iron replete cells, indicating that TonB has additional roles to heme- and siderophore-mediated iron acquisition *in vivo*[224]. Moreover, it has been demonstrated that mutants unable to synthesize guanine, thymine or p-aminobenzoic acid are severely impaired in intracellular multiplication[36]. Recent proteomic data suggest that intracellular *Shigella* scavenges a wide range of carbon sources as many transport systems for a variety of sugars and peptides are expressed[216]. In addition, these transport systems are robust and redundant as single mutations in genes as *fruA*, *manX*, or *dpp* do not affect the ability of the pathogen to grow intracellular[216]. *Shigella* seems to metabolize the carbon sources through glycolysis and mixed-acid fermentation. Mutants unable to metabolize pyruvate to formate and lactate did not grow well in the intracellular environment[216]. Although there is increasing knowledge about bacterial factors that are adapted within the host cell and participate in metabolism, little is known about host factors that contribute to or restrict bacterial growth.

3 Modulation of pro-inflammatory signaling cascades

3.1 Inflammation, a tightrope walk for both, *Shigella* and the host

Inflammation is a pivotal point of *Shigella* infection as it can be beneficial or detrimental for both, the pathogen and the host. The consequence is a tug war between the host and the pathogen for the adjustment of inflammation in favor of each side. Inflammation is fundamental for the initiation of an immune response, leading to the clearance of infection. However, excessive inflammation can lead to severe tissue damage and even allow further bacteria to gain access to the submucosa. This already implies the dependency of the pathogen towards a beneficial amount of inflammation. A low level of inflammation appears to be optimal for the pathogen because this would allow evasion of the immune response. However, *Shigella* also relies on a certain amount of inflammation, leading to the manifestation of the diarrheal symptom that promotes the spread of the pathogen. In this section, strategies of *Shigella* to interfere with the host signaling towards an inflammatory response will be described.

3.2 Pathogen sensing

The innate immune system senses invading microbial pathogens by receptors recognizing specific conserved bacterial patterns. These receptors, collectively referred as pattern recognition receptors (PRRs) recognize specific pathogen-associated molecular patterns (PAMPs) including LPS, lipoproteins and peptidoglycan (PGN) that are broadly expressed on pathogens but not found on host cells [265]. The most prominent PRR family are the Toll-like receptors (TLRs), that recognize different PAMPs (also referred as microbe-associated molecular patterns (MAMPs)) including lipids, lipoproteins, proteins, glycans and nucleic acids [265]. TLRs are either expressed on the cell surface to sense extracellular PAMPs or can be found on intracellular vesicles such as endosomes or lysosomes [265].

The gut is a special organ, regarding the huge number of comprised microbes building the gut microbiota. To avoid constant inflammation triggered by the massive presence of PAMPs, many TLRs are predominantly expressed on the baso-lateral side of the epithelium [1]. Invading pathogens are sensed by soluble intracellular PRR including the RIG-I like receptors (RLRs) and Nod-like receptors (NLRs) whose members Nod1 and Nod2 play an important role upon *S. flexneri* infection [48] [88]. NLRs typically consist of three distinct domains, including a N-terminal caspase recruitment domain (CARD) important

for protein interaction, a central nucleotide-binding NACHT domain and a C-terminal leucine-rich repeat (LRR) domain which mediates PAMP sensing[48]. Nod1 recognizes the PGN derived structural motif g-D-glutamyl-meso-diaminopimelic acid (iE-DAP) commonly found in the PGN structure of all gram-negative as well as in several gram-positive bacteria[86][37]. Nod2 recognizes muramyl dipeptide (MDP) a large compound of PGN that is present in all gram-negative as well as gram-positive bacteria, making it a more general sensor for bacteria[87]. Invading *S. flexneri* are sensed by a pool of membrane located Nod1 proteins that become recruited to the site of bacterial entry and also remain at the membrane fragments after rupture of the vacuole. In addition, peptidoglycan-derived peptides released from multiplying bacteria in the cytoplasm are sensed by Nod1 and further contribute to its activation. Peptidoglycan sensing induces the homodimerization of Nod1, mediated by the nucleotide-binding NACHT domain, and subsequently the recruitment and polyubiquitination of the kinase receptor-interacting serine/threonine-protein kinase 2 (RIP2) by CARD-CARD interaction. RIP2 then activates TAK1, a member of the MAP3K family. TAK1 forms a complex with TAB1, TAB2 and TAB3 that controls the further activation of downstream pathways including NF-κB and MAPKs[225].

3.3 NF-κB and the MAPKs - two important signaling pathway in response to bacterial infection

Several *Shigella* TTSS translocated effector proteins have been identified that target the NF-κB pathway in order to prevent nuclear translocation and subsequent expression of pro-inflammatory cytokines like IL-8. Another *S. flexneri* effector protein inactivates the MAPK cascade and thus prevents chromatin remodeling, a prerequisiste for the expression of pro-inflammatory cytokines. Thus, the NF-κB and MAPK pathway are important signaling pathways upon bacterial infection and key players in the induction of an innate immune response. The transcription factor NF-κB was discovered in 1986 to bind selectively to the kappa light chain enhancer DNA element in extracts of B-cell tumors, leading to the abbreviation NF-κB[252]. The NF-κB transcription factor family regulates the expression of many genes that are involved in diverse biological processes like inflammatory and immune responses, cell growth and development[186]. Five distinct members of this transcription factor family have been identified and termed as p65 (RelA), RelB, c-Rel, NF-κB1 and NF-κB2. NF-κB2 is synthesized as pro-forms (p105 and p100) and becomes proteolytically processed to p50 and p52, respectively. In its inactive form, NF-κB is sequestered in the cytoplasm by binding to its inhibitor inhibitor of NF-κB (IκB), that masks the nuclear localization sequence (NLS) of NF-κB and prevents its nuclear translocation and subsequent DNA binding. Activation of NF-κB occurs by release from IκB or by cleavage of p100 and p105. This is achieved by proteasomal degradation of IκB or

by partial degradation of the precursors. IκB becomes Lys-48 linked polyubiquitinated which is catalyzed by SCF$^{\beta\text{-TrCP}}$ type E3 ligase. A prerequisite for polyubiquitination is the prior specific double phosphorylation of IκB. The phosphorylation is mediated by an enzyme complex containing inhibitor of nuclear factor κ-B kinase (IKK)α and IKKβ and the non-catalytic accessory protein NEMO. The IKK complex itself becomes activated by upstream kinases, including NIK, MEKK1,2,3 and TAK1. In the canonical NF-κB pathway, proinflammatory signals such as cytokines, PAMPs and danger-associated molecular patterns (DAMPs) activate a signaling cascade that leads to the activation of IKK which induces the release of NF-κB for nuclear translocation and activation of gene transcription (Figure 3.6.1). In the specific case of bacterial invasion, their PAMPs and DAMPs are detected by various PRRs, including TLRs and NLRs as well as some components of the autophagic machinery, leading to the activation of the MAPK and NF-κB pathways[14].

The MAPK pathway coordinates diverse cellular functions such as gene expression, cell cycle, metabolism, motility, differentiation, survival and apoptosis[146]. Six distinct MAPK classes have been characterized in mammalians including extracellular-signal regulated kinase (ERK)1/2, ERK3/4, ERK5, ERK7/8, c-Jun N-terminal kinase (JNK) and p38[157]. For conceptual reasons, the focus of the brief MAPK signaling overview will be restricted to the most extensively studied groups ERK1/2, JNK and p38, all becoming activated upon *S. flexneri* infection by the Nod1, RIP2, MAP3K and MAP2K cascade. The MAPK cascade is typically tripartite and begins with a serine/threonine kinases from the MAP3K family which becomes activated by phosphorylation or by interaction with small GTPases from the Ras/Rho family in response to extracellular stimuli. Activated MAP3K phosphorylates MAP2Ks which are dual specificity kinases and thus phosphorylate their substrates the MAPK on both, threonine and tyrosine[146]. Activated MAPKs subsequently phosphorylate and activate their substrates including transcription factors, other kinases and histones. In particular, JNK and p38 regulate the activity of the transcription factor AP-1. In parallel, p38 and ERK remodel the chromatin structure by phosphorylation of histone H3 via the kinases MSK1 and MSK2, making the DNA accesible for transcription factors like AP-1 and NF-κB[205] [146]. The MAPK and NF-κB signaling cascades collectively initiate an inflammatory response, leading to the transcription of pro-inflammatory genes including the chemokine IL-8 which was shown to be more than 300-fold up-regulated during *S. flexneri* infection[209]. Pathogens have evolved strategies to circumvent the secretion of pro-inflammatory cytokines, which will be discussed in the following sections.

3.4 Several *Shigella* effectors interfere with the NF-κB pathway

Among the effector molecules that have been shown to interfere with NF-κB signaling is OspG which inhibits nuclear translocation of NF-κB by preventing degradation of the phosphorylated form of inhibitor of NF-κB alpha (IκBα)[132]. It was found that OspG binds the unbiquitinylated E2 UbcH5 which is a component of the $SCF^{\beta\text{-TrCP}}$ complex that promotes phospho-IκBα ubiquitination and its subsequent degradation by the proteasome. As a consequence of this OspG down-regulates the transcription of NF-κB-dependent genes and thus the pro-inflammatory response[132]. In addition, nuclear translocation of NF-κB is also impaired by the effector OspZ, which is a homologue to the EPEC/EHEC NleE effector, although the molecular mechanism of this observation remains to be resolved[190]. Two effectors of the IpaH family which are E3 ubiquitin ligases have also been demonstrated to interfere with NF-kB signaling. These include the *Shigella* effector IpaH9.8 that was shown to downregulate inflammation by binding to the mammalian splicing factor U2AF35, indicating that IpaH9.8 can dampen the expression of pro-inflammatory cytokines at the post-transcriptional level[202]. Moreover, IpaH9.8 interacts with NEMO/Inhibitor of nuclear factor κ-B kinase subunit γ (IKKγ) and the ubiquitin binding adaptor protein ABIN-1 and promotes ABIN-1-dependent polyubiquitination of NEMO. Subsequently, polyubiquitinated NEMO undergoes proteasome-dependent degradation, severely impairing NF-κB activation[11].

In addition to the activation of NF-κB through Nod1-dependent recognition of peptidoglycan moieties, NF-κB can also become activated by PKC signaling in response to membrane damage through *Shigella* invasion of epithelial cells. In this pathway IpaH0722, another member from the IpaH family, ubiquitinates TRAF2, a downstream molecule of PKC and promotes its proteasomal degradation[12]. As a consequence, the downstream signaling towards IKK, IκB/NF-κB is dampened during *Shigella* infection. Interestingly, NF-κB activation through PKC signaling is also targeted by the effector and glutamine deamidase OspI that impairs inflammatory signaling by targeting NF-κB activation via the TRAF6 pathway[236]. OspI deamidates UBC13 and impairs its E2 ubiquitin ligase activity which is required for TRAF6 polyubiquitination. As a consequence, nuclear translocation of NF-kB is impaired. Surprisingly, there has also been an effector described that seems to activate NF-κB signaling[80]. OspB was shown to activate NF-κB through GEF-H1 and Nod1 leading to Rho-associated protein kinase (ROCK)-dependent phosphorylation of NF-κB. However, Zurawski and colleagues found OspB to reduce the pro-inflammatory response by interacting with retinoblastoma protein[304].

The fact that *S. flexneri* has several effector proteins targeting NF-κB, clearly puts much attention on this pathway in the context of bacterial induced inflammation. However, it is not easy to explain why a pathogen evolved different effector molecules for the apparently

same purpose. Although the different effectors tackle the NF-κB pathway at distinct sites, the outcome is expected to be similar. Redundancy may serve as an explanation however, by considering the fact that deletion of a single effector can strongly promote inflammation as claimed in different studies, it is not very plausible. Otherwise, multiple deletion mutants would have been required for the observation of an effect. A more plausible explanation is the temporal factor. The distinct effectors may deploy their activity at different time-points of infection and may thus all be important for a successful inactivation of NF-κB signaling. More work is required to unravel the impact of these effectors on the NF-κB pathway. Especially a systems biology approach would be suitable to study the different effectors in context instead of an isolated view on single effectors as already carried out.

3.5 OspF prevents MAPK activation via its phosphothreonine lyase activity

As described in the previous paragraph, *Shigella* targets the NF-κB pathway and inhibits nuclear translocation of the transcription factor. This is not the only strategy the pathogen employs to down-regulate the expression of pro-inflammatory genes in infected cells. In addition, the MAPK pathway, which synergistically with the NF-κB pathway induces the expression of pro-inflammatory genes, is also subverted by *Shigella*[250]. This is achieved by OspF, a TTSS secreted effector protein, that inactivates the MAPKs p38 and ERK and thereby dampens host immunity[9]. The OspF family, includes OspF from *Shigella spp.*, SpvC from nontyphoid *Salmonella spp.* and HopAI1 from plant pathogen *Pseudomonas syringae*[207]. MAPKs are activated by dual phosphorylation on a pT-X-pY motif in the activation loop. Inactivation of MAPKs by OspF is mediated by its phosphothreonine lyase activity that irreversibly removes the phosphate group from the phosphothreonine in the MAPK activation loop, a process called β-elimination (Figure 3.5.1). More precisely, OspF converts phosphothreonine into β-methyldehydroalanine and thereby irreversibly inactivates the MAPKs. Biochemical analysis has shown that OspF is specific for dual phosphorylated MAPKs, with high activity towards phosphorylated p38, moderate towards ERK, but almost no activity towards phosphorylated JNK[300]. Once secreted into the epithelial host cell, OspF rapidly translocates to the nucleus where it inactivates p38/ ERK and subsequently prevents the phosphorylation of histone H3 on serine 10[9]. Besides transcription factors like NF-κB, histone modifications play a major role in the control of transcription. The N-terminus of the four core histones H2A, H2B, H3 and H4 are accessible for post-translational modification (PTM), because they protrude out of the nucleosome. Histone modifying PTM include amongst others acetylation, phosphorylation and methylation. These modifications affect gene regulation by altering

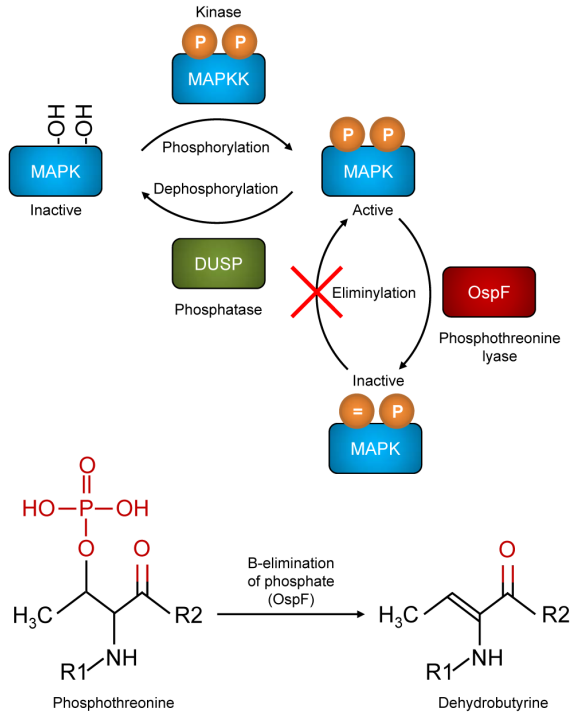

Figure 3.5.1 OspF has phosphothreonine lyase activity. MAPK (blue) become activated by dual phosphorylation on a Thr-Xaa-Tyr motif of the activation loop through an upstream MAPKK. The MAPK can become inactivated by removal of the phosphorylation through a dual-specificity phosphatase (DUSP) (green). OspF (red) can irreversibly inactivate phosphorylated MAPK by a beta-elimination reaction where phosphothreonine becomes modified to dehydrobutyrine which due to its lack of a hydroxyl group cannot be re-phosphorylated. This post-translational modification is termed eliminylation, represented by (=). Monophosphorylated MAPK is inactive *Adapted with modifications from Brennan and Barford 2009* [51].

the accessibility of transcription factors to chromatin [122]. Phosphorylation of histone H3 on serine 10 can be induced by the MAPKs signaling pathways. The phosphorylation selectively occurs on the promotors of immediate early genes like FOS and on a subset of NF-κB-dependent pro-inflammatory cytokine and chemokine genes as IL-8. Altough its not yet entirely clear, it is most likely that downstream of the MAPKs, mitogen- and stress-activated kinase (MSK) is the kinase responsible for Histone H3 phosphorylation upon *Shigella* infection [9].

Altogehther, it has been demonstrated that OspF is an effector that dampens the inflammatory response by inhibiting the MAPK pathway and subsequently Histone H3 phosphorylation, preventing the transcription of NF-κB regulated pro-inflammatory genes, particularly IL-8 [9]. IL-8 attracts PMN cells through the lamina propria as well as through the epithelial layer. This is in concordance with *in vivo* data showing that an *ospF* deletion strain compared to wild type causes a much more severe inflammation including leukocyte recruitment [9]. Recently, it was shown that OspF can also indirectly affect the activity of proteins by interfering with a negative feedback loop [225]. In particular, p38 repression by OspF leads to an interruption of the negative feedback towards TGF-beta activated kinase 1 (TAK1) and subsequently potentiates the activity of the downstream MAPK JNK and the transcription factor NF-κB [225]. Therefore it is tempting to speculate that OspF may affect even more cellular targets downstream of the MAPK cascade and may have a broader impact on the host cell signaling as described so far.

3.6 IpgD also dampens inflammation

In 2013, *in vivo* work has assigned an additional function to IpgD and revealed its role in immune evasion by down-regulating the inflammatory response[219]. Earlier, it has been proposed that *Shigella* infection induces the opening of connexin 26 hemichannels, allowing adenosine triphosphate (ATP) to be released from the cell. Although it has been reported that this ATP release can increase bacterial invasion and spreading, the pathophysiological meaning of this process remained unclear[274]. In the recent years, it became evident that extracellular ATP plays a role in immunity and that it can modulate inflammation in a concentration-dependent manner[30]. Puhar and colleagues[219] now described that *Shigella* infection induces an early innate immune response caused by ATP release through connexin hemichannels. They could show that PI5P produced by IpgD can block *Shigella* induced ATP release by closing connexin hemichannels. This *in vivo* data reveals that beyond controlling the survival state of an infected cell, IpgD plays also a major role in the maintenance of the *Shigella* epithelial niche by down-regulating the inflammatory response.

3.7 Mechanism of bystander cell activation

Recently, a study from our laboratory was published revealing a host strategy to circumvent the anti-inflammatory activity of *Shigella* effectors by amplification of IL-8 expression during bacterial infection[128]. It was shown, that epithelial cells infected with *Shigella* are not able to produce IL-8 due to the activity of different *Shigella* effectors, in particular OspF. Surprisingly, uninfected neighboring bystander cells produced IL-8. In addition, nuclear NF-kB translocation as well as MAPK activation rapidly propagated from infected to uninfected bystander cells, altogether resulting in the observed IL-8 production. Bystander IL-8 production was also observed upon *Salmonella Typhimurium* and *Listeria monocytogenes* infection, indicating a general host defense mechanism. It was subsequently shown that the bystander cells were alerted by infected cells through gap junction-dependent cell-cell communication[128].

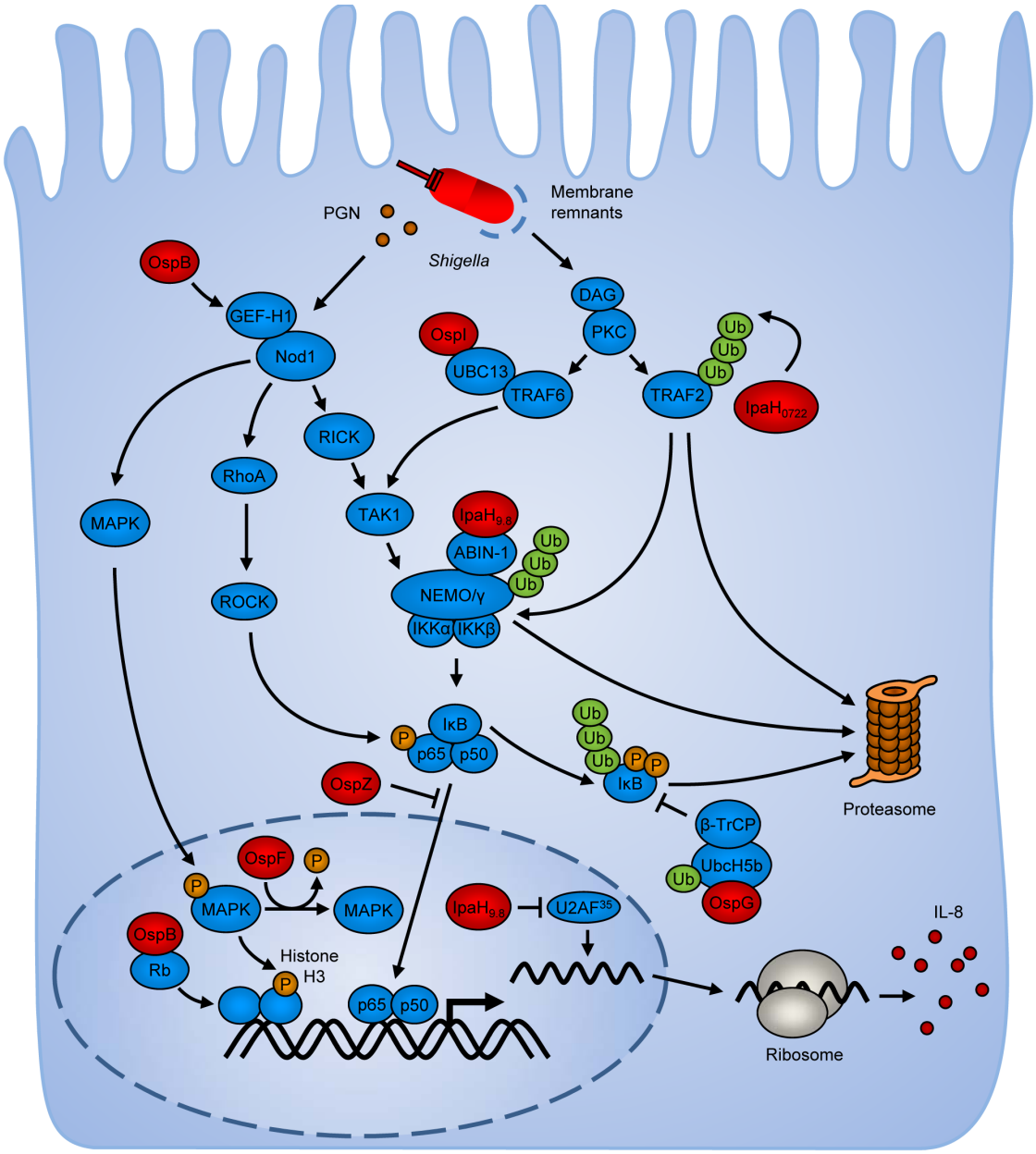

Figure 3.6.1 *Shigella* modulates the host immune response. Several effector proteins (red) are secreted by intracellular *Shigella* and interfere with the NF-κB and MAPK signaling cascades in order to downregulate the inflammatory response. For more details, refer to the manuscript. *Adapted with modifications from Ashida et al.*[14].

4 Study of the host signaling network

4.1 Systems biology of *S. flexneri* infection

Infection of epithelial cells by *S. flexneri* has been well investigated by reductionist approaches resulting in important discoveries regarding specific molecular aspects of infection, as well as general concepts of infection biology and immunology [223] [13]. However, the host-pathogen interaction is a multifarious process that is far more complex than it can be comprehended by isolated observations of specific aspects of the infection. Systems biology is following the assumption, that a comprehensive understanding of biological processes, which are influenced by a multitude of factors, can be extracted from global network data. This type of information can be obtained from different technology platforms which are capable to sensitively and accurately acquire large scale data sets of a certain cellular state. One possibility are perturbations of the biological system and the consequent measurement of the impact on a cellular state as it can be achieved by RNA interference (RNAi) screens. In addition, systems biological approaches often rely on different "omics" disciplines such as transcriptomics, metabolomics or proteomics. Transcriptomic data to study the differential gene expression profiles upon perturbations or changed environments, can be acquired by DNA microarray technologies. This technique has been applied to study the gene expression pattern of epithelial cells infected with *S. flexneri* [209]. The expression of 12'000 genes was monitored, revealing the induction of a pro-inflammatory gene expression pattern. Although, a biological dogma proposes a hierarchical information flow from DNA to mRNA to proteins to metabolites, this flow can be influenced by the cell or extrinsic factors at different stages. mRNA expression for instance, does not necessarily correlate with protein expression, highlighting the importance of proteomic data as complementation of transcriptomics [95]. Proteomics deals with the large-scale determination of gene and cellular functions directly at the protein level [3]. The *Shigella* proteome has been characterized in different states of growth or environmental conditions. However, a broad host cell proteome upon *Shigella* infection is lacking [217] [299] [216]. Even though information about a host cell proteome upon *S. flexneri* infection would be valuable, its suitability to capture signaling events that occur early in the infection process would be very limited. Rapid signaling events often occur through PTM of proteins which allow a faster response than regulation at the protein level would. Thus, studying PTM modifications upon *S. flexneri* infection is an attractive strategy towards a global understanding of the host-pathogen interaction.

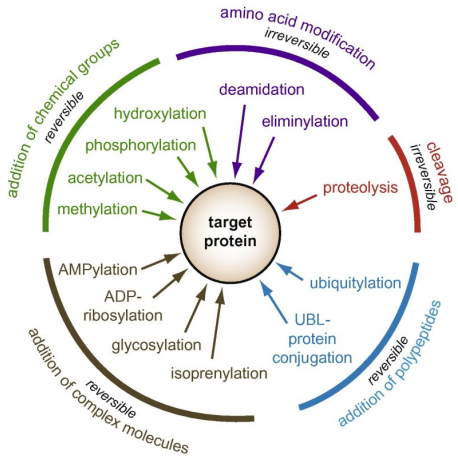

Figure 4.2.1 Diversity of PTM. PTM are modifications of target proteins after their translation. PTM can be distinguished based on different criteria: The modification of the chemical structure of the amino acid side chain, the addition of chemical groups or complex molecules to specific amino acids, the covalent linkage of polypeptides, or the proteolytic cleavage of proteins. For each class the reversibility of the modification as well as examples are indicated. *From Ribet and Cossart 2010* [226].

4.2 Post-translational modifications

Proteins are large macromolecules consisting of specific sequences of amino acids. Although the sequence determines the fold and consequently the function of a protein to a high degree, modifications of amino acids and their side chains contribute essentially. The ability of proteins to undergo modifications at the post-translational level dramatically enhances the complexity of proteomes in several orders of magnitude more than the gene code alone could. More than 300 different PTMs have been reported, already indicating the complexity added to the proteome by modification of proteins [226]. The complexity even becomes unbounded assuming that a single protein can undergo several different modifications at different sites which in turn may affect the modification state of other proteins.

PTMs can be classified based on the chemical nature and on the reversibility of the modification. Most simply, the proteolytic cleavage of a protein is an irreversible PTM modification. In addition, irreversible amino acid modifications include deamidation and eliminylation, two chemical reactions which can become catalyzed by *S. flexneri* effectors. Deamidation is a chemical reaction occuring on asparagine and glutamine in which the amide group of the side chain becomes removed yielding an aspartic or glutamic acid, respectively. Deamidation of Ubc13 by the *S. flexneri* effector OspI downregulates the inflammatory response as described in section 3.4. Eliminylation was discovered based on the delineated mechanism of the *S. flexneri* OspF and *Salmonella* SpvC phosphothreonine lyases. These effectors employ a β-elimination reaction, where the phosphate from phosphothreonine is removed and converted into dehydrobutyrine (section 3.5).

Other PTM are characterized either by the addition of polypeptides, complex molecules or chemical groups. The most prominent example of a PTM that is based on addition of polypeptides is ubiquitination. Lysine residues can become modified by the small protein ubiquitin. Ubiquitination is a reversible PTM, associated with regulation of the half-life of

proteins, as ubiquitinated proteins can rapidly undergo proteasomal degradation. Ubiquitination can be different in the way that a substrate can become monoubiquitinated or polyubiquitinated. Lys48 linked polyubiquitination is associated with proteasomal degradation whereas Lys63 linked polyubiquitin chains can mediate signaling functions. Thus, ubiquitination is a complex PTM and executes a variety of biological functions within a cell[140]. It is not surprising that *S. flexneri* evolved TTSS effector molecules that interfere with the host ubiquitination machinery like the E3 ubiquitin ligases IpaH9.8 and IpaH0722 that have been described in section 3.4.

Besides the addition of polypeptides also other complex molecules can be attached to a protein and thus affect its function. These modifications are usually reversible and prominent examples are AMPylation, ADP-ribosylation, glycosylation or isoprenylation. AMPylation, also known as adenylation describes the reversible, covalent attachment of an adenosinmonophosphate (AMP) to hydroxyl side chains of protein substrates. AMPylation was shown to play an important role upon bacterial infection where T3SS or T4SS translocated proteins harboring a filamentation induced by cAMP (Fic) domain, catalyze the AMPylation of cellular targets. Prominent bacterial effector Fic proteins are the TTSS effector VopS from *Vibrio parahaemolyticus* as well as the T4SS effector VbhT from *Bartonella Schoenbuchensis*, both AMPylating RhoGTPases leading to the collapse of the cytoskeleton[293] [65].

Besides the above mentioned PTM, there are also irreversible modifications of proteins with complex molecules. An example of such a PTM is myristoylation where a myristoyl group becomes covalently attached to the N-terminal glycine residue of target proteins, typically promoting membrane binding[290]. As described in section 2.5, the *S. flexneri* TTSS effector IpaJ cleaves the peptide bond of N-myristoylated glycine-2 and asparagine-3 of human ARF1 and thereby inhibits the host secretion machinery[34]. The most prominent example for a reversible PTM characterized by the addition of chemical groups is phosphorylation which will be elucidated in more detail in the next section.

Altogether, these examples illustrate that PTMs are involved in diverse cellular aspects and thus targeted by many different bacterial effectors. Therefore, recently developed proteomic approaches including ubiquitomics, acetylomics or phosphoproteomics will shed new light on the signaling map of host-pathogen interactions[136,164,229].

4.3 Protein phosphorylation

One of the most important PTM with regard to signal transduction is phosphorylation. Phosphorylation is a reversible modification and involved in nearly all aspects of cellular life. It was first discovered in the 1950's that the metabolic enzyme phosphorylase which converts glycogen to glucose-1-phosphate exists in either an active or an inactive

state[144]. It was found that a protein kinase could catalyze the attachment of a phosphate to phosphorylase and therefore renders it active[77]. For these discoveries, Edwin Krebs and Edmond Fischer received the Nobel prize in 1992. In addition, it was shown that phosphorylase kinase itself becomes activated by the protein kinase A (PKA)[105] leading to the birth of the concept of protein phosphorylation as a key biochemical regulatory mechanism. The transfer of the γ-phosphate group from a high energy donor molecule to its substrate is mediated by enzymes named kinases or phosphotransferases. Donor molecules are typically ATP or less frequently guanosine-5'-triphosphate (GTP). The γ-phosphate of ATP or GTP is preferentially transferred to hydroxyl groups (OH) but also to nucleophilic centers of other functional groups of acceptor molecules containing oxygen, sulfur or nitrogen. This attachment process of a phosphorus containing group is termed phosphorylation, where a phosphono- or short phospho (also named phosphoryl) group is transferred to an acceptor molecule.

A hallmark of phosphorylation signaling is its rapid character. A cell can adapt to various stimuli by modification of the total protein amount. Although degradation of proteins by the proteasome is rather fast, synthesis of new proteins will clearly need more time. As a cell has to rapidly respond to various stimuli this cannot solely be achieved by adjusting relative protein amounts. Therefore fast signaling events are often mediated by PTM of proteins whereby phosphorylation has a prominent role. It has been shown for instance, that cells treated with epidermal growth factor (EGF) undergo phosphorylation on more than 500 different proteins already within 5 minutes after treatment[203].

4.3.1 Chemical properties of amino acid phosphorylation

Biochemically, phosphorylation can be subdivided into different classes, based on the acceptor amino acid that becomes modified. In eukaryotic cells, hydroxy-linked or O-phosphorylation is by far the most extensively studied. In O-phosphorylation a phosphate group becomes bound to one of the three amino acids serine, threonine or tyrosine containing a hydroxyl-group within the side chain[60]. The frequency of phosphorylation is not identical for all potential acceptor amino acids. In eukaryotic proteins, phosphorylation occurs mainly on serine (86%) followed by threonine (12%) and only a minor fraction on tyrosines (2%)[203]. It is noteworthy to mention, that the general abundance of the amino acid tyrosine is much lower than for serine and threonine. Although tyrosine phosphorylation seems to be underrepresented it appears to be very dynamic and crucial for the building of extensive interaction networks with its binding partners, through specific binding domains as src homology 2 (SH2) domain or 14-3-3 domains, to note just two examples[161]. Nitrogen phosphorylation of histidine, arginine and lysine are formed by a phosphoramidate linkage and are named N-phosphorylation[60]. Histidine phosphorylation for instance, has been found in all kingdoms of life and histidine kinases are prominent

in plants and bacteria. In eukaryotic cells the relative contribution of N-linked phosphorylation to the total phospho-amino acids has been estimated to approximately 6% and is exceeding the relative amount of tyrosine phosphorylation [104]. However, N-linked phosphorylation is highly acid-labile and therefore remained undiscovered for a long time. This is also the reason why research progress on histidine phosphorylation is slow, although it became obvious that histidine phosphorylation may play an important role in different mammalian signaling pathways and has also been linked to several diseases [15]. Additionally, the sulfur of cysteine can form a phosphate thioester or S-phosphate. Aspartate and glutamate can form an acid anhydride (acyl phosphate). Yet, thio- and acyl phosphates are extremely rare in eukaryotic cells [60].

4.3.2 Biochemical and structural consequences of protein phosphorylation

Phosphorylation can affect the structure and subsequently also the functionality of a protein. The phosphoryl group is predominantly dianionic at physiological pH and consequently forms two negative charges. Such a double negative charge is not present in protein coding amino acids. The addition of a phosphoryl group can therefore have a major impact on the net charge of the substrate and thus can affect the conformation of a protein [124]. On one hand, a conformational change of a protein can be due to repulsive force from the phosphoryl towards other negative charges found in the protein. On the other hand, the negative phosphoryl group can form ion pairs with positively charged amino acid side chains such as harbored by arginine. Phosphoryl oxygens are therefore able to form multiple hydrogen bonds forming strong interactions. At tight binding sites, phosphate groups are known to frequently interact with the side chain of arginine residues which can stabilize the conformational state of a protein. On sites with less tight phosphoryl-group interactions, main-chain nitrogens at the beginning of an α-helix are involved in binding, due to the positive charge of the helix dipole [161]. Furthermore other polar residues including lysine, histidine, tyrosine, serine and threonine may also be able to form contacts to phosphoryl groups. The sum of newly formed and broken hydrogens bonds determines the conformational and structural consequences of protein phosphorylation. Thus, a protein can undergo phosphorylation-dependent structural changes, which can affect the specific function of the protein. By this, phosphorylation can activate enzyme activity through allosteric conformational changes, as it is observed for many kinases that become activated through phosphorylation by upstream kinases [161]. However, phosphorylation can also inhibit enzymatic activity, when the phosphate group acts a steric blocking agent preventing conformational changes, or when phosphorylation impedes substrate recognition [116] [286]. Phosphorylation can also be an important mechanism to provide a recognition site for other proteins. For example, proteins harboring a SH2 domain specifically interact with proteins that are tyrosine phosphorylated. Another example is a regulatory domain found

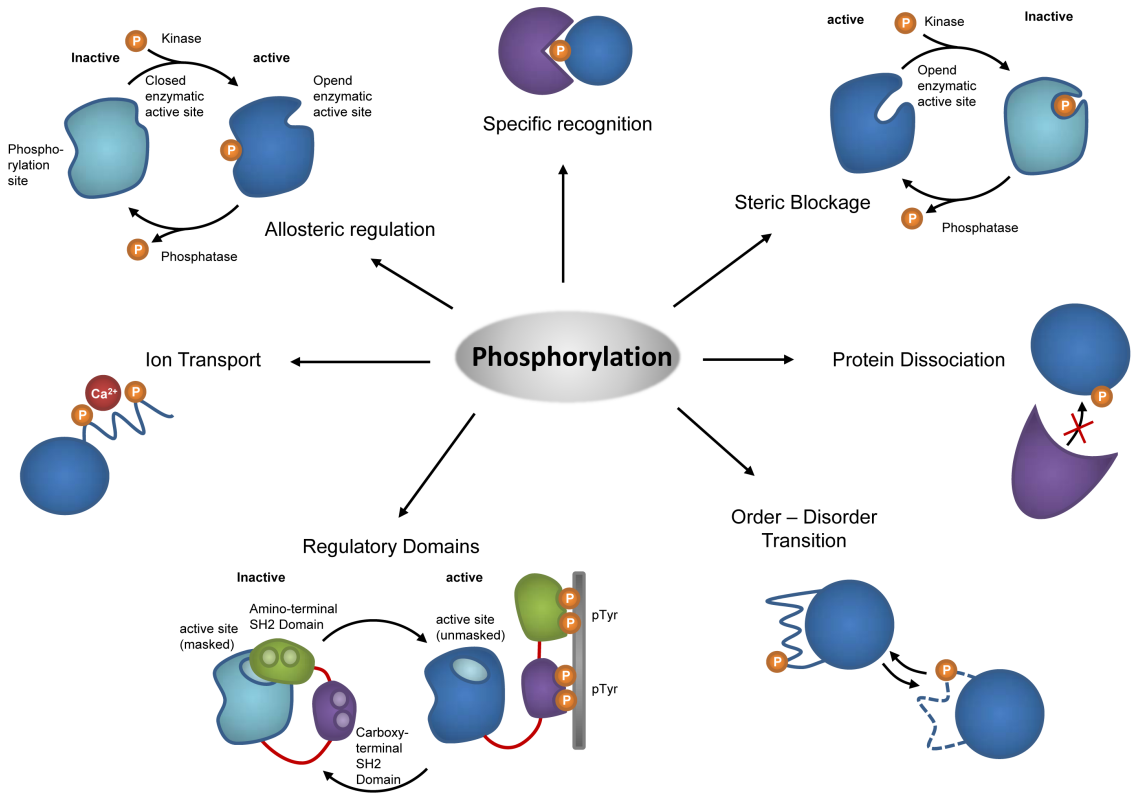

Figure 4.3.1 Phosphorylation affects the function of proteins. The addition of a negative charge by the attachment of a phosphoryl group to a protein can influence the function of a protein in different ways: Phosphorylation can lead to allosteric regulation of an enzyme, influence the recognizability by another protein, lead to steric blockage of an enzymatic active site, promote protein-protein dissociation, promote order - disorder transition, activate enzymes by phosphorylation of regulatory domains, and facilitate ion transport.

on 14-3-3 proteins that recognize phosphoserine or phosphothreonine. The Polo-like kinase is targeted to its substrate by a similar mechanism, where a phosphoserine on the target protein is recognized by the Polo-box domain of the Polo-like kinase[161]. Phosphorylation can thus promote conformational changes leading to protein association as well as protein dissociation. In addition, order to disorder transition, as well as disorder to order transition of proteins can be mediated by phosphorylation. An overview of the structural consequences of protein phosphorylation is depicted in figure 4.3.1.

4.3.3 Kinases and phosphatases

By transferring the γ-phosphate group of ATP to specific amino acids in proteins, protein kinases, collectively referred as kinome, act as key regulators of diverse cellular functions and are involved in different diseases including cancer. Thus, kinases are attractive drug

targets and many different inhibitors exist[161]. Kinases are one of the largest protein families of genes, corresponding to 2% of the genome in eukaryotes[169]. There are more than 500 different human protein kinases, grouped into different families, of which an overview is provided in table 4.1 and table 4.2[169]. All eukaryotic protein kinases (EPK) are structurally related and harbor a catalytic domain consisting of approximately 200-300 residues which can further be divided into subdomains[101][60]. A structural feature shared by all EPK is the designated protein kinase fold. The catalytic domain of kinases consist of two lobes where the typically small N-terminal lobe of β-sheets is responsible for binding and orientation of ATP and the typically large C-terminal lobe consisting of α-helices is required for substrate binding and initiation of the phosphoryl transfer. It is noteworthy, that the residues directly involved in catalysis are always entirely conserved[60]. ATP binds in the cleft between the two lobes, keeping the adenosine part in a hydrophobic pocket and the phosphate backbone oriented outwards. The substrate will then bind along the cleft and the transfer of the terminal γ-phosphate of ATP to the hydroxyl oxygen of serine, threonine or tyrosine, is catalyzed by different conserved residues of the kinase catalytic domain[277].

Although all classical kinases share a common fold domain, there is specificity of different kinases towards their substrates. Substrate specificity is of great importance, as there are approximately 700'000 potential phosphorylation sites within a cell and around 30% of all proteins become at least once phosphorylated at some point in their existence[277]. There are different strategies used to ensure substrate specificity, starting with the structure of the catalytic cleft. Although sharing the same catalytic domain structures, the catalytic cleft of the two main kinase groups, Ser/Thr and Tyr kinases is slightly different[277][7]. Tyr kinases have a deeper catalytic cleft, allowing the larger Tyr residues to span the distance between the peptide backbone and the γ-phosphate of ATP, whereas the smaller side chains of Ser and Thr cannot[277]. However, the specificity mediated by the depth of the cleft is not absolute as Ser/thr kinases sometimes can phosphorylate tyrosine residues, whereas the converse is less common.

The next layer of specificity is imparted by specific substrate consensus sequences typically consisting of four amino acids on either side of the phosphorylated residue, significantly contributing to the specificity of kinase-substrate recognition[277]. Consensus sequences for many kinases have been experimentally elucidated and allow the prediction of new potential kinase substrates based on their homology to known consensus motifs[154]. Nevertheless, the presence of a consensus sequence must not strictly be present to relate to a certain kinase, as *in vivo* phosphorylation sites have been found to not match the consensus[278].

A second layer of substrate specificity is given by the interaction between docking motifs on the kinase and the substrate thereby increasing their affinity. These include specific

binding sites on MAPK substrates as well as SH2 domains on non-receptor tyrosine kinases. It is assumed that these docking motifs enhance specificity by increasing the local concentration of the substrate around the kinase[277]. Besides kinase-substrate docking domains also binding partners exist, that target the kinase to specific substrates. This may allow a single kinase to interact with different substrates in different contexts. Furthermore, kinases can be recruited to their substrates that have been primed by previous phosphorylation via another kinase. And eventually, the subcellular localization of a kinase is crucial for specificity, by spatially limiting the number of potential substrates.

While a lot is known about kinases less knowledge exits about phosphatases. There are three different classes of phosphatases, consisting of Ser/Thr phosphatases (∼40), Tyr phosphatases (∼100) and dual specific phosphatases (∼50). Although there are around 400 Ser/Thr protein kinases, only approximately 40 Ser/Thr phosphatases are described which raises the question about their specificity. It is assumed that phosphatase specificity is mainly achieved through the association of phosphatase catalytic domains with regulatory subunits that target the catalytic domain to substrates[214]. Tyrosine kinases and phosphatases are approximately equal in number and it appears that Tyr phosphatases also tend to be modular proteins consisting of catalytic and targeting domains including SH2, as Tyr kinases[277].

4.4 Phosphoproteomics

Different methods can be used when assessing phosphorylation, based on the question being asked and the resources available. Kinase activity for instance, which is an important parameter in signaling, can be estimated by an *in vitro* kinase assay, where a purified or immunoprecipitated kinase is incubated with an exogenous substrate in the presence of ATP. Although this technique provides information about the enzymatic activity and kinetics of a certain kinase towards a substrate, such an assay cannot reflect the signaling landscape of a kinase nor can it reveal the identity of previously unknown targets. In addition, *in vitro* kinase activity does not necessarily reflect an *in vivo* situation with endogenous protein levels and the presence of phosphatases and counteracting phosphorylation events. Thus, direct detection of protein phosphorylation can provide further information about the cellular response towards a certain stimuli. A classical method for detection of phosphorylation is radiolabeling. Whole cells become incubated with ^{32}P-orthophosphate and the corresponding protein extracts are subsequently separated by SDS page and exposed to films[152] [277]. As more direct method, in 1981, the first documented phospho-specific antibody was developed by immunizing rabbits with benzonyl phosphonate conjugated to keyhole limpet hemocyanin (KLH). The antibody could broadly recognize tyrosine phosphorylated proteins[234]. Ten years later, phospho-specific antibodies were developed

Table 4.1 Conventional eukaryotic protein kinase classification

Conventional eukaryotic protein kinases		
Group	Definition	Examples
AGC	The name of the AGC kinases is derived from the member as follows: cyclic nucleotide-dependent family (PKA/cAPK and PKG), the "PKC" family, PKB/AKT/RAC-alpha PSTK, βARK, the ribosomal S6 kinase family, and other close relatives. These kinases have a strong preference for phosphorylation of Ser/Thr residues that are located in a consensus sequence containing the basic amino acids Lys and Arg [210].	AKT (PKB), PKC, PKG, S6K, RSK, MSK, PDK1 and GRK
CamK	The members of the CaMK group are Ser/Thr kinases taking their name from Ca^{2+}/calmodulin-regulated kinases and structurally related families including CaMK and SNF1/AMP-activated PKs. Most of the members of this group exhibit activation by the binding of Ca^{2+} or calmodulin to a small C-terminal domain in close proximity to the catalytic core. These kinases tend to be directed towards substrates containing basic residues.	CaMK, CaMK-like, CDPK, MAPK-associated PK, MLCK, TRIBBLES, KIN1/SNF1/Nim1, and AMPK, EF2K, PhK
GMGC	This group is named after the member families (cyclin-dependent kinase (CDK), mitogenactivated protein kinase (MAPK), glycogen synthase kinase (GSK), CDC-like kinase (CLK)) group of protein kinases). The CMGC kinases are an essential and typically large group of kinases found in all eukaryotes [281]	Cdk1, MAPK,GSK-3, CLK/CKL, CK2a, SRPK, DYRK
CK1	The protein kinase CK1 (formerly called Casein Kinase 1) CK1 is a family of monomeric serine/threonine (Ser/Thr)-selective protein kinases. CK1 is evolutionary conserved in eukaryotes and regulates diverse cellular processes. Including, Wnt signaling, membrane trafficking, cytoskeleton maintenance, DNA replication, DNA damage response, RNA metabolism and parasitic infections. [40]	CK1, Tau tubulin kinase
RGC	The members of the small group of receptor guanylate cyclases (RGCs) are similar in sequence to the metazoan Tyr kinases which are lacking in plants, fungi, and protists. Their properties are distinct from other known EPKs; the RGC kinase domain appear to be all but catalytically inactive. It is thought that this group evolved late in the expansion of the EPK superfamily.	Photoreceptor membrane guanylate cyclase
STE	The STE group includes homologs of the *S. cerevisiae* sterile kinases sterile 7, sterile 11, and sterile 20. This group contains the MAPK cascade kinases, in which a MAPK is phosphorylated and activated by a MAP2K, which itself is activated by a MAP3K. The family of Raf-related MAP4K is structurally distinct from the Ste20 family, and belongs to the TKL group. [130]	Ste7-like (MAP2K, NIMA/NEK and NEK-like), Ste11-like (MAP3K, Cdc7), Ste20-like (MAP4K)
TK	The Tyr kinase (TK) group contains conventional phosphotyrosine kinases (PTKs). The active members specifically phosphorylate tyrosine residues of proteins, are distinct from DSKs which also phosphorylate Ser/Thr and are scattered within other kinase groups. TKs are found in metazoans and play important roles in intracellular signaling cascades. Two classes of PTKs are present in cells: the transmembrane receptor PTKs and the cytoplasmic PTKs. [21]	EGFR, Jak, VEGFR, Src, LRR-TK, Abelson kinase (c-Abl), LCK
TKL	The Tyr kinase-like (TKL) group is the most diverse of all groups, is closely related to TKs, and is integrated within important signaling pathways. However, TKLs are in fact serine/threonine protein kinases and present in metazoans and plants but virtually absent from fungi. TKLs represent the largest group of EPKs in land plants, where they often constitute up to 80% of the kinome	LRR kinases, MLKs, TGFBR1, Raf, IRAK, RLK/PELLE family (RTK-like, Pti1-like, WAK-like)

Table 4.2 Atypical eukaryotic protein kinase classification

Atypical eukaryotic protein kinases		
Group	Definition	Examples
Alpha	The Alpha group of kinases is a small and only recently discovered group of atypical EPKs (APKs). In mammals, channel-kinases are members of Alpha APKs. Alpha kinases contain both a fold similar to EPKs and key amino acid residues known to be important for catalysis from EPKs	EEF2K, Dictyostelium MHCK, two channel-kinases, TRPMs ion channel-kinases
PIKK	The members of the small phosphatidyl inositol 3 kinase- related kinase (PIKK) family are involved in signaling of DNA damage, apoptosis/ survival and cell growth. PIKK kinases have a high molecular weight and in mammals. [49]	PIKK, ATM, ATR, mTOR, DNA-PK, SMG-1
PDHK	The pyruvate dehydrogenase kinases (PDHKs) are a small and ubiquitous group of APKs; five members were identified in humans. PDHKs phosphorylate a subunit of the pyruvate dehydrogenase multienzyme complex and thus plays an important role in oxidative metabolism, i.e. in controlling glucose and lipid oxidation	PDHK, PKAK1
RIO	The RIO ("right open reading frame") group is named after the divergently transcribed founding member which was one of the two adjacent genes. RIO is a small group of essential eukaryotic APKs. They share the overall EPK fold, however, distinct substrate-binding domains were not yet discovered and the mode of ATP-binding also seems to be different from other kinases. Some RIO kinases autophosphorylate [151]	Rio1-family and Rio2
Others	This group contains several kinases and families that do not fit within any of the other main kinase groups	Wee1, Myt1/Mik1, Caks, CAKAK, Aurora, Mos, CaMKK, NIMA/NEK, TOUSLED, PPK1

by immunizing rabbits with synthetic phosphopeptides covering amino acid sequence of a certain protein, sourrounding the phosphosite of interest [59]. The availability of phospho-specific antibodies opened a new avenue in the phosphoproteomic field as it can be applied to different immunoassay techniques as western blot, immunofluorescence, flow cytometry or ELISA. As it will be exemplified in section 4.4.1 phosphoresidue-specific antibodies can also be used for phosphopeptide enrichment prior to identification and quantitation using mass spectrometry. Although phospho-specific antibodies are widely used in different techniques, a caveat is still the availability as well as the specificity and sensitivity of antibodies towards a certain phosphosite on a phosphoprotein of interest. For large-scale studies aiming for the identification of phosphorylation events in response to a certain stimuli the use of phospho-specific antibodies can be a limiting factor, as it couples the identification of phosphosite to previous knowledge, preventing the identification of new substrates.

As an alternative, an emerging approach for large scale phosphoproteomics is based on the selective enrichment of phosphopeptides followed by liquid chromatography tandem mass spectrometry (LC-MS/MS) for quantitation and identification. An overview of LC-MS/MS based proteomics is provided in figure(4.4.2). This approach allowed for example the identification of hundreds of phosphorylation events upon EGF stimulation of

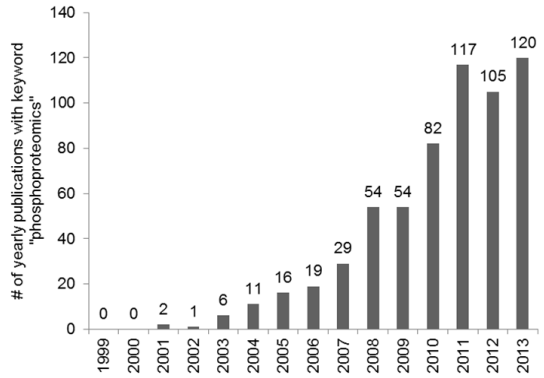

Figure 4.4.1 Increase in the application of phosphoproteomics within the last decade. The pubmed database was searched for publications assigned with the keyword "phosphoproteomic". The number of publications found was plotted against the year of publication.

HeLa cells as described by Olsen et al.[203]. The development of quantitative phosphoproteomics not only allows the identification and cataloging of phosphorylation sites but also provides valuable information about the stoichiometry of phosphorylation between different cellular states and ultimate in health and disease. Quantitative phosphoproteomic is a tool of interest for basic research but can also be used in translational biology and diagnostics[160]. Thus, it is not surprising that the field of phosphoproteomics is emerging as indicated in figure 4.4.1. According to the pubmed database the first publication with the keyword "phosphoproteomics" has been published in the year 2001. Since 2011 there are more than 100 articles annually published.

A typical phosphoproteomic workflow consists of several steps starting with cell harvesting and lysis. If desired the lysate can be fractionated to study different cellular compartments individually. Proteins from the lysates are subsequently digested. Trypsin is commonly used to digest protein extracts, often in combination with alternate enzymes (e.g. Lys-C, Asp-N, Glu-C, chymotryppsin) for an improved sequence coverage and phosphosite mapping[289] [24]. Phosphopeptides are usually present in low proportion compared to non-phosphorylated peptides and the number of phosphorylation sites can be very dynamic on a wide range of expressed proteins. Thus phosphopeptides have to become enriched to enhance their relative abundance to a level detectable by mass spectrometry. Common phosphopeptide enrichment methods will be explained in section 4.4.1. The phosphopeptides can be further fractionated to reduce sample complexity as described in section 4.4.2 followed by analysis with LC-MS/MS. A brief overview about quantification strategies of phosphopeptides is provided in section 4.4.3.

4.4.1 Phosphopeptide enrichment methods

4.4.1.1 IMAC and MOAC

The most common materials for phosphopeptide enrichement are immobilized IMAC and MOAC. IMAC was initially developed to affinity purify proteins based on the interac-

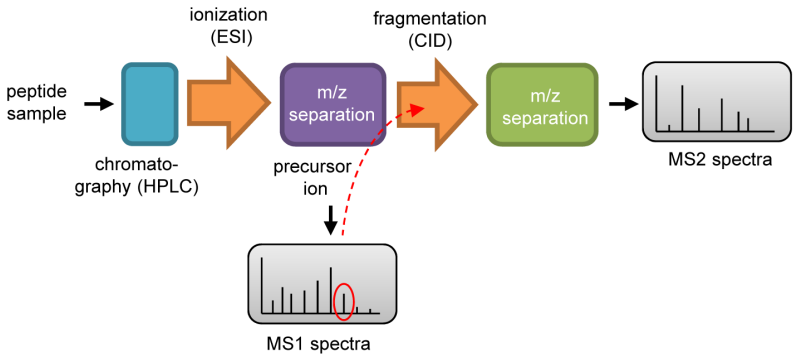

Figure 4.4.2 Principle of tandem mass spectrometry. Mass-spectrometry has become the method of choice for the analysis of complex protein samples and is thus also applied to phosphoproteomics. A mass spectrometer consist of an ion source, a mass analyzer that measures the mass to charge ratio (m/z) of the ionized analytes and a detector that registers the number of ions on each m/z value. In LC-MS/MS, peptides are usually separated by high-pressure liquid chromatography (HPLC) and eluted into an electrospray ion source that generates small charged droplets. A spectrum of the eluted protonated peptides at this time-point is generated by the mass analyser (MS1). Selected peptides are then fragmented by collision with gas (CID) and an MS2 or MS/MS spectrum is obtained from the fragments. In addition to the peptide mass, the peak pattern of the MS/MS spectra provides information about peptide sequence. These spectra are scanned against comprehensive protein sequence databases by the use of different algorithms. By the combination of such an obtained amino acid sequence together with the mass information, the originated peptide can be identified [3].

tion of histidine and cysteine towards the IMAC resin. However the finding that metal ions bind phosphorylated proteins or phosphoaminoacids opened a new avenue of application [8]. Subsequently the technique was expanded to enrich for phosphopeptides derived from proteolytic digested proteins [189]. IMAC is one of the most extensively used enrichment methods and represented a big step towards sensitive and selective enrichment of phosphopeptides [76] [191]. The method makes use of the affinity of negative charged phosphate groups towards metal ions like Fe^{3+} (iron) or Ga^{3+} (gallium) [83] (Figure 4.4.3 A). These ions can become chelated on beads to facilitate the enrichment procedure. IMAC has been successfully used in many large scale phosphoproteomic studies allowing detection of more than 10'000 phosphopeptides [148]. However this approach requires significant amount of protein as starting material [269]. Another drawback of IMAC is its additional affinity for carboxyl groups, resulting in co-purification of acidic peptides beside phosphopeptides. Modifications of the pH and ionic strength of solvents can be used to control the specificity of binding and elution [19]. An alternative to IMAC is MOAC which is based on the affinity of phosphate groups for metal oxides (Figure 4.4.3 B). The most frequently used metal oxide is titanium dioxide (TiO_2). IMAC using Fe^{3+} or Ga^{2+} was

shown to be less selective in the enrichment for phosphopeptides than MOAC using TiO_2, while IMAC allowed the identification of more multiple phosphorylated peptides [10] [153]. A further advantage of TiO_2 chromatography over IMAC is that it is less sensitive towards the presence of salt and detergents and it does not compete with nucleic acids for binding with the material [158]. The advantages of applying MOAC seem to outweigh IMAC but it is important to note that the two methods should rather be considered to be complementary than competitive. Bodenmiller and colleagues demonstrated by comparing various methods of phosphopeptide enrichment, including IMAC and MOAC, that the different methods yielded in different distinct datasets with an overlap of only around 30% [27]. This indicates that phosphoproteomic coverage can only be improved by using different enrichment strategies in parallel, although such an approach would be expensive and laborious.

4.4.1.2 Antibody based phosphopeptide enrichment

Antibody based affinity purification is based on selective enrichment for phosphorylated residues of proteins or peptides that are recognized by the antibodies. Thus, it is in the nature of the method that this approach is limited by the specificity of the available antibodies. In use are antibodies that are supposed to recognize a specific phosphorylated residue like phospho-serine (pS), phospho-threonine (pT) or phospho-tyrosine (pY) (Figure 4.4.3 C). The success of applying pS and pT antibodies for phosphoproteomics is limited. In 2002 Gronbor and colleagues were only able to identify seven phosphoproteins using a pS and pT antibody based enrichment method which is far from opening an avenue as general approach to study the phosphoproteome [94]. The usage of pY antibody based phosphoprotein or phosphopeptide enrichment is more frequently used and more successful. This is also due to the fact that tyrosine phosphorylations is least abundant (1.8%) compared to threonine (11.8%) and serine (86.4%) phosphorylation, as investigated in HeLa cells stimulated with EGF [203]. Non residue specific enrichment methods like IMAC or MOAC typically result in a low yield of tyrosine phosphorylated peptides compared to serine and threonine which makes an approach that selectively enriches for pY very attractive. Due to the chemical properties of tyrosine which harbors an electron rich aromatic ring, pY has more opportunities to form bonds with the antibody binding pocket than the aliphatic side chains of pS and pT which results in a stronger and more specific binding [19]. Many studies made successfully use of this method for example Krüger and colleagues investigated in 2008 the tyrosine phosphoproteome of the insulin pathway by the use of pY immunoprecipitation [145]. Another antibody based purification method represents the usage of phosphomotif specific antibodies (Figure 4.4.3 D). The concept is based on the fundamental observation, that different kinases phosphorylate their substrates on specific conserved phosphorylation motifs [154]. Kosako and colleagues intended to identify novel

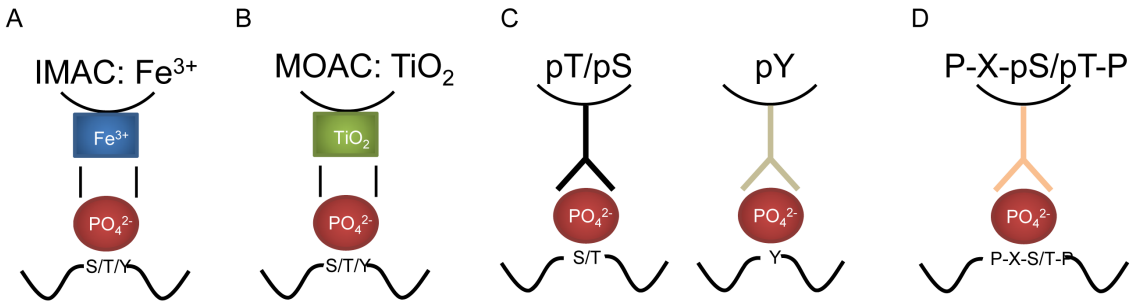

Figure 4.4.3 Principles of commonly used phosphopeptide enrichment methods. A) IMAC using Fe^{3+} B) MOAC using TiO_2 C) phosphoresidue-specific antibodies D) phosphomotif-specific antibodies (ERK) *Adapted with modifications from Beltran et al.*[19]

ERK substrates using ERK phospho-motif specific antibodies[141]. ERK is known to preferentially phosphorylate its substrates on the consensus amino acid sequence (P)-X-S/T-P where the first proline is optional, X represents any amino acid and the serine or threonine becomes phosphorylated[91]. Antibodies raised against this sequence allow the purification of potential ERK substrates. Out of 24 new candidate ERK targets, 13 were found to be *in vitro* ERK substrates and follow-up experiments revealed Nup50 as a bona fide ERK substrate[141]. Nowadays several phosphomotif specific antibodies are commercially available as for example for substrates of AKT, PKA, PKC and ATM/ataxia telangiectasia and Rad3 related protein (ATR). The latest for example, has already been used in a phosphoproteomic study for identification of novel ATM/ATR substrates[183]. Thus phospho-motif specific antibodies are a promising tool for the detection of novel kinase substrates by phosphoproteomics, although it had to be kept in mind that the specificity of a kinase to a consensus motif is not absolute.

4.4.2 Prefractionation methods

The complexity of a sample can limit the proteomic coverage, even considering the improvement in speed and sensitivity of tandem mass spectrometry as well as performance of liquid chromataography. Therefore, it can be beneficial to reduce the complexity of the sample by prefractionation, splitting the samples into several fractions, each with a decreased complexity prior to mass spectrometry. This approach implies the use of a significant amount of starting material, it increases the number of samples and consequently the following working procedures as well as the time needed for measurements by mass spectrometry[178]. A frequently applied method is strong cation exchange (SCX) where tryptic digested peptides are separated with respect to their charge[63]. Alternatively, isoelectric focusing (IEF) can be applied to separate peptides according to their isolectric point (pI)[168]. A separation based on the molecular weight of the proteins can be achieved

by SDS-PAGE and in-gel digestion. If a broad coverage of the proteome is of high importance, multiple prefractionation approaches must be taken into consideration [168].

4.4.3 Quantification strategies

Mass spectrometry does not only provide information about the identity of peptides but also about the relative abundance among different biological samples. SILAC, iTRAQ and label-free quantification are commonly used strategies for relative peptide quantification.

The principle of stable isotope labeling in cell culture (SILAC) relies on the introduction of heavy stable isotopes as ^{2}H, ^{13}C, ^{15}N or ^{18}O to the proteins of a sample (Figure 4.4.4). This is achieved by growing cell populations used for comparison in media containing light and heavy isotopically labeled amino acids (typically Lysine and/or Arginine). After full incorporation, the samples derived from differentially labeled cells can be distinguished based on a mass shift of the peptide isotopes [66]. The differences of the MS1 signal intensities among these peptide ion pairs can be measured in the mass spectrometer and reflect relative protein abundances. A different approach is the isobaric *in vitro* labeling method using isobaric tags for relative and absolute quantitation (iTRAQ) (Figure 4.4.4). The initial used iTRAQ reagent allows parallel quantification of up to 4 samples, whereas recently developed 8-plex iTRAQ reagent allows parallel comparison of up to eight different samples. iTRAQ labeled identical peptides from different sample cannot be distinguished on the MS1 precursor level. However, fragmentation of the labeled peptides generates different reporter ions allowing quantification of the sample on MS/MS level [68]. Beside the use of common labeling techniques for quantitative proteomics, as exemplified by SILAC and iTRAQ, there is an increasing application of label-free quantification strategies [68]. As already implicated in the name, there is no requirement for protein or peptide labeling (Figure 4.4.4). The method makes use of the high resolution power and increase in mass accuracy of modern MS instrumentation. Label-free quantitative mass spectrometry is based on the observation of a correlation between abundance of proteins and the chromatographic peak area of a corresponding peptide as well as between the number of spectra and the abundance of MS/MS spectra and the protein amount [188]. Based on these observations two different label-free techniques emerged for protein quantification: area under the curve (AUC) measurement and spectral counting. AUC is based on the integrated measurement of chromatographic peak areas that arise over time for any given peptide at the MS1 level in LC-MS runs. The AUC measurement is linearly proportional to the concentration of the measured peptide. Ionised peptides elute from the reversed-phase column into the mass spectrometer and the ion intensities are subsequently measured and together with the retention time information leading to an intensity peak whose area correlates with peptide concentration. Subsequent MS/MS scans will then confirm the identity of these peptides [188]. Spectral counting is based on the observation

that more abundant peptides will produce more MS/MS spectra and is therefore proportional to the corresponding protein amount [188]. Although labeling techniques are often used for quantitative proteomics, for different reasons a label-free approach can be more appropriate compared to conventional label techniques. First, it overcomes the limitation of sample number than can be analyzed in a single experiment which is currently restricted to 2 or 3 for SILAC and up to 8 for iTRAQ. Because there is no need for distinguishable labels, the sample number for a label-free approach is theoretically not restricted. A further advantage of a label-free approach is its relative reasonable price compared to more expensive labeling techniques. A disadvantage of label-free proteomics is the parallel workflow of the samples. SILAC samples can be mixed even prior to digestion, and all subsequent working steps are thus applied similarly to all conditions, leading to very low introduction of variation during the workflow. Because proteins are not labeled in the label-free approach and samples can thus not be distinguished, all samples have to be treated in parallel within the whole workflow. This may introduce more variation as different samples may be treated slightly different. Nevertheless, it is generally accepted that label-free quantification can accurately estimate protein abundance and can provide larger dynamic range of quantification than labeling techniques [188]. It is therefore not surprising that label-free proteomics is emerging and now the most published approach for quantitative proteomics [68].

4.4.4 Phosphoproteomics in the field of infection biology

Host cell phosphorylation events upon infection with pathogens have been studied for decades and many signaling cascades involving pathogen triggered phosphorylations have been described. This was mainly achieved by targeted approaches incidentally leading to the discovery of pathogen triggered phosphorylation events. However, also explorative approaches with the direct goal for the systematic identification of host protein phosphorylations were undertaken. The examples shown in this section, represent the evolutionary improvement of methods applied as well as the diversity of host-pathogen interactions studied by phosphoproteomics, including plants and mammalian cells as host as well as bacteria, viruses and protozoa as pathogens. In 2001, Peck and colleagues conducted an Arabidopsis "phosphoprotein proteome" in response to treatment with flagellin 22 peptide (flg22), mimicking pathogenic exposure [211]. Untreated or flg22 treated Arabidopsis cells were incorporated with ^{32}P- or ^{33}P-ortho-phosphate and solubilized proteins were visualized by 2D gel electrophoresis. Gel fragments were subsequently subjected to nanoESI-MS-MS revealing the protein AtPhos43 to become phosphorylated after flaggelin exposure. Although the 2D-gels provide an overview of spots representing proteins that are differentially phosphorylated upon treatment, the lack of information about the identity of the proteins and phosphorylation sites is clearly preventing a thorough perception

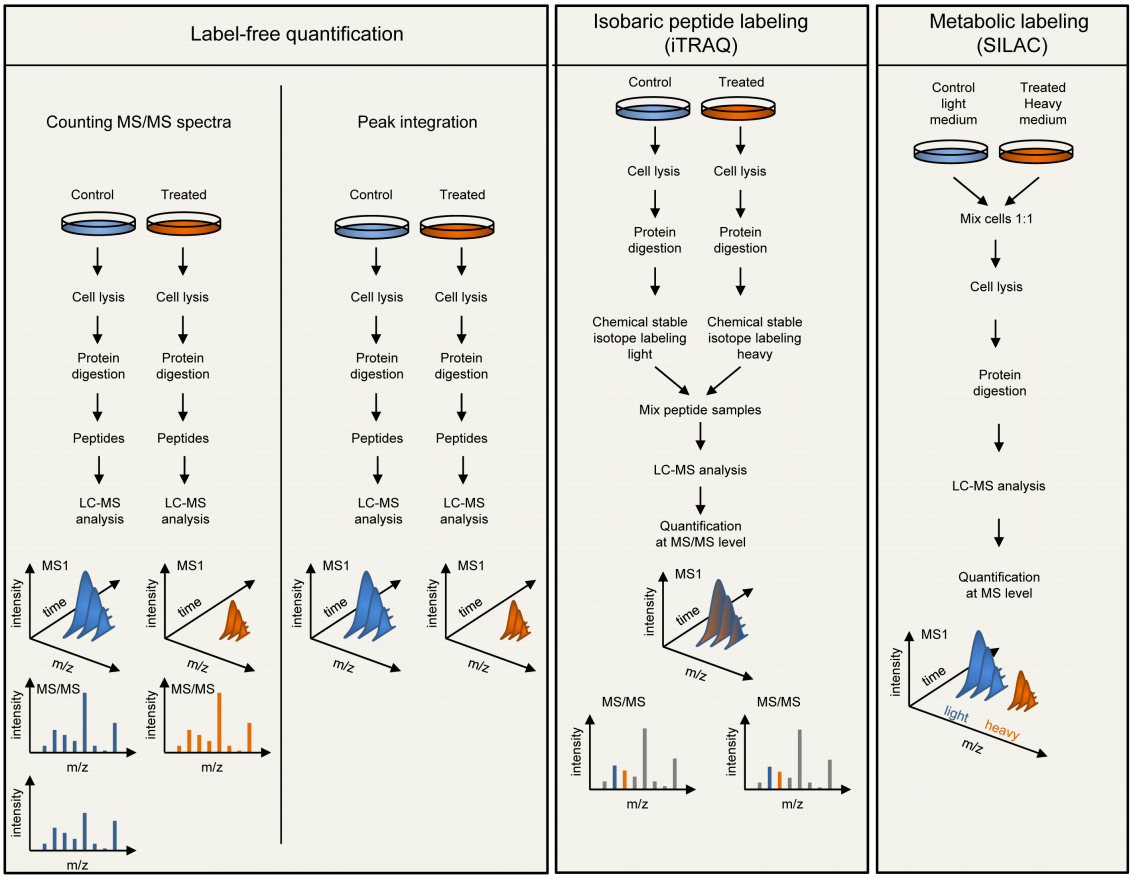

Figure 4.4.4 Three commonly used peptide quantification strategies. *Adapted with modifications from Käll and Vitek 2011*[138]

of the phosphoproteome. An approach that allows the systematic identification of phosphorylations is the usage of phospho-specific antibody arrays. This approach was used in 2003 to address host phosphorylations upon mycobacterial infection[109]. Several host proteins were identified to become phosphorylated upon infection, as JNK or Glycogen synthase kinase 3 alpha. Also the effect of *Salmonella* on host cell internalization has been addressed by the use of protein arrays. Lysates after different time-points of infection with wild-type *Salmonella Typhimurium* as well as several mutants were subjected to reverse-phase protein arrays mounted with phospho-specific antibodies[176].

First studies applying quantitative mass spectrometry based phosphoproteomics for the detection of host phosphorylation events upon pathogenic infection were published in the year 2009 and broad application of this technique is currently emerging indicated by a high number of publications in the year 2013. The first large-scale phosphoproteomic approach upon pathogenic infection was performed by Rogers and colleagues in 2011, leading to the identification of almost 2'000 different phosphoproteins[229]. They compared uninfected

cells and cells infected with *Salmonella Typhimurium* at different timepoints of infection up to twenty minutes and identified the kinases AKT, PKC, and PIM to play a role in the infection process. In addition, they investigated the role of the *Salmonella Typhimurium* effector protein SopB and showed that this effector is responsible for almost half of the observed phosphorylation events. In 2013, a complementary study was published, examining the effect of *Salmonella* Pathogenicity island 2 secreted effectors on the host phosphoproteome[117]. In contrast to *S. flexneri* which harbors only the mxi-spa TTSS, *Salmonella enterica* employs two distinct TTSS ecoded in *Salmonella* pathogenicity island 1 (SPI1) and *Salmonella* pathogenicity island 2 (SPI2). Whereas the SPI1 secreted effector proteins are required for bacterial internalization, SPI2 effectors play an important role at later stages of infection, ensuring successful intracellular replication[85]. There are about 30 different effector proteins secreted by the SPI2 TTSS. However, the function for most of them are still poorly understood[85]. Imami and colleagues addressed these open questions by measuring the global impact of SPI2 effectors on the host phosphoproteome of RAW264.7 and HeLa cells. They revealed that SPI2 effectors interfere with several cellular processes like trafficking, cytoskeletal regulations and immune signaling, which so far have not been attributed to *Salmonella* infection. In addition, HSP27 was identified as a new direct target of the SPI2 effector and kinase SteC that mediates actin manipulations through HSP27[117]. Beside bacterial pathogens, also viral infection has been subject of phosphoproteomic studies. As an example serves a study from 2013 that investigated the phosphorylation response of $CD4^+$ cells after infection with HIV-1. Already one minute after $CD4^+$ cell exposure to HIV-1, the phosphorylation state of 175 proteins changed significantly. These comprised proteins from pathways already known to become activated upon HIV-receptor binding but also previously unidentified host factors. To examine whether the HIV responsive phosphorylations regulate the HIV infection levels, a siRNA screen depleting 69 of these phosphoproteins in MAGI cells was performed. The siRNA screen revealed that SRRM2 suppression increases HIV-dependent gene expression. SRRM2 encodes the splicing factor SRm300 and through further mechanistic studies on this factor it was suggested that HIV-1 manipulates alternative splicing to facilitate viral replication and release[123]. This work demonstrates that coupling of phosphoproteomics to perturbation assays like RNAi, can serve as powerful approach to unravel mechanistic aspects of host-pathogen interactions and may allow the linkage of phosphoproteins to a certain cellular phenotype.

5 Aim of the thesis

Upon infection of host cells with *S. flexneri* a lot of signaling cascades become modified in favor of the invasion process. Thus, the main objective of the presented work was to investigate signaling events that take place during *S. flexneri* infection of epithelial cells. Phosphorylation as one of the most widespread post-translational modifications with a major role in signal transduction, was aimed to study in a systematic and comprehensive way. To this end we employed an LC-MS/MS approach for the identification and quantification of phosphopeptides generated from an *in vitro* model of infected HeLa cells. To capture as many aspects of the host-pathogen interaction as possible, our purpose was to cover several time intervals ranging from 15 to 120 minutes post-infection. Our laboratory has previously shown that the effector protein OspF does not only repress phosphorylation of the MAPKs p38 and ERK and some downstream targets, but is also able to promote additional phosphorylation events by a negative feedback loop. We hypothesized that OspF may have a broader impact on the phosphorylation network of the cell than previously reported and therefore our goal was to conduct an OspF dependent phosphoproteome analysis by comparing cells infected with wild type *S. flexneri* to cells exposed to an *ospF* deletion mutant. In a second project our objective was to unravel the activation mechanism of mTOR and AKT that were found to become activated during *S. flexneri* infection. We used a novel *Yersinia enterocolitica* derived TTSS dependent protein translocation tool to directly inject the *S. flexneri* effector protein IpgD into HeLa cells and to study its impact on mTOR and subsequent AKT activation. By the use of different kinase inhibitors we aimed to find or exclude kinases important for mTOR/AKT activation.

Chapter II

Systems-level overview of host protein phosphorylation during *Shigella flexneri* infection revealed by phosphoproteomics.

1 Summary

The enteroinvasive bacterium *Shigella flexneri* injects several effector proteins to promote its uptake and the subsequent manipulation of host signaling pathways in favor of the bacteria. To systematically address the dynamics of signaling cascades triggered by bacterial invasion, we studied host cell phosphorylation using liquid chromatography coupled to tandem mass spectrometry (LC-MS/MS). We could identify several hundreds of proteins becoming differentially phosphorylated during the first two hours of infection. the temporal dynamics of phosphorylation was addressed by fuzzy c-means clustering, revealing six distinct patterns of phosphorylations. We could approve that one cluster, related to genotoxic stress, is mainly regulated by the kinase ATM. A search for activated signaling pathways revealed mTOR as the most overrepresented pathway. Whe demonstrated that during *S. flexneri* infection, mTORC1 and mTORC2 are required for the phosphorylation of the substrates S6K and AKT, respectively. In addition, a comparison to a recently published phosphoproteomic dataset of *Salmonella typhimurium* infection of epithelial cells revealed a large cluster of co-regulated phosphoproteins. Eventually, the impact of the *S. flexneri* effector OspF an the host signaling network was determined by the use of phosphoproteomics. OspF was shown to affect the phosphorylation state of several hundred proteins, demonstrating the wide-reaching impact a single bacterial effector can have on a host cell.

2 Statement of contribution

I conducted most of the experiments mentioned in the paper. Including sample preparation and phosphopeptide enrichment of the different phosphoroteomic experiments as well as the additional experiments. I performed different bioinformatic analysis in collaboration with Erik Ahrné. Christoph A. Kasper performed quantitative image analysis. Therese Tschon, Isabel Sorg and Roland F. Dreier contributed to the infection assays and sample preparation for several phosphoproteomic experiments. Alexander Schmidt performed the LC-MS/MS measurements and quantifications together with Erik Ahrné. Biological interpretation of the phosphoproteomic data as well as manuscript preparation was done by Cécile Arrieumerlou and myself.

This chapter has been published as:

Schmutz C, Erik A, Kasper CA, Tschon T, Sorg I, Dreier RF, Schmidt A, Arrieumerlou C. Systems-Level Overview of Host Protein Phosphorylation During *Shigella flexneri* Infection Revealed by Phosphoproteomics. *Molecular & Cellular Proteomics*, 12(10):2952-68, 2013.

Research

This paper is available on line at http://www.mcponline.org

Systems-Level Overview of Host Protein Phosphorylation During *Shigella flexneri* Infection Revealed by Phosphoproteomics*[S]

Christoph Schmutz‡, Erik Ahrné‡, Christoph A. Kasper‡, Therese Tschon‡, Isabel Sorg‡, Roland F. Dreier‡, Alexander Schmidt‡, and Cécile Arrieumerlou‡§

The enteroinvasive bacterium *Shigella flexneri* invades the intestinal epithelium of humans. During infection, several injected effector proteins promote bacterial internalization, and interfere with multiple host cell responses. To obtain a systems-level overview of host signaling during infection, we analyzed the global dynamics of protein phosphorylation by liquid chromatography-tandem MS and identified several hundred of proteins undergoing a phosphorylation change during the first hours of infection. Functional bioinformatic analysis revealed that they were mostly related to the cytoskeleton, transcription, signal transduction, and cell cycle. Fuzzy c-means clustering identified six temporal profiles of phosphorylation and a functional module composed of ATM-phosphorylated proteins related to genotoxic stress. Pathway enrichment analysis defined mTOR as the most overrepresented pathway. We showed that mTOR complex 1 and 2 were required for S6 kinase and AKT activation, respectively. Comparison with a published phosphoproteome of *Salmonella typhimurium*-infected cells revealed a large subset of coregulated phosphoproteins. Finally, we showed that *S. flexneri* effector OspF affected the phosphorylation of several hundred proteins, thereby demonstrating the wide-reaching impact of a single bacterial effector on the host signaling network. ***Molecular & Cellular Proteomics 12: 10.1074/mcp.M113.029918, 2952–2968, 2013.***

The enteroinvasive bacterium *Shigella flexneri* invades the intestinal epithelium of humans, causing an acute mucosal inflammation called shigellosis or bacillary dysentery that is responsible for 1.1 million deaths annually (1). During the infectious process, bacteria use a sophisticated delivery system, the type III secretion apparatus, to inject multiple effector proteins that subvert cellular and immune functions of macrophages and epithelial cells (2). First, *S. flexneri* crosses the colonic epithelium by transcytosis via M cells (3, 4). Released in the M cell pocket, it invades resident macrophages and induces cell death (5, 6). Dying macrophages release bacteria and several proinflammatory cytokines including IL-1β and IL-18 that contribute to acute intestinal inflammation (7, 8). *S. flexneri* is then able to invade epithelial cells via the basolateral surface, and uses them as replication niche (9). Although infection of epithelial cells represents a key aspect of infection, there is currently no comprehensive model that describes the molecular processes occurring in the first hours of infection.

The entry of *S. flexneri* into epithelial cells is a multistep process that requires the secretion of effector proteins into the cytoplasm of target cells via type III secretion. Upon contact between the tip complex of the type III apparatus and host cell receptors, including $\alpha5\beta1$-integrins and CD44, the secreted proteins IpaB and IpaC insert into the plasma membrane and form a pore into the host membrane through which several effectors translocate (10–14). Among these, IpaA, IpaB, IpaC, IpgB1, IpgB2, IpgD, and VirA act synergistically to induce membrane ruffling and bacterial internalization (2). Local remodeling of the cell surface depends on the interplay between these effectors and small Rho GTPases, kinases, and other regulators of the actin cytoskeleton and microtubules (15, 16). Engulfed bacteria rapidly lyse the membrane of their internalization vacuole and escape into the cytoplasm where they multiply, and use actin based motility to spread from cell-to-cell (17). *Shigella*-actin based motility is mediated by the virulence factor IcsA/VirG (18, 19). This autotransporter, which accumulates at one pole of the bacterium, recruits the host protein N-WASP and forms together with vinculin and Arp2/3, a complex that serves as actin polymerization nucleator (20).

Although, epithelial cells are not professional immune cells, they can detect invasion and contribute to acute inflammation by secreting several proinflammatory cytokines such as interleukin-8 (IL-8) and tumor necrosis factor α (21). During *S. flexneri* infection, peptidoglycan-derived muramyl peptides are recognized via the receptor Nod1 (22). This recognition leads to the activation of multiple signaling pathways including NF-κB and MAP kinase (MAPK)[1]. Bacteria manipulate

From the ‡Biozentrum, University of Basel, Klingelbergstrasse 50/70, 4056 Basel, Switzerland

Received April 12, 2013, and in revised form, June 14, 2013
Published, MCP Papers in Press, July 4, 2013, DOI 10.1074/mcp.M113.029918

[1] The abbreviations used are: Mitogen-activated protein kinase, MAPK; *Shigella flexneri, S. flexneri;* wt, wild-type*;* interleukin-8, IL-8; mammalian target of rapamycin, mTOR; liquid chromatography tandem mass spectrometry, LC-MS/MS; Database for Annotation Visu-

host signaling in infected cells by secreting effectors that affect different signaling pathways. For instance, the effector OspF, which functions as a phosphothreonine lyase, dephosphorylates MAPKs p38 and ERK in the nucleus of infected cells (23, 24). It was proposed that this mechanism leads to reduced histone H3 phosphorylation and selective repression of gene transcription. Expression of the gene encoding for IL-8, a potent chemoattractant for polymorphonuclear cells, is specifically decreased in presence of OspF. A recent study from our laboratory reported a mechanism of cell–cell communication between infected and uninfected bystander cells that restores IL-8 expression in infected cell monolayers, and potentiates inflammation during infection (25).

S. flexneri infection of epithelial cells has been well investigated by reductionist approaches that led to important findings regarding specific molecular aspects of infection, and general concepts of infection biology and immunology (26, 27). In addition, DNA microarrays were instrumental in the systematic identification of genes regulated during infection and the characterization of host cell responses (28, 29). However, these approaches were not well-suited to obtain a systems-level overview of early host signaling during infection.

Protein phosphorylation is the most widespread known post-translational modification. It can either activate or inactivate biological processes, and is commonly used to switch enzyme activity "on" or "off." Protein kinases and phosphatases are abundant in the human genome, giving rise to countless phosphorylation and dephosphorylation events that control the most diverse cellular pathways. Incidentally, the importance of protein phosphorylation has been already described for several aspects of *S. flexneri* infection, and few kinases have been identified (30–33). Based on this, we reasoned that the complexity of host signaling during *S. flexneri* infection may be addressed by a systematic and unbiased analysis of protein phosphorylation. Here we describe a label-free quantitative phosphoproteomics approach that reveals the dynamics of host protein phosphorylation during infection. Although this method can only capture a sub-portion of the entire phosphoproteome, several hundred of proteins undergoing a change in phosphorylation during the first two hours of infection were identified and functionally annotated. Bioinformatic tools were used to recognize six different temporal profiles of phosphorylation, a functional module composed of ATM-phosphorylated proteins related to genotoxic stress, and the central role of mammalian target of rapamycin (mTOR). By comparing our data to a recently published phosphoproteomics analysis of *Salmonella typhimurium* infection (34), we identified a large set of coregulated phosphoproteins. Finally, we showed that *S. flexneri* effector OspF alters the phosphorylation of several hundred proteins, thereby demonstrating its broad impact during infection.

alization and Integrated Discovery, DAVID; nuclear pore complex, NPC; mTOR complex 1, mTORC1; mTOR complex 2, mTORC2; regulatory-associated protein of mTOR, Raptor; mammalian LST8/G-protein β-subunit like protein, mLST8/GβL; rapamycin-insensitive companion of mTOR, Rictor; mammalian stress-activated protein kinase interacting protein 1, mSIN1; anaphase-promoting complex/cyclosome, APC/C; inducible Rictor-knockout, iRiKO; mouse embryonic fibroblasts, MEFs; tryptic soy broth, TSB.

MATERIALS AND METHODS

Reagents and Antibodies—PP242 was obtained from Chemdea, Ridgewood, NJ (#CD0258), Rapamycin from LC Laboratories, Woburn, MA (#R-5000), KU-60019 (#S1570), SB203580 (#S1076) and PD98059 (#S1177) from Selleck Chemicals, Houston, TX. Antibodies against MAPK p38 (#9212), phospho-MAPK p38 Thr180/Tyr182 (#4631), ERK (#9102), pospho-ERK (Thr202/Tyr204) (#4377), RIP2 (#4982), phospho-RIP2 Ser176 (#4364), CREB (#9197), phospho-CREB Ser133 (#9198), phospho-AKT Ser473 (#4058), phospho-ATM Ser1981 (#5883), phospho-S6 ribosomal protein Ser235/Ser236 (#4858), phospho-S6K Thr389 (#9205), Rictor (#2114), phospho-TBCD4 Ser588 (#8730), phospho-p90RSK Thr359/Ser363 (#9344), phospho-MYPT1 Ser507 (#3040) were obtained from Cell Signaling Technology, Danvers, MA. Antibodies against ATM (#05–513) and actin (#MAB1501) were purchased from Millipore, Billerica, MA. The antibody against vinculin was purchased from Sigma, St. Louis, MO (#V9131).

Cell Culture—HeLa CCL-2™ human epithelial cells were purchased from ATCC, Manassas, VA and cultured in DMEM, supplemented with 10% FCS, antibiotics and L-glutamine. Inducible Rictor-knockout (iRiKO) mouse embryonic fibroblasts (MEFs) and the corresponding control cells were generously provided by Prof. M. Hall (35). MEFs were cultured in DMEM, supplemented with 10% FCS, antibiotics and L-glutamine. The knockout of Rictor was induced by culturing the cells for 3 days in the presence of 1 μM Tamoxifen.

Bacterial Strains—The M90T *S. flexneri* and M90T *S. flexneri* Δ*virG* strains were generously provided by Prof. P. Sansonetti (Institut Pasteur, Paris, France). The *ospF* deletion mutant (Δ*ospF*) was generated by allelic exchange using a modification of the lambda red-mediated gene deletion as previously described (36). *S. flexneri* M90T Δ*virG* pCK100 (P_{uhpT}::DsRed) was generated by transforming the non-motile *S. flexneri* strain M90T Δ*virG* with the plasmid pCK100. pCK100 contains the fluorescent marker DsRed under the control of the native promoter of the *S. flexneri* gene *uhpT*, which is up-regulated in presence of glucose-6-phosphate. Briefly, the 251bp promoter region upstream of *uhpT* was amplified by PCR (Primers used: GAGAGAGAATGCAGTGCTCGATACCTGGCACT, GCTCTAGAGGGTTACTCCTGAAATGAATACCT) and ligated into the pMW211 plasmid using *Bsm*I and XbaI.

Infection Assay—M90T *S. flexneri* strain was grown in tryptic soy broth (TSB) to exponential growth phase at 37 °C and coated with poly-L-lysine. 30 min before infection, complete growth medium was replaced by DMEM supplemented with 10 mM Hepes and 2 mM L-glutamine (assay medium). Assay medium (uninfected control) or bacteria were added to 6-well plates at a multiplicity of infection of 40. Infection was initiated by centrifugation of the plates for 5 min and their incubation at 37 °C for the indicated time periods. Extracellular bacteria were killed by adding gentamycin (50 μg/ml) 30 min after infection.

Microscopy and Automated Image Analysis—Infection rates were determined by using automated image analysis. Images were automatically acquired with an ImageXpress Micro (Molecular devices, Sunnyvale, USA). At each site, images were acquired at 360 nm, 480 nm, 594 nm and 640 nm to visualize Hoechst, FITC-phalloidin, DsRed-expressing *S. flexneri* and Alexa 647-conjugated secondary antibodies, respectively. Infection rates were determined by image analysis using CellProfiler (37) and MATLAB (The MathWorks, Inc, Natick, USA). The Hoechst staining was used as a mask to automatically identify cell nuclei. The cellular area was defined by extension of the nuclear mask. In parallel, the presence of bacteria within the area

of each cell was quantified. Performance of bacterial detection was checked by visual inspection of several images prior to automated processing. In control images (no infection), the algorithm generally classified less than 1% of cells as infected (25).

SDS-PAGE and Immunoblotting—Uninfected control and infected cells were washed twice in ice cold PBS, lysed in PhosphoSafe™ extraction reagent (Millipore, Billerica, MA), incubated on ice for 10 min, and subsequently centrifuged at 4 °C for 20 min at 16′000g. BCA Protein Assay kit (Pierce, Rockford, IL) was used to determine protein concentration. 10–15 μg of protein was subjected to SDS-polyacrylamide gels and electroblotted onto nitrocellulose membranes. Immunoblotting was performed using primary antibodies diluted in phosphate buffered saline containing 0.1% tween and 5% bovine serum albumin. HRP-conjugated secondary antibodies were purchased from GE Healthcare, Chalfont St Giles, United Kingdom or Cell Signaling Technology, Danvers, MA. The blots were developed with an enhanced chemiluminescence method (Pierce, Rockford, IL).

Immunofluorescence—After fixation in 4% PFA for 10 min, cells were permeabilized in 0.3–0.5% Triton X-100 for 10 min. Phospho-AKT antibody was incubated overnight at 4 °C in PBS followed by a secondary staining using Alexa 647-conjugated secondary antibody (Invitrogen, Carlsbad, CA). Additionally, DNA and F-actin were stained for 1 h at room temperature with Hoechst and FITC-phalloidin (Invitrogen, Carlsbad, CA), respectively.

Sample Preparation for Phosphoproteomics—For each condition, two 6-well plates of HeLa CCL-2™ cells were grown to confluency. Cells were infected as described above. At the indicated time-points, the plates were put on ice and washed twice with ice-cold phosphate-buffered saline (PBS). Samples were then collected in urea solution [8 M Urea (AppliChem, Darmstadt, Germany), 0.1 M Ammoniumbicarbonate (Sigma, St. Louis, MO), 0.1% RapiGest (Waters, Milford, MA), 1× PhosSTOP (Roche, Basel, Switzerland)]. The samples were briefly vortexed, sonicated at 4 °C (Hielscher, Teltow, Germany), shaked for 5 min on a thermomixer (Eppendorf, Hamburg, Germany) and centrifuged for 20 min at 4 °C and 16′000g. Supernatants were collected and stored at −80 °C for further processing. BCA Protein Assay (Pierce, Rockford, IL) was used to measure protein concentration.

Phosphopeptide Enrichment—Disulfide bonds were reduced with tris(2-carboxyethyl)phosphine at a final concentration of 10 mM at 37 °C for 1 h. Free thiols were alkylated with 20 mM iodoacetamide (Sigma, St. Louis, MO) at room temperature for 30 min in the dark. The excess of iodoacetamide was quenched with N-acetyl cysteine at a final concentration of 25 mM for 10 min at room temperature. Lys-C endopeptidase (Wako, Osaka, Japan) was added to a final enzyme/protein ratio of 1:200 (w/w) and incubated for 4 h at 37 °C. The solution was subsequently diluted with 0.1 M ammoniumbicarbonate (Sigma, St. Louis, MO) to a final concentration below 2 M urea and digested overnight at 37 °C with sequencing-grade modified trypsin (Promega, Madison, WI) at a protein-to-enzyme ratio of 50:1. Peptides were desalted on a C18 Sep-Pak cartridge (Waters, Milford, MA) and dried under vacuum. Phosphopeptides were isolated from 2 mg of total peptide mass with TiO_2 as described previously (38). Briefly, dried peptides were dissolved in an 80% acetonitrile (ACN)–2.5% trifluoroacetic acid (TFA) solution saturated with phthalic acid. Peptides were added to the same amount of equilibrated TiO_2 (5-μm bead size, GL Sciences, Tokyo, Japan) in a blocked Mobicol spin column (MoBiTec, Goettingen, Germany) that was incubated for 30 min with end-over-end rotation. The column was washed twice with the saturated phthalic acid solution, twice with 80% ACN and 0.1% TFA, and finally twice with 0.1% TFA. The peptides were eluted with a 0.3 M NH_4OH solution. The pH of the eluates was adjusted to be below 2.5 with 5% TFA solution and 2 M HCl. Phosphopeptides were again desalted with microspin C18 cartridges (Harvard Apparatus, Holliston, MA).

LC-MS/MS Analysis—Chromatographic separation of peptides was carried out using an EASY nano-LC system (Thermo Fisher Scientific, Waltham, MA), equipped with a heated RP-HPLC column (75 μm x 37 cm) packed in-house with 3 μm C18 resin (Reprosil-AQ Pur, Dr. Maisch). Aliquots of 1 μg total phosphopeptide sample were analyzed per LC-MS/MS run using a linear gradient ranging from 98% solvent A (0.15% formic acid) and 2% solvent B (98% acetonitrile, 2% water, 0.15% formic acid) to 30% solvent B over 90 min at a flow rate of 200 nl/min. Mass spectrometry analysis was performed on a dual pressure LTQ-Orbitrap mass spectrometer equipped with a nano-electrospray ion source (Thermo Fisher Scientific, Waltham, MA). Each MS1 scan (acquired in the Orbitrap) was followed by collision-induced dissociation (CID, acquired in the LTQ) of the 10 most abundant precursor ions with dynamic exclusion for 30 s with enabled multistage activation. Total cycle time was ~2 s. For MS1, 10^6 ions were accumulated in the Orbitrap cell over a maximum time of 300 ms and scanned at a resolution of 60,000 FWHM (at 400 *m/z*). MS2 scans were acquired using the normal scan mode, a target setting of 10^4 ions, and accumulation time of 50 ms. Singly charged ions and ions with unassigned charge state were excluded from triggering MS2 events. The normalized collision energy was set to 32%, and one microscan was acquired for each spectrum.

Label-free Quantification and Database Searching—The acquired raw-files were imported into the Progenesis software tool (Nonlinear Dynamics, Version 4.0) for label-free quantification using the default parameters. MS2 spectra were exported directly from Progenesis in mgf format and searched using the MASCOT algorithm (Matrix Science, Version 2.4) against a decoy database (39) containing normal and reverse sequences of the predicted SwissProt entries of *Homo sapiens* (www.ebi.ac.uk, release date 16/05/2012) and commonly observed contaminants (in total 41,250 sequences) generated using the SequenceReverser tool from the MaxQuant software (Version 1.0.13.13) . To identify proteins originating from *S. flexneri*, non phosphopeptide enriched samples were searched against the same database above including predicted SwissProt entries of *S. flexneri* (www.ebi.ac.uk, release date 16/05/2012, in total 49,610 sequences) The precursor ion tolerance was set to 10 ppm and fragment ion tolerance was set to 0.6 Da. The search criteria were set as follows: full tryptic specificity was required (cleavage after lysine or arginine residues unless followed by proline), 2 missed cleavages were allowed, carbamidomethylation (C) was set as fixed modification and phosphorylation (S,T,Y) or oxidation (M) as a variable modification for TiO2 enriched or not enriched samples, respectively. Finally, the database search results were exported as a xml-file and imported back to the Progenesis software for MS1 feature assignment. For phosphopeptide quantification, a csv-file containing the MS1 peak abundances of all detected features was exported and for not enriched samples, a csv-file containing all protein measurements based on the summed feature intensities of all identified peptides per protein was created. Importantly, the Progenesis software was set that proteins identified by similar sets of peptides are grouped together and that only non-conflicting peptides with specific sequences for single proteins in the database were employed for protein quantification. Both files were further processed using the in-house developed SafeQuant v1.0 R script (unpublished data, available at https://github.com/eahrne/SafeQuant/). In brief, the software sets the identification level False Discovery Rate to 1% (based on the number of decoy protein sequence database hits) and normalizes the identified MS1 peak abundances (extracted ion chromatogram, XIC) across all samples, *i.e.* the summed XIC of all confidently identified peptide features is scaled to be equal for all LC-MS runs. Next, all quantified phosphopeptides/proteins are assigned an abundance ratio for each time point, based on the median XIC per time point. The statistical significance of each ratio is given by its q-value (false discovery rate

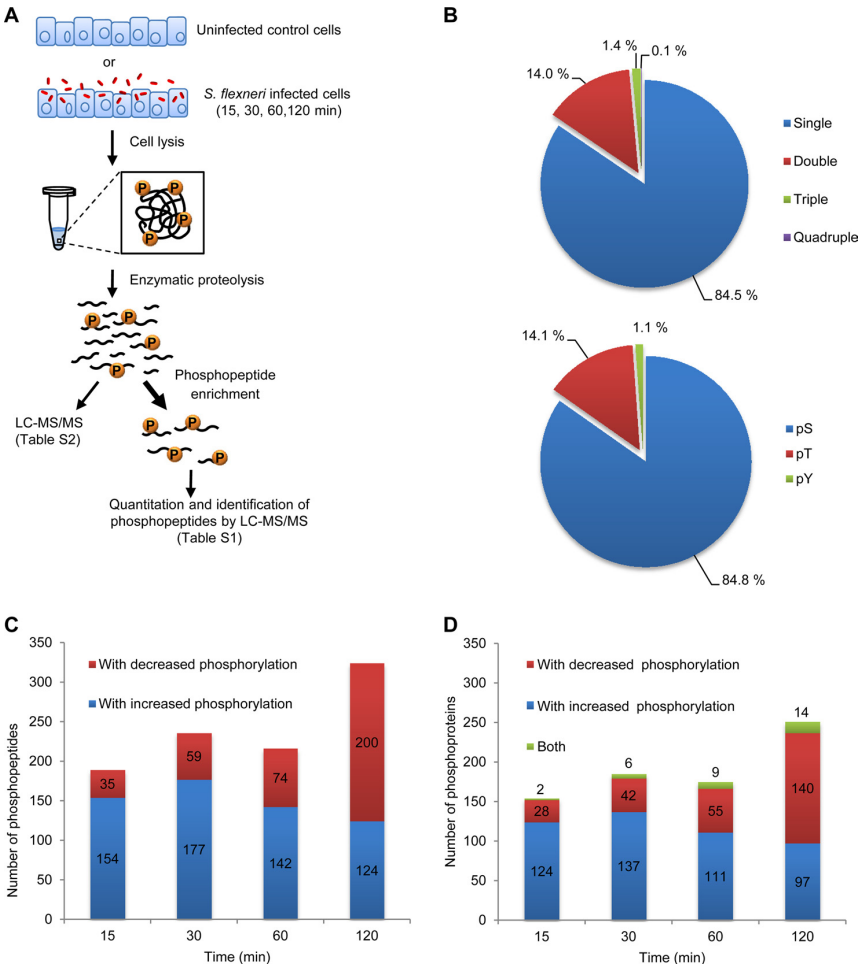

FIG. 1. **Phosphoproteomics analysis applied to *S. flexneri* infection.** *A*, Diagram of the phosphoproteomics protocol applied to *S. flexneri* infection of HeLa cells. *B*, Distribution of single, double, triple, and quadruple peptide phosphorylation based on 3234 detected phosphopeptides (upper panel). Distribution of serine, threonine and tyrosine phosphorylation based on 3109 detected phospho-sites (lower panel). *C*, Dynamics of phosphorylation changes after *S. flexneri* infection of HeLa cells. Data represent the number of phosphopeptides for which a significant increase (in blue) or a decrease (in red) of phosphorylation was observed after *S. flexneri* infection compared with uninfected cells. A minimum twofold change and a q-value <0.01 were used to select phosphopeptides for quantification. *D*, Dynamics of phosphorylation changes at the protein level after *S. flexneri* infection of HeLa cells. Data represent the number of proteins for which an increase of phosphorylation (in blue), a decrease of phosphorylation (in red) or both (in green) was observed after *S. flexneri* infection compared with uninfected cells. All proteins containing at least one phosphopeptide with a minimum twofold change and a q-value <0.01 were considered for analysis.

adjusted *p* values), obtained by calculating modified t-statistic *p* values (40) and adjusting for multiple testing (41). The final list of all quantified phosphopeptides/proteins is presented in supplemental Table S1 and S2. The location of the phosphorylated residues was automatically assigned by MASCOT (score >10). All annotated spectra can be found in supplemental information file 12 (annotated spectra) and, together with the MS raw files and search parameters employed, have been deposited to the ProteomeXchange Consortium (http://proteomecentral.proteomexchange.org) via the PRIDE partner repository (42) (data submitted).

RESULTS

Label-Free Quantitative Phosphoproteomics Reveals the Massive Impact of S. flexneri Infection on Host Protein Phosphorylation—To analyze the impact of *S. flexneri* infection on protein phosphorylation in epithelial cells, we used a phosphoproteomics strategy that combines phosphopeptide enrichment and label-free quantification based on liquid chromatography coupled to tandem mass spectrometry (LC-MS/MS) (Fig. 1*A*) (38, 43). In three independent experiments, HeLa cells were left untreated or infected with *S. flexneri* for 15, 30, 60, and 120 min at a multiplicity of infection of 40 (Fig. 1*A*). Cell lysis, enzymatic proteolysis, phosphopeptide enrichment on titanium dioxide beads, identification and quantification of individual phosphopeptides were performed as described in Methods. A total of 3234 phosphopeptides corresponding to

3109 phospho-sites and 1183 phosphorylated proteins were identified (supplemental Table S1). Analysis of all detected phosphopeptides revealed that the distribution of phosphorylated peptides was strongly biased toward single and dual phosphorylations (Fig. 1*B*, upper panel). As previously described (44), the large majority of phosphorylation events were found on serine and threonine residues (Fig. 1*B*, lower panel). Correlation analysis based on squared Pearson correlation coefficient R^2 between the three biological replicates showed robust reproducibility between independent experiments for all infection conditions (supplemental Fig. S1*A*). This was confirmed by data showing that the coefficients of variance calculated for all infection conditions as described in Methods varied between 18 and 29% (supplemental Fig. S1*B*), a range of values expected for label-free quantification methods (45, 46). Significant changes in phosphorylation were defined by a q-value (moderated *t* test adjusted for multiple testing) cutoff of < 0.01 using the SafeQuant tool (47) and a minimum twofold increase or decrease in peptide phosphorylation between infected and uninfected control cells (supplemental Table S1). Based on these criteria, 14.3% of all detected phosphopeptides showed a significant change in phosphorylation after *S. flexneri* infection. A parallel LC-MS/MS analysis, performed before phosphopeptide enrichment (Fig. 1*A*), showed no significant changes in protein amount after infection for significantly altered phosphopeptides (supplemental Table S2), demonstrating that changes in phosphopeptide detection reflected true changes in phosphorylation for at least 56.9% of the identified phosphoproteins (supplemental Fig. S1*C*). Phosphorylation events were visible at all time-points with a peak at 30 min at which 177 phosphopeptides corresponding to 137 phosphorylated proteins showed an increase in phosphorylation compared with control cells (Figs. 1*C* and 1*D*). Decreased phosphorylation was also detected at all time-points with a maximum of 200 peptides corresponding to 140 proteins showing reduced phosphorylation 2 h postinfection (Figs. 1*C* and 1*D*). For simplification, we defined as phosphoproteome the subset of 334 proteins undergoing a significant change of phosphorylation on at least one phosphopeptide after infection (supplemental Table S1). Phosphoproteomics data showing an increase in phosphorylation of TBCD4 at serine 588, RSK (KS6A1) at threonine 359 and serine 363, and MYPT1 at serine 507 were confirmed by Western blot using phospho-specific antibodies (supplemental Fig. S2). Previous data showing dual phosphorylation of ERK at residues threonine 202 and tyrosine 204 after *S. flexneri* infection (48) were confirmed by our phosphoproteomics data (supplemental Table S1). Taken together, these results showed that *S. flexneri* has a massive impact on host protein phosphorylation, and that label free quantitative phosphoproteomics is well suited to reproducibly identify and quantify the phosphorylation changes occurring during infection of epithelial cells.

Phosphoproteomics Reveals New Cellular Functions Affected by Infection—The biological functions of proteins from the phosphoproteome of *S. flexneri*-infected cells were investigated by gene ontology analysis with the functional annotation tool of the Database for Annotation, Visualization, and Integrated Discovery (DAVID, http://david.abcc.ncifcrf.gov/) (49, 50). Results showed that proteins were involved in diverse cellular functions (supplemental Table S3) with a specific enrichment in proteins related to cytoskeleton, cell death and small GTPases signaling (Fig. 2*A* and supplemental Table S3). Gene ontology was completed by a manual functional annotation based on literature (Fig. 2*B*, supplemental Table S4). This analysis revealed that 40 proteins were implicated in the organization and rearrangement of the actin cytoskeleton. This included actin-binding proteins that regulate actin polymerization (*i.e.* ARPC1, PALLD, CTTN), GTP exchange factors (*i.e.* ARHGEF7, DOCK9, ARHGEF16, and ARHGEF17), GTPase activating proteins (*i.e.* ARHGAP29, IQGAP2) and downstream effectors (*i.e.* BORG5) of the small GTPases Cdc42, Rac and RhoA known to be involved in filopodia, membrane ruffling and stress fiber formation, respectively (51, 52). The comparison with the phosphoproteome of cells infected by a deletion virG mutant (Δ*virG*) that cannot perform actin-based motility (19) suggested that proteins undergoing similar phosphorylation changes after both types of infection were important for the cortical actin rearrangements taking place during bacterial internalization (supplemental Tables S1 and S5). In contrast, phosphoproteins found exclusively in the wild-type data set may be either important for actin-based motility or not detected in the LC-MS/MS experiment for technical reasons (supplemental Table S5). In addition to proteins regulating the actin cytoskeleton, proteins associated with the network of microtubules (*i.e.* MAP1B, MAP7, ELM4) and intermediate filaments (*i.e.* PLEC, SYNM) were found. These results were expected as it is well documented that *S. flexneri* induces a profound remodeling of actin and microtubules for bacterial uptake and intra- and intercellular motility (2). In line with data showing that *S. flexneri* interferes with cell–cell adhesion (53), the phosphorylation of proteins involved in the assembly of tight junctions in enterocytes (ZO-1 and ZO-2) and the regulation of adherens junctions (CTNA1, CTND1) was altered in infected cells (supplemental Table S4). With around 50 members, proteins implicated in signal transduction were also highly represented in the phosphoproteome. They mainly correspond to receptors, adaptors, kinases, and phosphatases involved in well-characterized signaling pathways, including EGFR, MAPK, NF-κB, mTOR, and PKA. In addition, 24 proteins related to endocytosis (*i.e.* SH3GL1, DNMBP), exocytosis (*i.e.* STXB5), and vesicular trafficking (*i.e.* BET1, Rab7A, WDR44) were also present in the phosphoproteome (supplemental Table S4). In line with previous data showing that *S. flexneri* interferes with host cell cycle (54), we found that infection affected the phosphorylation of regulators of mitotic progression that control spindle

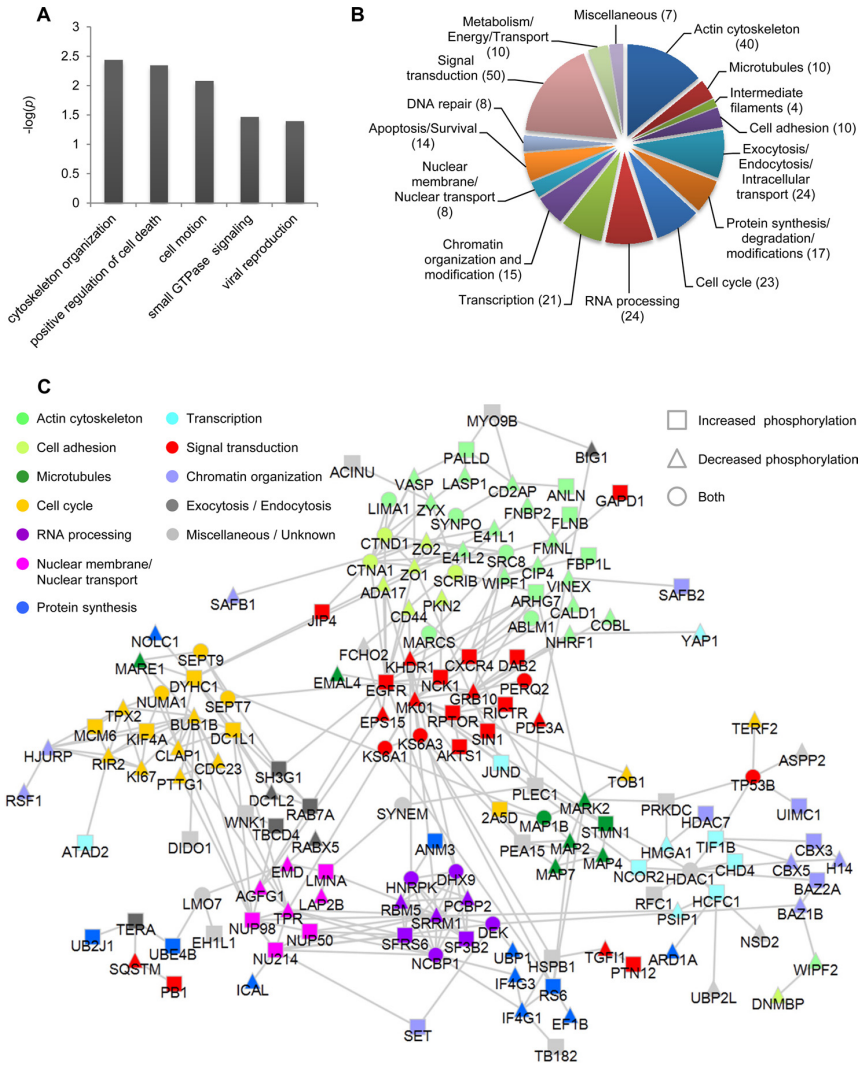

FIG. 2. **Cellular processes affected by *S. flexneri.*** *A*, Gene ontology analysis of proteins with altered phosphorylation after *S. flexneri* infection performed with DAVID (GO term BP FAT, $p < 0.05$). All proteins (334) containing at least one phosphopeptide with a minimum twofold change and a q-value <0.01 were considered for analysis. A subset composed of all detected phosphoproteins was used as background. Full list of GO terms is shown in supplemental Table S3. *B*, Literature-based manual annotation of the phosphoproteome. Numbers in brackets indicate the number of corresponding proteins. *C*, Graphical representation of the phosphoproteome using STRING (high confidence 0.7) combined with manual functional annotation and the direction of phosphorylation changes. Square, triangle and circle representations correspond to an increase, a decrease or an increase and a decrease in phosphopeptide abundance for a given phosphoprotein. Only proteins with at least one connection in STRING are represented.

dynamics and chromosome separation (*i.e.* NEK9, BOD1L, PDS5B). To note, the proteins SEPT7 and SEPT9 of the septin family, known to be involved in cytokinesis (55) and more recently, in the formation of septin cages around intracellular bacteria (56, 57), were found phosphorylated after *S. flexneri* infection (supplemental Table S4). In agreement with data reporting that cell fate is controlled by opposite signals (58), we found that the phosphorylation of both pro- and anti-apoptotic proteins (*i.e.* PDCD4, BAG3, PAWR) was altered in infected cells. For the first time, our data showed that the phosphorylation of several proteins (Nup98, Nup50, Nu214, and TPR) from the nuclear pore complex (NPC) was modified after infection. NPCs are large multiprotein channels embedded in the nuclear envelope that mediate the transport of macromolecules including proteins and RNA between the cytoplasm and the nucleus of eukaryotic cells. The phosphoproteome was graphically illustrated by combining data from the STRING database that assembles protein networks based

on known and predicted protein–protein interactions (59), with a functional description of proteins. Only proteins with at least one connection in STRING were represented (Fig. 2*C*). Data showed a complex network with several distinct functional modules containing highly interconnected nodes. As expected, proteins involved in signal transduction were highly connected with members from other groups, including cytoskeleton and cell adhesion.

To identify the phosphorylation motifs overrepresented in the phosphoproteome, the Motif-X algorithm (60) was applied to all up-regulated phosphopeptides. Six distinctive motif sequences, all phosphorylated on a serine, including the motifs RXRXX*S*, RRX*S*, RXX*S*, *S*P, *S*Q, and *S*XE, were extracted (supplemental Fig. S3). To predict the putative kinases of these motifs, we compared them to those of all known substrates of 107 kinase families (61). The first three motifs showed striking similarities to substrates of the AGC kinases AKT, PKG/PKA/PKC, RSK, and of CamKII (supplemental Fig. S3). The proline directed *S*P motif can be phosphorylated by MAPK, CDC2, and CDK whereas the *S*Q motif is known to be a substrate of ATM/ATR or DNAPK. Finally, the motif *S*XE remotely resembled a substrate motif of CK2. Although AKT was absent from the phosphoproteome (supplemental Table S1), we experimentally confirmed its activation and localization at sites of *S. flexneri* entry (supplemental Figs. S4*A* and S4*B*), as previously reported (62). The high connectivity of AKT within the STRING graphical representation of the phosphoproteome network suggested that this kinase played a central function during infection (supplemental Fig. S4*C*). In particular, AKT was highly connected to proteins associated with the actin cytoskeleton and apoptosis/survival regulation. Phosphopeptides corresponding to active RSK and ERK were found in the phosphoproteome (supplemental Table S1) suggesting that these two kinases may be responsible for the phosphorylation of RXX*S* and *S*P motifs during infection, respectively.

Taken together, these results show that *S. flexneri* infection alters the phosphorylation of a complex network of proteins that are involved in several key aspects of epithelial cell biology. They confirm the large impact of *S. flexneri* infection on the actin cytoskeleton and transcription, and show that numerous proteins related to cell cycle, microtubules, intracellular trafficking, and the nuclear pore are also affected during infection.

Spatiotemporal Dynamics of Protein Phosphorylation During S. flexneri Infection—To capture the spatial dynamics of phosphorylation during *S. flexneri* infection, we used the UniProt database (http://www.uniprot.org) to analyze the subcellular localization of proteins with altered phosphorylation during infection. With 86% coverage of the phosphoproteome, results showed that phosphorylation changes mainly occurred in proteins localized in the cytoplasm, at the plasma membrane, in the nucleus, in cell junctions, at the Golgi apparatus and the endoplasmic reticulum (supplemental Fig. S5*A* and S5*B*). Weak differences were observed over time, indicating for rapid and sustained signaling in different subcellular compartments during infection. Early phosphorylation changes after 15 min in the nucleus may result from a fast nuclear translocation of host signaling proteins and/or from a rapid translocation of bacterial effectors to the nucleus of infected cells.

Analysis of the temporal dynamics of individual peptides revealed a large heterogeneity in the patterns of phosphorylation changes after *S. flexneri* infection (supplemental Fig. S5*C*). Analysis of all peptides taken individually by fuzzy c-means clustering (63) revealed six main profiles (Fig. 3*A*, supplemental Table S6). Clusters 1 and 2 corresponded to fast and slow decrease in phosphorylation, respectively. Clusters 3, 4, and 5 corresponded to peptides with fast increase in phosphorylation followed by slow, intermediate and fast decrease, respectively. Cluster 6 grouped peptides showing late phosphorylation with a maximum at 2 h. Computational analysis indicated that the functional categories were not equally represented in all clusters (supplemental Table S6). For instance, proteins associated with the cytoskeleton were overrepresented in clusters 1 and 2. In contrast, proteins involved in the p53 pathway and DNA repair were in majority found in cluster 6. In the same line, the most frequent phospho-motif varied between clusters (Fig. 3*A*). A thorough analysis of cluster 6 revealed that among its 23 members, 15 were phosphorylated on a *S*Q motif. As this motif is the consensus sequence for the major sensor of DNA double-strand breaks ATM (64, 65), we checked the activation profile of this kinase after *S. flexneri* infection by monitoring its phosphorylation at serine 1981. As shown in Figs. 3*B* and 3*C*, an increase of ATM phosphorylation was observed at 30 min and phosphorylation was maximal after two hours, suggesting that several cluster 6 proteins were targets of ATM. This hypothesis was validated by showing that the phosphorylation of 11 proteins from this cluster was sensitive to the ATM inhibitor KU-60019 (supplemental Figs. S6*A* and S6*B*, supplemental Table S7). More generally, dynamics analysis of all peptides phosphorylated on a *S*Q motif after infection revealed also an earlier profile of phosphorylation (supplemental Fig. S6*C*), suggesting that another kinase was implicated. In conclusion, analysis of the dynamics of phosphorylation revealed several temporal profiles of phosphorylation associated with specific enriched phospho-motifs and distinct functional descriptions. In particular, we identified one group of proteins showing maximal phosphorylation on a *S*Q motif two hours post-infection. As literature indicates that TP53B, PRKDC, UIMC1, and TR150 are linked to the p53 pathway or DNA repair (66–69), our results suggest that part of group 6 proteins is involved in a genotoxic stress response to infection. More broadly, these results illustrate how phosphorylation dynamics and phospho-motif enrichment data combined with functional annotation can be used to identify and characterize the host pathways regulated during bacterial infection.

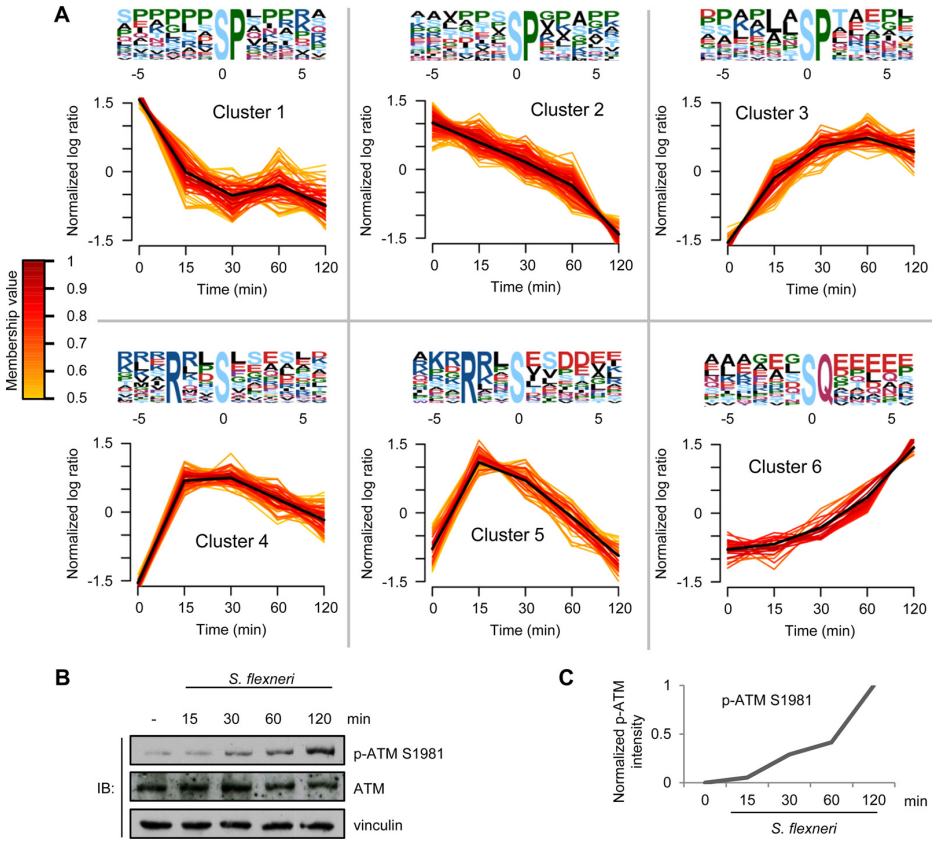

FIG. 3. **Dynamics of phosphorylation changes after *S. flexneri* infection of epithelial cells.** *A*, Dynamics of phosphorylation changes for individual phosphopeptides analyzed by fuzzy c-means clustering using the MFuzz algorithm. All individual phosphopeptides showing a significant change at least at one time point were considered. Fold phosphorylation changes (log Ratio values) obtained for all time-points were normalized to have a standard deviation of 1 and a mean of 0 (z-score). For each cluster, the black line corresponds to an optimal membership of 1. The most overrepresented phospho-motif extracted with the motif-X algorithm was shown for each cluster. *B*, Immunoblot of ATM phosphorylation at Ser-1981 in HeLa cells infected for the indicated time periods by *S. flexneri*. Vinculin was used as a loading control. *C*, Densitometric quantification of ATM phosphorylation at Ser-1981 using the gel analysis tool from Fiji (88) (results representative of 2 independent experiments).

mTORC1 and mTORC2 Control S6 Kinase and AKT Phosphorylation Respectively—The KEGG database was used to identify the overrepresented pathways in the phosphoproteome of *S. flexneri*-infected cells (70, 71). With 7 KEGG-annotated proteins, the mTOR signaling pathway was the most overrepresented pathway (Fig. 4*A*, supplemental Table S8). mTOR is a central serine/threonine protein kinase that regulates cell growth and metabolism, autophagy, the actin cytoskeleton, cell proliferation, cell survival, protein synthesis, and transcription (72). It is found as part of two different protein complexes. mTOR complex 1 (mTORC1) is composed of mTOR, regulatory-associated protein of mTOR (Raptor), mammalian LST8/G-protein β-subunit like protein (mLST8/GβL) and the recently identified partners PRAS40 and DEPTOR (73). This complex functions as a sensor for nutrient, redox balance and energy, and controls protein synthesis. mTOR complex 2 (mTORC2) is composed of mTOR, rapamycin-insensitive companion of mTOR (Rictor), mLST8, DEPTOR and mammalian stress-activated protein kinase interacting protein 1 (mSIN1) (73). mTORC2 has been shown to function as an important regulator of the actin cytoskeleton (74). As indicated on the mTOR signaling map (Fig. 4*B*), components of both mTOR complexes but also regulators and effectors proteins of mTOR, showed altered phosphorylation after *S. flexneri* infection (supplemental Table S1). In order to test the implication of mTORC1 during infection, we monitored the effect of rapamycin on the activation of ribosomal S6 kinase, a protein implicated in protein translation known to be a substrate of mTORC1, and found in the phosphoproteome (supplemental Table S1). An antibody that recognizes S6 kinase phosphorylated at threonine 389 was used in an immunoblotting experiment. Although a strong activation of S6 kinase was confirmed after infection, a short treatment of rapamycin blocked this induction (Fig.

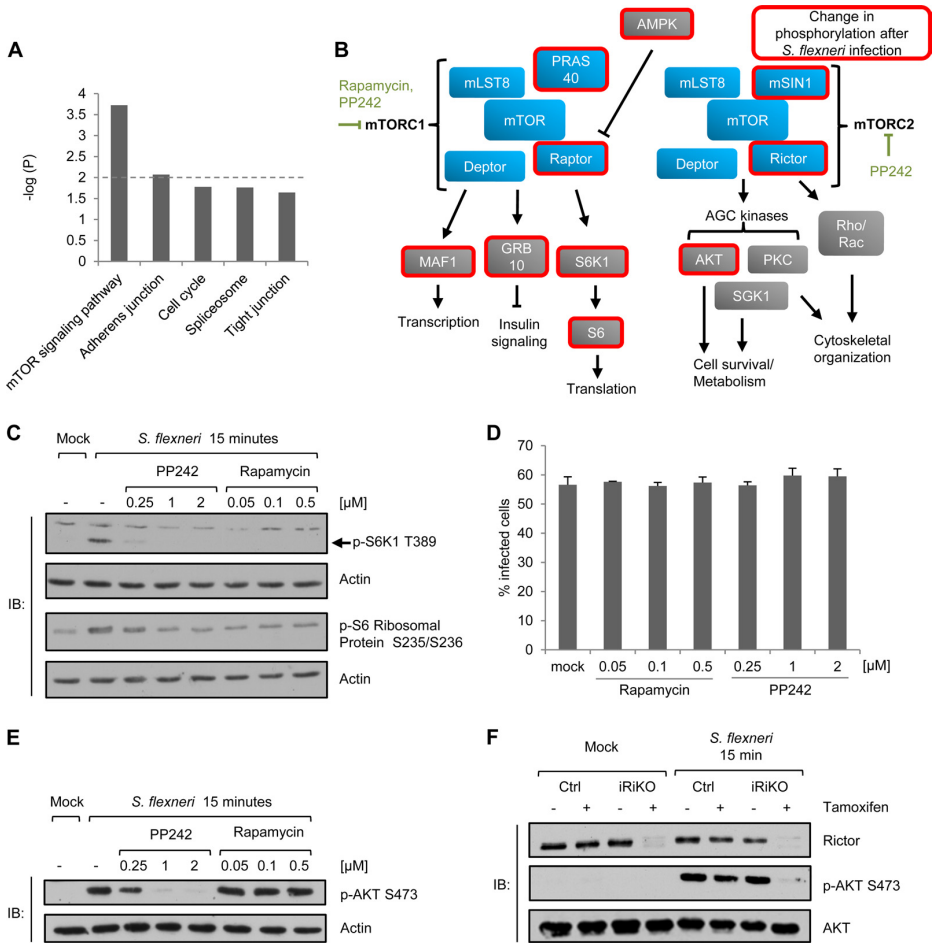

FIG. 4. **mTORC1 and mTORC2 control S6 kinase and AKT phosphorylation respectively.** *A*, Analysis of the most overrepresented KEGG signaling pathways of the phosphoproteome using DAVID. The dashed line indicates a negative log *p* value threshold of 2. *B*, Projection of mTOR-related proteins identified by phosphoproteomics onto an mTOR signaling map. Proteins from the phosphoproteome of *S. flexneri*-infected cells are surrounded by red borders. mLST8, mTOR, Deptor, SGK1, Rho/Rac were not detected in the phosphoproteomics study. PKC alpha was detected but not significantly regulated. *C*, mTORC1 is required for S6 kinase and S6 ribosomal protein phosphorylation during *S. flexneri* infection. HeLa cells were left untreated or pretreated with rapamycin or PP242 for 60 min prior to *S. flexneri* infection (15 min) and analyzed by immunoblotting for the phosphorylation of S6 kinase at residue Thr-389 and of S6 ribosomal protein at Ser-235/236. Actin is used as a loading control. *D*, The mTOR inhibitors rapamycin and PP242 do not affect *S. flexneri* entry. HeLa cells were pretreated either with rapamycin or PP242 at indicated concentrations for one hour, and infected with *S. flexneri* ΔvirG- pCK100 (P_{uhpT}::Dsred) for 3 h. These bacteria, only fluorescent when they are intracellular, form large microcolonies that are effectively detected by automated image analysis. Quantification of the infection rate shows that inhibition of mTORC1 and mTORC2 fails to affect the entry process of *S. flexneri* into HeLa cells. Results are expressed as the mean ± S.D. corresponding to three different wells of a 96-well plate and are representative of two independent experiments. *E*, *S. flexneri* infection-induced activation of AKT is mTORC2 dependent. HeLa cells were left untreated or pretreated with rapamycin or PP242 for 60 min prior to *S. flexneri* infection (15 min) and analyzed by immunobloting for the phosphorylation of AKT at Ser-473. Actin is used as a loading control. *F*, mTORC2 component Rictor is required for the phosphorylation of AKT during *S. flexneri* infection. Control (Ctrl) and inducible-Rictor knockout (iRiKO) mouse embryonic fibroblasts were left untreated or infected with *S. flexneri* for 15 min and analyzed for the expression of Rictor and the level of AKT phosphorylation at Ser-473 by immunoblotting. Inducible Rictor-knockout was obtained by tamoxifen pretreatment. AKT is used as loading control. All results were representative of at least two independent experiments.

4*C*, upper panel). The phosphorylation of S6 ribosomal protein, the main substrate of S6 kinase, was also sensitive to rapamycin (Fig. 4*C*, lower panel). In the same condition of drug treatment, rapamycin had no effect on *S. flexneri* entry into cells (Fig. 4*D*). Taken together, these results show that mTORC1 is involved in the early activation of S6 kinase following *S. flexneri* infection, and suggest that it may control protein translation.

In addition to mTORC1, proteins from the mTORC2 pathway were also found in the phosphoproteome (Fig. 4*B*, supplemental Table S1). Although this complex is known to control the actin cytoskeleton, inhibition of mTORC2 had no effect on bacterial invasion (Fig. 4*D*). As AKT was activated during *S. flexneri* infection (supplemental Fig. S4*A* and S4*B*) and is a known substrate of mTORC2, we tested whether mTORC2 played a role in the activation of AKT during infection. Interestingly, AKT phosphorylation was blocked by PP242, an inhibitor of both complexes, but unchanged after rapamycin treatment (Fig. 4*E*), showing that mTORC2 alone was implicated in the activation of AKT during infection. This result was confirmed by showing that AKT phosphorylation was abrogated in inducible Rictor-knockout mouse embryonic fibroblasts (35) treated by tamoxifen (Fig. 4*F*). In conclusion, these data show that, mTORC1 controls the phosphorylation of S6 kinase whereas mTORC2 is involved in the activation of AKT. As these two kinases control translation and host cell survival, respectively (62, 75, 76), our study indicates that mTOR plays a critical role in the control of host cell responses to *S. flexneri* infection.

S. flexneri and S. typhimurium Infections Trigger Common Host Phosphorylation Changes—In order to better characterize the phosphoproteome of *S. flexneri*-infected cells, we compared it to a recently published phosphoproteome dataset generated from HeLa cells infected by *Salmonella typhimurium* (34). This bacterium is also an enteroinvasive pathogen that uses type III secretion to inject multiple effector proteins that facilitate its internalization. However, in contrast to *S. flexneri*, *S. typhimurium* remains enclosed in a vacuole where it replicates. Although different quantitative phosphoproteomics methods were employed, the comparison between the phosphoproteomes of cells infected by *S. flexneri* or *S. typhimurium* showed an overlap of 62 phosphopeptides corresponding to 57 phosphoproteins (Fig. 5*A*, supplemental Table S9). Hierarchical clustering and correlation analysis performed on shared phosphopeptides showed a strong correlation of phosphorylation changes with 61 phosphopeptides co-regulated after both infections (supplemental Fig. S7*A* and S7*B*). As expected, proteins involved in the actin cytoskeleton, microtubules, cell-cell adhesion, cell cycle or gene regulation were similarly regulated during infection by both pathogens (Fig. 5*B*). Taken together, these results identify new common molecular processes triggered by *S. flexneri* and *S. typhimurium* in infected epithelial cells, and provide the first large-scale comparison of host signaling after infection by different bacteria.

OspF has a Wide-Reaching Impact on Host Protein Phosphorylation—During infection, *S. flexneri* injects several type III effectors that manipulate the signaling pathways controlling the inflammatory response of infected cells. Several mechanisms of action have been characterized based on the enzymatic activity, the structure or the intracellular binding partners of these effectors. For instance, the effector OspF attenuates IL-8 expression via its phosphothreonine lyase activity that irreversibly dephosphorylates MAPKs p38 and ERK on a T-X-Y motif, thereby preventing downstream histone H3 phosphorylation (23). We experimentally confirmed that p38 and ERK phosphorylation was restored when cells were infected with a deletion mutant of OspF (Δ*ospF*) compared with wild-type-infected cells (Fig. 6*A*). Interestingly, we found that OspF interfered also with the phosphorylation of the kinase RIP2 and the transcription factor CREB (Fig. 6*A*), two proteins involved in the control of inflammation (77, 78), suggesting that OspF had a more complex effect on host signaling than expected. To evaluate its impact, the phosphoproteome of HeLa cells infected by Δ*ospF S. flexneri* was determined by LC-MS/MS. When we directly compared the phosphorylation changes triggered by Δ*ospF versus* wild-type infection (differential phosphoproteome) by hierarchical clustering, we found 377 peptides with increased phosphorylation and 86 with decreased phosphorylation (supplemental Table S10 and Fig. 6*B*), showing that OspF had a massive net negative impact on phosphorylation. As expected, phosphoproteomics data confirmed that OspF strongly dephosphorylated ERK and p38 at residues T202/Y204 and T180/Y182, respectively (supplemental Table S10). A systematic search for the T-X-Y motif, known to be the consensus motif for the OspF phosphothreonine lyase activity (79), identified GSK3A as a potential new target. To test this hypothesis, we tested whether a treatment with the ERK and p38 inhibitors, PD98059 and SB203580 respectively, abolished all OspF-dependent phosphorylation changes (supplemental Table S10). With a q value <0.01 and a minimum twofold-ratio, none of the phosphopeptides differentially regulated by OspF (supplemental Fig. S8*A*) remained significantly different from wild-type infection after pretreatment with MAPK inhibitors (supplemental Fig. S8*B*). In particular, PD98059 and SB203580 completely abolished GSK3A phosphorylation at T201 and Y203 (supplemental Fig. S8*B*), indicating that this protein was not a direct substrate of OspF. Taken together, these data suggest that the OspF-sensitive phosphorylation changes identified in this study result from the phosphothreonine lyase activity of this effector toward ERK and p38.

A STRING network representation of the differential phosphoproteome showed a core network of 136 proteins connected at least once (Fig. 6*C*). Some of these have direct or indirect connections to ERK and p38. A systematic search for the overrepresented phosphorylation motifs identified among others the *SP*/*TP* motif shared by the MAPKs, Cdc2 and Cdks as well as RXX*S*, which can be phosphorylated by RSK, a kinase identified in the differential phosphoproteome (Fig. 6*C*, supplemental Fig. S9).

It has been shown that OspF interferes with IL-8 expression in *S. flexneri*-infected cells (23). To further characterize the role of this effector during infection, we analyzed the biological functions of the differential phosphoproteome (Figs. 6*C* and 6*D*, supplemental Table S11). In line with an inhibition of

Protein Phosphorylation During Bacterial Infection

A

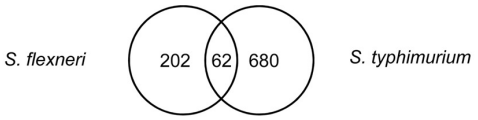

B

Protein ID	Protein Name	Phosphosites	Phosphorylation changes		Function
			S. flex.	*S. typhi.*	
TRIO	Triple functional domain protein	S2455/ S2459	↑	↑	Cytoskeleton
FMNL	Formin-like protein 1	S184	↓	↓	
IQGA2	Ras GTPase-activating-like protein	S16	↑	↑	
FBP1L	Formin-binding protein 1-like	S488	↑	↑	
PALLD	Palladin	S641/ S893	↑	↑	
CD2AP	CD2-associated protein	S458	↓	↓	
CTND1	Catenin delta-1	S252/ S268	↓	↓	
ZO1	Tight junction protein ZO-1	S617	↓	↓	
EPIPL	Epiplakin	S2691	↑	↑	
PLEC1	Plectin-1	S4626	↑	↑	
MAP1B	Microtubule-associated protein 1B	S2209/ S2211	↓	↓	
MAP7	Ensconsin	S365	↓	↓	
MYPT1	Protein phosphatase 1 regulatory subunit 12A	S507	↑	↑	
HSPB1	Heat shock protein beta-1	S15/ S82	↑	↑	
AHNK	Neuroblast differentiation-associated protein AHNAK	S210/ S5780/ S5784	↑	↑	Signaling
CXCR4	C-X-C chemokine receptor type 4	S324/ S325	↑	↑	
GAPD1	GTPase-activating protein and VPS9 domain-containing protein 1	S903	↑	↑	
TENS3	Tensin-3	S776	↑	↑	
PHIP	PH-interacting protein	S674	↑	↑	
AKP13	A-kinase anchor protein 13	S2567	↑	↑	
AKAP1	A kinase anchor protein 1, mitochondrial	S151	↑	↑	
APBB2	Amyloid beta A4 precursor protein-binding family B member 2	S123	↑	↑	
PB1	Protein polybromo-1	S39	↑	↑	
SH24A	SH2 domain-containing protein 4A	S315	↑	↑	
KIF4A	Chromosome-associated kinesin KIF4A	S801	↑	↑	Cell cycle
RIR2	Ribonucleoside-diphosphate reductase subunit M2	S20	↓	↓	
2A5D	Serine/threonine-protein phosphatase 2A regulatory subunit delta	S573	↑	↑	
BOD1L	Biorientation of chromosomes in cell division protein 1-like	S635	↑	↑	
SIPA1	Signal-induced proliferation-associated protein 1	S55	↑	↑	
SEPT9	Septin-9	S30	↑	↑	
DC1L1	Cytoplasmic dynein 1 light intermediate chain 1	T513/ T515	↑	↑	
BET1	BET1 homolog	S50	↑	↑	Transport
RAB7A	Ras-related protein Rab-7a	S72	↑	↑	
DEN4C	DENN domain-containing protein 4C	S1089	↑	↑	
GOGA5	Golgin subfamily A member 5	S116	↑	↑	
ACLY	ATP-citrate synthase	S455	↑	↑	Metabolism
S39A6	Zinc transporter ZIP6	S472	↑	↑	
NU214	Nuclear pore complex protein Nup214	S1023	↑	↑	Nuclear pore
NUP50	Nucleoporin 50 kDa	S221	↑	↑	
SNUT1	U4/U6.U5 tri-snRNP-associated protein 1	S448	↑	↑	Gene regulation
NCBP1	Nuclear cap-binding protein subunit 1	S22	↑	↑	
NUFP2	Nuclear fragile X mental retardation-interacting protein 2	S652	↑	↑	
PAIRB	Plasminogen activator inhibitor 1 RNA-binding protein	S330	↑	↑	
RBM14	RNA-binding protein 14	S618	↑	↑	
NELFE	Negative elongation factor E	S115	↑	↑	
HCFC1	Host cell factor	S666	↑	↑	
TR150	Thyroid hormone receptor-associated protein 3	S575	↑	↑	
PDCD4	Programmed cell death protein 4	S76/ S457	↑	↑	Miscellaneous/ Unknown
PRKRA	Interferon-inducible double stranded RNA-dependent protein kinase activator A	T20	↑	↑	
ZC11A	Zinc finger CCCH domain-containing protein 11A	S758	↑	↑	
FCHO2	FCH domain only protein 2	S387	↓	↓	
ZC3HD	Zinc finger CCCH domain-containing protein 13	S1014/ S1017	↓	↓	
PXDC2	Plexin domain-containing protein 2	S506	↑	↑	
EH1L1	EH domain-binding protein 1-like protein 1	S310	↑	↑	
TB182	182 kDa tankyrase-1-binding protein	S836	↑	↑	
K1522	Uncharacterized protein KIAA1522	S862	↓	↓	
CT2NL	CTTNBP2 N-terminal-like protein	T570	↓	↑	

FIG. 5. **S. flexneri and *S. typhimurium* infections trigger common host phosphorylation changes.** *A*, Venn diagram showing the overlap of phosphopeptides undergoing significant phosphorylation changes after *S. flexneri* infection (15 and 30 min) and *S. typhimurium* infection (10 and 20 min). For *S. typhimurium* infection, the phosphorylation events identified in different cellular compartments were compiled. B, Phosphoproteins undergoing significant phosphorylation changes after both *S. flexneri* and *S. typhimurium* infections. Phosphoproteins were grouped according to different biological functions. Arrows indicate whether there is an increase or decrease in phosphorylation.

gene expression (23), many proteins involved in transcription, chromatin modification and RNA processing were affected by OspF. Phosphorylation changes in several NPC proteins were also observed. In addition, phosphoproteins related to various biological functions including actin cytoskeleton, microtubules, apoptosis and cell cycle were also affected by OspF (Fig. 6*D*). Altogether, these results show that OspF has a massive impact on host protein phosphorylation and illustrate

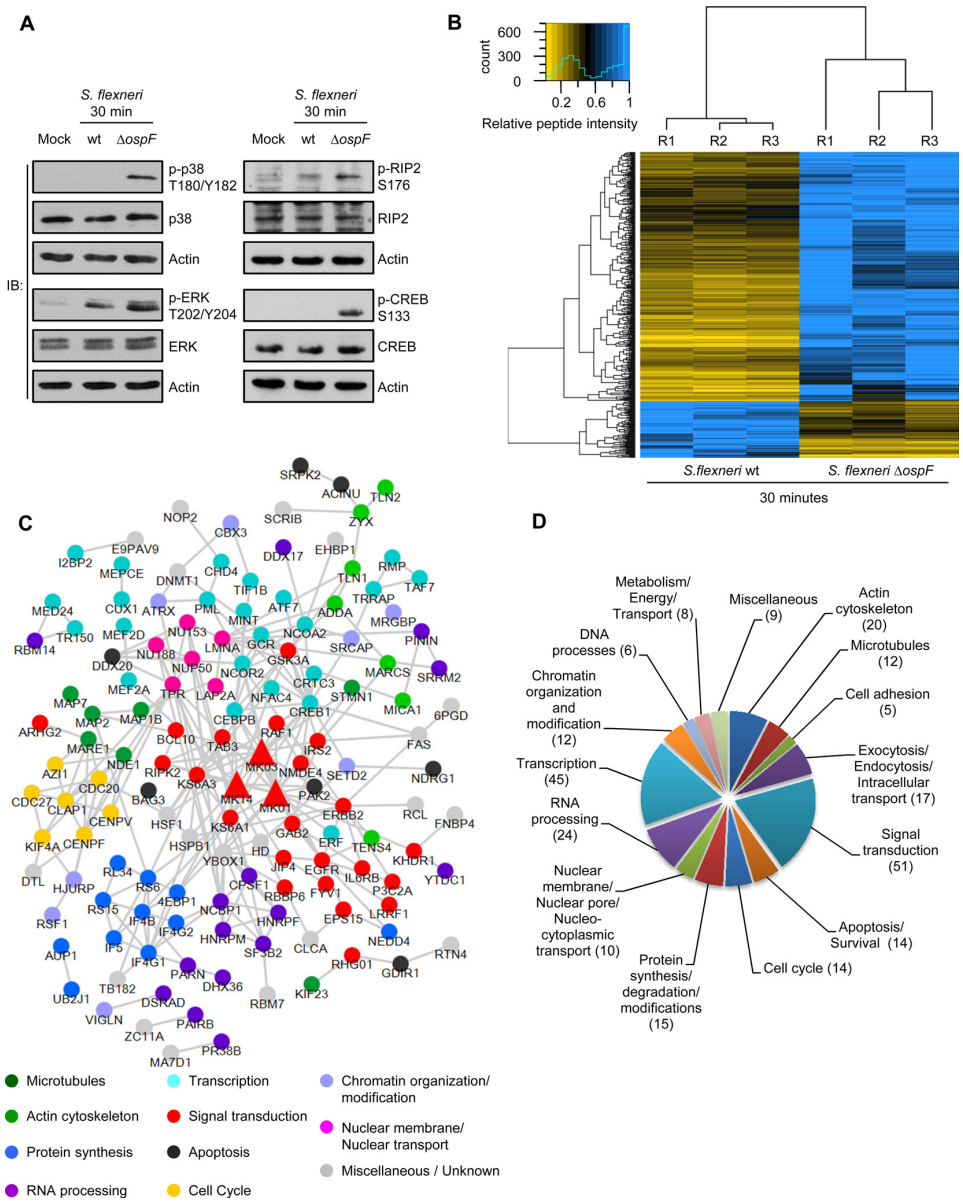

FIG. 6. **OspF has a wide -reaching impact on host protein phosphorylation.** *A*, OspF affects the phosphorylation of several signaling proteins involved in inflammation signaling. Left panels: OspF blocks the activation of p38 and ERK during *S. flexneri* infection. HeLa cells were left untreated or infected with either *S. flexneri* wild-type or Δ*ospF* for 30 min. The phosphorylation of p38 and ERK on residues T180/Y182 and T202/Y204 respectively, was analyzed by immunoblotting using the indicated phospho-specific antibodies. Right panels: OspF affects the phosphorylation of RIP2 and CREB on residue S176 and S133 respectively. Cells were left untreated or infected with *S. flexneri* wild-type or Δ*ospF* for 30 min. The phosphorylation of RIP2 and CREB was analyzed by immunoblotting using the indicated phospho-specific antibodies. Actin was used as loading control (results representative of two independent experiments). *B*, Hierarchical clustering analysis of relative peptide intensities obtained from the three independent replicates of cells infected for 30 min with either *S. flexneri* wild-type or Δ*ospF*. Phosphopeptides showing a significant change between Δ*ospF* and wild-type condition (2-fold change, q-value <0.01) were taken for the hierarchical clustering. *C*, Graphical representation of the network of phosphoproteins affected by OspF (differential phosphoproteome). Phosphoproteins differentially phosphorylated between wild-type and Δ*ospF S. flexneri* were subjected to STRING (high confidence 0.7). Only proteins with at least one connection are represented. STRING data were combined to manual functional annotation. The known OspF targets p38 (MK14), ERK1 (MK03), and ERK2 (MK01) are highlighted by an increased node size. *D*, Manual functional annotation of proteins from the differential phosphoproteome. Numbers in brackets indicate the number of corresponding proteins.

that, by targeting the central hubs p38 and ERK, this effector shuts down a large fraction of the cellular network.

DISCUSSION

For the first time, we used phosphoproteomics to address the dynamics of protein phosphorylation during the first two hours of *S. flexneri* infection in epithelial cells. Using a label-free LC-MS/MS-based approach, we found more than three hundred proteins undergoing a significant change in phosphorylation after infection. This corresponded to 28% of all detected phosphoproteins, showing that infection by the enteroinvasive bacterium *S. flexneri* has a massive impact on host protein phosphorylation. Although label-free LC-MS/MS is not a comprehensive method, our study covered a large portion of the phosphoprotein space and was well-suited to reproducibly identify and quantify host phosphorylation changes after bacterial infection.

Gene ontology analysis and manual functional annotation of the phosphoproteome confirmed the importance of the actin cytoskeleton and microtubules during infection. This result was expected because the first two hours of infection cover the entry mechanism of *S. flexneri* and actin based-motility, two processes highly dependent on actin and microtubule remodeling and controlled by protein phosphorylation (33, 80). The identification of around 50 new phosphoproteins related to the cytoskeleton and the comparison between wild-type and Δ*virG* infection open a new avenue to elucidate the mechanisms of bacterial entry and actin-based motility, two critical processes that contribute to successful colonization of the intestinal epithelium in humans.

Further functional analysis of the phosphoproteome showed that the phosphorylation of proteins related to cell cycle was affected by infection. This result was consistent with a report by Iwai *et al.* showing that the secreted effector IpaB causes cell-cycle arrest of epithelial cells by targeting Mad2L2, an anaphase-promoting complex/cyclosome (APC/C) inhibitor (54). The addition of Mad2L2 to the STRING network representation of the phosphoproteome shows that this protein interconnects with CDC23 and BUB1, component and substrate of APC/C respectively, which are important for cell cycle checkpoint enforcement. Interestingly, phosphoproteomics revealed that *S. flexneri* infection alters the phosphorylation of NPC proteins including Nup98, Nup50, Nu214 and TPR. NPCs are composed of around 30 different nucleoporins divided into scaffolding proteins that are important for nuclear pore assembly and maintenance, and peripheral proteins that function directly in nucleo-cytoplasmic transport. Noticeably, all proteins affected by *S. flexneri* infection belong to this second class. Follow up work is required to elucidate how infection impacts nuclear transport, and if trafficking of important host proteins or mRNA is affected during infection. Besides transport, recent studies indicate that peripheral proteins of NPCs can also directly contribute to gene regulation by interacting with chromatin and coupling transcription with mRNA export (81). It would be of particular interest to investigate whether changes in NPC protein phosphorylation can affect the expression of proinflammatory genes by this mechanism.

To better understand the host phosphorylation dynamics of *S. flexneri* infection and extract useful information regarding the roles of functional modules during infection, we used fuzzy c-means clustering to group all individual phosphopeptide based on the direction and the temporal profiles of phosphorylation changes after infection. Each cluster was then analyzed for the most frequent phospho-motifs and functional annotation of proteins. For clusters showing a fast (cluster 1) or slow reduction (cluster2) of phosphorylation, the *S*P phospho-motif was highly enriched. As this motif can be phosphorylated by MAPKs, we hypothesize that, for some proteins, the reduction of phosphorylation results from the phosphothreonine lyase activity of OspF on p38 and ERK. Alternatively, a reduction of *S*P phosphorylation can also be explained by the inhibition of other kinases like CDC2 and CDK. In a nonexclusive manner, the activation of phosphatases may also play a role. Remarkably, proteins from cluster 1 were in majority involved in the regulation of the actin cytoskeleton, microtubules and cell adhesion. In contrast, proteins belonging to cluster 2 were essentially related to transcription. Among the other profiles of phosphorylation changes, cluster 6 showed maximal phosphorylation two hours post-infection. For this cluster, 14 proteins out of 21 were phosphorylated on an *S*Q motif, a known substrate of ATM, ATR and DNAPK. By monitoring the activation of ATM at different time-points of infection by immunoblotting, we observed a very similar kinetics of activation, suggesting that ATM phosphorylated the *S*Q-containing proteins of cluster 6. This hypothesis was confirmed by showing that the ATM inhibitor KU60019 inhibited the phosphorylation of most of them. As some of these proteins were associated with the p53 pathway and DNA repair, we propose that they compose a functional module related to genotoxic stress. This assumption is supported by a recent article reporting *S. flexneri*-induced genotoxic stress and ATM activation (82).

Finally, in the clusters showing an increase in phosphorylation, the *S*P and RXX*S* phospho-motifs were overrepresented. The latter can be phosphorylated by AGC kinases such as AKT, PKA, PKC, S6 kinase and the members of the RSK family. Whereas our phosphoproteomics data supported the activation of S6 kinase and RSK during infection, phosphorylated AKT was not detected. By using an antibody that recognizes the active form of AKT, we confirmed its activation after *S. flexneri* infection and localization at entry foci. Although it was reported that AKT activation requires an IpgD-dependent production of phosphatidylinositol 5 monophosphate (62) and EGF receptor signaling (83), its exact mechanism of activation remains unclear. Here we found that AKT activation was sensitive to PP242 but not to rapamycin, and was abolished in cells depleted of Rictor, showing clearly

that AKT activation was dependent on mTORC2. The implication of mTORC2 was also supported by the phosphoproteomics data showing that both mSin1 and Rictor underwent a change in phosphorylation during *S. flexneri* infection. Further experiments are required to test how mTORC2 is activated during infection. Because AKT controls the survival of infected cells (62, 76), our data indicated that mTORC2 was involved in the regulation of cell fate during infection. Interestingly, although mTORC2 can regulate the actin cytoskeleton (74), bacterial entry was not affected by the inhibition of mTORC2. In addition, phosphoproteomics revealed a rapid change in phosphorylation for the two mTORC1 components Raptor and PRAS40, indicating that mTORC1 was implicated in the early phase of infection. This finding was supported by the observation that the phosphorylation of S6 kinase and S6 ribosomal protein observed 15 min post infection was sensitive to rapamycin and PP242 treatment. Because these two proteins are known to regulate protein translation, these results suggested that mTORC1 participates to the control of host protein synthesis during *S. flexneri* infection. Interestingly, a recent report by Tattoli *et al.* shows that *S. flexneri* infection leads to amino acid starvation and to a subsequent down-regulation of mTORC1 activity that induces autophagy (84). The authors report that amino acid starvation is sensed by GCN2 which becomes phosphorylated within the first hour of infection. Altogether, these two studies support the roles of both mTORC1 and mTORC2, and identify mTOR as a central host player of *S. flexneri* infection.

Phosphoproteomics is a method that has been applied only recently to the field of bacterial infection with a first study by Rogers *et al.* investigating *S. typhimurium* infection of epithelial cells (34). As *S. flexneri* and *S. typhimurium* are closely related and both harbor a type III secretion system with several homologue effectors, we compared the respective phosphoproteomes of infected HeLa cells. Although major differences in sample preparation and phosphoproteomics methodology exist between the two studies (85), 61 coregulated phosphopeptides were discovered. Considering that phosphoproteomics techniques fail to capture all cellular phosphoproteins, this number is mostly likely underestimated. These results demonstrated that *S. flexneri* and *S. typhimurium* induce various common host molecular processes in infected cells. Among the shared phosphopeptides, many belong to proteins related to the cytoskeleton and its regulation. For instance, the protein palladin, strongly phosphorylated after *S. flexneri* and *S. typhimurium* infection, is known to localize at sites of actin remodeling including ruffles and lamellipodia. The protein IQGAP2 interacts with CDC42 and Rac1, two GTPases required for efficient bacterial entry (86, 87). Taken together, these data constitute the first large-scale comparison of host signaling after infection by different pathogenic bacteria. By identifying the common phosphorylation events, this approach allows to define the host pathways that are co-regulated by pathogens, and may facilitate the identification of processes that could be targeted by broad-spectrum drugs in the perspective of treatments against bacterial infections.

As previously described, *S. flexneri* secretes different effectors that manipulate host signaling to finely tune the inflammatory response of infected cells. For instance, it was proposed that OspF blocks the expression of IL-8 by altering the phosphorylation of histone H3 and the access of transcription factors to chromatin (23). Phosphoproteomics revealed that OspF affects the phosphorylation of more than three hundred proteins, showing that this effector has a wider impact than anticipated. The MAPK inhibitors, PD98059 and SB203580, abolished all OspF-dependent phosphorylation changes, suggesting that they resulted from its phosphothreonine lyase activity toward p38 and ERK. In line with an effect of OspF on gene regulation, the phosphorylation of various proteins associated with transcription, chromatin modification and RNA processing was strongly affected. However, the biological functions and the number of proteins impacted by OspF strongly suggested that a reduction of histone H3 phosphorylation was not the only mechanism by which the effector OspF affected IL-8 expression in infected cells. Further functional analysis revealed that phosphoproteins associated with the actin cytoskeleton, microtubules, cell cycle and intracellular transport were also altered by OspF. Altogether, these results illustrate how *S. flexneri* effectively alters a large fraction of the host protein phosphorylation network via a single effector. They also demonstrate that OspF can be used as a molecular tool to discover new targets of MAPKs, and decipher novel downstream regulatory mechanisms.

In summary, we used quantitative phosphoproteomics to investigate host signaling during *S. flexneri* infection of epithelial cells. We found several hundred of proteins undergoing a significant change in phosphorylation during the first two hours of infection. Dynamics studies combined with functional annotation and phospho-motif enrichment demonstrated alterations of proteins involved in different cellular functions, including the cytoskeleton, cell cycle, transcription, and genotoxic stress responses. In addition, we discovered an early signaling function of mTOR during infection, and characterized the impact of OspF on host protein phosphorylation. In conclusion, these data provide the first systems-level overview of host signaling during the first hours of a bacterial infection, and constitute a valuable resource for generating testable hypotheses related to host-pathogen interactions.

Acknowledgments—We thank Prof. Mike Hall (Biozentrum, University of Basel) for the use of inducible rictor-knockout mouse embryonic fibroblasts, Dr. Timo Glatter for advice regarding LC-MS/MS sample preparation and data analysis, and Dr. Simon Ittig for critical reading of the manuscript.

* This work was supported by the Swiss National Science Foundation (grant 310030-138377/1 to C.A.) and the InfectX and BattleX projects from SystemsX.ch.

§ To whom correspondence should be addressed: Focal Area Infection Biology, Biozentrum, University of Basel, Klingelbergstrasse 50/70, CH-4056 Basel, Switzerland. Tel.: +41 61 267 21 20; Fax: +41 61 267 21 18; E-mail: cecile.arrieumerlou@unibas.ch.

S This article contains supplemental Figs. S1 to S9, Tables S1 to S12 and File S1.

Author Contributions: Conceived and designed the experiments: CS, CA, AS. Performed the experiments: CS, IS, TT, RD. Analyzed the data: CS, AS, EA, CA, CK. Contributed materials/analysis tools: AS, EA, CK. Wrote the paper: CA, CS.

Conflict of Interest: The authors declare that they have no conflict of interest.

REFERENCES

1. Kotloff, K. L., Winickoff, J. P., Ivanoff, B., Clemens, J. D., Swerdlow, D. L., Sansonetti, P. J., Adak, G. K., and Levine, M. M. (1999) Global burden of Shigella infections: implications for vaccine development and implementation of control strategies. *Bull. World Health Organ.* **77,** 651–666
2. Schroeder, G. N., and Hilbi, H. (2008) Molecular Pathogenesis of Shigella spp.: Controlling Host Cell Signaling, *Invasion, and Death by Type III Secretion. Clin. Microbiol. Rev.* **21,** 134–156
3. Sansonetti, P. J., Arondel, J., Cantey, J. R., Prévost, M. C., and Huerre, M. (1996) Infection of rabbit Peyer's patches by Shigella flexneri: effect of adhesive or invasive bacterial phenotypes on follicle-associated epithelium. *Infect. Immun.* **64,** 2752–2764
4. Wassef, J. S., Keren, D. F., and Mailloux, J. L. (1989) Role of M cells in initial antigen uptake and in ulcer formation in the rabbit intestinal loop model of shigellosis. *Infect. Immun.* **57,** 858–863
5. Nonaka, T., Kuwabara, T., Mimuro, H., Kuwae, A., and Imajoh-Ohmi, S. (2003) Shigella-induced necrosis and apoptosis of U937 cells and J774 macrophages. *Microbiology* **149,** 2513–2527
6. Zychlinsky, A., Prevost, M. C., Sansonetti, P. J. (1992) Shigella flexneri induces apoptosis in infected macrophages. *Nature* **358,** 167–169
7. Sansonetti, P. J., Phalipon, A., Arondel, J., Thirumalai, K., Banerjee, S., Akira, S., Takeda, K., and Zychlinsky, A. (2000) Caspase-1 activation of IL-1β and IL-18 are essential for Shigella flexneri–induced inflammation. *Immunity* **12,** 581–590
8. Zychlinsky, A., Fitting, C., Cavaillon, J. M., and Sansonetti, P. J. (1994) Interleukin 1 is released by murine macrophages during apoptosis induced by Shigella flexneri. *J. Clin. Invest.* **94,** 1328–1332
9. Mounier, J., Vasselon, T., Hellio, R., Lesourd, M., and Sansonetti, P. J. (1992) Shigella flexneri enters human colonic Caco-2 epithelial cells through the basolateral pole. *Infect. Immun.* **60,** 237–248
10. Blocker, A., Gounon, P., Larquet, E., Niebuhr, K., Cabiaux, V., Parsot, C., and Sansonetti, P. (1999) The tripartite type III secreton of Shigella flexneri inserts Ipab and Ipac into host membranes. *J. Cell Biol.* **147,** 683–693
11. Parsot, C. (2009) Shigella type III secretion effectors: how, where, when, for what purposes? *Curr. Opin. Microbiol.* **12,** 110–116
12. Frank Lafont, G. T. V. N., Kentaro, H., Sansonetti, P., and Gisou van der Goot F. (2002) Initial steps of Shigella infection depend on the cholesterol/sphingolipid raft-mediated CD44–IpaB interaction. *EMBO J.* **21,** 4449–4457
13. Watarai, M. F. S., Sasakawa C. (1996) Interaction of Ipa proteins of Shigella flexneri with alpha5beta1 integrin promotes entry of the bacteria into mammalian cells. *J. Exp. Med.* **183,** 991–999
14. Skoudy, A., Mounier, J., Aruffo, A., Ohayon, H., Gounon, P., Sansonetti, P., and Tran Van Nhieu, G. (2000) CD44 binds to the Shigella IpaB protein and participates in bacterial invasion of epithelial cells. *Cell Microbiol.* **2,** 19–33
15. Boquet, P., and Lemichez, E. (2003) Bacterial virulence factors targeting Rho GTPases: parasitism or symbiosis? *Trends Cell Biol.* **13,** 238–246
16. Mounier, J., Laurent, V., Hall, A., Fort, P., Carlier, M. F., Sansonetti, P. J., and Egile, C. (1999) Rho family GTPases control entry of Shigella flexneri into epithelial cells but not intracellular motility. *J. Cell Sci.* **112,** 2069–2080
17. Sansonetti, P. J., Ryter, A., Clerc, P., Maurelli, A. T., and Mounier, J. (1986) Multiplication of Shigella flexneri within HeLa cells: lysis of the phagocytic vacuole and plasmid-mediated contact hemolysis. *Infect. Immun.* **51,** 461–469
18. Bernardini, M. L., Mounier, J., d'Hauteville, H., Coquis-Rondon, M., and Sansonetti, P. J. (1989) Identification of icsA, a plasmid locus of Shigella flexneri that governs bacterial intra- and intercellular spread through interaction with F-actin. *Proc. Natl. Acad. Sci. U.S.A.* **86,** 3867–3871
19. Goldberg, M. B., and Theriot, J. A. (1995) Shigella flexneri surface protein IcsA is sufficient to direct actin-based motility. *Proc. Natl. Acad. Sci. U.S.A.* **92,** 6572–6576
20. Egile, C., Loisel, T. P., Laurent, V., Li, R., Pantaloni, D., Sansonetti, P. J., and Carlier, M. F. (1999) Activation of the Cdc42 effector N-Wasp by the Shigella flexneri Icsa protein promotes actin nucleation by Arp2/3 complex and bacterial actin-based motility. *J. Cell Biol.* **146,** 1319–1332
21. Sansonetti, P. J., Arondel, J., Huerre, M., Harada, A., and Matsushima, K. (1999) Interleukin-8 controls bacterial transepithelial translocation at the cost of epithelial destruction in experimental shigellosis. *Infect. Immun.* **67,** 1471–1480
22. Girardin, S. E., Boneca, I. G., Carneiro, L. A. M., Antignac, A., Jéhanno, M., Viala, J., Tedin, K., Taha, M.-K., Labigne, A., Zähringer, U., Coyle, A. J., DiStefano, P. S., Bertin, J., Sansonetti, P. J., and Philpott, D. J. (2003) Nod1 detects a unique muropeptide from gram-negative bacterial peptidoglycan. *Science* **300,** 1584–1587
23. Arbibe, L., Kim, D. W., Batsche, E., Pedron, T., Mateescu, B., Muchardt, C., Parsot, C., and Sansonetti, P. J. (2007) An injected bacterial effector targets chromatin access for transcription factor NF-[kappa]B to alter transcription of host genes involved in immune responses. *Nat. Immunol.* **8,** 47–56
24. Li, H., Xu, H., Zhou, Y., Zhang, J., Long, C., Li, S., Chen, S., Zhou, J. M., and Shao, F. (2007) The phosphothreonine lyase activity of a bacterial type III effector family. *Science* **315,** 1000–1003
25. Kasper, C. A., Sorg, I., Schmutz, C., Tschon, T., Wischnewski, H., Kim, M. L., and Arrieumerlou, C. (2010) Cell-Cell Propagation of NF-κB transcription factor and MAP kinase activation amplifies innate immunity against bacterial infection. *Immunity* **33,** 804–816
26. Ray, K., Marteyn, B., Sansonetti, P. J., and Tang, C. M. (2009) Life on the inside: the intracellular lifestyle of cytosolic bacteria. *Nat. Rev. Micro.* **7,** 333–340
27. Ashida, H., Ogawa, M., Kim, M., Mimuro, H., and Sasakawa, C. (2012) Bacteria and host interactions in the gut epithelial barrier. *Nat. Chem. Biol.* **8,** 36–45
28. Pédron, T., Thibault, C., and Sansonetti, P. J. (2003) The invasive phenotype of Shigella flexneri directs a distinct gene expression pattern in the human intestinal epithelial cell line Caco-2. *J. Biol. Chem.* **278,** 33878–33886
29. Faherty, C. S., Merrell, D. S., Semino-Mora, C., Dubois, A., Ramaswamy, A. V., and Maurell, A. T. (2010) Microarray analysis of Shigella flexneri-infected epithelial cells identifies host factors important for apoptosis inhibition. *BMC Genomics* **11,** 272–290
30. Stephen, E., Girardin, R. T., Mavris, M., Page, A. L., Li, X., Stark, G. R., Bertin, J., DiStefano, P. S., Yaniv, M., Sansonetti, P., J., and Philpott, D. J. (2001) CARD4/Nod1 mediates NF-κB and JNK activation by invasive Shigella flexneri. *EMBO Rep* **2,** 736–742
31. Kim, M. L., Jeong, H. G., Kasper, C. A., and Arrieumerlou, C. (2010) IKKα Contributes to Canonical NF-κB Activation Downstream of Nod1-Mediated Peptidoglycan Recognition. *PLoS ONE* **5,** e15371
32. Reiterer, V., Grossniklaus, L., Tschon, T., Kasper, C. A., Sorg, I., and Arrieumerlou, C. (2011) Shigella flexneri type III secreted effector OspF reveals new crosstalks of proinflammatory signaling pathways during bacterial infection. *Cell Signal.* **23,** 1188–1196
33. Tran Van Nhieu, G., Enninga, J., Sansonetti, P., and Grompone, G. (2005) Tyrosine kinase signaling and type III effectors orchestrating Shigella invasion. *Curr. Opin. Microbiol.* **8,** 16–20
34. Rogers, L. D., Brown, N. F., Fang, Y., Pelech, S., and Foster, L. J. (2011) Phosphoproteomic analysis of salmonella-infected cells identifies key kinase regulators and SopB-dependent host phosphorylation events. *Sci. Signal.* **4,** rs9
35. Cybulski, N., Zinzalla, V., and Hall, M. N. (2012) Inducible raptor and rictor Knockout Mouse Embryonic Fibroblasts. *Methods Mol. Biol.* **821,** 267–278
36. Kim, M. L., Jeong, H. G., Kasper, C. A., and Arrieumerlou, C. (2010) IKKalpha contributes to canonical NF-kappaB activation downstream of Nod1-mediated peptidoglycan recognition. *PLoS One* **5,** e15371
37. Carpenter, A., Jones, T., Lamprecht, M., Clarke, C., Kang, I., Friman, O., Guertin, D., Chang, J., Lindquist, R., Moffat, J., Golland, P., and Sabatini,

D. (2006) CellProfiler: image analysis software for identifying and quantifying cell phenotypes. *Genome Biol.* **7,** R100
38. Bensimon, A., Schmidt, A., Ziv, Y., Elkon, R., Wang, S.-Y., Chen, D. J., Aebersold, R., and Shiloh, Y. (2010) ATM-dependent and -independent dynamics of the nuclear phosphoproteome after DNA damage. *Sci. Signal*. **3,** rs3
39. Perkins, D. N., Pappin, D. J. C., Creasy, D. M., and Cottrell, J. S. (1999) Probability-based protein identification by searching sequence databases using mass spectrometry data. *Electrophoresis* **20,** 3551–3567
40. Smyth, and Gordon, K. (2004) Linear Models and Empirical Bayes Methods for Assessing Differential Expression in Microarray Experiments. *Stat. Appl. Genet. Mol. Biol.* **3**
41. Ting, L., Cowley, M. J., Hoon, S. L., Guilhaus, M., Raftery, M. J., and Cavicchioli, R. (2009) Normalization and statistical analysis of quantitative proteomics data generated by metabolic labeling. *Mol. Cell. Proteomics* **8,** 2227–2242
42. Vizcaíno, J. A., Côté, R. G., Csordas, A., Dianes, J. A., Fabregat, A., Foster, J. M., Griss, J., Alpi, E., Birim, M., Contell, J., O'Kelly, G., Schoenegger, A., Ovelleiro, D., Pérez-Riverol, Y., Reisinger, F., Ríos, D., Wang, R., and Hermjakob, H. (2013) The proteomics identifications (PRIDE) database and associated tools: status in 2013. *Nucleic Acids Res.* **41,** D1063–D1069
43. Huber, A., Bodenmiller, B., Uotila, A., Stahl, M., Wanka, S., Gerrits, B., Aebersold, R., and Loewith, R. (2009) Characterization of the rapamycin-sensitive phosphoproteome reveals that Sch9 is a central coordinator of protein synthesis. *Genes Dev.* **23** 1929–1943
44. Olsen, J. V., Blagoev, B., Gnad, F., Macek, B., Kumar, C., Mortensen, P., and Mann, M. (2006) Global, in vivo, and site-specific phosphorylation dynamics in signaling networks. *Cell* **127,** 635–648
45. Schilling, B., Rardin, M. J., MacLean, B. X., Zawadzka, A. M., Frewen, B. E., Cusack, M. P., Sorensen, D. J., Bereman, M. S., Jing, E., Wu, C. C., Verdin, E., Kahn, C. R., MacCoss, M. J., and Gibson, B. W. (2012) Platform-independent and label-free quantitation of proteomic data using MS1 extracted ion chromatograms in Skyline. *Mol. Cell. Proteomics* **11,** 202–214
46. Schmidt, A., Beck, M., Malmstrom, J., Lam, H., Claassen, M., Campbell, D., and Aebersold, R. (2011) Absolute quantification of microbial proteomes at different states by directed mass spectrometry. *Mol. Syst. Biol.* **7**
47. Glatter, T., Ludwig, C., Ahrné, E., Aebersold, R., Heck, A. J. R., and Schmidt, A. (2012) Large-scale quantitative assessment of different in-solution protein digestion protocols reveals superior cleavage efficiency of tandem Lys-C/trypsin proteolysis over trypsin digestion. *J. Proteome Res.* **11,** 5145–5156
48. Köhler, H., R., S., and McCormick, B. A. (2002) Shigella flexneri interactions with the basolateral membrane domain of polarized model intestinal epithelium: role of lipopolysaccharide in cell invasion and in activation of the mitogen-activated protein kinase ERK. *Infect. Immun.* **70,** 1150–1158
49. Huang, D. W., Sherman, B. T., and Lempicki, R. A. ((2008) Systematic and integrative analysis of large gene lists using DAVID bioinformatics resources. *Nat. Protocols* **4,** 44–57
50. Huang, D. W., Sherman, B. T., and Lempicki, R. A. (2009) Bioinformatics enrichment tools: paths toward the comprehensive functional analysis of large gene lists. *Nucleic Acids Res.* **37,** 1–13
51. Nobes, C. D., and Hall, A. (1995) Rho, Rac, and Cdc42 GTPases regulate the assembly of multimolecular focal complexes associated with actin stress fibers, lamellipodia, and filopodia. *Cell* **81,** 53–62
52. Ridley, A. J. H. A. (1992) Distinct patterns of actin organization regulated by the small GTP-binding proteins Rac and Rho. *Cold Spring Harb. Symp. Quant. Biol.* **57,** 10
53. Sakaguchi, T., Köhler, H., Gu, X., McCormick, B. A., and Reinecker, H. C. (2002) Shigella flexneri regulates tight junction-associated proteins in human intestinal epithelial cells. *Cell Microbiol.* **4,** 367–381
54. Iwai, H., Kim, M., Yoshikawa, Y., Ashida, H., Ogawa, M., Fujita, Y., Muller, D., Kirikae, T., Jackson, P. K., Kotani, S., and Sasakawa, C. (2007) A bacterial effector targets Mad2L2, an APC inhibitor, to modulate host cell cycling. *Cell* **130,** 611–623
55. Cao, L., Y., W., Wu, Y., and Yu, L. (2009) The evolution, complex structures and function of septin proteins. *Cell Mol. Life Sci.* **66,** 3309–3323
56. Mostowy, S., Bonazzi, M., Hamon, M. A., Tham, T. N., Mallet, A., Lelek, M., Gouin, E., Demangel, C., Brosch, R., Zimmer, C., Sartori, A., Kinoshita, M., Lecuit, M., and Cossart, P. (2010) Entrapment of intracytosolic bacteria by septin cage-like structures. *Cell Host Microbe* **8,** 433–444
57. Mostowy, S., Nam Tham, T., Danckaert, A., Guadagnini, S., Boisson-Dupuis, S., Pizarro-Cerdá, J., and Cossart, P. (2009) Septins regulate bacterial entry into host cells. *PLoS ONE* **4,** e4196
58. Carneiro, L. A. M., Travassos, L. H., Soares, F., Tattoli, I., Magalhaes, J. G., Bozza, M. T., Plotkowski, M. C., Sansonetti, P. J., Molkentin, J. D., Philpott, D. J., and Girardin, S. E. (2009) Shigella induces mitochondrial dysfunction and cell death in nonmyeloid cells. *Cell Host Microbe* **5,** 123–136
59. Szklarczyk, D., Franceschini, A., Kuhn, M., Simonovic, M., Roth, A., Minguez, P., Doerks, T., Stark, M., Muller, J., Bork, P., Jensen, L. J., and Mering, C. v. (2011) The STRING database in 2011: functional interaction networks of proteins, globally integrated and scored. *Nucleic Acids Res.* **39,** D561–D568
60. Schwartz, D., and Gygi, S. P. (2005) An iterative statistical approach to the identification of protein phosphorylation motifs from large-scale data sets. *Nat. Biotech.* **23,** 1391–1398
61. Manning, G., Whyte, D. B., Martinez, R., Hunter, T., and Sudarsanam, S. (2002) The protein kinase complement of the human genome. *Science* **298,** 1912–1934
62. Pendaries, C., Tronchere, H., Arbibe, L., Mounier, J., Gozani, O., Cantley, L., Fry, M. J., Gaits-Iacovoni, F., Sansonetti, P. J., and Payrastre, B. (2006) PtdIns(5)P activates the host cell PI3-kinase/Akt pathway during Shigella flexneri infection. *EMBO J.* **25,** 1024–1034
63. M., F. (2005) Noise-robust soft clustering of gene expression time-course data. *J. Bioinform. Comput. Biol.* **3,** 965–988
64. Kim, S. T., Lim, D. S., Canman, C. E., and Kastan, M. B. (1999) Substrate specificities and identification of putative substrates of ATM kinase family members. *J. Biol. Chem.* **274,** 37538–37543
65. O'Neill, T., Dwyer, A. J., Ziv, Y., Chan, D. W., Lees-Miller, S. P., Abraham, R. H., Lai, J. H., Hill, D., Shiloh, Y., Cantley, L. C., and Rathbun, G. A. (2000) Utilization of oriented peptide libraries to identify substrate motifs selected by ATM. *J. Biol. Chem.* **275,** 22719–22727
66. Wang, B., Matsuoka, S., Carpenter, P. B., and Elledge, S. J. (2002) 53BP1, a Mediator of the DNA damage checkpoint. *Science* **298,** 1435–1438
67. Hartley, K. O., Gell, D., Smith, G. C. M., Zhang, H., Divecha, N., Connelly, M. A., Admon, A., Lees-Miller, S. P., Anderson, C. W., and Jackson, S. P. (1995) DNA-dependent protein kinase catalytic subunit: A relative of phosphatidylinositol 3-kinase and the ataxia telangiectasia gene product. *Cell* **82,** 849–856
68. Kim, H., Chen, J., and Yu, X. (2007) Ubiquitin-binding protein RAP80 mediates BRCA1-dependent DNA damage response. *Science* **316,** 1202–1205
69. Beli, P., Lukashchuk, N., Wagner, Sebastian A., Weinert, Brian T., Olsen, Jesper V., Baskcomb, L., Mann, M., Jackson, Stephen P., and Choudhary, C. (2012) Proteomic investigations reveal a role for RNA processing factor THRAP3 in the DNA a *Mol. Cell* **46,** 212–225
70. Kanehisa, M., and Goto, S. (2000) KEGG: Kyoto encyclopedia of genes and genomes. *Nucleic Acids Res.* **28,** 27–30
71. Kanehisa, M., Goto, S., Sato, Y., Furumichi, M., and Tanabe, M. (2012) KEGG for integration and interpretation of large-scale molecular data sets. *Nucleic Acids Res.* **40,** D109–D114
72. Wullschleger, S., Loewith, R., and Hall, M. N. (2006) TOR Signaling in growth and metabolism. *Cell* **124,** 471–484
73. Laplante, M., and Sabatini, D. M. (2009) mTOR signaling at a glance. *J. Cell Sci.* **122,** 3589–3594
74. Jacinto, E., Loewith, R., Schmidt, A., Lin, S., Ruegg, M. A., Hall, A., and Hall, M. N. (2004) Mammalian TOR complex 2 controls the actin cytoskeleton and is rapamycin insensitive. *Nat. Cell Biol.* **6,** 1122–1128
75. Magnuson, B. E. B., and Fingar, D. C. (2012) Regulation and function of ribosomal protein S6 kinase (S6K) within mTOR signalling networks. *Biochem. J.* **441,** 1–21
76. Knodler, L. A., Finlay, B. B., and Steele-Mortimer, O. (2005) The salmonella effector protein SopB protects epithelial cells from apoptosis by sustained activation of Akt. *J. Biol. Chem.* **280,** 9058–9064
77. Newton, K., and Dixit, V. M. (2012) Signaling in innate immunity and inflammation. **4,** a006049
78. Chin, A. I., Dempsey, P. W., Bruhn, K., Miller, J. F., Xu, Y., and Cheng, G. (2002) Involvement of receptor-interacting protein 2 in innate and adaptive immune responses. *Nature* **416,** 190–194
79. Zhu, Y., Li, H., Long, C., Hu, L., Xu, H., Liu, L., Chen, S., Wang, D. C., and

Shao, F. (2007) Structural insights into the enzymatic mechanism of the pathogenic MAPK phosphothreonine lyase. *Mol. Cell* **28,** 899–913
80. Burton, E. A., Oliver, T. N., and Pendergast, A. M. (2005) Abl kinases regulate actin comet tail elongation via an N-WASP-dependent pathway. *Mol. Cell. Biol.* **25,** 8834–8843
81. Liang, Y., and Hetzer, M. W. (2011) Functional interactions between nucleoporins and chromatin. *Curr. Opin. Cell Biol.* **23,** 65–70
82. Bergounioux, J., Elisee, R., Prunier, A.-L., Donnadieu, F., Sperandio, B., Sansonetti, P., and Arbibe, L. (2012) Calpain activation by the Shigella flexneri effector VirA regulates key steps in the formation and life of the bacterium's epithelial niche. *Cell Host Microbe* **11,** 240–252
83. Ramel, D., Lagarrigue, F., Pons, V., Mounier, J., Dupuis-Coronas, S., Chicanne, G., Sansonetti, P. J., Gaits-Iacovoni, F., Tronchere, H., and Payrastre, B. (2011) Shigella flexneri infection generates the lipid PI5P to alter endocytosis and prevent termination of EGFR signaling. *Sci. Signal.* **4,** ra61
84. Tattoli, I., Sorbara, M. T., Vuckovic, D., Ling, A., Soares, F., Carneiro, Leticia A. M., Yang, C., Emili, A., Philpott, Dana J., and Girardin, Stephen E. (2012) Amino acid starvation induced by invasive bacterial pathogens triggers an innate host defense program. *Cell Host Microbe* **11,** 563–575
85. Eyrich, B., Sickmann, A., and Zahedi, R. P. (2011) Catch me if you can: Mass spectrometry-based phosphoproteomics and quantification strategies. *Proteomics* **11,** 554–570
86. Briggs, M. W., and Sacks, D. B. (2003) IQGAP proteins are integral components of cytoskeletal regulation. *EMBO Rep.* **4,** 571–574
87. Ohya, K., Handa, Y., Ogawa, M., Suzuki, M., and Sasakawa, C. (2005) IpgB1 is a novel shigella effector protein involved in bacterial invasion of host cells. *J. Biol. Chem.* **280,** 24022–24034
88. Schindelin, J., Arganda-Carreras, I., Frise, E., Kaynig, V., Longair, M., Pietzsch, T., Preibisch, S., Rueden, C., Saalfeld, S., Schmid, B., Tinevez, J.-Y., White, D. J., Hartenstein, V., Eliceiri, K., Tomancak, P., and Cardona, A. (2012) Fiji: an open-source platform for biological-image analysis. *Nat. Meth.* **9,** 676–682

SUPPLEMENTARY INFORMATION

Table of content

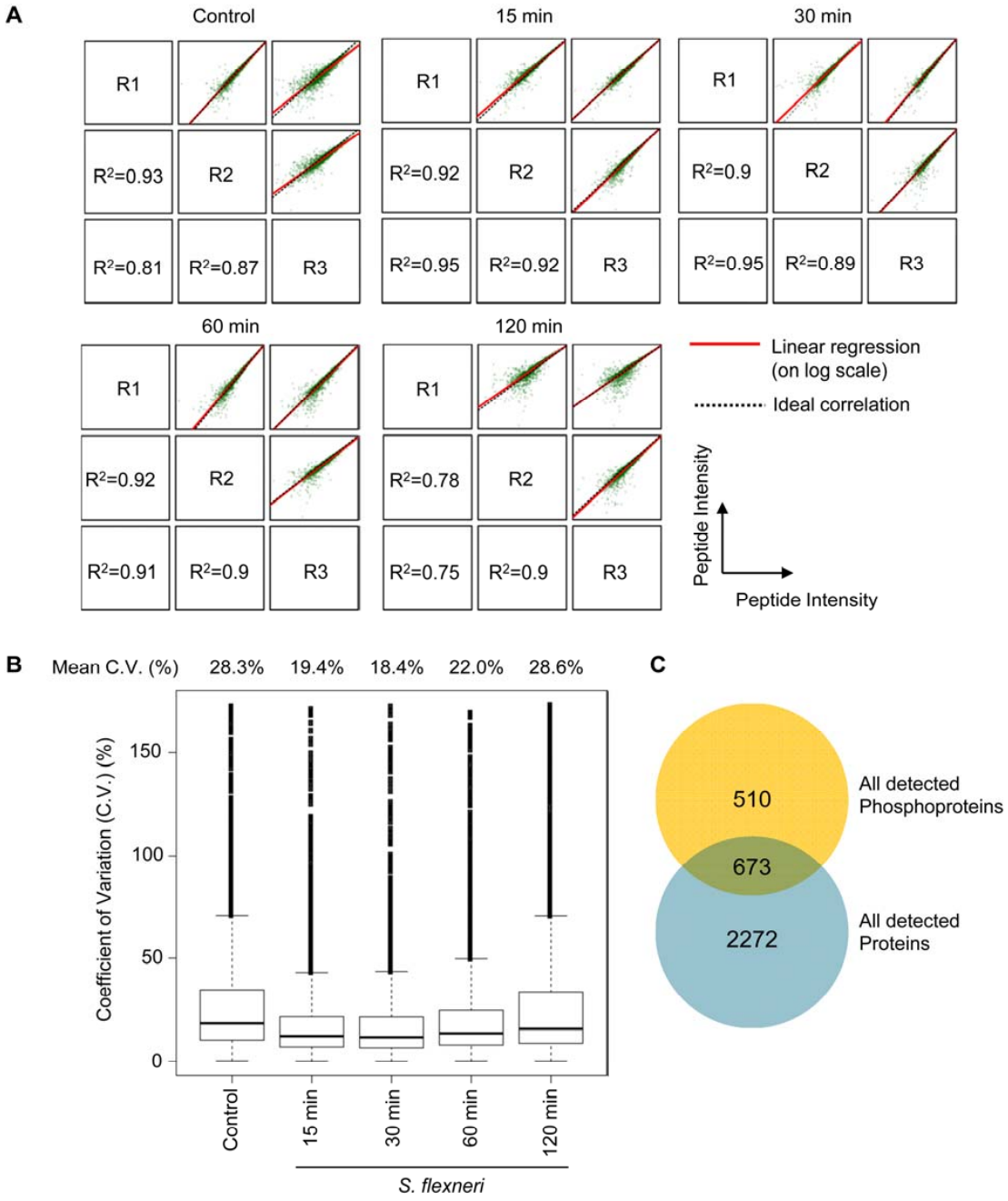
A
Control
15 min
30 min
R1
R2
R3
R²=0.93
R²=0.81
R²=0.87
R²=0.92
R²=0.95
R²=0.9
R²=0.89
60 min
120 min
R²=0.92
R²=0.91
R²=0.9
R²=0.78
R²=0.75
Linear regression (on log scale)
Ideal correlation
Peptide Intensity
Peptide Intensity
B
Mean C.V. (%)
28.3%
19.4%
18.4%
22.0%
28.6%
Coefficient of Variation (C.V.) (%)
150
100
50
0
Control
15 min
30 min
60 min
120 min
S. flexneri
C
510
673
2272
All detected Phosphoproteins
All detected Proteins

Figure S1

Figure S1: Quality control of the phosphoproteomics data

(A) Squared Pearson correlation coefficient R^2 of integrated peptide feature intensities between different replicates (R1, R2 and R3) of each condition. The linear regression of the integrated peptide feature intensities of two conditions is indicated in red, whereas the dashed line corresponds to direct proportionality. **(B)** Boxplot showing the coefficient of variance (C.V. in %) of the replicates for each condition. The median C.V. is indicated by the line in the box, the mean C.V. is indicated at the top of each boxplot. **(C)** Venn diagram showing the overlap between identified phosphoproteins and proteins.

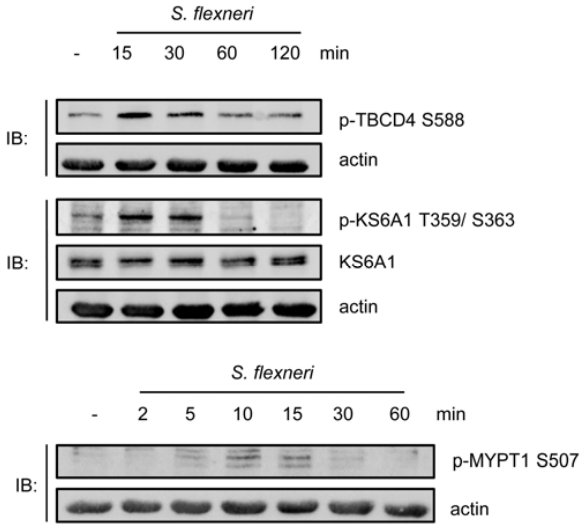

Figure S2

Figure S2: Validation of phosphoproteomics data by western blotting

TBCD4 becomes phosphorylated on S588, KS6A1 (RSK) on T359/ S363 and MYPT1 on S507 after *S. flexneri* infection. Cells were left untreated or infected for indicated time-periods with *S. flexneri*. Actin is shown as loading control. For KS6A1 (RSK), the total protein amount is shown. Data is representative of two independent experiments.

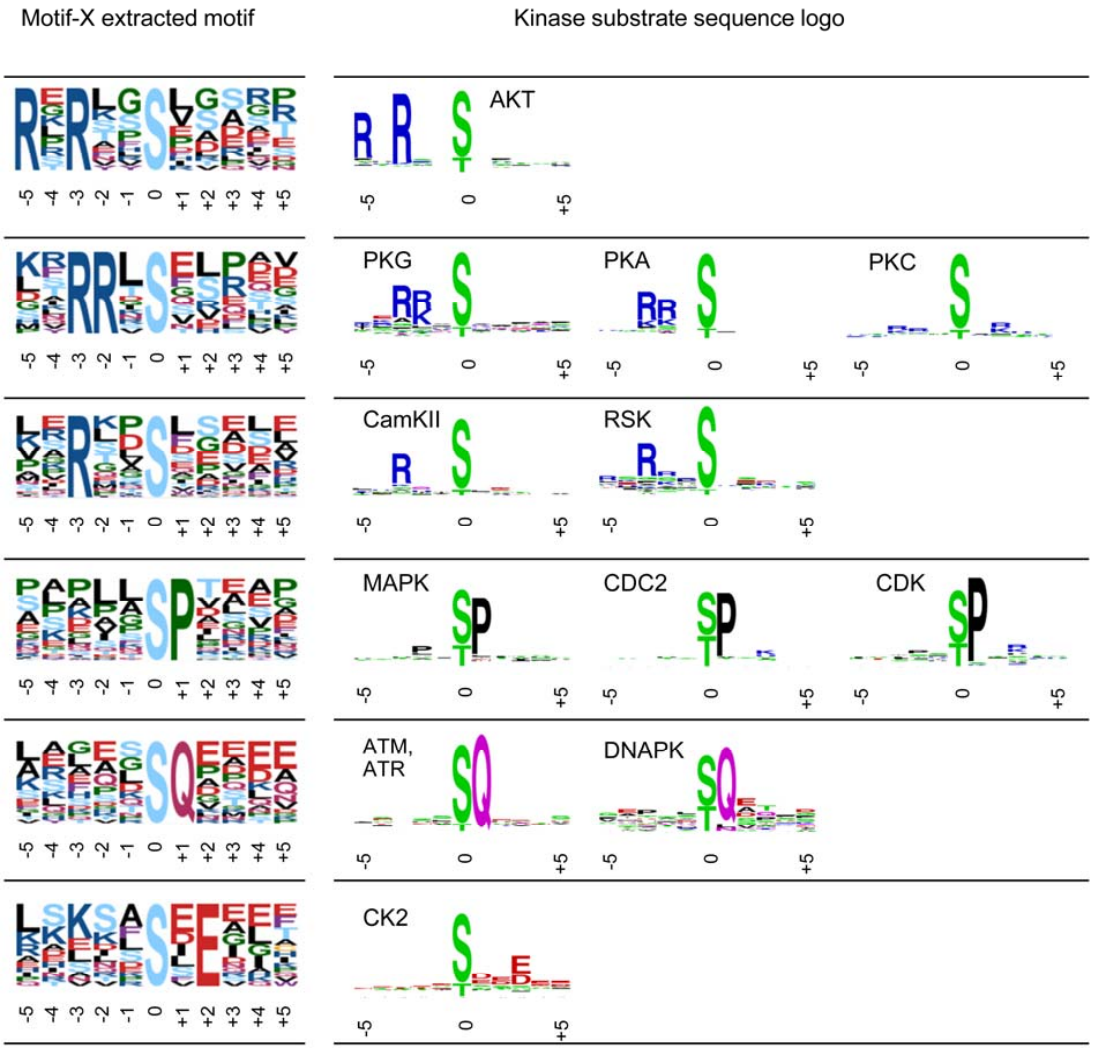

Figure S3

Figure S3: Overrepresented phosphorylation motifs upon *S. flexneri* infection

The overrepresented phosphorylation motifs were extracted with the software tool Motif-X. With a p-value < 0.0005 and a minimal occurrence of 15, six distinct motifs corresponding to phosphopeptides with increased phosphorylation were identified (left panel). Putative kinases responsible for the phosphorylation of the observed motifs and

their corresponding substrate sequences, are shown in the right panel [1]. Kinase substrate motifs were taken from RegPhos, a platform collecting experimentally verified kinase substrates from the databases PhosphoELM and SwissProt [2,3].

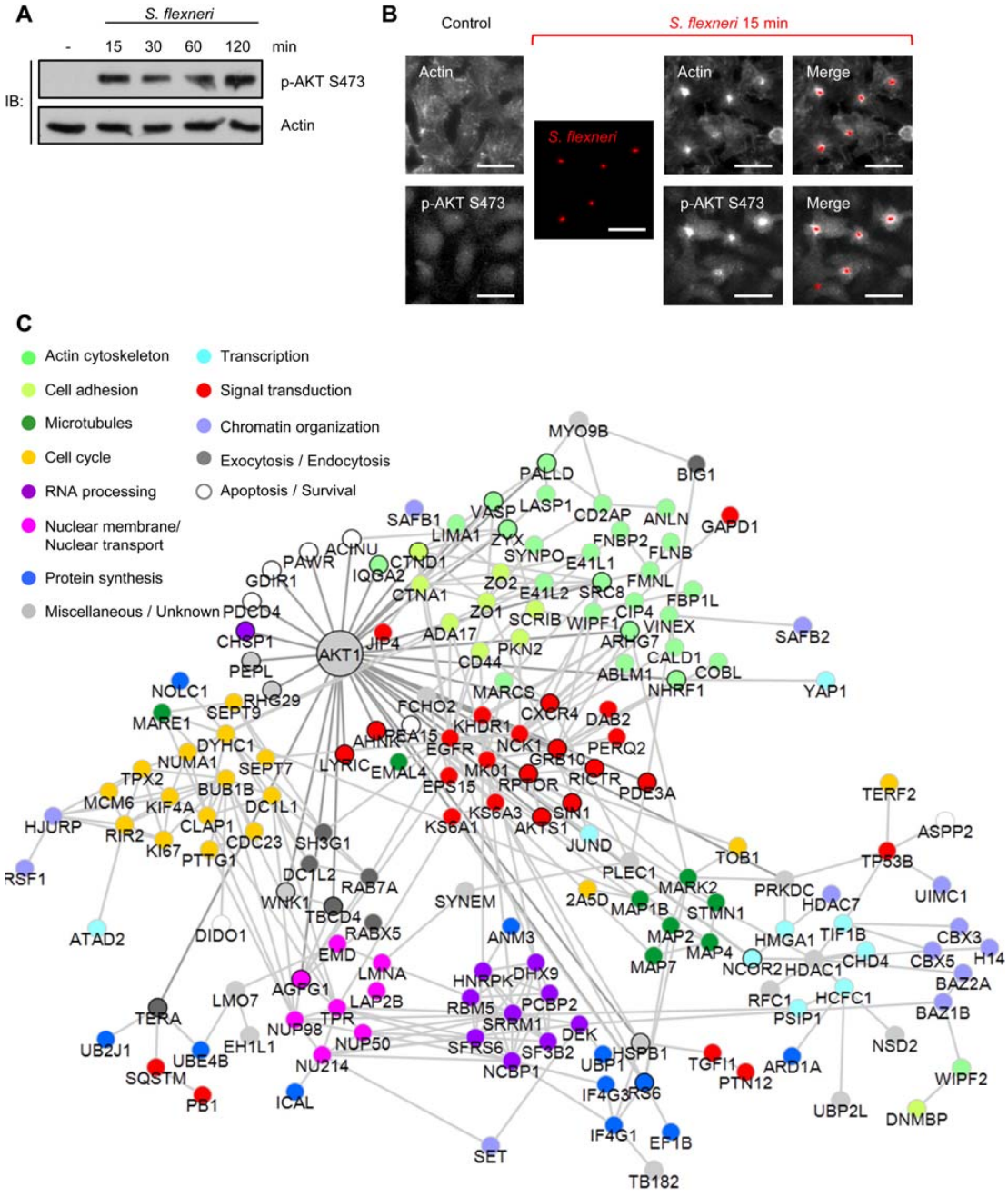
A
S. flexneri
- 15 30 60 120 min
IB:
p-AKT S473
Actin
B
Control
S. flexneri 15 min
Actin
S. flexneri
Actin
Merge
p-AKT S473
p-AKT S473
Merge
C
Actin cytoskeleton
Cell adhesion
Microtubules
Cell cycle
RNA processing
Nuclear membrane/ Nuclear transport
Protein synthesis
Miscellaneous / Unknown
Transcription
Signal transduction
Chromatin organization
Exocytosis / Endocytosis
Apoptosis / Survival
AKT1
MYO9B
PALLD
BIG1
VASP
LASP1
CD2AP
ANLN
GAPD1
SAFB1
LIMA1
ZYX
FNBP2
FLNB
SYNPO
E41L1
ACINU
PAWR
CTND1
IQGA2
GDIR1
ZO2
FMNL
CTNA1
E41L2
SRC8
FBP1L
ZO1
SCRIB
WIPF1
CIP4
VINEX
PDCD4
CHSP1
JIP4
ADA17
ARHG7
SAFB2
PKN2
CD44
CALD1
PEPL
ABLM1
COBL
NOLC1
RHG29
NHRF1
YAP1
SEPT9
MARCS
FCHO2
CXCR4
DAB2
MARE1
KHDR1
DYHC1
AHNK
PEA15
EGFR
NCK1
PERQ2
NUMA1
SEPT7
LYRIC
EMAL4
GRB10
TPX2
MK01
RICTR
BUB1B
EPS15
RPTOR
PDE3A
MCM6
KIF4A
DC1L1
KS6A3
SIN1
TERF2
HJURP
CLAP1
KS6A1
AKTS1
ASPP2
RIR2
CDC23
SH3G1
JUND
TOB1
KI67
PTTG1
TP53B
RSF1
DC1L2
PLEC1
RAB7A
MARK2
PRKDC
UIMC1
WNK1
SYNEM
2A5D
MAP1B
STMN1
HDAC7
TBCD4
ATAD2
DIDO1
RABX5
ANM3
MAP2
HMGA1
TIF1B
CBX3
EMD
MAP4
MAP7
NCOR2
HDAC1
CHD4
CBX5
H14
LMNA
HNRPK
DHX9
BAZ2A
AGPG1
LMO7
LAP2B
RBM5
PCBP2
RFC1
HCFC1
TERA
TPR
SRRM1
PSIP1
BAZ1B
NUP98
DEK
UB2J1
EH1L1
NUP50
SFRS6
SF3B2
HSPB1
NSD2
UBE4B
NU214
UBP1
TGFI1
ARD1A
SQSTM
NCBP1
PTN12
WIPF2
IF4G3
RS6
PB1
ICAL
UBP2L
DNMBP
IF4G1
EF1B
SET
TB182

Figure S4

Figure S4: Activation and roles of AKT during *S. flexneri* infection

(A) AKT becomes phosphorylated at Ser473 upon *S. flexneri* infection. Cells were left untreated or infected for indicated time-points and collected for immunoblotting against phospho-Akt Ser473. Actin is shown as loading control. Data is representative of two independent experiments. **(B)** Phosphorylated AKT is recruited to sites of bacterial entry. HeLa cells were infected for 15 min with dsRed-expressing *S. flexneri* and stained for AKT phosphorylated at Ser473 and F-actin (phalloidin). Scale bars represent 40 µm. **(C)** Graphical representation of the network of the phosphoproteome including AKT1 using the STRING database (high confidence score 0.7) combined with manually annotated biological functions. Only proteins with at least one connection in STRING are represented. Several proteins connected to AKT are related to cell death and survival (white nodes). All proteins connected to AKT are highlighted with black rings.

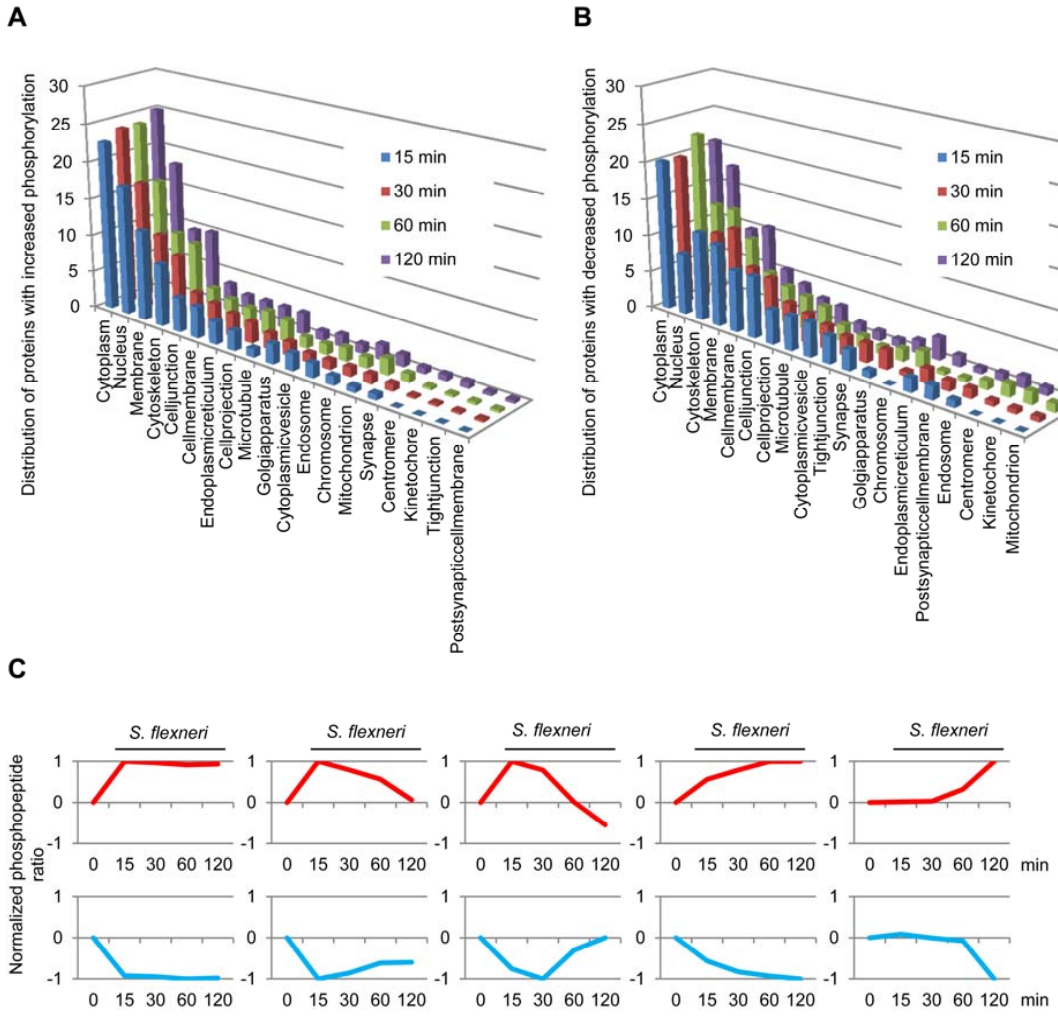
A
B
C
Distribution of proteins with increased phosphorylation
Distribution of proteins with decreased phosphorylation
15 min
30 min
60 min
120 min
Cytoplasm
Nucleus
Membrane
Cytoskeleton
Celljunction
Cellmembrane
Endoplasmicreticulum
Cellprojection
Microtubule
Golgiapparatus
Cytoplasmicvesicle
Endosome
Chromosome
Mitochondrion
Synapse
Centromere
Kinetochore
Tightjunction
Postsynapticcellmembrane
Tightjunction
Synapse
Golgiapparatus
Chromosome
Endoplasmicreticulum
Postsynapticcellmembrane
Endosome
Centromere
Kinetochore
Mitochondrion
S. flexneri
Normalized phosphopeptide ratio
0 15 30 60 120
min

Figure S5

Figure S5: Spatio-temporal dynamics of protein phosphorylation during *S. flexneri* infection

(A) Subcellular localization of proteins with increased phosphorylation during *S. flexneri* infection using UniProt database [3]. **(B)** Subcellular localization of proteins with decreased phosphorylation during *S. flexneri* infection using UniProt database. **(C)** Analysis of the temporal dynamics of phosphorylation changes of individual phosphopeptides after *S. flexneri* infection. Peptides showing significant increase in phosphorylation are shown in red. Peptides showing significant decrease in phosphorylation are shown in blue.

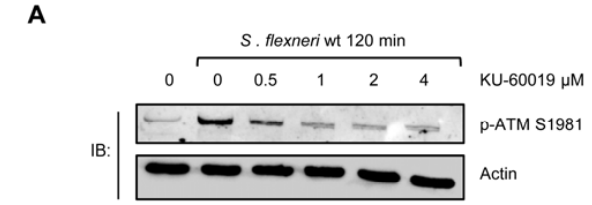

B

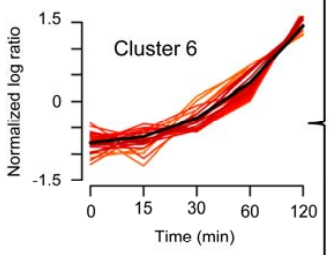

Protein Name	Phosphosite	Phospho-motif	KU-60019 sensitive
TP53B	S1068	LHFPSS*QGEEE	Yes
PRKDC	S3205	LPEDNS*MNVDQ	Yes
UIMC1	S101	AREVNS*QEEEE	Yes
TCAL3	S65	LEDEGS*QEKQG	Yes
FKBP5	S445	EKGTDS*QAMEE	Yes
RPP29	S10	IYHALS*QKEAN	Yes
TR150	S211	FSGGTS*QDTKA	Yes
TP53B	S831	VEQDSS*QPSLP	Yes
NUMA1	S395	LEEHLS*QLQDN	Yes*
CHD4	S1570	KIEENS*LKEEE	Yes*
ACINU	S243	KLSEGS*QPAEE	Yes*
DHX9	S321	AQFEPS*QRQNQ	Yes*
BA2D1	S2105	KLPDLS*PVENK	No
TCAL3	S121	RGTDDS*PKDSQ	No
FLNB	S2478	GQRLVS*PGSAN	No
CSN1	S474	PPREGS*QGELT	No
MCM6	S762	ESEIDS*EEELI	No
CBX3	T173	RLTWHS*CPEDE	Not detected
MAGD2	S162	EPEPES*AAAQS	Not detected
FKBP4	S453	TAGSQS*QVETEA	Not detected
CSN7A	S232	AAAATS*QDPEQ	Not detected
MAGD2	S265	AKLQSS*QEPEA	Not detected
RFC1	S190	KRKELS*QNTDE	Not detected

C

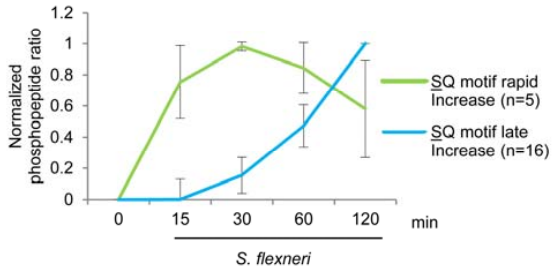

Figure S6

Figure S6: ATM inhibition abolishes the phosphorylation of several cluster 6-proteins

(A) KU-60019 prevents ATM phosphorylation at S1981 (p-ATM S1981). HeLa cells were left untreated or pretreated with KU-60019 for 1h and infected with wild-type *S. flexneri* for 2 h. Phosphorylation of ATM at Serine 1981 was measured by immunoblotting using a phospho-specific antibody. Actin is shown as loading control. **(B)** Phosphoproteomics of HeLa cells pretreated with 4µM KU-60019 for 1 hour and infected with *S. flexneri* for 2 hours. Data were compared to uninfected cells. Out of the 23 phosphopeptides of cluster 6, 19 were again detected. Among these, 9 were at least 2-fold down-regulated by KU-60019 with a q-value <0.01. In addition, 5 phosphopeptides were at least 1.5 fold down-regulated by KU-60019 with a q-value <0.05 (marked with an asterisk). Finally, 5 phosphopeptides were not considered to be KU-60019 sensitive according to these criteria. **(C)** Temporal dynamics of all peptides phosphorylated on a <u>S</u>Q motif. The phosphopeptides are grouped into two distinct clusters with an early and a late increase in phosphorylation.

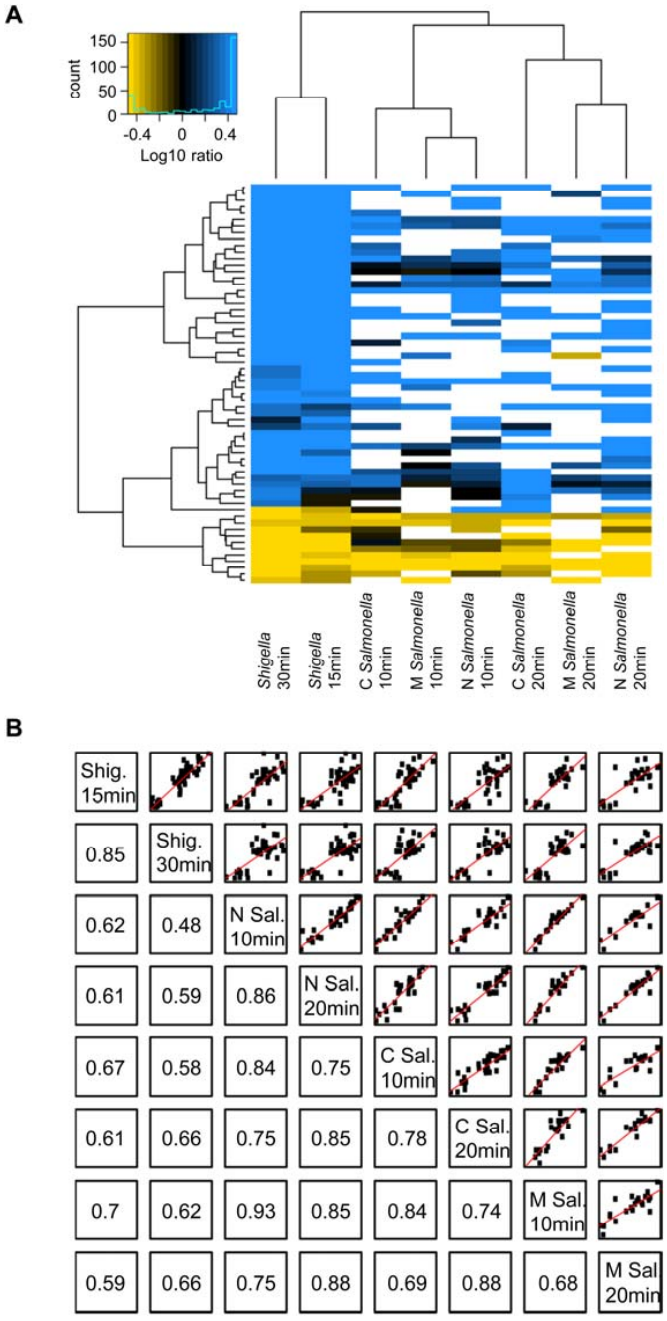
A
count
150
100
50
0
-0.4
0
0.4
Log10 ratio
Shigella 30min
Shigella 15min
C Salmonella 10min
M Salmonella 10min
N Salmonella 10min
C Salmonella 20min
M Salmonella 20min
N Salmonella 20min
B
Shig. 15min
Shig. 30min
N Sal. 10min
N Sal. 20min
C Sal. 10min
C Sal. 20min
M Sal. 10min
M Sal 20min
0.85
0.62 0.48
0.61 0.59 0.86
0.67 0.58 0.84 0.75
0.61 0.66 0.75 0.85 0.78
0.7 0.62 0.93 0.85 0.84 0.74
0.59 0.66 0.75 0.88 0.69 0.88 0.68

Figure S7

Figure S7: Comparison between *S. flexneri* and *S. typhimurium* phosphoproteomics data

(A) Hierarchical clustering of log10 abundance ratios, with respect to the uninfected samples, for the phosphopeptides that are common to the phosphoproteomes of *S. flexneri* and *S. typhimurium* infection. Protein phosphorylation was measured after 15 and 30 minutes for *S. flexneri* infection and after 10 and 20 minutes for *S. typhimurium* infection [4]. Phosphopeptides that underwent a minimum two-fold phosphorylation change and had a q-value <0.01 for at least one time-point, were taken for comparison between the two pathogens. The results obtained for *S. flexneri* infected cells were compared to the three *S. typhimurium* datasets corresponding to the membrane (M), cytoplasmic (C) and nuclear (N) fractions. White bands correspond to situations where no SILAC measurements were available [4]. **(B)** Correlation analysis of phosphorylation changes (log10 abundance ratios, with respect to the uninfected samples) across infection conditions and pathogens. Phosphopeptides undergoing a significant change in phosphorylation after infection by both *S. flexneri* and *S. typhimurium* infections were considered. Values in the lower triangle of the correlation matrix correspond to the squared Pearson's correlation coefficient (R^2). The linear regression for the indicated comparisons is shown in red.

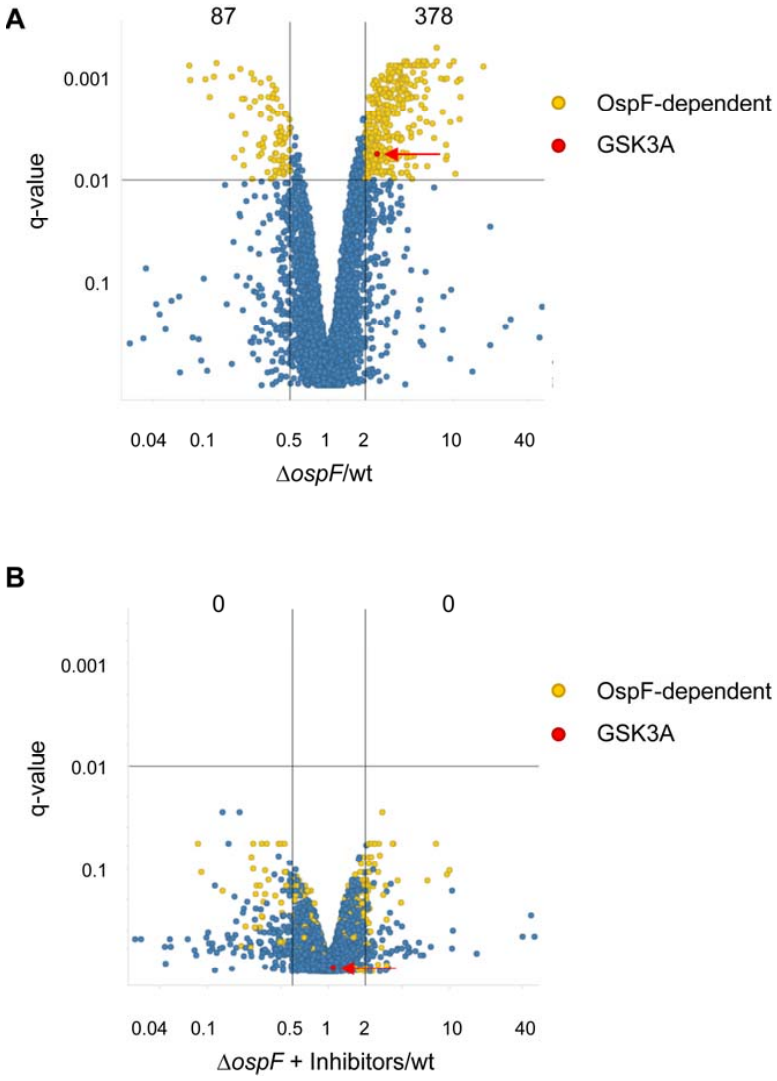
A
87
378
0.001
0.01
0.1
q-value
0.04
0.1
0.5
1
2
10
40
ΔospF/wt
OspF-dependent
GSK3A
B
0
0
0.001
0.01
0.1
q-value
0.04
0.1
0.5
1
2
10
40
ΔospF + Inhibitors/wt
OspF-dependent
GSK3A

Figure S8

Figure S8: Phosphoproteomic comparison between wild-type infection and Δ*ospF* infection in the presence of p38 and ERK inhibitors.

(A) Volcano plot representing significance (q-values) versus the Δ*ospF*/wild-type phosphorylation ratio on the y- and x-axes, respectively. Phosphopeptides showing a minimum 2-fold change in Δ*ospF*/wild-type phosphorylation ratio and a q-value <0.01 were considered significantly regulated by OspF, and represented in yellow. **(B)** Volcano plot representing significance (q-values) versus the Δ*ospF* + MAPK inhibitors/wild-type phosphorylation ratio on the y- and x-axes, respectively. The phosphopeptides significantly regulated by OspF as defined in (A) are represented in yellow. The phosphopeptide corresponding to GSK3A phosphorylation on T201 and Y203 is shown in red.

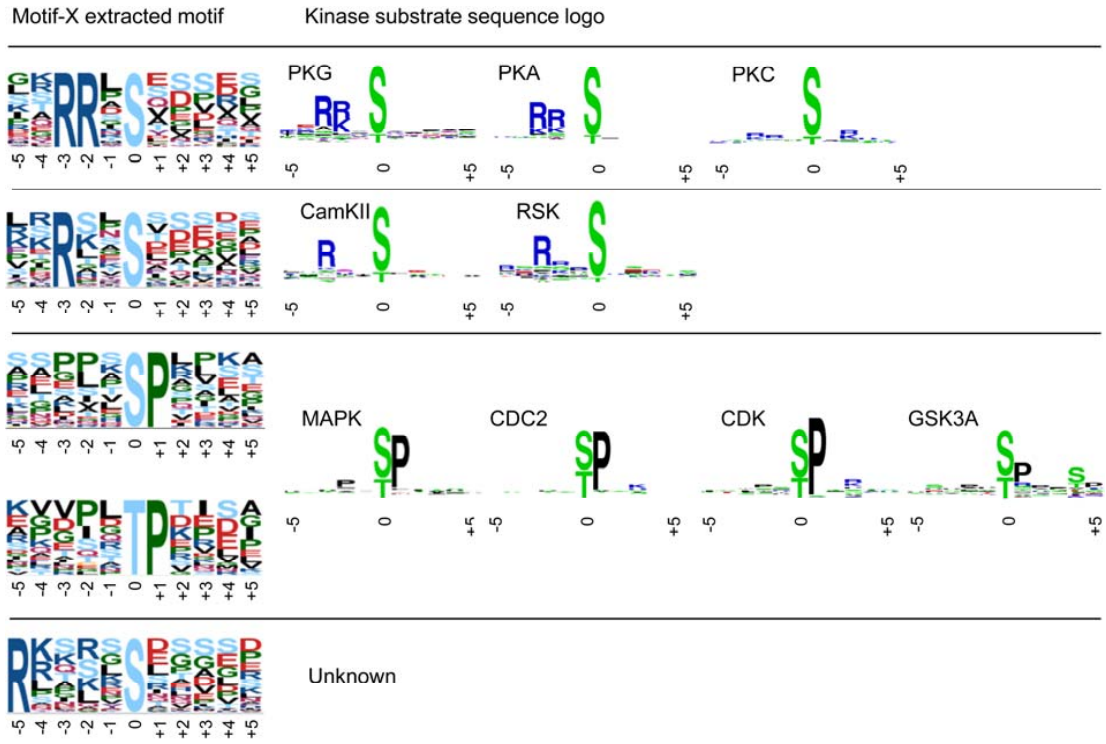

Figure S9

Figure S9: Overrepresented phosphorylation motifs of proteins from the differential phosphoproteome

The overrepresented phosphorylation motifs of proteins differentially phosphorylated between wild-type and *S. flexneri* Δ*ospF* infection were identified by the software tool Motif-X [5]. Using a p-value cutoff of 10^{-6} and a minimal occurrence of 20 peptides, five distinct phosphorylation motifs were identified. Putative kinases responsible for the phosphorylation of the observed motifs and their corresponding substrate sequences are shown in the right panel.

SUPPLEMENTARY INFORMATION FILE LEGENDS

Table S1: Quantification of all phosphopeptides detected by LC-MS/MS

Relative quantification of all confidently identified phosphopeptides in HeLa cells after infection with wild-type *S. flexneri* for 15, 30, 60 and 120 minutes. Abundance Ratios (with respect to the uninfected control condition) and q-values, calculated using SafeQuant v1.0 as described in Supplemental Methods, and used for the entire study, are shown in green and blue, respectively. All raw data are shown in "Raw data" Excel sheet. Data corresponding to individual time-points were highlighted in separated sheets. An explanation of specific terms used in the "Raw Data" sheet is provided in the "Table Description" sheet.

Table S2: Quantification of all proteins detected by LC-MS/MS

Relative quantification of all confidently identified proteins in HeLa cells after infection with wild-type *S. flexneri* for 15, 30, 60 and 120 minutes and *S. flexneri* Δ*ospF* for 30 min. Protein abundance is calculated as the summed MS1 peak abundances of its confidently identified constituting peptides. On this basis, protein abundance ratios (with respect to the uninfected control condition) and accompanying q-values are calculated using SafeQuant v1.0 as described in Supplemental Methods. An explanation of specific terms used in the "Raw Data" sheet is provided in the "Table Description" sheet.

Table S3: Gene ontology analysis of the phosphoproteome *of S. flexneri* infection in HeLa cells

Sheet 1: Gene ontology terms of the proteins of the phosphoproteome.

Sheet 2: Enrichment in gene ontology terms. All 334 proteins from the phosphoproteome were subjected to DAVID and the overrepresented GO Terms (GO_TERM_BP_FAT) with respect to all detected phosphoproteins, used as background, were extracted.

Table S4: Manual functional annotation of the phosphoproteome

All proteins from the phosphoproteome were manually annotated according to their published biological function. Only one function was assigned to a protein based on relative available literature. At the bottom of the page, a summary showing all annotations and their mode of classification can be found.

Table S5: Quantification of all phosphopeptides detected by LC-MS/MS upon *S. flexneri* Δ*virG* infection

Relative quantification of all confidently identified phosphopeptides in HeLa cells after infection with *S. flexneri* Δ*virG* for 15 and 60 minutes. Abundance Ratios (with respect to the uninfected control condition) and *q*-values calculated using SafeQuant v1.0 as described in Supplemental Methods, are shown in green and blue, respectively. An explanation of specific terms used in the sheet, is provided in the “Table Description” sheet. A comparison with wild-type infection is shown in “comparison with wt” sheet for the proteins related to actin.

Table S6: Temporal dynamics of protein phosphorylation during *S. flexneri* infection

The temporal dynamics of phosphorylation was analyzed by fuzzy c-means clustering. The phosphopeptides from the six clusters (on separated sheets) are listed with their corresponding membership value and functional annotation. For each cluster, the most enriched phosphorylation motif was extracted using the motif-X algorithm.

Table S7: Quantification of all phosphopeptides detected by LC-MS/MS upon *S. flexneri* infection and ATM inhibition by KU-60019 treatment

Relative quantification of all confidently identified phosphopeptides in HeLa cells after infection with *S. flexneri* for 120 minutes either untreated or treated with 4µM KU-60019. Abundance Ratios (with respect to the uninfected control condition) and q-values, calculated using SafeQuant v1.0 as described in Supplemental Methods, are shown in green and blue, respectively, in sheet 1. Abundance Ratios (with respect to the *S. flexneri* infected cells for 120 minutes condition) and q-values, calculated using SafeQuant v1.0 as described in Supplemental Methods, are shown in green and blue, respectively, in sheet 2. An explanation of specific terms used in the sheet, is provided in the “Table Description” sheet.

Table S8: KEGG pathways analysis of the phosphoproteome of *S. flexneri* infection

All proteins from the phosphoproteome were subjected to DAVID and the enrichment of KEGG pathways with respect to the human genome background was extracted.

Table S9: Comparison of the phosphoproteome of *S. flexneri* and *S. typhimurium* infected cells

The phosphoproteome of *S. flexneri* infection was compared to the phosphoproteome of *S. typhimurium* infection published by Rogers et al. [4]. The 15 and 30 min time-points from the *S. flexneri* dataset are compared to the 10 and 20 min time-points of the *S. typhimurium* dataset. Phosphopeptides, which are detected in both datasets to be regulated in a significant manner (2-fold change and q-value <0.01) in at least one condition, are shown.

Table S10: OspF and MAPK inhibitor sensitive phosphoproteome

Relative quantification of all confidently identified phosphopeptides in HeLa cells after infection with wild-type *S. flexneri,* *S. flexneri* Δ*ospF* and *S. flexneri* Δ*ospF* in the presence of 10 µM SB203580 and 50 µM PD98059. Abundance Ratios (with respect to the uninfected control condition) and *q*-values, calculated using SafeQuant v1.0 as described in Supplemental Methods, are shown in green and blue, respectively in sheet1. Abundance Ratios (with respect to the Δ*ospF* 30 minutes condition) and q-values, calculated using SafeQuant v1.0 as described in Supplemental Methods, are shown in green and blue, respectively in sheet2. An explanation of specific terms used, is provided in the “Table Description” sheet

Table S11: Manual annotation of the OspF-sensitive phosphoproteome

All phosphopeptides that are at least two fold up- or down-regulated with a *q*-value <0.01 in cells infected with Δ*ospF* compared to wild-type infected cells, were manually annotated according to their biological function. At the bottom of the page, a summary of the annotation from the OspF sensitive phosphoproteome can be found.

File S12: All annotated spectra

SUPPLEMENTARY MATERIALS AND METHODS

Functional annotation

DAVID [6] was used for functional annotation and Gene Ontology enrichment analysis. Enriched terms with a *p*-value below 0.05 were considered. Terms from the GOTERM_BP_FAT category were used to address overrepresented biological functions. KEGG pathway was used to address overrepresented pathways [7,8].

Motif analysis

The software tool Motif-X [5] was used to extract overrepresented phosphorylation motifs. We took 13-amino acid sequences centered on the phosphorylation sites as defined in our dataset. The complete human International Protein Index database was used as background. Occurrence and *p*-value cutoffs are indicated in the corresponding figure legends. To compare the obtained motifs to substrate motifs from known kinases, the resource RegPhos (http://regphos.mbc.nctu.edu.tw/) was used. There, experimentally verified kinase substrates were collected from the databases Phospho.ELM and SwissProt. The substrates were related to 107 kinases families corresponding to more than 300 individual kinases [9] and represented using WebLogo [10].

Network analysis

For graphical representations, lists of proteins were submitted to the STRING (v. 9.0) database [11] using a filter for high confidence interactions (score >0.7). Interaction data were downloaded and processed with Cytoscape 2.8.2 [12]. Cytoscape was also used to combine the STRING interaction data to manual functional annotation.

M Fuzz Clustering

The phosphorylation profiles of phosphopeptides undergoing a significant change compared to uninfected cells (a minimum 2-fold change and a q-value < 0.01) at least at one time point were clustered using Fuzzy c-means clustering [13]. The clustering algorithm was provided with normalized log ratio abundance profiles for each phosphopeptide (each profile was scaled to have a mean of 0 and a standard deviation of 1, z-scoring). The number of clusters was set to 6, after evaluating the decrease in minimum centroid distance over a range of cluster numbers, as suggested by Schwämmle and Jensen, 2010 [14]. The fuzzification parameter m was set to 2.15 after evaluation of fuzzy clustering applied to randomized datasets of the same dimension and number of profiles as our data. Finally, each cluster was filtered to include only the phosphopeptides with a membership-value larger than 0.5.

Comparison of *S. flexneri* and *S. typhimurium* phosphoproteomes

The comparison between both phosphoproteomes was performed as follows. For both datasets, significant changes in phosphorylation were defined as a minimum two-fold increase or decrease compared to uninfected cells, and a q-value < 0.01 for *S. flexneri* infection and a p-value < 0.01 for *S. typhimurium* infection. Phosphorylation was measured after 15 and 30 minutes of *S. flexneri* infection and 10 and 20 minutes of *S.*

typhimurium infection. For the latter, phosphorylation changes in at least one fraction (membrane, cytoplasmic or nuclear) were considered. Based on these criteria, 62 phosphopeptides showed a significant change in phosphorylation after infection by both pathogens (at least in one time-point and in one fraction for *S. typhimurium* infection*)*. For instance, if a phosphopeptide was found significantly phosphorylated at 15 minutes after *S. flexneri* and at 20 minutes post *S. typhimurium* infection in the nuclear fraction, it was considered as overlapping. Hierarchical clustering was used to compare the direction of the phosphorylation changes for the 62 shared phosphopeptides. Due to the nature of the SILAC method employed in the *S. typhimurium* study, each peptide was not necessarily identified and quantified in all fractions and time-points. The missing values are indicated by white bands in the heat-map (Figure S7A).

References

1. Lee T-Y, Bo-Kai Hsu J, Chang W-C, Huang H-D (2011) RegPhos: a system to explore the protein kinase–substrate phosphorylation network in humans. Nucleic Acids Res 39: D777-D787.
2. Dinkel H, Chica C, Via A, Gould CM, Jensen LJ, et al. (2010) Phospho.ELM: a database of phosphorylation sites—update 2011. Nucleic Acids Res.
3. Magrane M, Consortium U (2011) UniProt Knowledgebase: a hub of integrated protein data. Database 2011.
4. Rogers LD, Brown NF, Fang Y, Pelech S, Foster LJ (2011) Phosphoproteomic Analysis of Salmonella-Infected Cells Identifies Key Kinase Regulators and SopB-Dependent Host Phosphorylation Events. Sci Signal 4: rs9-.
5. Schwartz D, Gygi SP (2005) An iterative statistical approach to the identification of protein phosphorylation motifs from large-scale data sets. Nat Biotech 23: 1391-1398.
6. Huang DW, Sherman BT, Lempicki RA (2008) Systematic and integrative analysis of large gene lists using DAVID bioinformatics resources. Nat Protocols 4: 44-57.

7. Kanehisa M, Goto S (2000) KEGG: Kyoto Encyclopedia of Genes and Genomes. Nucleic Acids Res 28: 27-30.
8. Kanehisa M, Goto S, Sato Y, Furumichi M, Tanabe M (2012) KEGG for integration and interpretation of large-scale molecular data sets. Nucleic Acids Res 40: D109-D114.
9. Manning G, Whyte DB, Martinez R, Hunter T, Sudarsanam S (2002) The Protein Kinase Complement of the Human Genome. Science 298: 1912-1934.
10. Crooks GE, Hon G, Chandonia J-M, Brenner SE (2004) WebLogo: A Sequence Logo Generator. Genome Research 14: 1188-1190.
11. Szklarczyk D, Franceschini A, Kuhn M, Simonovic M, Roth A, et al. (2011) The STRING database in 2011: functional interaction networks of proteins, globally integrated and scored. Nucleic Acids Res 39: D561-D568.
12. Smoot ME, Ono K, Ruscheinski J, Wang P-L, Ideker T (2011) Cytoscape 2.8: new features for data integration and network visualization. Bioinformatics 27: 431-432.
13. M. F (2005) Noise-Robust Soft Clustering Of Gene Expression Time-Course Data. J Bioinform Comput Biol 3: 965–988.
14. Schwämmle V, Jensen ON (2010) A simple and fast method to determine the parameters for fuzzy c–means cluster analysis. Bioinformatics 26: 2841-2848.

5 Unpublished results related to the research article

This section contains additional unpublished results related to the research article "Systems-Level Overview of Host Protein Phosphorylation During *Shigella flexneri* Infection Revealed by Phosphoproteomics". These results were either excluded because of space limitations or due to lacking contribution to the principal message of the research article. However, these results still cover some important aspects related to the work and are therefore presented and discussed in the current section.

5.1 Statement of contribution

I performed all of the experiments shown in this section except the following. C. Kasper performed the siRNA screen and a comparison to the phosphoproteomic data. In addition, C. Kasper performed the automated image quantification for the nuclear transport experiments. R. Dreier contributed the p-MYPT1 immunoblot and a phosphoproteomic dataset covering the first 15 minutes of *S. flexneri* infection.

5.2 Results and discussion

5.2.1 Phosphoproteomics of *S. flexneri* infection upon mTOR inhibition

A KEGG pathway analysis of phosphoproteins revealed mTOR as the most overrepresented pathway during *S. flexneri* infection[248]. We could further validate that the pathway becomes activated during infection by monitoring activity of S6K and AKT, the downstream targets of mammalian target of rapamycin complex 1 (mTORC1) and mammalian target of rapamycin complex 2 (mTORC2), respectively. Therefore, we aimed to reveal potential roles of mTOR during infection. We applied phosphoproteomics to study the impact of mTOR inhibition upon *S. flexneri* infection. Cells were pretreated with the mTORC1 inhibitor rapamycin or with the mTORC1/2 inhibitor PP242 for an hour and subsequently infected with *S. flexneri* for 30 minutes. The infected cells were harvested, lysed, enzymatically digested and the derived peptides enriched for phosphopeptides using TiO_2 (Figure 5.2.1 A). The obtained phosphopeptides were subjected to mass spectrometry as previously described[248]. Inhibition of mTORC1 by rapamycin upon *S. flexneri* infection affected the phosphorylation on 13 different peptides compared to infection without treatment (Figure 5.2.1 B). The down-regulation of phosphorylation on Ser235/236 of the mTORC1 substrate RS6 upon rapamycin treatment validated the approach. In

addition, phosphorylation of EF2K, a kinase that was shown to be involved in insulin signaling towards mTOR, was also sensitive to rapamycin[31]. Interestingly, more phosphopeptides were found to undergo an increase than a decrease in phosphorylation during *S. flexneri* infection and rapamycin treatment. These include the Src substrate cortactin as well as LARP1 that has recently been shown to associate with mTORC1 and being required for protein synthesis[268]. Inhibition of both mTORC1 and mTORC2 by PP242 has as expected a higher impact on the phosphorylation network of the cell (Figure 5.2.1 C). We identified 33 phosphopeptides undergoing a significant change in phosphorylation upon infection with *S. flexneri* and PP242 treatment compared to infection without treatment. PP242 had a net negative impact on protein phosphorylation upon infection as 25 phosphopeptides were identified to be less phosphorylated compared to 8 phosphopeptides that showed an increase in phosphorylation upon PP242 treatment. The repression of RS6 phosphorylation upon PP242 treatment validated the inhibitory effect towards mTORC1 and the repression of phosphorylation of AKTS1, which is a substrate of AKT, validates the inhibitory effect towards mTORC2. A decrease in phosphorylation was again observed for EF2K and additionally for 4EBP1 and 4EBP2 two regulators of eIF4E a protein involved in regulation of translation[167]. Interestingly, LARP1 was found again to undergo a change in phosphorylation. However, PP242 represses LARP1 phosphorylation whereas rapamycin enhanced LARP1 phosphorylation. It has to be mentioned that different phosphosites were regulated among the two treatments which indicates that LARP1 phosphorylation becomes regulated at multiple sites in mTOR dependency as also previously observed[112,296]. Overall, these data show that repression of mTOR signaling during bacterial infection affects the phosphorylation of many different proteins that are mainly related to regulation of translation. Although this data may provide new targets of mTOR or indirect mTOR regulated proteins, a function of mTOR during bacterial infection could not be revealed.

5.2.2 The nuclear translocation of Rev-GR-GFP is affected upon *S. flexneri* infection

In the research article we showed that *S. flexneri* infection induces phosphorylation events of several components of the nuclear pore complex (NPC) including Nup98, Nup50, Nu214 and TPR. Because phosphorylation of nucleoporins is proposed to cause disassembly of NPCs during mitosis[141], we first examined whether these multiprotein structures remain intact after *S. flexneri* infection (Figure 5.2.2 A and B). The subcellular localization of the nuclear pore membrane protein Pom121 and the central transporter Nup62 was compared in uninfected and infected cells by confocal microscopy. As these proteins are respectively localized in the central part and the periphery of the nuclear pore, they are used to control the integrity of NPCs[141]. Data showed that bacteria did not alter the localization of these

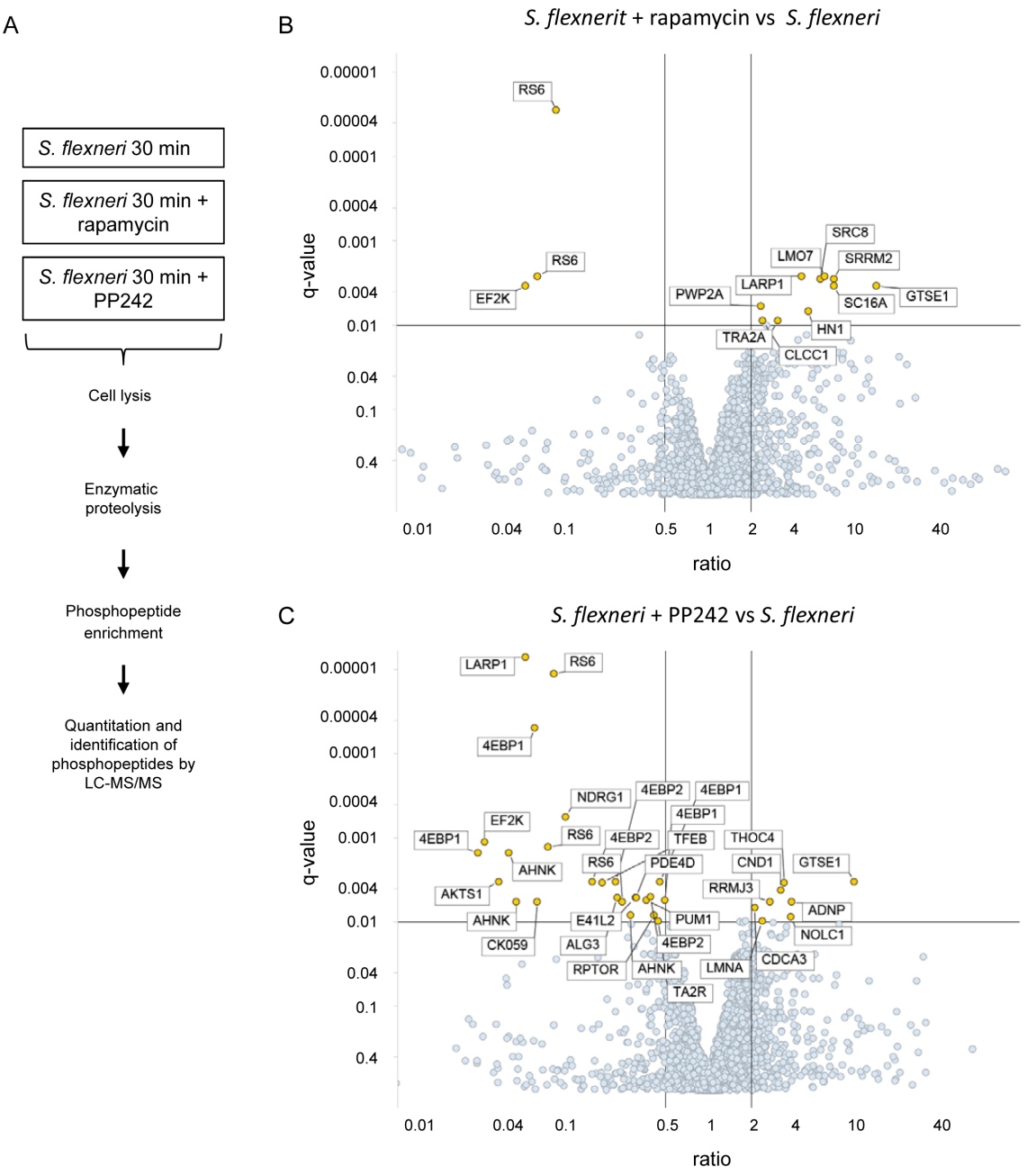

Figure 5.2.1 (Continued on the following page.)

Figure 5.2.1 Phosphoproteomics of *S. flexneri* infection upon mTOR inhibition. (A) Schematic workflow of the experiment. HeLa cells were either left untreated or pretreated with 100nM rapamycin or 2μM PP242 for one hour and subsequently infected with *S. flexneri* at an multiplicity of infection (MOI) of 40 for 30 minutes. Afterwards the standard phosphoproteomic workflow was applied. (B) Volcano plot representing significance (q-values) versus the *S. flexneri* + rapamycin/ *S. flexneri* phosphorylation ratio on the y- and x-axes, respectively. Phosphopeptides showing a minimum 2-fold change in *S. flexneri* + rapamycin/ *S. flexneri* phosphorylation ratio and a q-value <0.01 were considered significantly regulated by rapamycin, and represented in yellow. (C) Volcano plot representing significance (q-values) versus the *S. flexneri* + PP242/ *S. flexneri* phosphorylation ratio on the y- and x-axes, respectively. Phosphopeptides showing a minimum 2-fold change in *S. flexneri* + PP242/ *S. flexneri* phosphorylation ratio and a q-value <0.01 were considered significantly regulated by PP242, and represented in yellow.

proteins, suggesting that NPCs remained intact during infection (Figure 5.2.2 A and B). The impact of *S. flexneri* infection on nuclear import was then directly tested. We used a common nucleo-cytoplasmic shuttling assay employing the human immunodeficiency virus type 1 Rev protein fused to the glucocorticoid ligand binding domain and GFP (Rev-GR-GFP)[162,220]. In control cells, Rev-GR-GFP is located in the cytoplasm (Figure 5.2.3 A, upper panel). After treatment with dexamethasone, the fusion protein enters the nucleus to localize to the nucleolus (Figure 5.2.3 A, lower panel). A moderate but significant inhibition of nuclear import was observed in infected cells compared to control uninfected cells (Figure 5.2.3 A and B). Altogether, these results showed that the phosphorylation of several NPC proteins was altered during infection, and that nuclear import of proteins was partially inhibited in infected cells.

5.2.3 OspF affects the phosphorylation of Nup50 but has no effect on the nuclear translocation of Rev-GR-GFP

To validate the phosphorylation of the NPC we selected the protein Nup50, for which a phospho-specific antibody was available and adressed its phosphorylation at serine 221 by immunofluorescence. Whereas infection by the virulence plasmid-cured strain BS176 or the TTSS Δ*spa40*[254] had no effect, wild-type and Δ*ospF* bacteria induced a moderate and strong increase of Nup50 phosphorylation, respectively (Figure 5.2.4 A). These observations are in concordance with the phosphoproteomic data. Nup50 was shown to be an ERK substrate and Nup50 phosphorylation impaired the nuclear transport of importin-β and transportin[141]. Thus, we wondered whether we would observe a difference in dexamethasone-induced nuclear translocation of Rev-GR-GFP among wild-type infection or infection with the Δ*ospF* mutant, for which we observed an increase in phosphorylation of several nuceloporins including Nup50. However a change in Nup50 phosphorylation

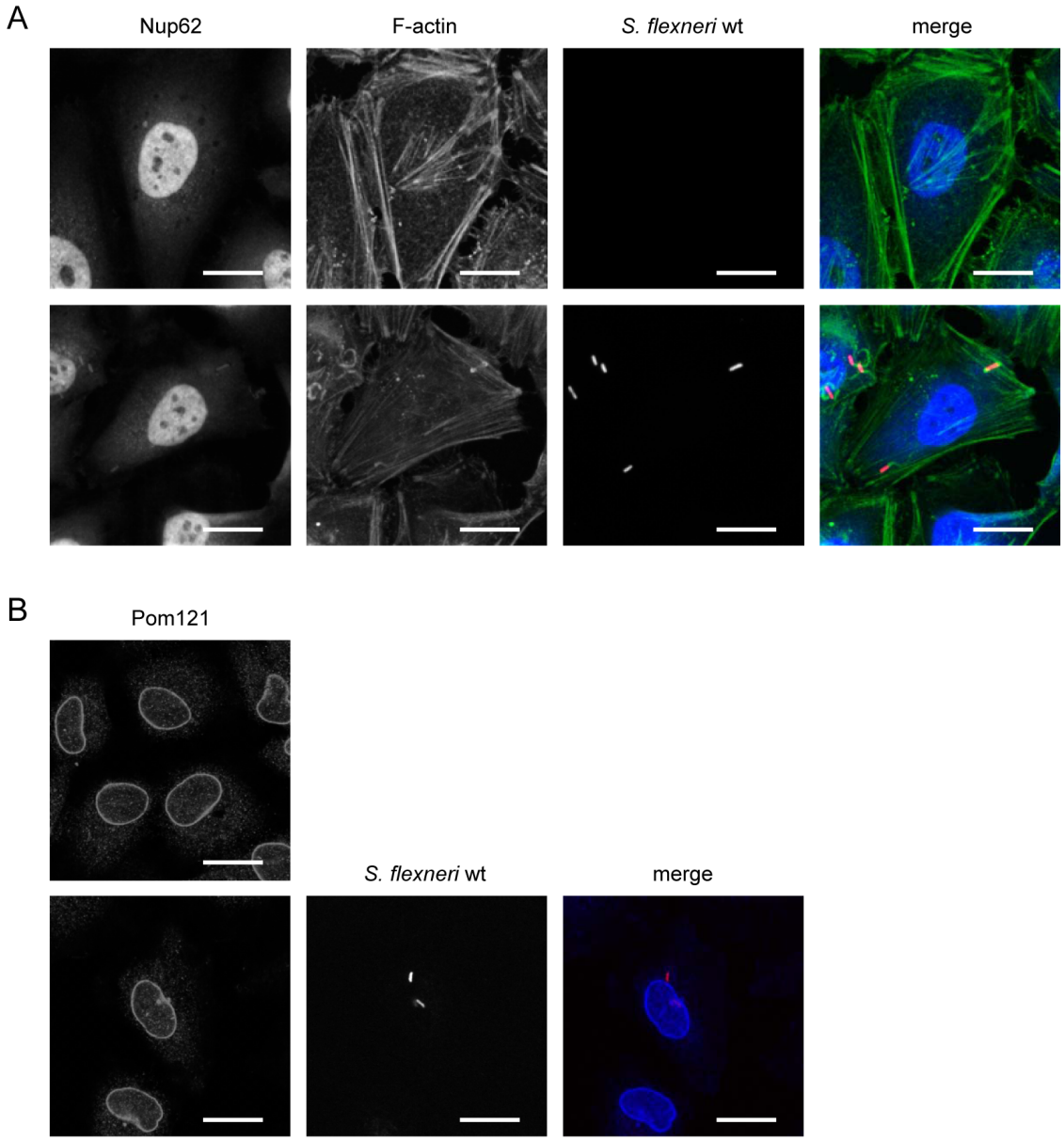

Figure 5.2.2 NPCs remain intact during *S. flexneri* infection. (A) The localization of Nup62 is not altered in infected cells. Analysis of Nup62 localization by immunofluorescence microscopy. HeLa cells were left untreated or infected with DsRed-expressing wild-type *S. flexneri* at an MOI of 10 for 60 minutes and stained for Nup62 and F-actin. Scale bars represent 20μm. (B) POM121 distribution is not altered in infected cells. Distribution of POM121 was analyzed by immunofluorescence microscopy. HeLa cells were left untreated or infected with DsRed-expressing wild-type *S. flexneri* at an MOI of 10 for 60 minutes and stained for POM121. Scale bars represent 20μm.

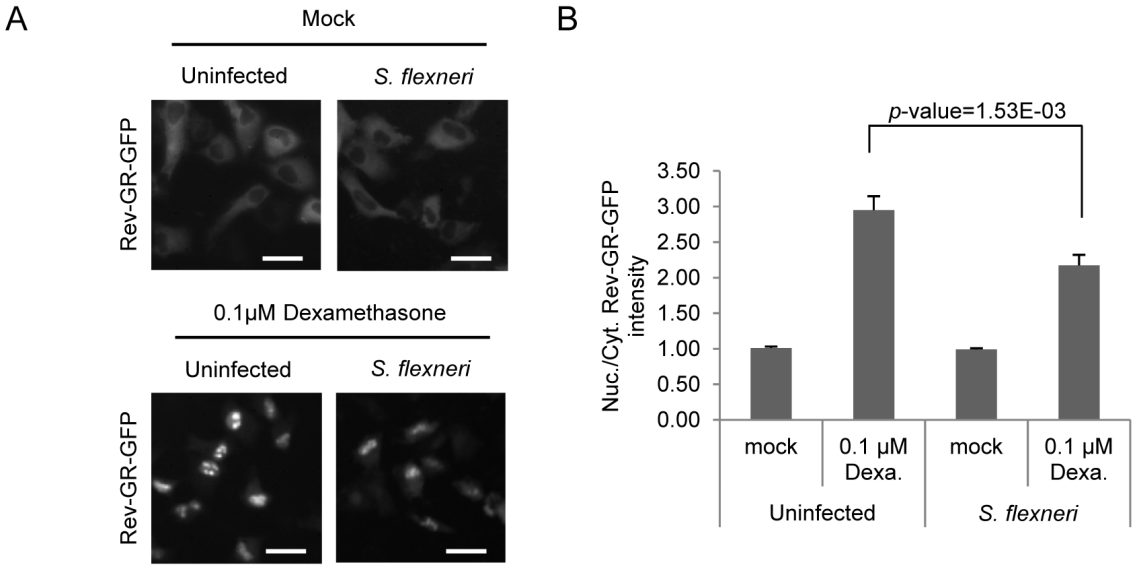

Figure 5.2.3 *S. flexneri* infection affects the nuclear translocation of of Rev-GR-GFP. (A) Cells expressing Rev-GR-GFP were left untreated or infected with *S. flexneri* for 30 minutes. Cells were then stimulated or not with 0.1μM dexamethasone for 40 minutes. (B) Nuclear translocation of Rev-GR-GFP was quantified by automated image analysis. Results are expressed as the mean ± SD of four wells. The data is representative for four independent experiments.

did not correlate with a general alteration in nuclear transport, as OspF failed to affect dexamethasone-induced nuclear translocation of Rev-GR-GFP (Figure 5.2.4 B). Overall, our data showed that although NPCs remained intact during infection, the nuclear translocation of Rev-GR-GFP was reduced in cells infected by wild-type bacteria. However the contribution of NPC protein phosphorylation to this phenomenon was not demonstrated. Indeed, Δ*ospF* infection, which triggers massive phosphorylation of several NPC proteins, affected nuclear transport in the same extent as wild-type infection. Additional work is required to elucidate how infection impacts nuclear transport, and if trafficking of important host proteins or mRNA is affected during infection.

5.2.4 Selected proteins showing an effect in phosphoproteomics and a siRNA screen on *S. flexneri* entry

In order to identify host factors important for the uptake of *S. flexneri* into HeLa cells, a genome-wide siRNA screen was performed by C. Kasper in the frame of the InfectX initiative. Hits from this screen were compared to phosphoproteomic data covering 2, 5, 10, 15, 30, 60 and 120 minutes of *S. flexneri* infection. The phosphoproteomic data derives from all datasets published in Schmutz et al. as well as a dataset covering the first 15 minutes of infection (R. Dreier unpublished) [248]. Figure 5.2.5 A depicts proteins that were identified in the siRNA screen to affect entry and in addition by phosphoproteomics

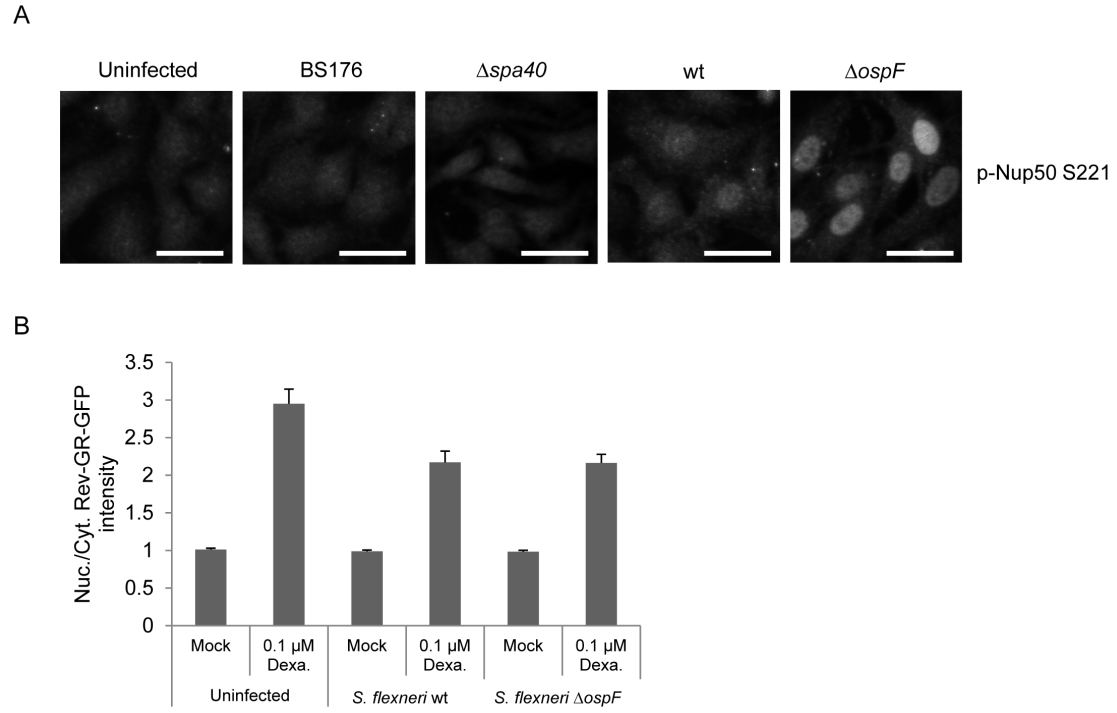

Figure 5.2.4 *S. flexneri* induced Nup50 phosphorylation does not affect nuclear translocation of of Rev-GR-GFP. (A) Immunofluorescence staining of p-Nup50 in infected HeLa cells. Cells were left untreated or infected with wild-type, non-invasive BS176, Δ*spa40* or Δ*ospF S. flexneri* strains. Scale bars represent 40 μm. (B) Nuclear translocation of Rev-GR-GFP was quantified by automated image analysis. Cells expressing Rev-GR-GFP were left untreated or infected with wild-type or *S. flexneri* Δ*ospF* for 30 minutes. Cells were then stimulated or not with 0.1μM dexamethasone for 40 minutes. Results are expressed as the mean ± SD of four wells. The data is representative for four independent experiments.

to undergo a change in phosphorylation upon infection. We could identify for example the phosphoproteins IQGAP2 and Myosin IXB to negatively affect entry. IQGAP2 has been shown to interact with activated CDC42 and Rac1 two important proteins during *S. flexneri* infection[201]. Myosin IXB acts as a GTPase activating protein on Rho[102], a protein that is targeted by the *S. flexneri* effector IpaA to promote remodeling of the actin cytoskeleton[57]. Thus, these two proteins are promising candidates for further research on the entry process. In addition, we revealed that the phosphoprotein MYPT1 is important for the uptake of *S. flexneri*. MYPT1 was shown to interact and beeing a substrate of ROCK[131], a protein becoming activated during *S. flexneri* infection[80]. Recently it was demonstrated that MYPT1 regulated the surface density of $\alpha5\beta1$ integrins, an important receptor for binding of *S. flexneri*[126,285]. Thus, we addressed the role of MYPT1 during the entry process in more detail by application of a commercially available phospho-specific antibody. HeLa cells were either left untreated or infected for different

time-points ranging from 2 to 60 minutes (Figure 5.2.5 B). Calyculin A was used as positive control for the detection of MYPT1 phosphorylation. Immunoblotting with a phospho-specific antibody against Ser507 of MYPT1 confirmed the induction of MYPT1 phosphorylation early during infection, as observed by phosphoproteomics (Figure 5.2.5 B). More precisely, MYPT1 phosphorylation was highest between 10 to 15 minutes post-infection, temporally correlating with the entry process of *S. flexneri*. As we confirmed the temporal phosphorylation pattern of MYPT1, we next aimed to resolve its spatial localization during infection. HeLa cells were infected with *S. flexneri* for 15 minutes followed by chemical fixation and staining for F-actin by phalloidin and p-MYPT1 on Ser507 by a phospho-specific antibody. The immunofluorescence images showed a co-localization of F-actin ruffles at the site of bacterial entry with phosphorylation of MYPT1 (Figure 5.2.5 C). These data show that MYPT1 phosphorylation does not only correlate temporally but also spatially with the entry process. Overall, these data demonstrate that the combination of a siRNA screen with phosphoproteomics can reveal host proteins that are important for *S. flexneri* entry. In particular, we could confirm that MYPT1 plays an important role in the uptake process of *S. flexneri*. However, more research would be required to elucidate the interaction of MYPT1 with other host proteins as ROCK or $\alpha 5\beta 1$ integrin during infection and the underlying molecular mechanisms.

5.3 Additional material and methods

5.3.1 Phosphoproteomics

Sample preparation for phosphoproteomics, Phosphopeptide enrichment and LC-MS/MS analysis were conducted as described in Schmutz et al.[248]

5.3.2 Immunofluorescence labeling of phospho-Nup50

Cells were fixed with 4% paraformaldehyde for 10 minutes at room temperature. After being washed with PBS, cells were permeabilized for 10 minutes with 0.1% Triton X-100. They were then incubated with p-Nup50 antibody diluted 1:200 in PBS containing 2% goat serum for two hours at room temperature. After several PBS washes, cells were incubated for one hour with a goat anti-rabbit secondary antibody diluted 1:500 in PBS containing 2% goat serum.

5.3.3 Nuclear import assay

HeLa cells were seeded into a 96 well plate at day 1, and transfected at day 2 with a Rev-GlucocorticoidReceptor-GFP construct[162] using FUGENE HD transfection reagent (Promega). Cells were serum-starved for 2 hours and infected with *S. flexneri* for 30

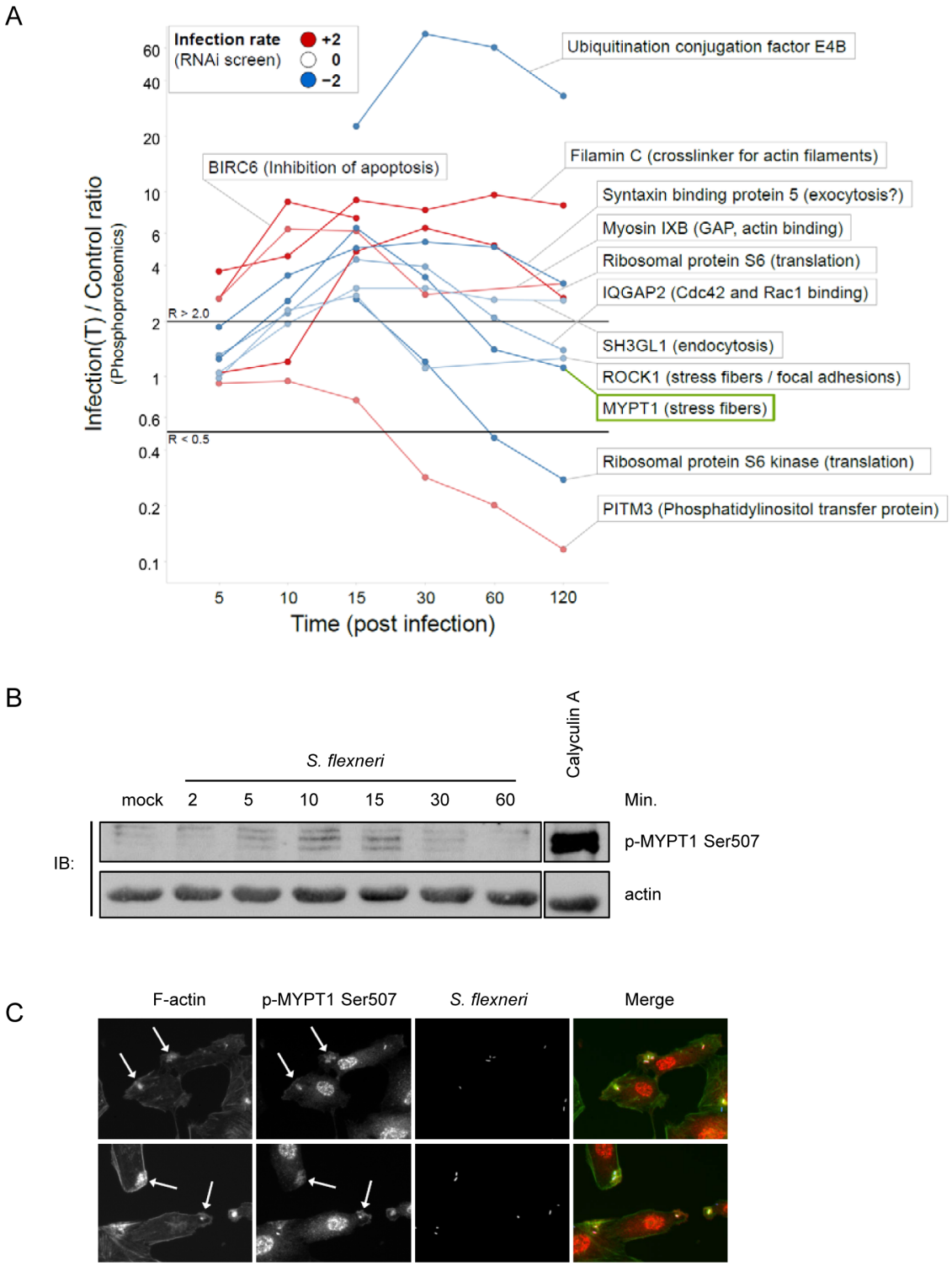

Figure 5.2.5 (Continued on the following page.)

Figure 5.2.5 Selected proteins showing an effect in phosphoproteomics and a siRNA screen of *S. flexneri* entry. (A) Selected hits from a siRNA screen on *S. flexneri* entry and proteins that were found to undergo a significant change in phosphorylation over time are depicted. The infection/ control phosphorylation ratio is plotted against the time of infection. Proteins whose depletion increases the infection rate are shown in red, whereas proteins whose depletion decreases the infection rate are shown in blue. MYPT1 which was selected for follow up experiments is depicted in green. (B) HeLa cells were left untreated or infected with *S. flexneri* for 2, 5, 10, 15, 30 and 60 min or treated with calyculin A as positive control. The phosphorylation of MYPT1 on Ser507 was analyzed by immunoblotting. Actin was used to ensure equal protein loading. (C) MYPT1 becomes phosphorylated on Ser507 at the *S. flexneri* entry site. HeLa cells were infected with *S. flexneri* for 15 minutes, followed by paraformaldehyde fixation. Cells were analyzed by immunofluorescence for phospho-MYPT1 Ser507, F-actin and dsRed expressing *S. flexneri*.

minutes at an MOI of 40. After 30 minutes, the medium was replaced by medium or medium containing 0.1 μM dexamethasone (Sigma). Cells were then incubated for 40 minutes, fixed using 4% paraformaldehyde, permeabilized using 0.1% Triton-X100 and stained with fluorescent phalloidin and Hoechst for 1 hour. Imaging and quantification was performed according to the standard automated image analysis protocol. F-actin staining was used to define cell contours. The translocation of Rev-GR-GFP protein was measured by the nuclear/cytoplasmic GFP intensity ratio.

5.3.4 siRNA screen on *S. flexneri* entry

The technical procedure for the siRNA screen on *S. flexneri* entry has been described in detail in the PhD thesis of C. Kasper[127].

Chapter III

Exploration of an IpgD dependent mTOR and AKT activation mechanism

The *Shigella flexneri* effector IpgD induces mTOR signaling and activates AKT in a PI3K independent manner involving IPMK

Christoph Schmutz, Simon Ittig, Marlise Amstutz and Cécile Arrieumerlou

Biozentrum, University of Basel, Klingelbergstrasse 50/70, 4056 Basel, Switzerland

Manuscript in preparation

1 Statement of contribution

Most of the experiments presented were performed by myself, unless differently stated. Simon Ittig developed the *Yersinia* type three secretion system (TTSS) based protein delivery tool including cloning of IpgD. Marlise Amstutz provided the IpgD C438S mutant and conducted the corresponding experiments.

2 Abstract

The *S. flexneri* effector IpgD is a phosphoinositide 4-phosphatase and translocated into the host cell where it generates phosphatidylinositol 5-phosphate (PI5P) ftom phosphatidylinositol 4,5-bisphosphate (PI(4,5)P2)and activates AKT by a mechanism involving PI3K, mTOR and tyrosine kinases. However, the activation mechanisms of the PI3K/AKT/mTOR pathway during infection remains poorly understood. We aimed to unravel the role of PI3K and mTOR during IpgD induced AKT activation and in addition, attempt to find new kinases involved in this pathway. By the use of a *Yersinia enterocolitica* type three secretion system (TTSS) based translocation assay, we were able to rapidly inject functionally active IpgD into HeLa cells and revealed that IpgD does not only activate AKT, but is also sufficient for mTOR activation. The additional application of chemical inhibitors targeting the PI3K and mTOR pathway showed that early IpgD induced AKT activation is mTORC2 but not PI3K-dependent. However, an IpgD induced pro-survival response was found to be dependent on mTORC2 and PI3K signaling, which is in concordance with the observation made at later time-points of IpgD delivery or *S. flexneri* infection, where also AKT activation was found to be dependent on PI3K signaling. Thus, our data suggests two temporally distinct mechanisms of mTORC2 and AKT activation. Contradictory to previous findings, treatment with two different EGFR inhibitors showed that the kinase is not required for *S. flexneri* induced AKT activation. However, we could demonstrate that the kinase inositol polyphosphate multikinase (IPMK) is required for IpgD induced AKT activation and is present at the entry site of *S. flexneri* where it co-localizes with phosphorylated AKT.

3 Introduction

S. flexneri are bacterial pathogens and the causative agent of bacillary dysentery. *S. flexneri* harbor a type three secretion system (TTSS) allowing the translocation of bacterial effector proteins into the epithelial host cell for the induction of its uptake and interference with host signaling cascades that are essential for the maintenance of the pathogens replicative niche. An important aspect of the infection process is the prevention or delay of host cell apoptosis, allowing bacterial replication and dissemination within the tissue. So far, two different TTSS effector proteins have been identified that promote host cell survival, namely VirA and IpgD[22,193,212]. IpgD is a phosphoinositide 4-phosphatase generating phosphatidylinositol 5-phosphate (PI5P) from phosphatidylinositol 4,5-bisphosphate (PI(4,5)P2)[193]. It has been demonstrated that PI5P is rapidly produced at the *S. flexneri* entry site and co-localizes with phosphorylated AKT[212]. Furthermore, IpgD-dependent PI5P production was shown to be a requirement for AKT phosphorylation upon *S. flexneri* infection[212]. AKT is one of the most frequently activated kinases in cancer and plays an important role in different cellular processes, including metabolism, apoptosis, survival, growth and protein synthesis[79]. Canonically, AKT becomes activated within the PI3K/AKT/mTOR cascade. More precisely, receptor tyrosine kinases, G-protein-coupled receptors and other stimuli were shown to activate PI3K and induce the formation of phosphatidylinositol (3,4,5)-trisphosphate (PI(3,4,5)P3) in the plasma membrane. PI(3,4,5)P3 serves as membrane bound docking anchor for proteins harboring a pleckstrin homology domain including AKT and its upstream activator PDK1. In addition, mTORC2 was shown to have kinase activity towards AKT and promoting phosphorylation on Ser 473[108]. AKT activation is typically short-lived due to the rapid hydrolysis of PI(3,4,5)P3 by different phosphoinositide phosphatases including PTEN[119]. However upon *S. flexneri* infection AKT phosphorylation is sustained which has been linked to the inhibition of PP2A phosphatases[221]. Still, the mechanisms by which IpgD induces PI5P-dependent AKT activation are poorly understood. Ramel and colleagues could demonstrate that EGFR is required for IpgD induced AKT activation[222]. More is known for the *Salmonella* IpgD homologue SopB. A screen for kinases involved in SopB-dependent AKT activation revealed the contribution of several kinases, including inositol polyphosphate multikinase (IPMK), although class 1 PI3K did not contribute[233]. Despite the fact that IpgD and SopB were shown to have slightly different substrate specificities[196,193], this finding is surprising and also questions the role of PI3K

upon IpgD-dependent AKT activation. In addition, it has recently been demonstrated that mTORC2 activity is also essential for AKT activation upon *S. flexneri* infection[248]. However, little is known about the activation mechanisms of mTORC2 although this is of great importance due to its involvement in cancer by regulating AKT activity. By the use of a new *Yersinia enterocolitica* type three secretion system (TTSS) based protein delivery tool, we could demonstrate that IpgD is sufficient for the induction of mTOR signaling. We could validate that IpgD-dependent AKT activation is dependent on mTOR but interestingly not on canonical PI3K signaling. Treatment with the well characterized PI3K inhibitors wortmannin and LY294002 did not abolish AKT phosphorylation on Ser 473 during early signaling within the first 15 minutes of IpgD delivery or *S. flexneri* infection. However, at later time-points of IpgD presence, AKT activation was found to be dependent on canonical PI3K signaling which fits the observation that an IpgD induced pro-survival response was dependent on both, mTORC2 and PI3K signaling. Furthermore, we demonstrated that IPMK is required for IpgD induced AKT activation and is present at the site of bacterial entry where it co-localizes with phosphorylated AKT. Our studies provide new insight in the IpgD-dependent activation mechanism of AKT and reveals that mTOR becomes activated downstream of IpgD. Our data may therefore contribute to a better understanding of mTOR activation.

4 Results

4.1 The *S. flexneri* effector IpgD activates the mTOR pathway

In line with a previous observation, we could show that *S. flexneri* induced AKT activation is mammalian target of rapamycin complex 2 (mTORC2)-dependent [248]. HeLa cells were either left untreated or pretreated with the mTOR inhibitor PP242 or the mammalian target of rapamycin complex 1 (mTORC1) inhibitor rapamycin for 1 hour prior to infection with *S. flexneri* for 15 minutes. Rapid phosphorylation of AKT on Ser473 was observed by immunoblotting. Furthermore, AKT phosphorylation was insensitive to pretreatment with the mTORC1 inhibitor rapamycin, whereas PP242, an inhibitor of both mTORC1 and mTORC2, abolished *S. flexneri* induced AKT activation. These data strongly indicates the requirement of mTORC2 in *S. flexneri* induced AKT activation, as previously described [248] (Figure 4.0.1 A). To elucidate whether mTOR itself becomes phosphorylated, a time-course of *S. flexneri* infection covering the first 15 minutes of infection was performed (Figure 4.0.1 B,C). Immunoblotting with phospho-specific mTOR antibodies revealed a moderate but clearly observable increase in mTOR phosphorylation over time on both, the autophosphorylation site Ser2481 and the S6K phosphorylation site Ser2448, which have been associated with mTORC2 and mTORC1 activity, respectively [45]. These data shows that mTORC2 is required for AKT activation during *S. flexneri* infection and reveals that mTOR becomes rapidly activated. It is well established that AKT becomes activated during *S. flexneri* infection due to the activity of the TTSS effector IpgD. However, the precise mechanism of IpgD-dependent AKT activation remains incompletely understood. To study the activation mechanism of mTOR and AKT during *S. flexneri* infection, we applied a *Yersinia enterocolitica* derived TTSS-dependent protein translocation tool. The tool allows the direct translocation of IpgD into target cells in a temporal tightly controlled manner and without interference of other effectors (Figure 4.0.1 D). Thus, a *Yersinia enterocolitica* strain mutated in all six effector genes (YopH, O, P, E, M and T) as well as *asd*, leading to obligate requirement for diaminopimelic acid (DAP), was fused to YopE containing a signal required for TTSS-dependent secretion and IpgD, yielding in the $\Delta HOPEMT\ asd\ +\ YopE_{signal}$ - *IpgD* strain [147]. As control, the background strain $\Delta HOPEMT\ asd\ +\ YopE_{signal}$ was used. To test these strains, HeLa cells were either infected with $\Delta HOPEMT\ asd\ +\ YopE_{signal}$ - *IpgD* or $\Delta HOPEMT\ asd\ +\ YopE_{signal}$ for 15 minutes and phosphorylation of AKT on Ser473 was visualized by immunoblotting. The background strain was not capable to induce AKT phosphorylation, whereas

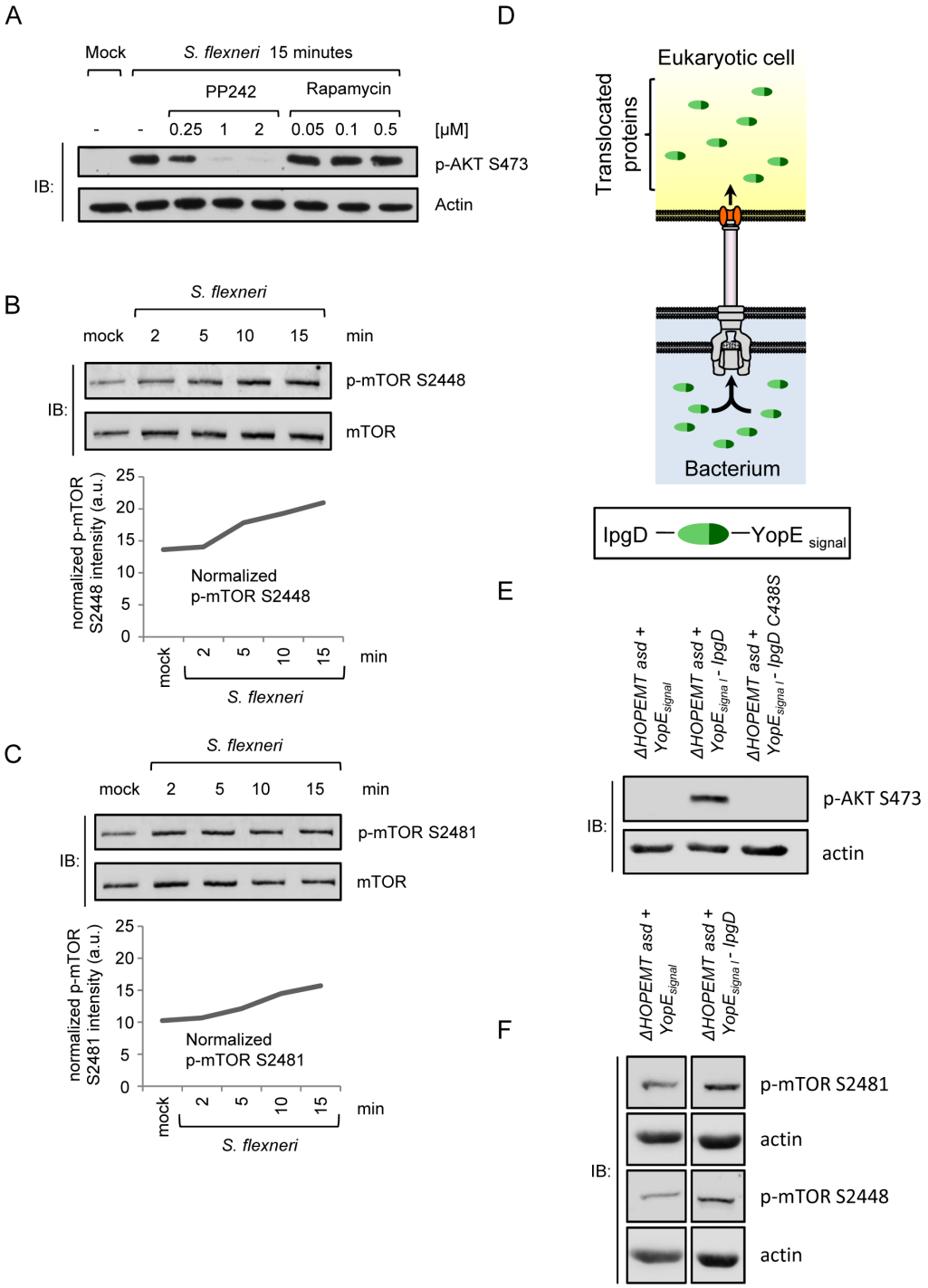

Figure 4.0.1 (Continued on the following page.)

Figure 4.0.1 *S. flexneri* activates the mTOR pathway. (A) *S. flexneri* activates AKT in a mTOR-dependent manner. HeLa cells were pretreated for one hour with indicated concentrations of PP242 or rapamycin and infected with *S. flexneri* at an MOI of 40 for 15 minutes. The phosphorylation of AKT on Ser473 was analyzed by immunoblotting. Actin was used to ensure equal protein loading. (B) HeLa cells were infected for 2, 5, 10 and 15 minutes with *S. flexneri* at an MOI of 40 and analyzed by immunoblotting for the phosphorylation of mTOR on Ser2448. Total mTOR was used as loading control. The lower diagram shows the increase in mTOR Ser 2448 phosphorylation normalized to the total mTOR protein amount over time. (C) HeLa cells were infected for 2, 5, 10 and 15 minutes with *S. flexneri* at an MOI of 40 and analyzed by immunoblotting for the phosphorylation of mTOR on Ser2481. Total mTOR was used as loading control. The lower diagram shows the increase in mTOR Ser2481 phosphorylation normalized to the total mTOR protein amount over time. (D) a *Yersinia enterocolitica* Δ*HOPEMT asd +* $YopE_{signal}$ *- IpgD* strain is used for the rapid and synchronized TTSS-dependent translocation of IpgD into HeLa cells, without interference of additional effectors. (E) The phosphatidylinositol-4-posphatase activity of IpgD is required for AKT activation. HeLa cells were infected for 15 minutes with either Δ*HOPEMT asd +* $YopE_{signal}$ or Δ*HOPEMT asd +* $YopE_{signal}$ *- IpgD* or Δ*HOPEMT asd +* $YopE_{signal}$ *- IpgD C438S* for 15 minutes. Cell extracts were analyzed by immunoblotting for the phosphorylation of AKT on Ser473. Actin was used to ensure equal protein loading. (F) IpgD induces mTOR phosphorylation. HeLa cells were infected for 15 minutes with either Δ*HOPEMT asd +* $YopE_{signal}$ or Δ*HOPEMT asd +* $YopE_{signal}$ *- IpgD* and phosphorylation of mTOR on Ser 2448 and Ser2481 was analyzed by immunoblotting. Actin was used as loading control (preliminary data).

the IpgD translocating strain efficiently did (Figure 4.0.1 E). In addition, we aimed to validate that the catalytic activity of IpgD is required for AKT activation. We mutated the proposed catalytic domain of IpgD (C438S) which fully abolished AKT phosphorylation on Ser473[193] (Figure 4.0.1 E). Therefore, the effect of IpgD towards activation of AKT can be attributed to PI5P which is the product of the catalytic activity of IpgD . Furthermore, our data shows that IpgD is sufficient to induce mTOR activation. By immunoblotting with antibodies recognizing phosphorylated mTOR, a moderate increase in mTOR phosphorylation on both, Ser2481 and Ser2448 was observed upon infection with Δ*HOPEMT asd +* $YopE_{signal}$ *- IpgD* compared to Δ*HOPEMT asd +* $YopE_{signal}$ (Figure 4.0.1 F). These data indicate that the *Yersinia* tool can be applied to study the impact of IpgD on mTOR and AKT activation.

4.2 IpgD induced AKT and mTOR activation is not PI3K-dependent

We aimed to elucidate the mechanism of IpgD-dependent AKT activation in more detail. Thus, we wanted to reproduce the PI3K-dependency of IpgD induced AKT phosphorylation as it was previously observed[212] and contradictory to findings based on the

Salmonella homologue SopB[233]. IpgD was translocated by the use of the *Yersinia* protein delivery system into cells pretreated with the PI3K inhibitors wortmannin or LY294002 or the mTOR inhibitor PP242. AKT phosphorylation on Ser473 was monitored after 15 minutes of IpgD delivery by immunoblotting. As already shown, PP242 treatment almost fully abolished AKT activation (Figure 4.2.1 A). To our surprise, neither wortmannin nor LY294002 treatment could abolish AKT phosphorylation, implementing an AKT activation mechanism independent of canonical PI3K signaling. Insulin induced AKT phosphorylation was sensitive to wortmannin and LY294002 treatment confirming the efficacy of the drug treatment. Using the same experimental context, we aimed to visualize mTOR activity by monitoring the phosphorylation on Ser2481 and Ser2448 (Figure 4.2.1 B). IpgD induced phosphorylation of mTOR on Ser2481 also appeared to be PI3K insensitive as treatment with wortmannin or LY294002 did not affect the phosphorylation. Phosphorylation of mTOR on Ser2448 seems to be at least partially sensitive to LY294002. Next, we aimed to prove whether AKT activation is also insensitive to PI3K inhibition upon *S. flexneri* infection of HeLa cells. Using the same conditions of drug treatment, we found that neither LY294002 nor wortmannin could abolish AKT phosphorylation on Ser473 whereas PP242 efficiently did (Figure 4.2.1 C). Overall, these data demonstrate that IpgD induces AKT and mTOR activation but independent of canonical PI3K signaling.

4.3 IpgD induced pro-survival response is mTOR and PI3K-dependent

Although a pro survival-effect of IpgD has been proposed, we aimed to validate this finding upon translocation of IpgD by the *Yersinia* TTSS protein delivery tool. This method allowed us to study the effect of IpgD on host cell survival in a temporal tightly controlled manner and additionally circumvented an adaption of the cell to the effector, as one could expect using transient overexpression of IpgD. HeLa cells were either infected with $\Delta HOPEMT\ asd\ +\ YopE_{signal}$ or $\Delta HOPEMT\ asd\ +\ YopE_{signal}$ - *IpgD* for one hour. Bacteria were subsequently removed by washing and gentamycin application. In addition, cells were treated for further two hours with 0.5μM staurosporine for induction of apoptosis. After chemical fixation, nuclei, actin cytoskeleton and cleaved-caspase 3 were stained with Hoechst, fluorescein phalloidin and fluorescently labeled antibodies, respectively (Figure 4.2.2 A). In staurosporine-treated cells infected with the $\Delta HOPEMT\ asd\ +\ YopE_{signal}$, an apoptotic phenotype was observable, characterized by nuclei shrinkage, cell shrinkage and detachment as well as caspase 3 cleavage. Translocation of IpgD attenuated these symptoms, indicating that IpgD is responsible for pro-survival signals. Next, we were interested whether the pro-survival effect of IpgD is dependent on mTOR and PI3K signaling. Thus, cells were pretreated with rapamycin to inhibit mTORC1, PP242 to inhibit both mTORC1 and mTORC2 signaling as well as LY294002 for inhibition of PI3K

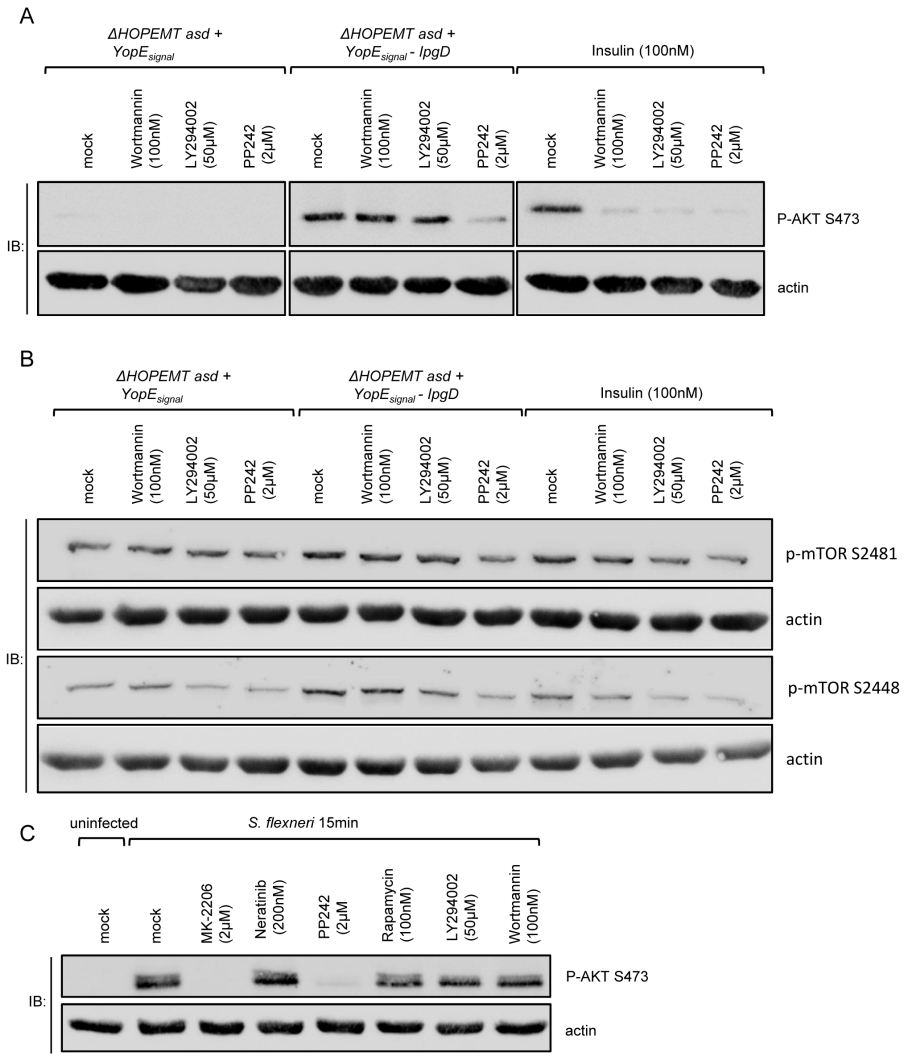

Figure 4.2.1 The IpgD indcuced AKT activation is mTOR but not PI3K-dependent. (A) HeLa cells were either left untreated or pretreated with wortmannin, LY294002 or PP242 for 1 hour. IpgD was translocated into the Hela cells by the *Yersinia* protein translocation system for 15 minutes. As control for the inhibitory effect of the drugs, drug treated HeLa cells were stimulated with 100nM Insulin for 15 minutes. Cell extracts were analyzed by immunoblotting for the phosphorylation of AKT on Ser473. Actin was used as loading control. (B) mTOR phosphorylation is only partially sensitive to PI3K inhibition. In the same experimental conditions, phosphorylation of mTOR was visualized by immunoblotting on Ser2481 and Ser2448. Actin was used as loading control. (C) AKT activation upon *S. flexneri* infection is also PI3K independent. HeLa cells were left untreated or pre-treated with wortmannin, LY294002 or PP242 for 1 hour and subsequently infected with *S. flexneri* at an MOI of 40 for 15 minutes. Cell extracts were analyzed by immunoblotting for the phosphorylation of AKT on Ser473. Actin was used to ensure equal protein loading.

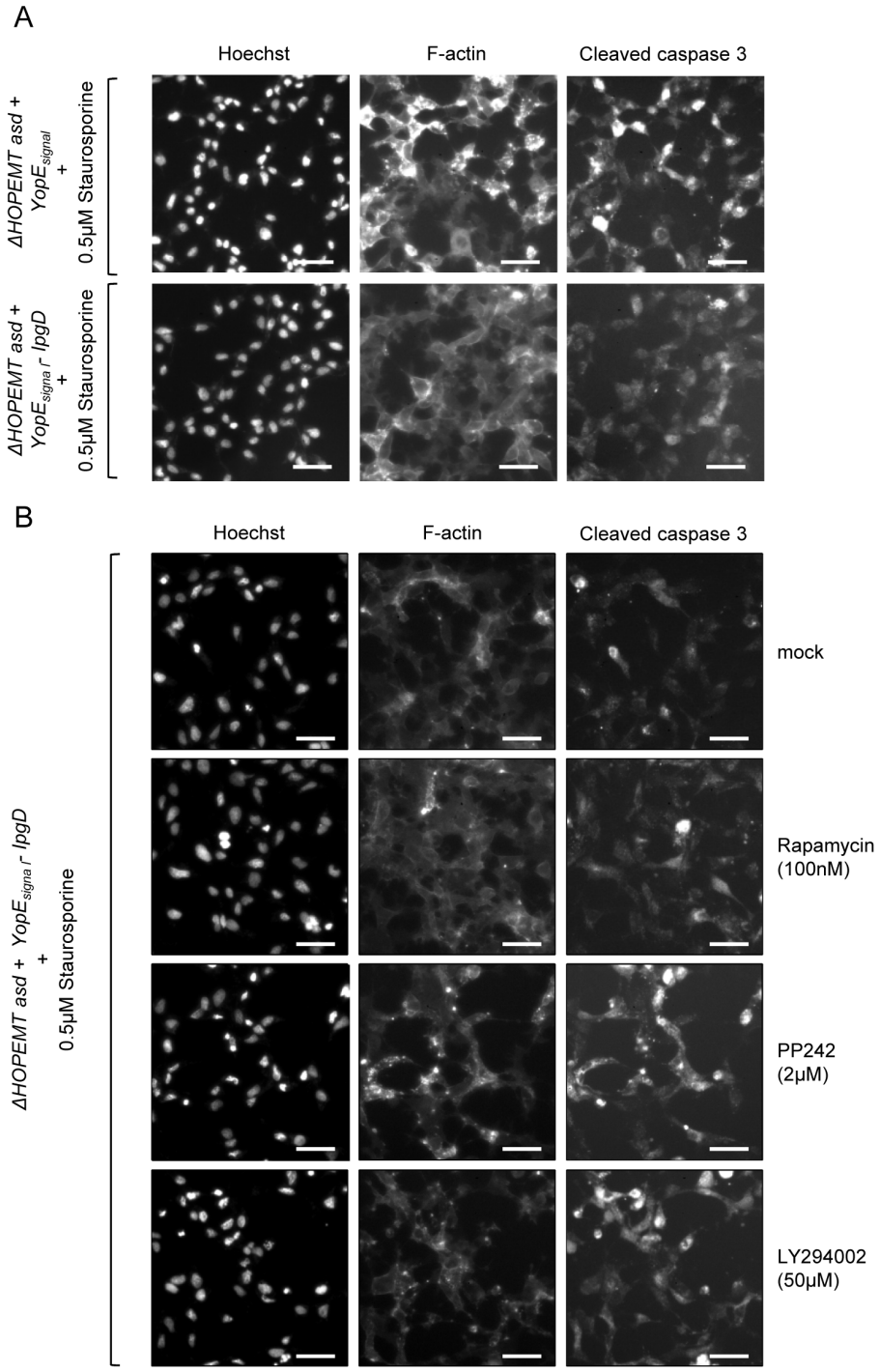

Figure 4.2.2 (Continued on the following page.)

Figure 4.2.2 IpgD protects cells from staurosporine induced apoptosis in dependence of mTORC2 and PI3K signaling. (A) IpgD protects HeLa cells from staurosporine indcued apoptosis. HeLa cells were infected with either Δ*HOPEMT asd + YopE*$_{signal}$ or Δ*HOPEMT asd + YopE*$_{signal}$ - *IpgD* for 1 hour allowing translocation of IpgD. Next, bacteria were removed and cells were challenged with 0.5μM staurosporine for further 2 hours, followed by paraformaldehyde fixation and staining of the nuclei, F-actin and cleaved caspase-3 for immunofluorescence. (B) The pro-survival effect of IpgD is dependent on mTORC2 and PI3K signaling. HeLa cells were either left untreated or pre-treated with rapamycin, PP242 or LY294002 for 1 hour. HeLa cells were subsequently infected with Δ*HOPEMT asd + YopE*$_{signal}$ - *IpgD* for 1 hour allowing translocation of IpgD. Next, bacteria were removed and cells were left untreated or challenged with 0.5μM staurosporine for further 2 hours, followed by paraformaldehyde fixation and staining of the nuclei, F-actin and cleaved caspase-3 for immunofluorescence. Scale bars represent 50μm.

signaling. Again, IpgD was allowed to translocate into the cells for one hour, followed by staurosporine treatment (Figure 4.2.2 B). Inhibition of mTORC1 using rapamycin did not affect host cell survival upon staurosporine and IpgD treatment compared to cells that have only been treated with staurosporine and IpgD. However, treatment with PP242, known to inhibit both, mTORC1 and mTORC2 markedly attenuated the protective effect of IpgD. Because mTORC1 inhibition alone did not affect survival, it is tempting to speculate that mTORC2 is important for the transduction of an IpgD-dependent pro-survival response. As we have shown, that PI3K signaling is not required for IpgD-dependent AKT activation, we expected that it would neither be important for an IpgD induced pro-survival response. Surprisingly, pretreatment of cells with the PI3K inhibitor LY294002 attenuated the IpgD-dependent pro-survival response to a similar extend as PP242. Although PI3K signaling is not necessary for IpgD induced AKT activation it appears to play together with mTORC2 a role in an IpgD-dependent survival response.

4.4 PI3K is responsible for AKT activation at later time points

Against previous assumptions, we demonstrated that PI3K are not involved in early IpgD induced AKT activation. Yet, the IpgD induced pro-survival response was PI3K-dependent. As IpgD induces not only a fast but also sustained AKT phosphorylation, we asked ourselves whether we observe differences in the AKT activation mechanism over time. To address this question, HeLa cells were pretreated with LY294002 or PP242 for one hour and subsequently infected with Δ*HOPEMT asd + YopE*$_{signal}$ - *IpgD* or Δ*HOPEMT asd + YopE*$_{signal}$ for 30, 60 and 120 minutes (Figure 4.4.1 A). Immunoblotting revealed that AKT phosphorylation on Ser473 was strongest after 30 minutes and got weaker over time but was still observable after 120 minutes, confirming that IpgD induces sustained AKT activation. The mTORC1/2 inhibitor PP242 abolished AKT phosphorylation at all

time-points, validating that mTOR is crucial for AKT activation throughout the whole time-course of infection. Further, our data showed that IpgD induced AKT phosphorylation on Ser473 was not affected by LY294002 treatment after 30 minutes of infection with Δ*HOPEMT asd + YopE*$_{signal}$ - *IpgD*, but surprisingly LY294002 treatment reduced AKT phosphorylation after 60 minutes and almost completely abolished AKT phosphorylation after 2 hours of IpgD delivery.

This is in concordance with the observation that PI3K signaling is important for the induction of a pro-survival response that was monitored 3 hours post-infection. To confirm the significance of this observation, we repeated the experiment using *S. flexneri* infection as model. Again, cells were left untreated or pretreated either with LY294002 or PP242 and subsequently infected with *S. flexneri* for different periods of time (Figure 4.4.1 B). *S. flexneri* induced AKT activation is largely independent of PI3K signaling at 30 minutes post-infection as treatment with LY294002 could not abolish AKT phosphorylation on Ser473. However, after 60 and 120 minutes, LY294002 almost completely abolished AKT phosphorylation. This observation based on *S. flexneri* infection is congruent with the data obtained from IpgD translocation alone. Altogether, these data implies at least two distinct mechanism of AKT activation. Namely, an early mechanism which is independent from canonical PI3K signaling and a later one which relies on canonical PI3K signaling.

4.5 EGFR activity is not required for AKT activation

It was proposed that tyrosine kinases are also involved in AKT activation downstream of PI5P signaling[212]. Ensuing, it was shown that EGFR is required for IpgD-dependent AKT activation[222]. We aimed to validate that EGFR activity is required for AKT activation upon *S. flexneri* infection by immunoblotting for phosphorylated AKT and EGFR (Figure 4.5.1). HeLa cells were pretreated with LY294002, PP242 or with the EGFR inhibitors neratinib or AG-1478. EGF stimulation was used to confirm the inhibitory effect of the different drugs towards EGFR signaling. As expected, EGF stimulation induced AKT phosphorylation on Ser473 as well as on Thr308, whereas PP242 or LY294002 treatment fully abolished the observed AKT activation, confirming the requirement for mTOR and PI3K signaling in EGF-dependent AKT activation. Treatment with neratinib or AG-1478 prior to EGF stimulation also fully abolished EGF induced AKT phosphorylation on Ser473 and Thr308 approving the inhibitory effect of the drugs. In addition, EGFR activity was assessed by the use of an antibody recognizing EGFR autophosphorylation on Tyr1068. Pretreatment with LY294002 and PP242 did not reduce EGFR phosphorylation on Tyr1068 upon EGF stimulation as shown by immunoblotting. Interestingly, treatment with PP242 even enhanced EGFR autophosphorylation, although the relevance of this observation remains elusive. Treatment with neratinib or AG-1478 fully abolished EGF

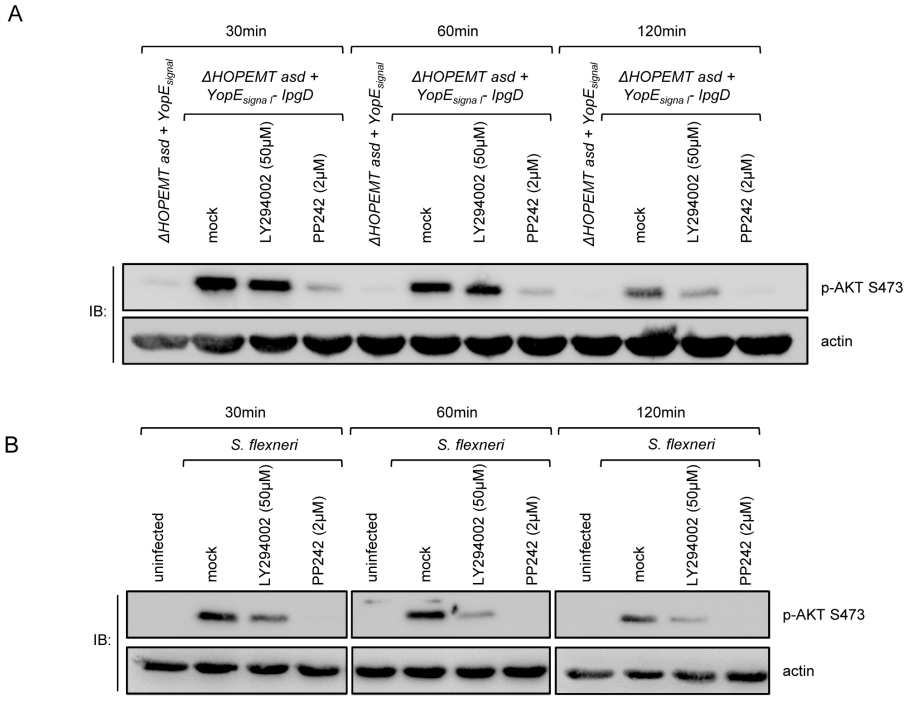

Figure 4.4.1 IpgD indcuced AKT activation is PI3K-dependent at later timepoints. (A) HeLa cells were either left untreated or pretreated with wortmannin, LY294002 or PP242 for 1 hour. IpgD was translocated into the Hela cells by the *Yersinia* system for either 30, 60 or 120 minutes. After 30 minutes, cells were treated with gentamycin to kill the *Yersinia*. Cell extracts were analyzed by immunoblotting for the phosphorylation of AKT on Ser473. Actin was used as loading control. (B) AKT activation upon *S. flexneri* infection is also PI3K-dependent at later timepoints of infection. HeLa cells were either left untreated or pre-treated with wortmannin, LY294002 or PP242 for 1 hour and subsequently infected with *S. flexneri* at an MOI of 40 for 30, 60 or 120 minutes. After 30 minutes, cells were treated with gentamycin to kill extracellular *S. flexneri*. Cell extracts were analyzed by immunoblotting for the phosphorylation of AKT on Ser 473. Actin was used as loading control.

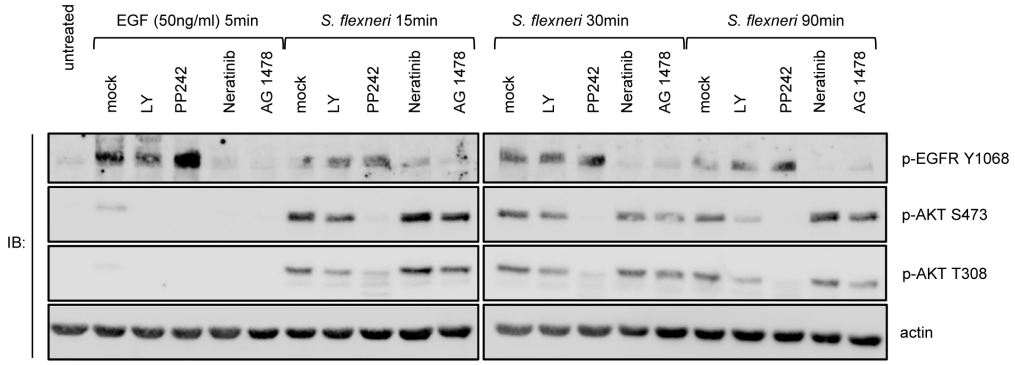

Figure 4.5.1 *S. flexneri* induced AKT activation is independent of EGFR signaling. HeLa cells were either left untreated or pre-treated with, LY294002, PP242, neratinib or AG-1478 for 1 hour. HeLa cells were subsequently treated with EGF (50ng/ml) for 5 minutes or infected for 15, 30 or 90 minutes with *S. flexneri* at a MOI of 40. Cell extracts were analyzed by immunoblotting for the phosphorylation of EGFR on Tyr1068 and phosphorylation of AKT on Ser473 and Thr308. Actin was used as loading control.

induced EGFR autophosphorylation on Tyr1068, further indicating that the experimental setup is suitable to study the effect of EGFR inhibition upon *S. flexneri* infection. In the same conditions of drugs treatment, cells were infected with *S. flexneri* for 15, 30 or 90 minutes. *S. flexneri* infection induced EGFR autophosphorylation on Tyr1068 that was sensitive to treatment with neratinib or AG1478. As previously observed, infection with *S. flexneri* induced a fast and sustained phosphorylation of AKT on Ser473 and Thr308 that was sensitive to PP242 treatment and in a temporal distinct manner sensitive to LY294002 treatment. However AKT phosphorylation on Ser473 and Thr308 was not affected upon neratinib or AG1478 treatment, showing that EGFR activity is not required for *S. flexneri* induced AKT activation. Therefore, other kinases than EGFR may be involved in *S. flexneri* induced AKT activation.

4.6 IPMK is required for IpgD induced AKT activation and recruited to the entry foci

Because class 1 PI3K that are targeted by LY294002 or wortmannin are not involved in the early IpgD and thus PI5P-dependent AKT activation, other kinases with PI3K activity must be involved. Recently, a siRNA screen revealed the inositol phosphokinase IPMK as candidate for AKT activation downstream of the *Salmonella* IpgD homologue SopB[233]. In order to test whether IpgD induced AKT activation relies on IPMK, we monitored AKT phosphorylation on Ser473 in IPMK deficient MEFs (Figure 4.5.2 A). To control the ability of the IPMK deficient MEF cells (IPMK-/-) to induce AKT activation, cells were

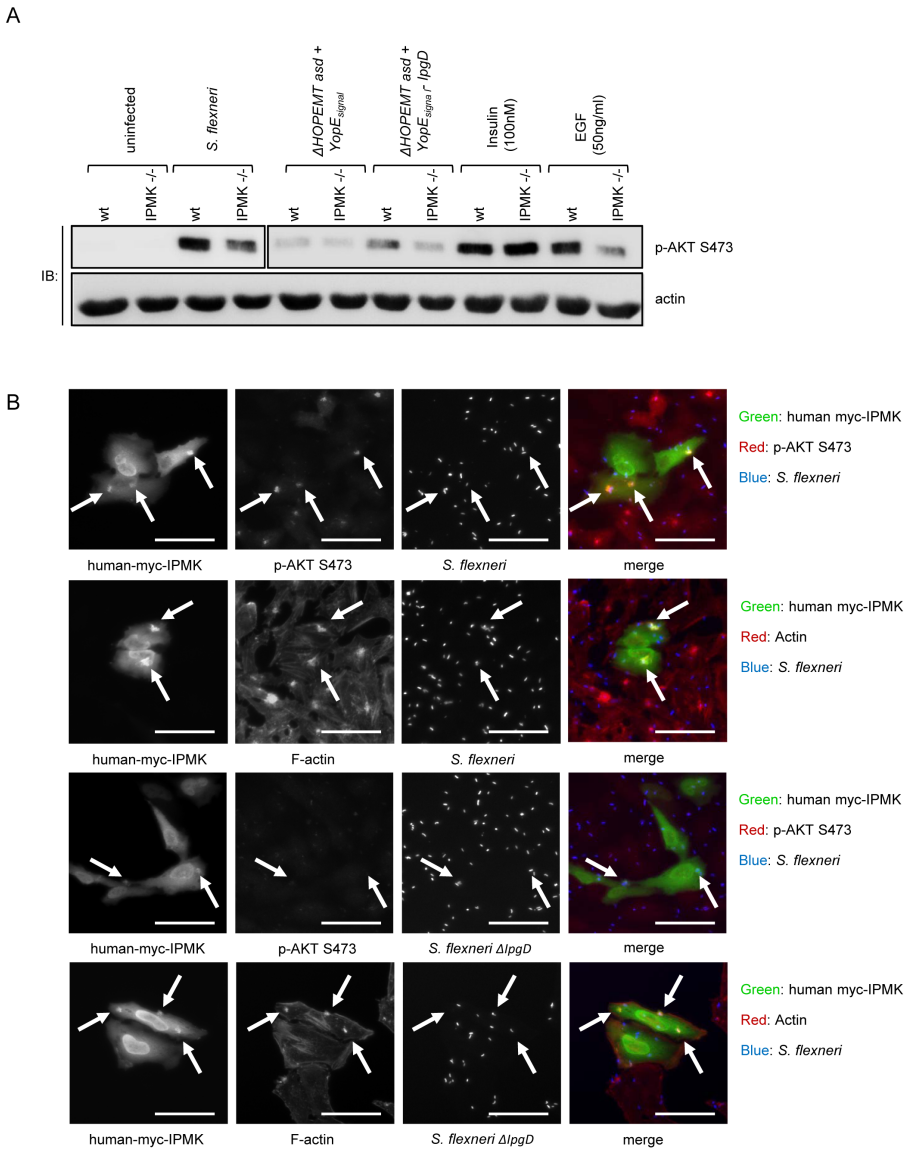

Figure 4.5.2 IPMK is required for IpgD-dependent AKT activation. (A) Wild-type (wt) and IPMK deficient mouse embryonic fibroblasts (MEF) cells (IPMK -/-) were either left untreated or treated with 100nM insulin, 50ng/ml EGF or infected with *S. flexneri* at a MOI of 40, Δ*HOPEMT asd + YopE*$_{signal}$ or Δ*HOPEMT asd + YopE*$_{signal}$ - *IpgD* at a MOI of 100 for 15 minutes. Cell extracts were analyzed by immunoblotting for the phosphorylation of AKT on Ser 473. Actin was used to ensure equal protein loading. (B) IPMK co-localizes with phosphorylated AKT at the *S. flexneri* entry site. HeLa cells were transfected with myc-tagged human-IPMK for 24 hours and subsequently infected with either wild-type *S. flexneri* or *S. flexneri* Δ*ipgD* for 15 minutes, followed by paraformaldehyde fixation. Cells were analyzed by immunofluorescence for myc-tagged human-IPMK, phospho-AKT Ser 473, F-actin and dsRed expressing *S. flexneri*. Scale bars represent 50μm.

either treated with insulin or EGF and AKT phosphorylation was monitored on Ser473 by immunoblotting. Upon stimulation with insulin, in both the wild-type and IPMK-/- MEF cells strong AKT phosphorylation on Ser473 was observed. Upon stimulation with EGF, AKT in wild-type MEF became phosphorylated whereas AKT in IPMK-/- MEF cells only got weakly activated. These data indicated that AKT can become phosphorylated in IPMK-/- MEFs but IPMK can interfere with AKT activation in a stimulus-dependent way. Next, we investigated whether IpgD can induce AKT phosphorylation in IPMK-/- cells. Cells were infected either with Δ*HOPEMT asd +* $YopE_{signal}$ or Δ*HOPEMT asd +* $YopE_{signal}$ *- IpgD* at a MOI of 100. As expected, infection with the background strain did not induce AKT phosphorylation in either wild-type or in IPMK-/- MEF cells. However, translocation of IpgD into wild-type MEF cells induced AKT phosphorylation on Ser473 within 15 minutes post-infection, showing that the *Yersinia* tool can also be used to target MEF cells. Interestingly, the ability to activate AKT in an IpgD-dependent manner is severely impaired in IPMK-/- cells, indicating that IPMK is essential for IpgD induced AKT phosphorylation. Hereafter, we tested whether this observation can be confirmed upon *S. flexneri* infection. Wild-type and IPMK-/- MEF cells were infected with *S. flexneri* at a MOI of 40 for 15 minutes and subsequently analyzed by immunoblotting. As already observed upon IpgD translocation, *S. flexneri* infection induces AKT phosphorylation in wild-type MEF cells. But again, the ability of *S. flexneri* to induce AKT phosphorylation in IPMK-/- cells was reduced. These data indicate, that IPMK is important for AKT activation upon IpgD delivery.

Since AKT is recruited to the entry foci we investigated whether IPMK was also localized at this site. HeLa cells were transfected with myc tagged human-IPMK for 24 hours and subsequently infected with *S. flexneri* for 15 minutes and fixed. Myc tagged human-IPMK as well as AKT phosphorylated on Ser473 was visualized by immunofluorescence (Figure 4.5.2 B). As already published[212], AKT rapidly became phosphorylated at the site of *S. flexneri* entry. In addition, we also found IPMK to be enriched at the entry foci. We next raised the question whether the presence of IPMK on the entry site is dependent on IpgD activity. Therefore, we compared cells transfected with human IPMK upon infection with wild-type and Δ*ipgD S. flexneri*. The *ipgD* deficient *S. flexneri* mutant was unable to induce AKT phosphorylation. However, IPMK was still observable at the site of entry, suggesting that IpgD is not a requirement for its recruitment. Overall, these data support the hypothesis that IPMK is necessary for IpgD induced AKT activation, while the recruitment of IPMK to the entry site is not IpgD-dependent.

5 Discussion

In the course of this study, we addressed an IpgD-dependent AKT and mTOR activation mechanism and aimed to identify novel components of this signaling pathway. Our data revealed that IpgD is sufficient for mTOR activation and induces AKT phosphorylation on Ser473 by a mechanism including mTORC2 but not canonical PI3K signaling. Furthermore, we demonstrated that EGFR is not involved in IpgD induced AKT activation, whereas IPMK is. It has previously been described, that *S. flexneri* infection affects mTOR signaling but the published data so far are not consistent. It was proposed, that *S. flexneri* infection causes amino acid starvation in the host cell, leading to downregulation of mTOR signaling after 2-6 hours of infection and the subsequent induction of autophagy[267]. A recent phosphoproteomic publication from our laboratory demonstrated that *S. flexneri* infection activates mTOR signaling within 15 minutes of infection as indicated by phosphorylation of the downstream effectors AKT and S6K[248]. The differences in the mTOR activation pattern between these two studies may mainly arise from monitoring different timescales of infection and could therefore indicate temporal distinct roles for mTOR during bacterial infection. The here presented study demonstrates additionally that IpgD was sufficient to activate mTOR. A catalytic inactive mutant of IpgD failed to activate AKT, strongly suggesting that the catalytic activity which is required for PI5P production is also essential for the IpgD-dependent effects we observe. This directly implies that PI5P production can lead to the activation of mTOR, a relationship which has to our knowledge so far not been recognized. Whether this is a direct effect or several intermediate stages contribute to mTOR activation requires further investigations. We next examined whether PI3Ks are important for IpgD-dependent AKT activation on a short timescale. Canonically, activated receptors directly stimulate Class 1 PI3Ks that convert PIP2 to PIP3 which binds to AKT at the plasma membrane, allowing PDK1 to phosphorylate AKT on T308 and either mTORC2 or DNA-PK to phosphorylate AKT on Ser473 leading to full AKT activity[108]. However, our data indicates that AKT can become activated independently of PI3K activity. This is also true for IpgD-dependent AKT phosphorylation on Thr308 which is not affected by wortmannin and at the best slightly affected by LY294002 treatment, suggesting a widely PI3K independent AKT activation mechanism (data not shown). These data is conflicting with previous publications, where IpgD induced AKT activation was shown to be PI3K-dependent[212,222]. Data from the *Salmonella* homologue SopB revealed that SopB-dependent AKT activation is indepen-

dent of the PI3K inhibitor wortmannin although sensitivity towards LY294002 treatment was osbserved[44]. Oppositely, a complete class 1 PI3K independent mechanism for SopB-dependent AKT activation has recently been proposed by Roppenser and colleagues fitting our IpgD-dependent observations[233]. In addition, we provide an explanation which can partially resolve the contradictory aspect to previous findings on the PI3K dependency of AKT activation. A time-course experiment of IpgD translocation by *Yersinia* into HeLa cells revealed that PI3K is required for AKT activation at later time-points. In previous studies, the IpgD induced AKT activation mechanism was mainly studied by transient transfection leading to a prolonged presence of IpgD in the target cell which impedes an observation of the early effect of IpgD[212]. This observation also provides an explanation why the observed IpgD induced pro-survival effect is PI3K-dependent although its activity is not required for initial AKT phosphorylation. Cell survival was monitored after 3h of IpgD delivery which provides enough time for the induction of the PI3K-dependent AKT pathway and points out that PI3K activity is indeed important for repression of apoptosis. Our study also addressed a potential role of EGFR in IpgD induced AKT activation. It was proposed by Pendaries et al. that tyrosine kinases are involved in IpgD induced AKT activation[212]. Ramel et al. subsequently demonstrated that the tyrosine kinase EGFR is essential for IpgD-dependent AKT activation[222]. However, our data suggest a mechanism which is independent of EGFR signaling. Whether other tyrosine kinases are involved in this signaling cascade is so far unknown. It was demonstrated that despite the lack of requirement for class 1 PI3K, PI(3,4,5)P3 is still important for SopB-dependent AKT activation, as co-expression of the phosphatase PTEN abolished SopB-dependent AKT activation, indicating the involvement of other kinases in the production of this phosphatidylinositol[233]. A siRNa screen performed by Roppenser et al. revealed amongst other, IPMK to be involved in *Salmonella*-dependent AKT activation[233]. IPMK is a pleiotropic protein as it can have both, phosphate kinase and phosphatidylinositol kinase catalytic activity[133]. Thus we tested whether IPMK is also essential for IpgD induced AKT activation. Infection of IPMK deficient MEF cells revealed the requirement of IPMK for IpgD induced AKT phosphorylation on Ser473. As we observed IPMK deficient MEF cells not to be impaired in their ability to induce insulin stimulated AKT activation, we conclude that the impairment towards IpgD-dependent AKT activation was specific. Intriguingly, we found that IPMK is also necessary for EGF mediated AKT activation. This is of special interest because the EGFR-PI3K-AKT pathway is deregulated in different cancers and the finding of the involvement of IPMK may contribute to a better understanding of this pathway[41].

As it is known that AKT is becoming phosphorylated at the entry site of *S. flexneri*, we addressed whether we also observe IPMK in this compartment. It has been described, that IPMK is a nuclear protein. As previously described, we observe a predominant nuclear

localization of human IPMK upon transient transfection into HeLa cells[287]. Nevertheless, IPMK is also present in the cytosol and more pronounced at the site of bacterial entry. This data gives further evidence that IPMK is involved in IpgD-dependent AKT activation.

6 Material and methods

6.1 Reagents and antibodies

PP242 was obtained from Chemdea, Ridgewood, NJ (#CD0258), Rapamycin from LC Laboratories, Woburn, MA (#R-5000), LY294002 (#S1105), Wortmannin, Neratinib (#S2150), Tyrphostin AG-1478 (#S2728) from Selleck Chemicals, Houston, TX, Wortmannin (#W1628) and Staurosporine (#S-4400), were obtained from Sigma, St. Louis, MO. Antibodies against phospho-AKT Ser473 (#4058), phospho-AKT Thr308 (#2965) phospho-S6K Thr389 (#9205), phospho-mTOR Ser2448 (#5536), phospho-mTOR Ser2481 (#2974), phospho-EGFR Tyr1068 (#3777) were obtained from Cell Signaling Technology, Danvers, MA. Antibodies against actin (#MAB1501) were purchased from Millipore, Billerica, MA.

6.2 Cell culture

HeLa CCL-2^{TM} human epithelial cells were purchased from ATCC, Manassas, VA and cultured in DMEM, supplemented with 10% FCS, antibiotics and L-glutamine. The IPMK deficient mouse embryonic fibroblasts (MEF)s and the corresponding control cells were generously provided by Solomon H. Snyder[165]. MEFs were cultured in DMEM, supplemented with 10% FCS, antibiotics and L-glutamine.

6.3 Bacterial strains

The M90T *S. flexneri* was generously provided by Prof. P. Sansonetti (Institut Pasteur, Paris, France). The IpgD deletion mutant Δ*ipgD* was generated by allelic exchange using a modification of the λ red-mediated gene deletion as previously described[135]. All *S. flexneri* strains were transformed with the pMW211 plasmid to express the DsRed protein under control of a constitutive promoter. The pMW211 plasmid was a generous gift from Dr. D. Bumann (Biozentrum, University of Basel, Switzerland). The Δ*ipgD* deletion mutant was generated from the M90T strain by allelic exchange using a modification of the λ red-mediated gene deletion procedure[52]. The genes for λ red recombination were expressed from the pKM208 plasmid[184]. The ampicillin resistance cassette of the pKD13 plasmid was amplified using the following primers:

Table 6.1 Primers for λ red-mediated gene deletion

Mutant	Forward	Reverse
Δ*ipgD*	CTGCAATCAATGCCCCATTTATGA	GCAAATAACATCTGCTAAATCTTC
	CTGAGGATAATTAAATGCACATAA	CATATATTCCTCTTATACAAATGAC
	CTATTCCGGGGATCCGTCGACC	GGTGTAGGCTGGAGCTGCTTC

After *DpnI* digestion, the PCR product was electroporated into *M90T* strain. Recombinants were selected on TSB plates containing ampicillin. The Amp cassette was removed by transformation of pCP20 and incubation at 30°C on TSB plates containing 100 μg/ml ampicillin. Single colonies were screened by PCR.

The Δ*HOPEMT asd* + $YopE_{signal}$ - *IpgD*strain was generated by cloning IpgD from *S. flexneri* M90T genomic DNA into a bacterial expression vector as fusion to $YopE_{signal}$. This construct was electroporated into the Δ*HOPEMT asd* effectorless *Yersinia enterocolitica* strain. More details cannot be provided at this moment due to a pending patent from Ittig et al. but will be available from Ittig et al. (manuscript in preparation).

6.4 *S. flexneri* infection assay

M90T *S. flexneri* strain was grown to exponential growth phase at 37°C in tryptic soy broth (TSB) and coated with poly-L-lysine. HeLa or MEF cells were serum starved for two hours or overnight by replacing the complete growth medium with DMEM supplemented with 10 mM Hepes and 2 mM L-glutamine (assay medium). Cells were infected at a MOI of 40 by adding bacteria or assay medium only (uninfected control) to 96- or 6-well plates. Infection was initiated and synchronized by centrifugation of the cell culture plates for 2 minutes at 1750 rpm and subsequent incubation at 37°C for the indicated time periods. Extracellular bacteria were killed by adding gentamycin (50μg/ml) (Life technology, Carlsbad, CA), 30 minutes after infection, in assays exceeding this timepoint.

6.5 *Y. enterocolitica* infection assay

Yersinia enterocolitica strains were grown overnight at room temperature in BHI supplemented with DAP , Nal and ampicillin. The next day, bacteria were diluted to an OD_{600} of 0.2 in fresh BHI including the supplements and grown for 2 hours at room temperature followed by a 30 minute temperature shift to 37°C in a water bath shaker. The bacteria were collected by centrifugation (6000 rcf, 30 seconds) and washed once with DMEM supplemented with 10 mM HEPES and 2 mM L-glutamine. Cells were infected at a MOI of 100 in DMEM supplemented with 10 mM HEPES and 2 mM L-glutamine. The infection was initiated by centrifugation of the plates for 1 minute at 1750 rpm and subsequent incubation at 37°C for the indicated time-periods. Extracellular bacteria were killed by

adding gentamycin (50μg/ml) (Life technology, Carlsbad, CA) 30 minutes after infection, in assays exceeding this timepoint.

6.6 Drug treatments

Cells were treated with twice the indicated concentrations of the drugs and incubated for one hour in assay medium at 37°C. The final drug concentration was reached by adding the same amount of bacteria or assay medium only to the cells.

6.7 SDS-PAGE and immunoblotting

Cells were washed twice in ice-cold PBS and lysed in PhosphoSafe^{TM} extraction reagent (Millipore, Billerica, MA), after an incubation on ice for 10 min. Lysates were centrifuged at 4°C for 25 min at 16000g and the supernatant was collected. To determine the protein concentration the BCA Protein Assay kit (Pierce, Rockford, IL) was used. 10-20 μg of protein were loaded on SDS-polyacrylamide gels and electroblotted onto nitrocellulose membranes. Primary antibodies were diluted in phosphate buffered saline containing 0.1% tween and 5% bovine serum albumin and used for immunoblotting. HRP-conjugated secondary antibodies were purchased from GE Healthcare, Chalfont St Giles, United Kingdom or Cell Signaling Technology, Danvers, MA. The blots were developed with an enhanced chemiluminescence method (Pierce, Rockford, IL) using an ImageQuant LAS4000 digital imaging system (GE Healthcare, Chalfont St Giles, United Kingdom).

6.8 Immunofluorescence

After fixation in 4% PFA for 10 min, cells were permeabilized in blocking buffer (0.3% Triton^{TM} X-100/ 5% goat serum) for 1 hour. Primary antibodies were incubated overnight at 4°C in antibody dilution buffer (1X PBS/1% BSA/0.3% Triton^{TM} X-100) followed by secondary antibody application using an Alexa 647-conjugated antibody (Invitrogen, Carlsbad, CA) in antibody dilution buffer. In parallel, F-actin and DNA were stained for 1 h at room temperature using FITC-phalloidin (Invitrogen, Carlsbad, CA) and Hoechst, respectively.

6.9 Automated microscopy

Images were acquired by automatic microscopy using an ImageXpress Micro (Molecular devices, Sunnyvale, USA). Images were acquired for each site at 360 nm, 480 nm, 594 nm and 640 nm to visualize Hoechst, FITC-phalloidin, DsRed-expressing *S. flexneri* and Alexa 647-conjugated secondary antibodies, respectively.

6.10 Constructs

pcDNA3-based constructs of human IPMK with Myc-tag at N-terminus of IPMK were generously provided by Prof. Hsien-yu Wang (State University of New York, New York, USA).

6.11 Transient transfection

For transient transfection of DNA, HeLa CCL-2^{TM} human epithelial cells were seeded into 96-well plates and grown for 24 hours in complete growth medium without antibiotics. 2μg DNA were diluted in 100μl OptiMEM (Life technology, Carlsbad, CA), mixed with 8μl FuGENE 6 transfection reagent (Promega, Madison, WI) and incubated for 10 minutes at room temperature. Afterwards, 5μl of the FuGENE 6 ransfection reagent/ DNA mix were added to the cells in 100μl complete growth medium without antibiotics. Cells were incubated for further 24 hours.

6.12 Survival assay

For the survival assay, HeLa CCL-2^{TM} human epithelial cells were seeded into 96-well plates and grown to confluency for 24 hours in complete growth medium. Cells were pretreated with the indicated drugs for one hour in assay medium, as already described. Next, cells were infected either with Δ*HOPEMT asd* + $YopE_{signal}$ or with Δ*HOPEMT asd* + $YopE_{signal}$ - *IpgD* at a MOI of 100 and incubated for 1 hour. The medium containing bacteria was removed and replaced with assay medium containing gentamycin (50μg/ml) (Life technology, Carlsbad, CA), the corresponding drug at 1x concentration and 0.5μM staurosporine for indicated conditions. Cells were incubated for further two hours at 37°C followed by fixation using 4% paraformaldehyde.

Chapter IV

Discussion and outlook

1.1 Main findings

This work has made several contributions to the field. First, the data provides a valuable resource for future research in infection biology. We could demonstrate that phosphoproteomics can provide testable hypothesis revealing for example the kinase ATM to play an important role in the induction of genotoxic stress during infection or highlighting the activity of mTOR and unraveling its importance for the induction of a pro-survival response. In addition, the identification of the NPC as regulator of the nucleo-cytoplasmic transport during *S. flexneri* infection serves as starting point for the decipherment of a new process related to bacterial infection. Although no new direct targets of OspF were found, the data shows the massive impact a single effector can have on the cellular network. The obtained data may be useful in research beyond infection biology because it allows to study the MAPK pathway in presence of a specific inibitor (OspF) in relation to chemical MAPK inhibitors. Furthermore, work on the effector protein IpgD revealed a mTOR dependent AKT activation mechanism which is largely independent of canonical PI3K signaling.

1.2 Host-pathogen crosstalks: a predestinated field for the application of phosphoproteomics

For a successful invasion many bacterial pathogens have developed sophisticated tools allowing them to interfere with host communication and shape the output in favor of the bacteria. The TTSS and its translocated effector proteins are an example of a virulence factor that adapted the host "language". It manipulates signaling cascades of the host, promoting the uptake of the pathogen into enterocytes and is important for the establishment of a successful replicative niche. Many of these signaling events are mediated by phosphorylation cascades, thus the systematic study of this PTM is an attractive strategy to reveal cross-talks during host-pathogen interactions. Using a phosphoproteomic approach, we aimed to study signaling cascades of the host cell that become activated in response to *S. flexneri* infection, covering different aspects of the infection by monitoring phosphorylations at several timepoints post-infection. In addition, the cross-talk between host and pathogen was exemplified by studying the effect of a single translocated bacterial effector protein on the phosphorylation landscape of the host cell.

1.3 Bacterial infection affects many aspects of cellular life

Our phosphoproteomic approach revealed an astonishing high number of host phosphorylation events induced by *S. flexneri* infection. It is noteworthy to mention that a conservative threshold was used for the selection of significant regulated phosphopeptides.

The threshold consisted of a q-value smaller than 1% and a difference in abundance compared to control of at least two fold. However, in many phosphoproteomic publications no cut-offs for abundance regulation are used and all phosphopeptides having a significant q-value are considered for further evaluation[185]. Despite our conservative threshold, we were able to find more than 300 proteins undergoing a change in phosphorylation upon *S. flexneri* infection which corresponds to 28% of all detected phosphoproteins. Still, this number is probably underestimated as we were able to confirm even the phosphorylation of proteins by immunoblotting which we did not consider to be significantly regulated (data not shown). By the use of a more relaxed but still widely accepted threshold of a q-value smaller than 1% but no restriction on regulation cut-off, we identified almost 500 phosphoproteins. This emphasizes even more the dramatic impact a bacterial infection has on the signaling network of a cell. Remarkably, we found that already after 15 minutes of infection more than 150 proteins change their phosphorylation status. More recent data from our laboratory revealed, that already two minutes post-infection, the phosphorylation of host proteins is affected as illustrated by high AKT phosphorylation at Ser473 and further phosphoproteomic data covering 2, 5, 10 and 15 minutes of infection with *S. flexneri*. Interestingly, a non-virulent *S. flexneri* strain lacking the large virulene plasmid was not able to induce phosphorylation events (R. Dreier unpublished data).

A widely used approach to capture the dynamics of time resolved phosphoproteomics is to subject the quantitative data to unsupervised clustering. This approach allows the partitioning of identified phosphosites to a few clusters. Although each phosphorylation site has an unique dynamic profile, they can be grouped into more generally observed profiles corresponding to e.g. early responders or late responders. In the current study, the phosphoproteomic data was subjected to fuzzy c-means clustering revealing six distinct profiles of phosphorylation. The clusters comprise profiles related to an early or intermediate increase or decrease in phosphorylation as well as a more distinct profile characterized by a late increase in phosphorylation. Distinct temporal profiles of phosphorylation may correspond to the activity of certain kinases. Therefore, the coupling of temporal clustering and kinase motif analysis represents a promising approach for predicting kinase activity based on observed phosphorylation events. Using this approach, we were able to predict and experimentally validate a cluster of late phosphorylation events as substrates of the kinase ATM that becomes activated by DNA double strand breaks and regulates the cellular response to genotoxic stress[255].

In addition, we could show by immunofluorescence that the ATM substrate histone H2AX, a marker for DNA double-strand breaks[251], becomes phosphorylated after 2 hours of *S. flexneri* infection, giving further evidence for the genotoxic potential of *S. flexneri*. An induction of the DNA damage cascade has been reported for different bacterial pathogens. These include *E. coli* harboring a genomic island called pks, encoding

for the production of a genotoxin[50]. An *in vivo* infection using a mouse model revealed the formation of phosphorylated H2AX foci in enterocytes in a *pks* dependent manner. Furthermore, low dose exposure of cultured mammalian cells to *E. coli* induced a transient DNA damage response leading to chromosome aberrations. Those cells showed an increase in gene mutation frequency and anchorage-independent colony formation, a hallmark of cell transformation. The authors speculated that *E. coli* harboring the pks island could contribute to the development of colorectal cancer[50]. Whether the genotoxic stress induced upon *S. flexneri* infection can also lead to increased gene mutation frequency and anchorage-independent colony formation or whether those cells eventually undergo apoptotic or necrotic cell death, preventing such a transformation, may be an interesting subject of further studies. In addition, it has been demonstrated that infection with a high number of toxigenic bacteria induces an irreversible cell cycle arrest and eventually apoptotic cell death, an observation which is presumably more related to the experimental condition applied in our study[50]. This observation also indicates a potential relation between the genotoxic stress and the regulation of the host cell cycle, a cellular process involving phosphoproteins, that we found to be enriched during *S. flexneri* infection.

Our research was done in HeLa cells to allow a direct comparison to data obtained from an siRNA screen on *S. flexneri* entry (C. Kasper unpublished data). HeLa cells are epithelial cells but do not correspond to the physiological tissue that becomes infected by *S. flexneri in vivo*. Nevertheless, this cell line is often used in the field because it can easily be transfected. As a future perspective, it could provide additional insight to conduct a phosphoproteome in a cell line that is more related to the *in vivo* situation as for example the colon cancer derived cell line Caco-2. It would also be feasible to conduct a phosphoproteome from an animal model of bacterial infection, although major challenges would have to be overcome. Going even a step further, the effect of bacterial infection could be studied by phosphoproteomics of biopsies, derived from infected tissue from patients[16]. The emerging application of phosphoproteomics towards the usage in diagnosis by monitoring a subset of biomarkers derived from body fluids or tissue from biopsy, demonstrates the possibility to obtain quantitative phosphoproteomic data directly from patient derived cells[218].

1.4 Interference with the nucleo-cytoplasmic transport - A new working point of bacteria?

Interestingly, we observed altered phosphorylation of Nup98, Nup50, Nu214 and TPR, all belonging to the NPC which consists of about 30 different proteins that are important for nuclear pore assembly and maintenance as well as directly involved in the nucleo-cytoplasmic transport. This finding was surprising to us, as regulation of the NPC has

so far not been linked to bacterial infection. However, there is extensive research about the role of the NPC in the context of viral infections. Viruses affect the NPC for different reasons. Some of which could serve as starting point to unravel the role of the NPC upon bacterial infection. Some viruses alter the permeability of the NPC to deliver their viral genome into the nucleus for replication. In addition, it can be beneficial for viruses to block the nuclear transport of host proteins involved in the host antiviral response. Thus, we speculated whether *S. flexneri* infection may also interfere with the nucleo-cytoplasmic transport. This hypothesis was supported by the observation of Nup50 phosphorylation on Ser221 which has been described as ERK substrate and leads to inhibition of the nuclear import of importin-beta and transportin [141]. In our phosphopoteome we observed Nup50 phosphorylation in an OspF dependent manner, strongly suggesting that ERK may regulate the phosphorylation upon infection. Thus, we had an ideal model system to study the impact of infection on nuclear transport in dependency of a bacterial effector protein. We studied the impact on dexamethasone-induced nuclear transport of the protein Rev-GR-GFP, which had previously been used to study nucleo-cytoplasmic transport [162]. Although we observed a reduction of nuclear import upon wild-type *S. flexneri* infection, there was no difference upon infection with the Δ*ospF* mutant observable, making it unlikely that Nup50 phosphorylation regulates nuclear transport upon infection. Although we are lacking a mechanistic explanation how NPC phosphorylation is linked to the regulation of nuclear transport, the observation that nuclear transport is affected by bacterial infection is new and represents an interesting starting point for further studies. This is supported by the study of Rogers and colleagues that observed phosphorylation of the nucleoporin Nup50 and Nup214 after *Salmonella* infection, making it tempting to speculate that regulation of the NPC is a common feature upon bacterial infection [229].

Beside the regulation of nuclear transport, the NPC fulfills other functions which could play a role upon bacterial infection. Proteins of the NPC can directly contribute to gene regulation by interacting with chromatin [259] and could thus be important for the expression of pro-inflammatory cytokines upon bacterial infection. Future research about the role of the NPC during bacterial infection could reveal a new mechanism of gene regulation. Finally, it would be of special interest whether the phosphorylation of the NPCs and the impairment of the nucleo-cytoplasmic transport is directly triggered by bacterial effectors.

1.5 A single bacterial effector can massively influence the cellular response

Effector proteins are important molecular tools of bacteria to shape the response of the host in their favor. The molecular mechanism by which OspF renders its target ERK and p38

inactive is well described[9] [156]. OspF dependent MAPK inhibition and the subsequent inhibition of histone H3 phosphorylation impairs the accessibility of transcription factors to the DNA and thus reduces the expression of pro-inflammatory cytokines. However, recent research has shown that OspF can indirectly affect the activity of other proteins through disruption of a negative feedback loop[225]. Our phosphoproteomic approach revealed that OspF had a massive net negative impact on the phosphorylation network of the cell. OspF affects the phosphorylation of more than 300 different proteins which is not surprising when taking into consideration that the MAPKs play a pivotal role in cell signaling. The ability of effector proteins to strongly shape host signaling was also demonstrated for *Salmonella* where up to half of all observed phosphorylation events were dependent on the effector SopB[229]. However, SopB had a net positive impact indicating that effectors can either promote or suppress overall cellular phosphorylation. Our subsequent search for potential direct targets of OspF did not reveal any new candidates, suggesting that OspF shapes the phosphorylation network of the cell solely through inactivation of ERK and p38. It would be of interest to study the effect of OspF by a complementary approach where OspF is directly translocated into cells, that are stimulated with different MAPK activating agents. Due to the high specificity of OspF towards the MAPKs, this approach could also be of special interest for cancer related research. The OspF data we obtained by phosphoproteomics, are questioning the canonical view of linear pathways that lead to a cellular response and favor a model where the cellular response is due to the integration of all those individual signaling events.

1.6 A comparison of pathogen derived phosphoproteomic datasets: What can we learn?

To identify more general phosphorylation events that are induced upon bacterial infection, we compared our data to a phosphoproteomic dataset of *Salmonella* infection[229]. Although the overlap of the two phosphoproteomes was rather small, probably due to technical reasons as discussed in the introduction, we were able to find more than 60 phosphopeptides that were considered to be significantly regulated in both datasets. Interestingly, all but one of the identified phosphosites found on these proteins were regulated in the same direction by both *Shigella* and*Salmonella*. The two pathogens belong to the family of *Enterobacteriaceae* and use a TTSS to promote the uptake into the epithelial cell via a trigger mechanism. Moreover, many effector proteins of *Shigella spp.* and *Salmonella spp.* are homologues and fulfill similar functions, as exemplified by the *Salmonella* effector SopB which is a homologue to the *S. flexneri* effector IpgD.

The comparison derived data clearly indicates that both pathogens induce a similar host response during the first half hour of infection. It is therefore not surprising that many

phosphoproteins are linked to the actin cytoskeleton including IQGAP2 and Palladin. MYPT1, which may be involved in the entry process of *S. flexneri*, as revealed by a siRNA screen (C. Kasper, unpublished data), becomes phosphorylated upon infection of both pathogens, making it a promising candidate for an important host protein upon bacterial invasion. Because Rogers and colleagues have not examined later timepoints of infection, we cannot compare signaling events that take place at these timepoints. It is tempting to speculate that the phosphoproteome of the two pathogens would be more divergent at later timepoints due to the different cellular compartment the two pathogens occupy[250] [54]. *Salmonella spp.* remain enclosed within a vacuole which represents its replicative niche, whereas *S. flexneri* lyses the vacuole and replicates in the cytoplasm from where it can spread intra- and intercellularly by ABM, a process requiring many host proteins. A direct phosphoproteomic comparison of these two pathogens during a timecourse of infection would be valuable to answer this question.

Although these two datasets provide a set of co-regulated phosphoproteins that may correspond to a general cellular response to bacterial infection, further bacterial infection derived phosphoproteomes would contribute to the determination of important host factors during infection. In 2013, a host cell phosphoproteome of *Francisella novicida* infection has been published[185]. However, *Francisella spp.* replicate in macrophages which questions a comparison to an infection of epithelial cells. Nevertheless, the increasing application of phosphoproteomics in infection biology will presumably provide more data in near future that can be directly compared to *Shigella* and *Salmonella* infection of epithelial cells. Of special interest would be data allowing the direct comparison of pathogens pursuing different strategies of infection, namely frontal and stealth attack. Although *S. flexneri* developed many tools to evade the immune response it induces massive inflammation leading to severe disease symptoms and cannot establish chronic infections in healthy individuals. Thus, *S. flexneri* would rather represent a frontal attack pathogen. On the other hand, *Bartonella spp.* serve as a model for a stealth pathogen which persist for a long time in the host[20]. Although both pathogens occupy different cellular niches, a direct comparison would still be interesting to determine the differences and similarities between both infection models.

1.7 What can we learn by mapping of phosphoproteomic and siRNA screen derived data?

Phosphoproteomic data can point towards signaling hot spots, characterized by many phosphoproteins being related to a certain pathway or cellular process. This allows the identification of pathways or cellular processes that have not yet been related to the stimuli or perturbation of interest, as exemplified in this study by the mTOR pathway or the

nucleo-cytoplasmic transport. This renders phosphoproteomics a suitable technique for the exploration of the signaling landscape shaped by a certain stimuli. Although the identification of proteins and the corresponding phosphosites by shotgun mass spectrometry does not rely on a priori knowledge and is thus not biased, a priori knowledge is a prerequisite for the interpretation of the data. Information about the phosphorylation state of a protein can only be inferred to a testable hypothesis if the protein function or the modified residue is known. Although many phosphorylation sites have been discovered, mainly by large-scale phosphoproteomic studies, an experimentally validated function for most of them is lacking. This issue is less pronounced on the level of proteins where some functional aspects for many proteins have been described. However, the linkage of an observed protein phosphorylation to a certain phenotype can, without further data, only be achieved by a "trial and error" approach. Therefore, the coupling of phosphoproteomics, or "omics" techniques in general to perturbation assays like siRNA screens is a promising approach to integrate a phenotypic observation into a signaling context, yet this approach has its pitfalls. Only phosphoproteins that show a phenotype in an siRNA screen can be considered for further evaluation, therefore phosphoproteins that may play an important role in the context of interest but do not show an siRNA dependent phenotype due to biological redundancy or technical reasons are excluded. On the other hand, a relative small number of phosphoproteins are obtained by a conventional phosphoproteomic study compared to the number of genes being studied by a genome-wide siRNA screen. Therefore, it is not too surprising that only few proteins were found to undergo an infection dependent change in phosphorylation and at the same time to affect the entry of *S. flexneri* into the host cell in a genome-wide siRNA screen. Nevertheless, the few that are obtained can be considered as validated.

This comparison revealed the phosphoprotein MYPT1 as being important for the entry of *S. flexneri* into HeLa cells as shown in the additional result section. Even more interesting, the temporal phosphorylation pattern of MYPT1, which is highest between 10 and 15 minutes post-infection, matches the timing of the *S. flexneri* entry process which is also assumed to take place within the first 15 minutes. Furthermore, immunofluorescence of phosphorylated MYPT1 revealed a co-localization with F-actin ruffles at the site of bacterial entry. MYPT1 has been described as a substrate of ROCK, which itself is known to play an important role in the entry process of *S. flexneri*. Thus, MYPT1 may be a downstream effector of ROCK during infection and involved in bacterial internalization. More work is required to elucidate the molecular mechanisms of this observation.

Beside this comparative integration of phosphoproteomic data and a perturbation assay, also experimental coupling is a promising approach. This can for instance be done by comparing signaling in wild-type to knockout cells by phosphoproteomics. In addition, the protein of interest can also directly be studied by expressing or translocating it into a

cellular system, which is best exemplified by an IpgD phosphoproteome (data not shown). Here, the impact of a single delivered bacterial effector was studied, leading to the detection of different AKT substrates. Thus, phosphoproteomic may serve as an ideal approach for the exploration of potential molecular targets of an effector protein, especially if the effector provokes a well observable phenotype.

1.8 mTOR - multiple roles for the central cellular player during bacterial infection?

1.8.1 Regulation of translation

In the last two years it became evident that mTOR plays an important role upon bacterial infection beyond its function as a master regulator of metabolism. Our work contributed to this finding, as we recognized by phosphoproteomics that many components of the mTOR signaling pathway undergo phosphorylation changes during bacterial infection. These include components of both, mTORC1 and mTORC2, as well as corresponding downstream targets. This data was complemented by immunoblotting, showing in addition phosphorylation of mTOR itself on Ser2448 and Ser2481, strongly suggesting activation of mTOR signaling. We could validate mTORC1 activation by monitoring phosphorylation of the downstream kinase S6K as well as its substrate RS6, which were both sensitive to the mTORC1 inhibitor rapamycin. This pathway is involved in the regulation of translation and may affect the synthesis of pro-inflammatory cytokines upon *S. flexneri* infection. We addressed this question by monitoring IL-8 production upon *S. flexneri* infection and mTOR inhibition by rapamycin or PP242. Indeed, we could observe a reduction of IL-8 production upon rapamycin treatment and even more pronounced upon PP242 treatment, suggesting that mTOR signaling is crucial for the translation of IL-8 (data not shown). However, the significance of this finding remains unclear, as IL-8 synthesis is almost exclusively observed in uninfected bystander cells as described by Kasper et al[128]. Thus, the role of mTOR signaling should in addition be studied in bystander cells and it would be crucial to test whether mTOR inhibition broadly affects protein translation upon infection or shows specificity for the translation of some pro-inflammatory cytokines.

1.8.2 Regulation of autophagy

Tattoli and colleagues showed in 2012 that infection with *Salmonella* or *Shigella* induced an amino acid starvation which leads to down-regulation of mTOR signaling, resulting in the induction of autophagy[267]. This data seems to be conflicting with our observation of increased mTOR signaling as indicated by S6K and RS6 phosphorylation. This conflict can partially be explained by the fact that we monitored mTOR activity mainly within the first hour of infection whereas Tattoli and colleagues observed a decrease in mTOR

signaling after 2-5 hours post-infection. Yet, it remains contradictory that Tattoli and colleagues do not observe an initial increase in mTOR activity one hour post-infection. In addition, they measured a different activation pattern of mTORC2 as indicated by AKT phosphorylation which is observed after 1 hour and is decreasing again after 4 hours. We could reproducibly observe sustained AKT phosphorylation already within 15 minutes after infection which is in concordance with previous observations [212] [222]. These data may indicate, temporally distinct roles of mTOR during the infection process.

1.8.3 Regulation of survival via AKT

It has been shown that *S. flexneri* promotes a pro-survival response and can rescue cells from staurosporine induced apoptosis [43], which has been assigned to the activity of the *S. flexneri* effector IpgD that induces AKT activation and thus promotes host cell survival [212]. Our data revealed that the IpgD induced pro-survival response is indeed dependent on AKT but also on mTORC2 signaling which is an upstream AKT activator. These data allocates a further function for mTOR during bacterial infection which is the prevention of apoptosis, through the activation of AKT.

1.9 IpgD as tool to decipher mTOR activation

Although it has been described that IpgD activates AKT via the production of PI5P, the exact activation mechanism largely remains elusive. PI3K and tyrosine kinases, in particular EGFR, are crucial for AKT activation [212] [222]. In addition, we provided evidence that mTORC2 is responsible for AKT activation during infection. mTORC2 signaling is of medical importance because it is associated with cancer and diabetes [47]. Therefore, deciphering the upstream activation mechanisms is a pivotal task in the field. As demonstrated by Zinzalla and colleagues, mTORC2 becomes associated with the ribosome upon insulin stimulated PI3K signaling, suggesting that ribosomes activate mTORC2 directly [301]. Yet, the exact molecular mechanisms of mTORC2 activation are still not entirely clear. We could show that IpgD induced mTORC2 signaling which rapidly leads to AKT phosphorylation. Indeed, we could observe AKT phosphorylation already within two minutes of infection (R. Dreier unpublished data). Thus, IpgD is a promising tool to study mTORC2 signaling because it rapidly induces AKT activation in a confined cellular compartment, the entry foci. We further could demonstrate, that IpgD induced AKT activation is not necessarily PI3K dependent, as treatment with both, wortmannin and LY294002, did not abolish IpgD induced AKT activation at early timepoints, whereas mTOR inhibition efficiently does. This is conflicting with previous reports, where LY294002 was shown to abolish *S. flexneri* induced AKT phosphorylation [212] [222]. However, a recent publication about the activation mechanism of the *Salmonella* homologue SopB has reported,

that SopB dependent AKT activation is independent of LY294002 and wortmannin as observed in our study upon IpgD delivery [233]. Still, it was demonstrated by overexpression of the phosphoinositide 3-phosphatase PTEN that AKT activation downstream of SopB relies on PI(3,4,5)P3 and thus another kinase than the canonical PI3K must be involved in formation of this messenger. An siRNA screen by Roppenser et al. revealed multiple kinases contributing to SopB dependent AKT activation and indicated IPMK to play a role in AKT activation [233]. We could demonstrate that IPMK is also important in IpgD dependent AKT activation and further found that it becomes recruited to the site of entry, where it co-localizes with phosphorylated AKT. We therefore propose a model of mTORC2 and AKT activation which relies on the IpgD product PI5P but is independent of canonical PI3K signaling at early time-points of infection. Currently, a kinase inhibitor screen is ongoing, aiming to identify kinases important for the IpgD dependent AKT activation.

1.10 The direct delivery of effector proteins by *Yersinia enterocolitica* as tool to study their function

Our work has demonstrated the importance of temporal resolution when studying bacterial effectors. We were able to identify a time-dependent effect of IpgD as we did not rely on transient expression but on the temporally tightly controlled delivery of IpgD into the target cell by the use of a *Yersinia enterocolitica* TTSS based protein delivery tool (SJ Ittig, manuscript in preparation). The activity of bacterial effectors is often addressed by transient expression of the protein or by comparison to a deletion mutant. Yet, the temporal orchestration of the effectors may be of significance. Studying the activity of an effector which is, due to the expression method, present for several hours in the target cell may allow the cell to adapt to its presence by modifying certain signaling pathways or changing the level of proteins that are involved in the process. The *Yersinia* system allows the circumvention of this issue and therefore represents a valuable tool for studying different bacterial effector proteins. Especially effector proteins that induce cell toxicity are difficult to be addressed by transient transfection, but are predestinated for the analysis with the *Yersinia* tool.

1.11 Future perspectives of "omics" technologies in infection biology

Our study demonstrated that phosphoproteomics can be applied in the field of infection biology and generates a substantial amount of quantitative data which reveals new cellular processes related to infection and provides a resource for further research on different aspects of the host-pathogen interaction. Although many phosphosites have been identified, several obstacles have to be overcome towards the identification of a complete and

comprehensive phosphoproteome. A main obstacle is the bias of MS-based technologies towards the detection of high abundant peptides[228]. This is of particular interest as many signaling proteins fulfilling regulatory functions are of low abundance[228]. This is also a reason why usually not all members of an activated signaling cascade are detected by phosphoproteomics. A method to overcome this problem is the application of targeted MS allowing also detection of low abundant peptides. However, this methods requires a priori knowledge about the peptides of interest and the number of detectable peptides is limited. Nevertheless, this is a promising approach when the phosphorylation of several proteins of interest should be monitored simultaneously[159].

Due to the high number of phosphoproteomic studies being published in the last few years, many phosphosites have been detected and brought into context with different environmental conditions or stimuli. Yet, the knowledge about the precise molecular role of distinct phosphosites and their impact on the functionality of the protein is lagging behind and is thus becoming a major bottleneck. The functional characterization of phosphosites is a substantial requirement for the interpretation of phosphoproteomic data and there is an urgent need for the development of large-scale procedures for functional characterization of phosphosites in order to fully exploit the potential of phosphoproteomics. The coupling of phosphoproteomics to other techniques like siRNA screens, as already discussed, can help to relate the detected phosphoproteins to a certain cellular phenotype and may facilitate the functional characterization of single phosphosites.

A further challenge will be the expansion of "omics" technologies towards the detection and quantification of other PTM modifications and their cross-talks among each other during bacterial infection. Ubiquitylation has already successfully been addressed by mass spectrometry based technologies revealing more than tenthousand ubiquitylation sites highlighting the broad impact of this PTM on the cellular network[283] [136]. As described in the introduction, ubiquitylation plays an important role during *S. flexneri* infection as exemplified by the activation cascade of NF-κB signaling. Even more interesting, the *S. flexneri* effectors of the ipaH family have been described as E3 ubiquitin ligases[230]. Therefore, the generation of an ubiquitin proteome upon bacterial infection would be of great interest and may unravel new targets of bacterial E3 ubiquitin ligases.

Another PTM that has recently been addressed by a large-scale proteomic study is lysine acetylation which was shown to be a widespread PTM[42] [164]. Lysine acetylation has been demonstrated to play an important role in TLR4 signaling that regulates the innate immune response induced by LPS[113]. Lysine acetylation of the NF-κB subunit p65 was shown to be important for full transcriptional activity of NF-κB[38]. These findings render the proteomic profiling of lysine acetylation a promising approach for the identification of new signal transduction mechanism during bacterial infection.

The availability of proteomic datasets addressing different PTM derived from host cells

infected with the same pathogen would not only allow to obtain a broad overview about activated signaling cascaded but would also allow the identification of cross-talks between the different PTMs[280].

References

[1] Abreu, M. T. (2010, February). Toll-like receptor signalling in the intestinal epithelium: how bacterial recognition shapes intestinal function. *Nat Rev Immunol 10*(2), 131–144. 21

[2] Adler, B., C. Sasakawa, T. Tobe, S. Makino, K. Komatsu, and M. Yoshikawa (1989, May). A dual transcriptional activation system for the 230 kb plasmid genes coding for virulence-associated antigens of Shigella flexneri. *Molecular Microbiology 3*(5), 627–635. 6, 7

[3] Aebersold, R. and M. Mann (2003, March). Mass spectrometry-based proteomics. *Nature 422*(6928), 198–207. 29, 40

[4] Akeda, Y. and J. E. Galan (2005, October). Chaperone release and unfolding of substrates in type III secretion. *Nature 437*(7060), 911–915. 8

[5] Allaoui, A., J. Mounier, M.-C. Prévost, P. J. Sansonetti, and C. Parsot (1992, June). icsB: a Shigella flexneri virulence gene necessary for the lysis of protrusions during intercellular spread. *Molecular Microbiology 6*(12), 1605–1616. 10

[6] Ambuj Kumar, Vidya Rajendran, Rao Sethumadhavan, and Rituraj Purohit (2013). AKT Kinase Pathway: A Leading Target in Cancer Research. *The Scientific World Journal 2013*, 6. 17

[7] Andersen, J. N., O. H. Mortensen, G. H. Peters, P. G. Drake, L. F. Iversen, O. H. Olsen, P. G. Jansen, H. S. Andersen, N. K. Tonks, and N. P. H. Møller (2001, November). Structural and Evolutionary Relationships among Protein Tyrosine Phosphatase Domains. *Molecular and Cellular Biology 21*(21), 7117–7136. 35

[8] Andersson, L. and J. Porath (1986, April). Isolation of phosphoproteins by immobilized metal (Fe3+) affinity chromatography. *Analytical Biochemistry 154*(1), 250–254. 40

[9] Arbibe, L., D. W. Kim, E. Batsche, T. Pedron, B. Mateescu, C. Muchardt, C. Parsot, and P. J. Sansonetti (2007, Jan). An injected bacterial effector targets chromatin access for transcription factor NF-kappaB to alter transcription of host genes involved in immune responses. *Nat Immunol 8*(1), 47–56. 1529-2908 (Print) Journal Article Research Support, Non-U.S. Gov't. 10, 25, 26, 136

[10] Aryal, U. K. and A. R. S. Ross (2010). Enrichment and analysis of phosphopeptides under different experimental conditions using titanium dioxide affinity chromatography and mass spectrometry. *Rapid Communications in Mass Spectrometry 24*(2), 219–231. 41

[11] Ashida, H., M. Kim, M. Schmidt Supprian, A. Ma, M. Ogawa, and C. Sasakawa (2010, January). A bacterial E3 ubiquitin ligase IpaH9.8 targets NEMO/IKKγ to dampen the host NF-κB-mediated inflammatory response. *Nat Cell Biol 12*(1), 66–73. 10, 24

[12] Ashida, H., H. Nakano, and C. Sasakawa (2013, 06). Shigella IpaH0722 E3 Ubiquitin Ligase Effector Targets TRAF2 to Inhibit PKC-NF-κB Activity in Invaded Epithelial Cells. *PLoS Pathog 9*(6), e1003409. 10, 24

[13] Ashida, H., M. Ogawa, M. Kim, H. Mimuro, and C. Sasakawa (2012). Bacteria and host interactions in the gut epithelial barrier. *Nat Chem Biol 8*(1), 36–45. 29

[14] Ashida, H., M. Ogawa, H. Mimuro, T. Kobayashi, T. Sanada, and C. Sasakawa (2011). Shigella are versatile mucosal pathogens that circumvent the host innate immune system. *Current Opinion in Immunology 23*(4), 448–455. 12, 23, 28

[15] Attwood, P. V., M. J. Piggott, X. L. Zu, and P. G. Besant (2007). Focus on phosphohistidine. *Amino Acids 32*(1), 145–156. 33

[16] Barbut, F., L. Beaugerie, N. Delas, S. Fossati Marchal, P. Aygalenq, J.-C. Petit, and I. C. S. Group (1999, July). Comparative Value of Colonic Biopsy and Intraluminal Fluid Culture for Diagnosis of Bacterial Acute Colitis in Immunocompetent Patients. *Clinical Infectious Diseases 29*(2), 356–360. 134

[17] Bardhan, P., A. Faruque, A. Naheed, and D. Sack (2010). Decreasing shigellosis-related deaths without Shigella spp.-specific interventions. *Asia. Emerg Infect Dis 1*, internet. 2

[18] Barry, E. M., M. F. Pasetti, M. B. Sztein, A. Fasano, K. L. Kotloff, and M. M. Levine (2013). Progress and pitfalls in Shigella vaccine research. *Nat Rev Gastroenterol Hepatol 10*(4), 245–255. 2, 3

[19] Beltran, L. and P. R. Cutillas (2012). Advances in phosphopeptide enrichment techniques for phosphoproteomics. *Amino Acids 43*(3), 1009–1024. 40, 41, 42

[20] Ben Tekaya, H., J.-P. Gorvel, and C. Dehio (2013, August). Bartonella and Brucella-Weapons and Strategies for Stealth Attack. *Cold Spring Harbor Perspectives in Medicine 3*(8), –. 137

[21] Bergamin, E., P. T. Hallock, S. J. Burden, and S. R. Hubbard (2010, July). The Cytoplasmic Adaptor Protein Dok7 Activates the Receptor Tyrosine Kinase MuSK via Dimerization. *Molecular Cell 39*(1), 100–109. 37

[22] Bergounioux, J., R. Elisee, A.-L. Prunier, F. Donnadieu, B. Sperandio, P. Sansonetti, and L. Arbibe (2012). Calpain Activation by the Shigella flexneri Effector VirA Regulates Key Steps in the Formation and Life of the Bacterium's Epithelial Niche. *Cell Host & Microbe 11*(3), 240 – 252. 11, 17, 109

[23] Bernardini, M. L., J. Mounier, H. d'Hauteville, M. Coquis Rondon, and P. J. Sansonetti (1989, May). Identification of icsA, a plasmid locus of Shigella flexneri that governs bacterial intra- and intercellular spread through interaction with F-actin. *Proc Natl Acad Sci U S A 86*(10), 3867–71. 0027-8424 (Print) In Vitro Journal Article Research Support, Non-U.S. Gov't. 13

[24] Bian, Y., M. Ye, C. Song, K. Cheng, C. Wang, X. Wei, J. Zhu, R. Chen, F. Wang, and H. Zou (2012, April). Improve the Coverage for the Analysis of Phosphoproteome of HeLa Cells by a Tandem Digestion Approach. *J. Proteome Res. 11*(5), 2828–2837. 39

[25] Bjorge, J. D. and D. J. Jakymiw, Andrew andFujita (2000). Selected glimpses into the activation and function of Src kinase. *Oncogene 19*(49), 5620–35. 11

[26] Blocker, A., P. Gounon, E. Larquet, K. Niebuhr, V. Cabiaux, C. Parsot, and P. Sansonetti (1999). The Tripartite Type III Secreton of Shigella flexneri Inserts Ipab and Ipac into Host Membranes. *The Journal of Cell Biology 147*(3), 683–693. 6, 8, 10

[27] Bodenmiller, B., L. N. Mueller, P. G. A. Pedrioli, D. Pflieger, M. A. Junger, J. K. Eng, R. Aebersold, and W. A. Tao (2007). An integrated chemical, mass spectrometric and computational strategy for (quantitative) phosphoproteomics: application to Drosophila melanogaster Kc167 cells. *Mol. BioSyst. 3*, 275–286. 41

[28] Bongrand, C., P. J. Sansonetti, and C. Parsot (2012, March). Characterization of the Promoter, MxiE Box and 5' UTR of Genes Controlled by the Activity of the Type III Secretion Apparatus in Shigella flexneri. *PLoS ONE 7*(3), e32862–. 6

[29] Boquet, P. and E. Lemichez (2003). Bacterial virulence factors targeting Rho GTPases: parasitism or symbiosis? *Trends in Cell Biology 13*(5), 238–246. 11

[30] Bours, M., E. Swennen, F. Di Virgilio, B. Cronstein, and P. Dagnelie (2006). Adenosine 5'-triphosphate and adenosine as endogenous signaling molecules in immunity and inflammation. *Pharmacology & Therapeutics 112*(2), 358 – 404. 27

[31] Browne, G. J. and C. G. Proud (2004, April). A Novel mTOR-Regulated Phosphorylation Site in Elongation Factor 2 Kinase Modulates the Activity of the Kinase and Its Binding to Calmodulin. *Molecular and Cellular Biology 24*(7), 2986–2997. 95

[32] Brugnera, E., L. Haney, C. Grimsley, M. Lu, S. F. Walk, A.-C. Tosello Trampont, I. G. Macara, H. Madhani, G. R. Fink, and K. S. Ravichandran (2002, August). Unconventional Rac-GEF activity is mediated through the Dock180-ELMO complex. *Nat Cell Biol 4*(8), 574–582. 11

[33] Buchrieser, C., P. Glaser, C. Rusniok, H. Nedjari, H. d'Hauteville, F. Kunst, P. Sansonetti, and C. Parsot (2000). The virulence plasmid pWR100 and the repertoire of proteins secreted by the type III secretion apparatus of Shigella flexneri. *Molecular Microbiology 38*(4), 760–771. 6

[34] Burnaevskiy, N., T. G. Fox, D. A. Plymire, J. M. Ertelt, B. A. Weigele, A. S. Selyunin, S. S. Way, S. M. Patrie, and N. M. Alto (2013). Proteolytic elimination of N-myristoyl modifications by the Shigella virulence factor IpaJ. *Nature 496*(7443), 106–109. 10, 11, 18, 31

[35] Campbell Valois, F.-X., P. Schnupf, G. Nigro, M. Sachse, P. J. Sansonetti, and C. Parsot (2014, February). A Fluorescent Reporter Reveals On/Off Regulation of the Shigella Type III Secretion Apparatus during Entry and Cell-to-Cell Spread. *Cell Host & Microbe 15*(2), 177–189. 7

[36] Cersini, A., A. M. Salvia, and M. L. Bernardini (1998). Intracellular Multiplication and Virulence of Shigella flexneri Auxotrophic Mutants. *Infection and Immunity 66*(2), 549–557. 20

[37] Chamaillard, M., S. E. Girardin, J. Viala, and D. J. Philpott (2003, Sep). Nods, Nalps and Naip: intracellular regulators of bacterial-induced inflammation. *Cell Microbiol 5*(9), 581–92. 1462-5814 (Print) Journal Article Review. 22

[38] Chen, L.-f., Y. Mu, and W. C. Greene (2002, December). Acetylation of RelA at discrete sites regulates distinct nuclear functions of NFkappaB. *The EMBO Journal 21*(23), 6539–6548. 142

[39] Chen, M. Y., R. H. Insall, and P. N. Devreotes (1996, Feb). Signaling through chemoattractant receptors in Dictyostelium. *Trends Genet 12*(2), 52–7. 0168-9525 Journal Article Review Review, Tutorial. 10

[40] Cheong, J. K. and D. M. Virshup (2011). Casein kinase 1: Complexity in the family. *The International Journal of Biochemistry & Cell Biology 43*(4), 465 – 469. 37

[41] Chong, C. R. and P. A. Janne (2013, November). The quest to overcome resistance to EGFR-targeted therapies in cancer. *Nat Med 19*(11), 1389–1400. 124

[42] Choudhary, C., C. Kumar, F. Gnad, M. L. Nielsen, M. Rehman, T. C. Walther, J. V. Olsen, and M. Mann (2009, August). Lysine Acetylation Targets Protein Complexes and Co-Regulates Major Cellular Functions. *Science 325*(5942), 834–840. 142

[43] Clark, C. S. and A. T. Maurelli (2007). Shigella flexneri Inhibits Staurosporine-Induced Apoptosis in Epithelial Cells. *Infection and Immunity 75*(5), 2531–2539. 17, 140

[44] Cooper, K. G., S. Winfree, P. Malik Kale, C. Jolly, R. Ireland, L. A. Knodler, and O. Steele Mortimer (2011, 07). Activation of Akt by the Bacterial Inositol Phosphatase, SopB, is Wortmannin Insensitive. *PLoS ONE 6*(7), e22260. 124

[45] Copp, J., G. Manning, and T. Hunter (2009, March). TORC-Specific Phosphorylation of Mammalian Target of Rapamycin (mTOR): Phospho-Ser2481 Is a Marker for Intact mTOR Signaling Complex 2. *Cancer Research 69*(5), 1821–1827. 111

[46] Cornelis, G. R. (2006, Nov). The type III secretion injectisome. *Nat Rev Microbiol 4*(11), 811–25. 1740-1534 (Electronic) Journal Article Research Support, Non-U.S. Gov't Review. 7, 8

[47] Cornu, M., V. Albert, and M. N. Hall (2013, February). mTOR in aging, metabolism, and cancer. *Current Opinion in Genetics & Development 23*(1), 53–62. 140

[48] Correa, R. G., S. Milutinovic, and J. C. Reed (2012, December). Roles of NOD1 (NLRC1) and NOD2 (NLRC2) in innate immunity and inflammatory diseases. *Bioscience Reports 32*(6), 597–608. 21, 22

[49] Courtney A. Lovejoy and David Cortez (2009). Common mechanisms of PIKK regulation. *DNA Repair 8*(9), 1004 – 1008. Checkpoint response to {DNA} damage. 38

[50] Cuevas Ramos, G., C. R. Petit, I. Marcq, M. Boury, E. Oswald, and J.-P. Nougayrede (2010, June). Escherichia coli induces DNA damage in vivo and triggers genomic instability in mammalian cells. *Proceedings of the National Academy of Sciences 107*(25), 11537–11542. 134

[51] Damian F. Brennan and David Barford (2009). Eliminylation: a post-translational modification catalyzed by phosphothreonine lyases. *Trends in Biochemical Sciences 34*(3), 108 – 114. 26

[52] Datsenko, K. A. and B. L. Wanner (2000, Jun 6). One-step inactivation of chromosomal genes in Escherichia coli K-12 using PCR products. *Proc Natl Acad Sci U S A 97*(12), 6640–5. 0027-8424 (Print) Journal Article Research Support, U.S. Gov't, Non-P.H.S. 126

[53] De Chastellier, C. and L. Thilo (2006, February). Cholesterol depletion in Mycobacterium avium-infected macrophages overcomes the block in phagosome maturation and leads to the reversible sequestration of viable mycobacteria in phagolysosome-derived autophagic vacuoles. *Cellular Microbiology 8*(2), 242–256. 9

[54] de Jong, H. K., C. M. Parry, T. van der Poll, and W. J. Wiersinga (2012, October). Host-Pathogen Interaction in Invasive Salmonellosis. *PLoS Pathog 8*(10), e1002933–. 137

[55] Dehio, C. (2008, August). Infection-associated type IV secretion systems of Bartonella and their diverse roles in host cell interaction. *Cellular Microbiology 10*(8), 1591–1598. 8

[56] Dehio, C., M. C. Prévost, and P. J. Sansonetti (1995, Jun 1). Invasion of epithelial cells by Shigella flexneri induces tyrosine phosphorylation of cortactin by a pp60c-src-mediated signalling pathway. *EMBO J 14*(11), 2471–82. 0261-4189 (Print) Journal Article Research Support, Non-U.S. Gov't. 11

[57] Demali, K. A., A. L. Jue, and K. Burridge (2006). IpaA Targets beta1 Integrins and Rho to Promote Actin Cytoskeleton Rearrangements Necessary for Shigella Entry. *Journal of Biological Chemistry 281*(51), 39534–39541. 10, 100

[58] d'Hauteville, H., R. Dufourcq Lagelouse, F. Nato, and P. J. Sansonetti (1996, February). Lack of cleavage of IcsA in Shigella flexneri causes aberrant movement and allows demonstration of a cross-reactive eukaryotic protein. *Infection and Immunity 64*(2), 511–517. 14

[59] DiGiovanna, M. P., R. R. Roussel, and D. F. Stern (2001). Production of Antibodies That Recognize Specific Tyrosine-Phosphorylated Peptides. In *Current Protocols in Molecular Biology*, pp. –. John Wiley & Sons, Inc. 38

[60] Dissmeyer, N. and A. Schnittger (2011). The Age of Protein Kinases. In N. Dissmeyer and A. Schnittger (Eds.), *Methods in Molecular Biology*, Volume 779, pp. 7–52–. Humana Press. 32, 33, 35

[61] DuPont, H. L., Myron M. Levine, R. B. Hornick, and S. B. Formal (1989). Inoculum Size in Shigellosis and Implications for Expected Mode of Transmission. *The Journal of Infectious Diseases 159*(6), pp. 1126–1128. 2

[62] Dupont, N., S. Lacas Gervais, J. Bertout, I. Paz, B. Freche, G. T. Van Nhieu, F. G. van der Goot, P. J. Sansonetti, and F. Lafont (2009, August). Shigella Phagocytic Vacuolar Membrane Remnants Participate in the Cellular Response to Pathogen Invasion and Are Regulated by Autophagy. *Cell Host & Microbe 6*(2), 137–149. 12

[63] Edelmann, M. J. (2011). Strong Cation Exchange Chromatography in Analysis of Posttranslational Modifications: Innovations and Perspectives. *BioMed Research International 2011*, –. 42

[64] Egile, C., H. D'Hauteville, C. Parsot, and P. J. Sansonetti (1997). SopA, the outer membrane protease responsible for polar localization of IcsA in Shigella flexneri. *Molecular Microbiology 23*(5), 1063–1073. 14

[65] Engel, P., A. Goepfert, F. V. Stanger, A. Harms, A. Schmidt, T. Schirmer, and C. Dehio (2012, February). Adenylylation control by intra- or intermolecular active-site obstruction in Fic proteins. *Nature 482*(7383), 107–110. 31

[66] Engholm Keller, K. and M. R. Larsen (2013, March). Technologies and challenges in large-scale phosphoproteomics. *Proteomics 13*(6), 910–931. 43

[67] Espina, M., A. J. Olive, R. Kenjale, D. S. Moore, S. F. Ausar, R. W. Kaminski, E. V. Oaks, C. R. Middaugh, W. D. Picking, and W. L. Picking (2006, August). IpaD Localizes to the Tip of the Type III Secretion System Needle of Shigella flexneri. *Infection and Immunity 74*(8), 4391–4400. 8, 10

[68] Evans, C., J. Noirel, S. Ow, M. Salim, A. Pereira Medrano, N. Couto, J. Pandhal, D. Smith, T. K. Pham, E. Karunakaran, X. Zou, C. A. Biggs, and P. C. Wright (2012). An insight into iTRAQ: where do we stand now? *Anal Bioanal Chem. 404*(4), 1011–1027–. 43, 44

[69] Faherty, C. S. and A. T. Maurelli (December 2009). Spa15 of Shigella flexneri Is Secreted through the Type III Secretion System and Prevents Staurosporine-Induced Apoptosis. *Infection and Immunity 77*(12), 5281–5290. 17

[70] Faherty, C. S., D. S. Merrell, C. Semino Mora, A. Dubois, A. V. Ramaswamy, and A. T. Maurelli (2010). Microarray analysis of Shigella flexneri -infected epithelial cells identifies host factors important for apoptosis inhibition. *BMC Genomics 11*(1), 1–18. 17

[71] Faherty, C. S., J. C. Redman, D. A. Rasko, E. M. Barry, and J. P. Nataro (2012, July). Shigella flexneri effectors OspE1 and OspE2 mediate induced adherence to the colonic epithelium following bile salts exposure. *Molecular Microbiology 85*(1), 107–121. 10

[72] Fasano, A., F. R. Noriega, M. Liao, W. Wang, and M. Levine (1997). Effect of shigella enterotoxin 1 (ShET1) on rabbit intestine in vitro and in vivo. *Gut. 40*, 505–511. 6

[73] Fehr, A. R. and D. Yu (2013). Control the Host Cell Cycle: Viral Regulation of the Anaphase-Promoting Complex. *Journal of Virology 87*(16), 8818–8825. 15

[74] Fernandez Prada, C. M., D. L. Hoover, B. D. Tall, A. B. Hartman, J. Kopelowitz, and M. M. Venkatesan (2000, June). Shigella flexneri IpaH7.8 Facilitates Escape of Virulent Bacteria from the Endocytic Vacuoles of Mouse and Human Macrophages. *Infection and Immunity 68*(6), 3608–3619. 10

[75] Ferrari, G., H. Langen, M. Naito, and J. Pieters (1999, May). A Coat Protein on Phagosomes Involved in the Intracellular Survival of Mycobacteria. *Cell 97*(4), 435–447. 9

[76] Figeys, D., S. P. Gygi, Y. Zhang, J. Watts, M. Gu, and R. Aebersold (1998). Electrophoresis combined with novel mass spectrometry techniques: Powerful tools for the analysis of proteins and proteomes. *ELECTROPHORESIS 19*(10), 1811–1818. 40

[77] Fischer, E. H. and E. G. Krebs (1955). CONVERSION OF PHOSPHORYLASE b TO PHOSPHORYLASE a IN MUSCLE EXTRACTS. *Journal of Biological Chemistry 216*(1), 121–132. 32

[78] Fronzes, R., P. J. Christie, and G. Waksman (2009, October). The structural biology of type IV secretion systems. *Nat Rev Micro 7*(10), 703–714. 8

[79] Fruman, D. A. and C. Rommel (2014, February). PI3K and cancer: lessons, challenges and opportunities. *Nat Rev Drug Discov 13*(2), 140–156. 109

[80] Fukazawa, A., C. Alonso, K. Kurachi, S. Gupta, C. F. Lesser, B. A. McCormick, and H.-C. Reinecker (2008, 11). GEF-H1 Mediated Control of NOD1 Dependent NF-kB Activation by Shigella Effectors. *PLoS Pathog 4*(11), e1000228. 10, 24, 100

[81] Fukumatsu, M., M. Ogawa, S. Arakawa, M. Suzuki, S. Nakayama, Kazuhisa andi Shimizu, M. Kim, H. Mimuro, and C. Sasakawa (2012). Shigella Targets Epithelial Tricellular Junctions and Uses a Non-canonical Clathrin-Dependent Endocytic Pathway to Spread Between Cells. *Cell Host & Microbe 11*(4), 325 – 336. 14

[82] Fukushima, M., K. Kakinuma, and R. Kawaguchi (2002, August). Phylogenetic Analysis of Salmonella, Shigella, and Escherichia coli Strains on the Basis of the gyrB Gene Sequence. *Journal of Clinical Microbiology 40*(8), 2779–2785. 5

[83] Gaberc Porekar, V. and V. Menart (2001). Perspectives of immobilized-metal affinity chromatography. *Journal of Biochemical and Biophysical Methods 49*, 335 – 360. 40

[84] Gall, T. L., M. Mavris, M. C. Martino, M. L. Bernardini, E. Denamur, and C. Parsot (2005, March). Analysis of virulence plasmid gene expression defines three classes of effectors in the type III secretion system of Shigella flexneri. *Microbiology 151*(3), 951–962. 7

[85] Garai, P., S. Marathe, and D. Chakravortty (2011, May). Effectors of Salmonella Pathogenicity Island 2: An Island crucial to the life of Salmonella. *virulence 2*(2150-5594), 177–180. 46

[86] Girardin, S. E., I. G. Boneca, L. A. Carneiro, A. Antignac, M. Jehanno, J. Viala, K. Tedin, M. K. Taha, A. Labigne, U. Zähringer, A. J. Coyle, P. S. Di Stefano, J. Bertin, P. J. Sansonetti, and D. J. Philpott (2003, Jun 6). Nod1 detects a unique muropeptide from gram-negative bacterial peptidoglycan. *Science 300*(5625), 1584–7. 1095-9203 (Electronic) Journal Article. 5, 22

[87] Girardin, S. E., I. G. Boneca, J. Viala, M. Chamaillard, A. Labigne, G. Thomas, D. J. Philpott, and P. J. Sansonetti (2003, Mar 14). Nod2 is a general sensor of peptidoglycan through muramyl dipeptide (MDP) detection. *J Biol Chem 278*(11), 8869–72. 0021-9258 (Print) Journal Article. 22

[88] Girardin, S. E., R. Tournebize, M. Mavris, A. L. Page, X. Li, G. R. Stark, J. Bertin, P. S. DiStefano, M. Yaniv, P. J. Sansonetti, and D. J. Philpott (2001, Aug). CARD4/Nod1 mediates NF-kappaB and JNK activation by invasive Shigella flexneri. *EMBO Rep 2*(8), 736–42. 1469-221X (Print) Journal Article. 21

[89] Goldberg, M. B. (2001, December). Actin-Based Motility of Intracellular Microbial Pathogens. *Microbiology and Molecular Biology Reviews 65*(4), 595–626. 13

[90] Goldston, A. M., R. R. Powell, and L. A. Temesvari (2012, October). Sink or swim: lipid rafts in parasite pathogenesis. *Trends in Parasitology 28*(10), 417–426. 9

[91] Gonzalez, F. A., D. L. Raden, and R. J. Davis (1991). Identification of substrate recognition determinants for human ERK1 and ERK2 protein kinases. *Journal of Biological Chemistry 266*(33), 22159–63. 42

[92] Gorden, J. and P. L. Small (1993). Acid resistance in enteric bacteria. *Infection and Immunity 61*(1), 364–367. 3

[93] Gouin, E., M. D. Welch, and P. Cossart (2005). Actin-based motility of intracellular pathogens. *Current Opinion in Microbiology 8*(1), 35–45. 13, 14

[94] Grønborg, M., T. Z. Kristiansen, A. Stensballe, J. S. Andersen, O. Ohara, M. Mann, O. N. Jensen, and A. Pandey (2002). A Mass Spectrometry-based Proteomic Approach for Identification of Serine/Threonine-phosphorylated Proteins by Enrichment with Phospho-specific Antibodies: Identification of a Novel Protein, Frigg, as a Protein Kinase A Substrate. *Molecular & Cellular Proteomics 1*(7), 517–527. 41

[95] Gry, M., R. Rimini, S. Stromberg, A. Asplund, F. Ponten, M. Uhlen, and P. Nilsson (2009). Correlations between RNA and protein expression profiles in 23 human cell lines. *BMC Genomics 10*(1), 365. 29

[96] Gu, B., Y. Cao, S. Pan, L. Zhuang, R. Yu, Z. Peng, H. Qian, Y. Wei, L. Zhao, G. Liu, and M. Tong (2012). Comparison of the prevalence and changing resistance to nalidixic acid and ciprofloxacin of Shigella between Europe-America and Asia-Africa from 1998 to 2009. *International Journal of Antimicrobial Agents 40*(1), 9 – 17. 3

[97] Hachani, A., L. Biskri, G. Rossi, A. Marty, R. Ménard, P. Sansonetti, C. Parsot, G. Tran Van Nhieu, M. L. Bernardini, and A. Allaoui (2008). IpgB1 and IpgB2, two homologous effectors secreted via the Mxi-Spa type III secretion apparatus, cooperate to mediate polarized cell invasion and inflammatory potential of Shigella flexenri. *Microbes and Infection 10*(3), 260–268. 10

[98] Haglund, C. M. and M. D. Welch (2011). Pathogens and polymers: Microbe-host interactions illuminate the cytoskeleton. *The Journal of Cell Biology 195*(1), 7–17. 13

[99] Hamiaux, C., A. van Eerde, C. Parsot, J. Broos, and B. W. Dijkstra (2006, August). Structural mimicry for vinculin activation by IpaA, a virulence factor of Shigella flexneri. *EMBO Rep 7*(8), 794–799. 10, 12

[100] Handa, Y., M. Suzuki, K. Ohya, H. Iwai, N. Ishijima, A. J. Koleske, Y. Fukui, and C. Sasakawa (2007, January). Shigella IpgB1 promotes bacterial entry through the ELMO–Dock180 machinery. *Nat Cell Biol 9*(1), 121–128. 10, 11

[101] Hanks, S., A. Quinn, and T. Hunter (1988). The protein kinase family: conserved features and deduced phylogeny of the catalytic domains. *Science 241*(4861), 42–52. 35

[102] Hanley, P. J., Y. Xu, M. Kronlage, K. Grobe, P. Schön, J. Song, L. Sorokin, A. Schwab, and M. Bähler (2010, July). Motorized RhoGAP myosin IXb (Myo9b) controls cell shape and motility. *Proceedings of the National Academy of Sciences 107*(27), 12145–12150. 100

[103] Harrington, A., N. Darboe, R. Kenjale, W. L. Picking, C. R. Middaugh, S. Birket, and W. D. Picking (2006). Characterization of the Interaction of Single Tryptophan Containing Mutants of IpaC from Shigella flexneri with Phospholipid Membranes. *Biochemistry 45*(2), 626–636. PMID: 16401091. 9, 10

[104] Harry R Matthews (1995). Protein kinases and phosphatases that act on histidine, lysine, or arginine residues in eukaryotic proteins: A possible regulator of the mitogen-activated protein kinase cascade. *Pharmacology & Therapeutics 67*(3), 323 – 350. 33

[105] Hayes, S. J. and S. E. Mayer (1981). Regulation of guinea pig heart phosphorylase kinase by cAMP, protein kinase, and calcium. *Am J Physiol. 240*(3), E340–9. 32

[106] Hayward, R. D., R. J. Cain, E. J. McGhie, N. Phillips, M. J. Garner, and V. Koronakis (2005). Cholesterol binding by the bacterial type III translocon is essential for virulence effector delivery into mammalian cells. *Molecular Microbiology 56*(3), 590–603. 9, 10

[107] Heindl, J. E., I. Saran, C.-r. Yi, C. F. Lesser, and M. B. Goldberg (2010). Requirement for Formin-Induced Actin Polymerization during Spread of Shigella flexneri. *Infection and Immunity 78*(1), 193–203. 14

[108] Hemmings, B. A. and D. F. Restuccia (2012, September). PI3K-PKB/Akt Pathway. *Cold Spring Harbor Perspectives in Biology 4*(9), –. 109, 123

[109] Hestvik, A. L. K., Z. Hmama, and Y. Av Gay (2003). Kinome Analysis of Host Response to Mycobacterial Infection: a Novel Technique in Proteomics. *Infection and Immunity 71*(10), 5514–5522. 45

[110] Hilbi, H. (1999). Host responses to secreted Shigella virulence factors. *Current Opinion in Infectious Diseases 12*(3), –. 11

[111] Hilbi, H., J. E. Moss, D. Hersh, Y. Chen, J. Arondel, S. Banerjee, R. A. Flavell, J. Yuan, P. J. Sansonetti, and A. Zychlinsky (1998). Shigella-induced Apoptosis Is Dependent on Caspase-1 Which Binds to IpaB. *Journal of Biological Chemistry 273*(49), 32895–32900. 10

[112] Hsu, P. P., S. A. Kang, J. Rameseder, Y. Zhang, K. A. Ottina, D. Lim, T. R. Peterson, Y. Choi, N. S. Gray, M. B. Yaffe, J. A. Marto, and D. M. Sabatini (2011, June). The mTOR-Regulated Phosphoproteome Reveals a Mechanism of mTORC1-Mediated Inhibition of Growth Factor Signaling. *Science 332*(6035), 1317–1322. 95

[113] Hu, X., Y. Yu, Y. Eugene Chin, and Q. Xia (2013, November). The role of acetylation in TLR4-mediated innate immune responses. *Immunol Cell Biol 91*(10), 611–614. 142

[114] Huang, Z., S. E. Sutton, A. J. Wallenfang, R. C. Orchard, X. Wu, Y. Feng, J. Chai, and N. M. Alto (2009, August). Structural insights into host GTPase isoform selection by a family of bacterial GEF mimics. *Nat Struct Mol Biol 16*(8), 853–860. 11

[115] Hume, P. J., E. J. McGhie, R. D. Hayward, and V. Koronakis (2003, July). The purified Shigella IpaB and Salmonella SipB translocators share biochemical properties and membrane topology. *Molecular Microbiology 49*(2), 425–439. 10

[116] Hurley, J. H., A. M. Dean, P. E. Thorsness, D. E. Koshland, and R. M. Stroud (1990, March). Regulation of isocitrate dehydrogenase by phosphorylation involves no long-range conformational change in the free enzyme. *Journal of Biological Chemistry 265*(7), 3599–3602. 33

[117] Imami, K., A. P. Bhavsar, H. Yu, N. F. Brown, L. D. Rogers, B. B. Finlay, and L. J. Foster (2013). Global Impact of Salmonella Pathogenicity Island 2-secreted Effectors on the Host Phosphoproteome. *Molecular & Cellular Proteomics 12*(6), 1632–1643. 46

[118] Ireton, K. (2013). Molecular mechanisms of cell-cell spread of intracellular bacterial pathogens. *Open Biology 3*(7), –. 13, 14

[119] Ivetac, I., R. Gurung, S. Hakim, K. A. Horan, D. A. Sheffield, L. C. Binge, P. W. Majerus, T. Tiganis, and C. A. Mitchell (2009, March). Regulation of PI(3)K/Akt signalling and cellular transformation by inositol polyphosphate 4-phosphatase-1. *EMBO reports 10*(5), 487–493. 109

[120] Iwai, H., M. Kim, Y. Yoshikawa, H. Ashida, M. Ogawa, Y. Fujita, D. Muller, T. Kirikae, P. K. Jackson, S. Kotani, and C. Sasakawa (2007, Aug 24). A bacterial effector targets Mad2L2, an APC inhibitor, to modulate host cell cycling. *Cell 130*(4), 611–23. 0092-8674 (Print) Journal Article Research Support, Non-U.S. Gov't. 15

[121] Izard, T., G. Tran Van Nhieu, and P. R. Bois (2006). Shigella applies molecular mimicry to subvert vinculin and invade host cells. *The Journal of Cell Biology 175*(3), 465–475. 10, 12

[122] Jaskelioff, M. and C. L. Peterson (2003). Chromatin and transcription: histones continue to make their marks. *Nat Cell Biol 5*(5), 395–399. 26

[123] Jason A. Wojcechowskyj, Chuka A. Didigu, Jessica Y. Lee, Nicholas F. Parrish, Rohini Sinha, Beatrice H. Hahn, Frederic D. Bushman, Shane T. Jensen, Steven H. Seeholzer, and Robert W. Doms (2013). Quantitative Phosphoproteomics Reveals Extensive Cellular Reprogramming during HIV-1 Entry. *Cell Host & Microbe 13*(5), 613 – 623. 46

[124] Johnson, L. N. and R. J. Lewis (2001, July). Structural Basis for Control by Phosphorylation. *Chem. Rev. 101*(8), 2209–2242. 33

[125] Johnson, S., P. Roversi, M. Espina, A. Olive, J. E. Deane, S. Birket, T. Field, W. D. Picking, A. J. Blocker, E. E. Galyov, W. L. Picking, and S. M. Lea (2007). Self-chaperoning of the Type III Secretion System Needle Tip Proteins IpaD and BipD. *Journal of Biological Chemistry 282*(6), 4035–4044. 8

[126] Joo, E. E. and K. M. Yamada (2014, March). MYPT1 regulates contractility and microtubule acetylation to modulate integrin adhesions and matrix assembly. *Nat Commun 5*, –. 100

[127] Kasper, C. A. (2012). *Amplifying the innate immune response : cell-cell propagation of proinflammatory signals during bacterial infection.* Ph. D. thesis, University of Basel, Faculty of Science. 103

[128] Kasper, C. A., I. Sorg, C. Schmutz, T. Tschon, H. Wischnewski, M. L. Kim, and C. Arrieumerlou (2010). Cell-Cell Propagation of NF-kappaB Transcription Factor and MAP Kinase Activation Amplifies Innate Immunity against Bacterial Infection. *Immunity 33*(5), 804–816. 5, 27, 139

[129] Kayath, C. A., S. Hussey, N. El hajjami, K. Nagra, D. Philpott, and A. Allaoui (2010). Escape of intracellular Shigella from autophagy requires binding to cholesterol through the type III effector, IcsB. *Microbes and Infection 12*, 956–966. 10

[130] Keshet, Y. and R. Seger (2010). The MAP Kinase Signaling Cascades: A System of Hundreds of Components Regulates a Diverse Array of Physiological Functions. In R. Seger (Ed.), *MAP Kinase Signaling Protocols*, Volume 661 of *Methods in Molecular Biology*, pp. 3–38. Humana Press. 37

[131] Khromov, A., N. Choudhury, A. S. Stevenson, A. V. Somlyo, and M. Eto (2009, August). Phosphorylation-dependent Autoinhibition of Myosin Light Chain Phosphatase Accounts for Ca2+ Sensitization Force of Smooth Muscle Contraction. *Journal of Biological Chemistry 284*(32), 21569–21579. 100

[132] Kim, D. W., G. Lenzen, A. L. Page, P. Legrain, P. J. Sansonetti, and C. Parsot (2005, Sep 27). The Shigella flexneri effector OspG interferes with innate immune responses by targeting ubiquitin-conjugating enzymes. *Proc Natl Acad Sci U S A 102*(39), 14046–51. 0027-8424 (Print) Journal Article. 11, 24

[133] Kim, E., R. Tyagi, J.-Y. Lee, J. Park, Y.-r. Kim, J. Beon, P. Y. Chen, J. Y. Cha, S. H. Snyder, and S. Kim (2013, December). Inositol polyphosphate multikinase is a coactivator for serum response factor-dependent induction of immediate early genes. *Proceedings of the National Academy of Sciences 110*(49), 19938–19943. 124

[134] Kim, M., M. Ogawa, Y. Fujita, Y. Yoshikawa, T. Nagai, T. Koyama, S. Nagai, A. Lange, R. Fassler, and C. Sasakawa (2009, May). Bacteria hijack integrin-linked kinase to stabilize focal adhesions and block cell detachment. *Nature 459*(7246), 578–582. 10, 15

[135] Kim, M. L., H. G. Jeong, C. A. Kasper, and C. Arrieumerlou (2010). IKKalpha Contributes to Canonical NF-kappaB Activation Downstream of Nod1-Mediated Peptidoglycan Recognition. *PLoS ONE 5*(10), e15371. 126

[136] Kim, W., E. Bennett, E. Huttlin, A. Guo, J. Li, A. Possemato, M. Sowa, R. Rad, J. Rush, M. Comb, J. Harper, and S. Gygi (2011, October). Systematic and Quantitative Assessment of the Ubiquitin-Modified Proteome. *Molecular Cell 44*(2), 325–340. 31, 142

[137] Klink, B. U., S. Barden, T. V. Heidler, C. Borchers, M. Ladwein, T. E. B. Stradal, K. Rottner, and D. W. Heinz (2010). Structure of Shigella IpgB2 in Complex with Human RhoA. *Journal of Biological Chemistry 285*(22), 17197–17208. 10, 12

[138] Käll, L. and O. Vitek (2011, December). Computational Mass Spectrometry-Based Proteomics. *PLoS Comput Biol 7*(12), e1002277–. 45

[139] Kobayashi, T., M. Ogawa, T. Sanada, H. Mimuro, M. Kim, H. Ashida, R. Akakura, M. Yoshida, M. Kawalec, J.-M. Reichhart, T. Mizushima, and C. Sasakawa (2013, May). The Shigella OspC3 Effector Inhibits Caspase-4, Antagonizes Inflammatory Cell Death, and Promotes Epithelial Infection. *Cell Host & Microbe 13*(5), 570–583. 10

[140] Komander, D. (2009). The emerging complexity of protein ubiquitination. *Biochem Soc Trans. 37*, 937–953. 31

[141] Kosako, H., N. Yamaguchi, C. Aranami, M. Ushiyama, S. Kose, N. Imamoto, H. Taniguchi, E. Nishida, and S. Hattori (2009). Phosphoproteomics reveals new ERK MAP kinase targets and links ERK to nucleoporin-mediated nuclear transport. *Nat Struct Mol Biol 16*(10), 1026–1035. 10.1038/nsmb.1656. 42, 95, 97, 135

[142] Kosek, M., P. P. Yori, and M. P. Olortegui (2010). Shigellosis update: advancing antibiotic resistance, investment empowered vaccine development, and green bananas. *Current Opinion in Infectious Diseases 23*(5), 475–480. 5

[143] Kotloff, K., J. Winickoff, B. Ivanoff, J. Clemens, D. Swerdlow, P. Sansonetti, G. Adak, and Levine MM. (1999). Global burden of Shigella infections: implications for vaccine development and implementation of control strategies. *Bull World Health Organ. 77*(8), 651–66. 2, 5

[144] Krebs, E. G. and E. H. Fischer (1955). PHOSPHORYLASE ACTIVITY OF SKELETAL MUSCLE EXTRACTS. *Journal of Biological Chemistry 216*(1), 113–120. 32

[145] Krüger, M., I. Kratchmarova, B. Blagoev, Y.-H. Tseng, C. R. Kahn, and M. Mann (2008). Dissection of the insulin signaling pathway via quantitative phosphoproteomics. *Proceedings of the National Academy of Sciences 105*(7), 2451–2456. 41

[146] Krishna, M. and H. Narang (2008). The complexity of mitogen-activated protein kinases (MAPKs) made simple. *Cell Mol Life Sci. 65*(22), 3525–3544–. 23

[147] Kudryashev, M., M. Stenta, S. Schmelz, M. Amstutz, U. Wiesand, D. Castaño Díez, M. T. Degiacomi, S. Münnich, C. K. Bleck, J. Kowal, A. Diepold, D. W. Heinz, M. Dal Peraro, G. R. Cornelis, H. Stahlberg, and V. Dötsch (2013, July). In situ structural analysis of the Yersinia enterocolitica injectisome. *eLife Sciences 2*, –. 111

[148] Kuroda, I., Y. Shintani, M. Motokawa, S. Abe, and M. Furuno (2004). Phosphopeptide-selective Column-switching RP-HPLC with a Titania Precolumn. *Analytical Sciences 20*(9), 1313–1319. 40

[149] Lafont, F., G. Tran Van Nhieu, K. Hanada, P. Sansonetti, and F. G. van der Goot (2002, Sep 2). Initial steps of Shigella infection depend on the cholesterol/sphingolipid raft-mediated CD44-IpaB interaction. *EMBO J 21*(17), 4449–57. 0261-4189 (Print) Journal Article. 9

[150] Lan, R. and P. R. Reeves (2002, September). Escherichia coli in disguise: molecular origins of Shigella. *Microbes and Infection 4*(11), 1125–1132. 5

[151] LaRonde LeBlanc, N. and A. Wlodawer (2005). A Family Portrait of the RIO Kinases. *Journal of Biological Chemistry 280*(45), 37297–37300. 38

[152] Larsen, M., G. Sørensen, S. Fey, P. Larsen, and P. Roepstorff (2001). Phospho-proteomics: evaluation of the use of enzymatic de-phosphorylation and differential mass spectrometric peptide mass mapping for site specific phosphorylation assignment in proteins separated by gel electrophoresis. *Proteomics 1*, 223–238. 36

[153] Larsen, M. R., T. E. Thingholm, O. N. Jensen, P. Roepstorff, and T. J. D. Jørgensen (2005). Highly Selective Enrichment of Phosphorylated Peptides from Peptide Mixtures Using Titanium Dioxide Microcolumns. *Molecular & Cellular Proteomics 4*(7), 873–886. 41

[154] Lee, T.-Y., J. Bo-Kai Hsu, W.-C. Chang, and H.-D. Huang (2011). RegPhos: a system to explore the protein kinase-substrate phosphorylation network in humans. *Nucleic Acids Research 39*(suppl 1), D777–D787. 35, 41

[155] Leung, Y., S. Ally, and M. B. Goldberg (2008). Bacterial Actin Assembly Requires Toca-1 to Relieve N-WASP Autoinhibition. *Cell Host & Microbe 3*(1), 39 – 47. 14

[156] Li, H., H. Xu, Y. Zhou, J. Zhang, C. Long, S. Li, S. Chen, J. M. Zhou, and F. Shao (2007, Feb 16). The phosphothreonine lyase activity of a bacterial type III effector family. *Science 315*(5814), 1000–3. 1095-9203 (Electronic) Journal Article Research Support, Non-U.S. Gov't. 10, 136

[157] Li, M., J. Liu, and C. Zhang (2011, October). Evolutionary History of the Vertebrate Mitogen Activated Protein Kinases Family. *PLoS ONE 6*(10), e26999–. 23

[158] Li, Y., Y. Luo, S. Wu, Y. Gao, Y. Liu, and D. Zheng (2009). Nucleic Acids in Protein Samples Interfere with Phosphopeptide Identification by Immobilized-Metal-Ion Affinity Chromatography and Mass Spectrometry. *Mol Biotechnol. 43*(1), 59–66–. 41

[159] Liebler, D. C. and L. J. Zimmerman (2013, March). Targeted Quantitation of Proteins by Mass Spectrometry. *Biochemistry 52*(22), 3797–3806. 142

[160] Liu, Z., Y. Wang, and Y. Xue (2013, November). Phosphoproteomics-based network medicine. *FEBS J 280*(22), 5696–5704. 39

[161] Louise N. Johnson (2009). The regulation of protein phosphorylation. *Biochem Soc Trans. 37*, 627–641. 32, 33, 34, 35

[162] Love, D. C., T. D. Sweitzer, and J. A. Hanover (1998). Reconstitution of HIV-1 Rev nuclear export: Independent requirements for nuclear import and export. *PNAS 95*(18), 10608–10613. 97, 101, 135

[163] Lucchini, S., H. Liu, Q. Jin, J. C. D. Hinton, and J. Yu (2005, January 1, 2005). Transcriptional Adaptation of Shigella flexneri during Infection of Macrophages and Epithelial Cells: Insights into the Strategies of a Cytosolic Bacterial Pathogen. *Infect. Immun. 73*(1), 88–102. 20

[164] Lundby, A., K. Lage, B. Weinert, D. Bekker Jensen, A. Secher, T. Skovgaard, C. Kelstrup, A. Dmytriyev, C. Choudhary, C. Lundby, and J. Olsen (2012, August). Proteomic Analysis of Lysine Acetylation Sites in Rat Tissues Reveals Organ Specificity and Subcellular Patterns. *Cell Reports 2*(2), 419–431. 31, 142

[165] Maag, D., M. J. Maxwell, D. A. Hardesty, K. L. Boucher, N. Choudhari, A. G. Hanno, J. F. Ma, A. S. Snowman, J. W. Pietropaoli, R. Xu, P. B. Storm, A. Saiardi, S. H. Snyder, and A. C. Resnick (2011, January). Inositol polyphosphate multikinase is a physiologic PI3-kinase that activates Akt/PKB. *Proceedings of the National Academy of Sciences 108*(4), 1391–1396. 126

[166] Mabbott, N. A., D. S. Donaldson, H. Ohno, I. R. Williams, and A. Mahajan (2013). Microfold (M) cells: important immunosurveillance posts in the intestinal epithelium. *Mucosal Immunology 6*(4), 666–677. 3

[167] Mamane, Y., E. Petroulakis, L. Rong, K. Yoshida, L. W. Ler, and N. Sonenberg (2004). eIF4E - from translation to transformation. *Oncogene 23*(18), 3172–3179. 95

[168] Manadas, B., V. M. Mendes, J. English, and M. J. Dunn (2010, October). Peptide fractionation in proteomics approaches. *Expert Review of Proteomics 7*(5), 655–663. 42, 43

[169] Manning, G., D. B. Whyte, R. Martinez, T. Hunter, and S. Sudarsanam (2002). The Protein Kinase Complement of the Human Genome. *Science 298*(5600), 1912–1934. 35

[170] Maurelli, A. T., B. Baudry, H. d'Hauteville, T. L. Hale, and P. J. Sansonetti (1985, July). Cloning of plasmid DNA sequences involved in invasion of HeLa cells by Shigella flexneri. *Infection and Immunity 49*(1), 164–171. 6

[171] Mavris, M., A.-L. Page, R. Tournebize, B. Demers, P. Sansonetti, and C. Parsot (2002). Regulation of transcription by the activity of the Shigella flexneri type III secretion apparatus. *Molecular Microbiology 43*(6), 1543–1553. 7

[172] Menard, R., P. Sansonetti, C. Parsot, and T. Vasselon (1994, November). Extracellular association and cytoplasmic partitioning of the IpaB and IpaC invasins of S. flexneri. *Cell 79*(3), 515–525. 10

[173] Menard, R., P. J. Sansonetti, and C. Parsot (1993, September). Nonpolar mutagenesis of the ipa genes defines IpaB, IpaC, and IpaD as effectors of Shigella flexneri entry into epithelial cells. *Journal of Bacteriology 175*(18), 5899–5906. 10

[174] Menard, R., P. J. Sansonetti, and C. Parsot (1994). The secretion of the Shigella flexneri Ipa invasins is activated by epithelial cells and controlled by IpaB and IpaD. *EM 13*, 5293–5302. 8

[175] Miura, M., J. Terajima, H. Izumiya, J. Mitobe, T. Komano, and H. Watanabe (2006, May). OspE2 of Shigella sonnei Is Required for the Maintenance of Cell Architecture of Bacterium-Infected Cells. *Infection and Immunity 74*(5), 2587–2595. 10

[176] Molero, C., I. Rodriguez Escudero, A. Aleman, R. Rotger, M. Molina, and V. J. Cid (2009). Addressing the effects of Salmonella internalization in host cell signaling on a reverse-phase protein array. *PROTEOMICS 9*(14), 3652–3665. 45

[177] Morris, C. R., C. L. Grassel, J. C. Redman, J. W. Sahl, E. M. Barry, and D. A. Rasko (2013). Characterization of Intracellular Growth Regulator icgR by Utilizing Transcriptomics To Identify Mediators of Pathogenesis in Shigella flexneri. *Infection and Immunity 81*(9), 3068–3076. 20

[178] Mostovenko, E., C. Hassan, J. Rattke, A. M. Deelder, P. A. van Veelen, and M. Palmblad (2013). Comparison of peptide and protein fractionation methods in proteomics. *EuPA Open Proteomics 1*(0), 30 – 37. 42

[179] Mostowy, S. and P. Cossart (2011, July). Autophagy and the cytoskeleton: New links revealed by intracellular pathogens. *autophagy 7*(1554-8627), 780–782. 12, 14

[180] Mota, L. J. and G. R. Cornelis (2005, January). The bacterial injection kit: Type III secretion systems. *Ann Med 37*(4), 234–249. 7

[181] Mounier, J., M. R. Popoff, J. Enninga, M. C. Frame, P. J. Sansonetti, and G. T. Van Nhieu (2009, 01). The IpaC Carboxyterminal Effector Domain Mediates Src-Dependent Actin Polymerization during Shigella Invasion of Epithelial Cells. *PLoS Pathog 5*(1), e1000271. 11

[182] Mounier, J., T. Vasselon, R. Hellio, M. Lesourd, and P. J. Sansonetti (1992). Shigella flexneri enters human colonic Caco-2 epithelial cells through the basolateral pole. *Infection and Immunity 60*(1), 237–248. 3

[183] Mu, J.-J., Y. Wang, H. Luo, M. Leng, J. Zhang, T. Yang, D. Besusso, S. Y. Jung, and J. Qin (2007). A Proteomic Analysis of Ataxia Telangiectasia-mutated (ATM)/ATM-Rad3-related (ATR) Substrates Identifies the Ubiquitin-Proteasome System as a Regulator for DNA Damage Checkpoints. *Journal of Biological Chemistry 282*(24), 17330–17334. 42

[184] Murphy, K. and K. Campellone (2003). Lambda Red-mediated recombinogenic engineering of enterohemorrhagic and enteropathogenic E. coli. *BMC Molecular Biology 4*(1), 11. 126

[185] Nakayasu, E. S., R. Tempel, X. A. Cambronne, V. A. Petyuk, M. B. Jones, M. A. Gritsenko, M. E. Monroe, F. Yang, R. D. Smith, J. N. Adkins, and F. Heffron (2013). Comparative Phosphoproteomics Reveals Components of Host Cell Invasion and Post-transcriptional Regulation During Francisella Infection. *Molecular & Cellular Proteomics 12*(11), 3297–3309. 133, 137

[186] Napetschnig, J. and H. Wu (2013, May). Molecular Basis of NF-kB Signaling. *Annu. Rev. Biophys. 42*(1), 443–468. 22

[187] Neal M. Alto, Feng Shao, Cheri S. Lazar, Renee L. Brost, Gordon Chua, Seema Mattoo, Stephen A. McMahon, Partho Ghosh, Timothy R. Hughes, Charles Boone, and Jack E. Dixon (2006). Identification of a Bacterial Type III Effector Family with G Protein Mimicry Functions. *Cell 124*(1), 133–145. 10, 11

[188] Neilson, K. A., N. A. Ali, S. Muralidharan, M. Mirzaei, M. Mariani, G. Assadourian, A. Lee, S. C. van Sluyter, and P. A. Haynes (2011, February). Less label, more free: Approaches in label-free quantitative mass spectrometry. *Proteomics 11*(4), 535–553. 43, 44

[189] Neville, D. C. A., R. R. Townsend, C. R. Rozanas, A. S. Verkman, E. M. Price, and D. B. Gruis (1997). Evidence for phosphorylation of serine 753 in CFTR using a novel metal-ion affinity resin and matrix-assisted laser desorption mass spectrometry. *Protein Science 6*(11), 2436–2445. 40

[190] Newton, H. J., J. S. Pearson, L. Badea, M. Kelly, M. Lucas, G. Holloway, K. M. Wagstaff, M. A. Dunstone, J. Sloan, J. C. Whisstock, J. B. Kaper, R. M. Robins Browne, D. A. Jans, G. Frankel, A. D. Phillips, B. S. Coulson, and E. L. Hartland (2010, 05). The Type III Effectors NleE and NleB from Enteropathogenic E. coli and OspZ from Shigella Block Nuclear Translocation of NF-kappaB p65. *PLoS Pathog 6*(5), e1000898. 11, 24

[191] Nühse, T. S., A. Stensballe, O. N. Jensen, and S. C. Peck (2003). Large-scale Analysis of in Vivo Phosphorylated Membrane Proteins by Immobilized Metal Ion Affinity Chromatography and Mass Spectrometry. *Molecular & Cellular Proteomics 2*(11), 1234–1243. 40

[192] Nie, H., F. Yang, X. Zhang, J. Yang, L. Chen, J. Wang, Z. Xiong, J. Peng, L. Sun, J. Dong, Y. Xue, X. Xu, S. Chen, Z. Yao, Y. Shen, and Q. Jin (2006). Complete genome sequence of Shigella flexneri 5b and comparison with Shigella flexneri 2a. *BMC Genomics 7*(1), 173–. 6

[193] Niebuhr, K., S. Giuriato, T. Pedron, D. J. Philpott, F. Gaits, J. Sable, M. P. Sheetz, C. Parsot, P. J. Sansonetti, and B. Payrastre (2002, Oct 1). Conversion of PtdIns(4,5)P(2) into PtdIns(5)P by the S.flexneri effector IpgD reorganizes host cell morphology. *EMBO J 21*(19), 5069–78. 0261-4189 (Print) Journal Article. 10, 12, 17, 109, 113

[194] Niebuhr, K., N. Jouihri, A. Allaoui, P. Gounon, P. J. Sansonetti, and C. Parsot (2000, October). IpgD, a protein secreted by the type III secretion machinery of Shigella flexneri, is chaperoned by IpgE and implicated in entry focus formation. *Molecular Microbiology 38*(1), 8–19. 10

[195] Niyogi, S. (2005). Shigellosis. *The Journal of Microbiology 43*(2), 133–143. 2, 3, 5

[196] Norris, F. A., M. P. Wilson, T. S. Wallis, E. E. Galyov, and P. W. Majerus (1998, November). SopB, a protein required for virulence of Salmonella dublin, is an inositol phosphate phosphatase. *Proceedings of the National Academy of Sciences 95*(24), 14057–14059. 109

[197] Nougayrède, J.-P., F. Taieb, J. De Rycke, and E. Oswald (2005). Cyclomodulins: bacterial effectors that modulate the eukaryotic cell cycle. *Trends in Microbiology 13*(3), 103 – 110. 15

[198] Ogawa, M., Y. Handa, H. Ashida, M. Suzuki, and C. Sasakawa (2008, Jan). The versatility of Shigella effectors. *Nat Rev Microbiol 6*(1), 11–6. 1740-1534 (Electronic) Journal Article Research Support, Non-U.S. Gov't Review. 14

[199] Ogawa, M., T. Suzuki, I. Tatsuno, H. Abe, and C. Sasakawa (2003). IcsB, secreted via the type III secretion system, is chaperoned by IpgA and required at the post-invasion stage of Shigella pathogenicity. *Molecular Microbiology 48*(4), 913–931. 10

[200] Ogawa, M., T. Yoshimori, T. Suzuki, H. Sagara, N. Mizushima, and C. Sasakawa (2005). Escape of Intracellular Shigella from Autophagy. *Science 307*(5710), 727–731. 10, 12

[201] Ohya, K., Y. Handa, M. Ogawa, M. Suzuki, and C. Sasakawa (2005). IpgB1 Is a Novel Shigella Effector Protein Involved in Bacterial Invasion of Host Cells. *Journal of Biological Chemistry 280*(25), 24022–24034. 10, 100

[202] Okuda, J., T. Toyotome, N. Kataoka, M. Ohno, H. Abe, Y. Shimura, A. Seyedarabi, R. Pickersgill, and C. Sasakawa (2005, Jul 29). Shigella effector IpaH9.8 binds to a splicing factor U2AF(35) to modulate host immune responses. *Biochem Biophys Res Commun 333*(2), 531–9. 0006-291X (Print) Journal Article Research Support, Non-U.S. Gov't. 10, 24

[203] Olsen, J. V., B. Blagoev, F. Gnad, B. Macek, C. Kumar, P. Mortensen, and M. Mann (2006). Global, In Vivo, and Site-Specific Phosphorylation Dynamics in Signaling Networks. *Cell 127*(3), 635–648. 32, 39, 41

[204] Osiecki, J. C., J. Barker, W. L. Picking, A. B. Serfis, E. Berring, S. Shah, A. Harrington, and W. D. Picking (2001). IpaC from Shigella and SipC from Salmonella possess similar biochemical properties but are functionally distinct. *Molecular Microbiology 42*(2), 469–481. 12

[205] Pan, H., J. Xie, F. Ye, and S.-J. Gao (June 1, 2006). Modulation of Kaposi's Sarcoma-Associated Herpesvirus Infection and Replication by MEK/ERK, JNK, and p38 Multiple Mitogen-Activated Protein Kinase Pathways during Primary Infection. *Journal of Virology 80*(11), 5371–5382. 23

[206] Park, H., C. Valencia Gallardo, A. Sharff, G. T. Van Nhieu, and T. Izard (2011, July). Novel Vinculin Binding Site of the IpaA Invasin of Shigella. *Journal of Biological Chemistry 286*(26), 23214–23221. 12

[207] Parsot, C. (2009, Feb). Shigella type III secretion effectors: how, where, when, for what purposes? *Curr Opin Microbiol 12*(1), 110–6. 1879-0364 (Electronic) Journal Article Review. 25

[208] Parsot, C., E. Ageron, C. Penno, M. Mavris, K. Jamoussi, H. D'Hauteville, P. Sansonetti, and B. Demers (2005). A secreted anti-activator, OspD1, and its chaperone, Spa15, are involved in the control of transcription by the type III secretion apparatus activity in Shigella flexneri. *Molecular Microbiology 56*(6), 1627–1635. 7, 10

[209] Pédron, T., C. Thibault, and P. J. Sansonetti (2003, Sep 5). The invasive phenotype of Shigella flexneri directs a distinct gene expression pattern in the human intestinal epithelial cell line Caco-2. *J Biol Chem 278*(36), 33878–86. 0021-9258 (Print) Journal Article. 5, 23, 29

[210] Pearce, L. R., D. Komander, and D. R. Alessi (2010, January). The nuts and bolts of AGC protein kinases. *Nat Rev Mol Cell Biol 11*(1), 9–22. 37

[211] Peck, S. C., T. S. NÃ¼hse, D. Hess, A. Iglesias, F. Meins, and T. Boller (2001). Directed Proteomics Identifies a Plant-Specific Protein Rapidly Phosphorylated in Response to Bacterial and Fungal Elicitors. *The Plant Cell Online 13*(6), 1467–1475. 44

[212] Pendaries, C., H. Tronchere, L. Arbibe, J. Mounier, O. Gozani, L. Cantley, M. J. Fry, F. Gaits Iacovoni, P. J. Sansonetti, and B. Payrastre (2006, March). PtdIns(5)P activates the host cell PI3-kinase/Akt pathway during Shigella flexneri infection. *EMBO J 25*(5), 1024–1034. 10, 17, 18, 109, 113, 118, 122, 123, 124, 140

[213] Peng, J., X. Zhang, J. Yang, J. Wang, E. Yang, W. Bin, C. Wei, M. Sun, and Q. Jin (2006). The use of comparative genomic hybridization to characterize genome dynamics and diversity among the serotypes of Shigella. *BMC Genomics 7*(1), 218–. 6

[214] Peti, W., A. C. Nairn, and R. Page (2013, January). Structural basis for protein phosphatase 1 regulation and specificity. *FEBS Journal 280*(2), 596–611. 36

[215] Philpott, D. J., S. Yamaoka, A. Israel, and P. J. Sansonetti (2000, Jul 15). Invasive Shigella flexneri activates NF-kappa B through a lipopolysaccharide-dependent innate intracellular response and leads to IL-8 expression in epithelial cells. *J Immunol 165*(2), 903–14. 0022-1767 (Print) Journal Article. 5

[216] Pieper, R., C. R. Fisher, M.-J. Suh, S.-T. Huang, P. Parmar, and S. M. Payne (2013). Analysis of the Proteome of Intracellular Shigella flexneri Reveals Pathways Important for Intracellular Growth. *Infection and Immunity 81*(12), 4635–4648. 20, 29

[217] Pieper, R., Q. Zhang, P. P. Parmar, S.-T. Huang, D. J. Clark, H. Alami, A. Donohue Rolfe, R. D. Fleischmann, S. N. Peterson, and S. Tzipori (2009). The Shigella dysenteriae serotype 1 proteome, profiled in the host intestinal environment, reveals major metabolic modifications and increased expression of invasive proteins. *PROTEOMICS 9*(22), 5029–5045. 29

[218] Pierobon, M., J. Wulfkuhle, L. Liotta, and E. Petricoin (2014, March). Application of molecular technologies for phosphoproteomic analysis of clinical samples. *Oncogene Epub*, –. 134

[219] Puhar, A., H. Tronchere, B. Payrastre, G. Tran Van Nhieu, and P. Sansonetti (2013). A Shigella Effector Dampens Inflammation by Regulating Epithelial Release of Danger Signal ATP through Production of the Lipid Mediator PtdIns5P. *Immunity 39*(6), 1121 – 1131. 10, 27

[220] Rajanala, K. and V. K. Nandicoori (2012). Localization of nucleoporin Tpr to the nuclear pore complex is essential for Tpr mediated regulation of the export of unspliced RNA. *PLoS ONE 7*(1), e29921. 97

[221] Ramel, D., F. Lagarrigue, S. Dupuis Coronas, G. Chicanne, N. Leslie, F. Gaits Iacovoni, B. Payrastre, and H. Tronchère (2009, September). PtdIns5P protects Akt from dephosphorylation through PP2A inhibition. *Biochemical and Biophysical Research Communications 387*(1), 127–131. 109

[222] Ramel, D., F. Lagarrigue, V. Pons, J. Mounier, S. Dupuis Coronas, G. Chicanne, P. J. Sansonetti, F. Gaits Iacovoni, H. Tronchere, and B. Payrastre (2011). Shigella flexneri Infection Generates the Lipid PI5P to Alter Endocytosis and Prevent Termination of EGFR Signaling. *Sci. Signal. 4*(191), ra61. 10, 18, 109, 118, 123, 124, 140

[223] Ray, K., B. Marteyn, P. J. Sansonetti, and C. M. Tang (2009). Life on the inside: the intracellular lifestyle of cytosolic bacteria. *Nat Rev Micro 7*(5), 333–340. 10.1038/nrmicro2112. 29

[224] Reeves, S. A., A. G. Torres, and S. M. Payne (2000). TonB Is Required for Intracellular Growth and Virulence of Shigella dysenteriae. *Infection and Immunity 68*(11), 6329–6336. 20

[225] Reiterer, V., L. Grossniklaus, T. Tschon, C. A. Kasper, I. Sorg, and C. Arrieumerlou (2011). Shigella flexneri type III secreted effector OspF reveals new crosstalks of proinflammatory signaling pathways during bacterial infection. *Cellular Signalling 23*(7), 1188–1196. 22, 26, 136

[226] Ribet, D. and P. Cossart (2010, July). Post-translational modifications in host cells during bacterial infection. *FEBS Letters 584*(13), 2748–2758. 30

[227] Riethmüller, J., A. Riehle, H. Grassmé, and E. Gulbins (2006, December). Membrane rafts in host-pathogen interactions. *Biochimica et Biophysica Acta (BBA) - Biomembranes 1758*(12), 2139–2147. 9

[228] Rigbolt, K. T. and B. Blagoev (2012, October). Quantitative phosphoproteomics to characterize signaling networks. *Seminars in Cell & Developmental Biology 23*(8), 863–871. 142

[229] Rogers, L. D., N. F. Brown, Y. Fang, S. Pelech, and L. J. Foster (2011). Phosphoproteomic Analysis of Salmonella-Infected Cells Identifies Key Kinase Regulators and SopB-Dependent Host Phosphorylation Events. *Sci. Signal. 4*(191), rs9–. 31, 45, 135, 136

[230] Rohde, J. R., A. Breitkreutz, A. Chenal, P. J. Sansonetti, and C. Parsot (2007). Type III Secretion Effectors of the IpaH Family Are E3 Ubiquitin Ligases. *Cell Host & Microbe 1*(1), 77–83. 10, 142

[231] Rolland, K., N. Lambert Zechovsky, B. Picard, and E. Denamur (1998, September). Shigella and enteroinvasive Escherichia coli strains are derived from distinct ancestral strains of E. coli. *Microbiology 144*(9), 2667–2672. 5

[232] Romero, S., G. Grompone, N. Carayol, J. Mounier, S. Guadagnini, M.-C. Prevost, P. Sansonetti, and G. Tran Van Nhieu (2011). ATP-Mediated Erk1/2 Activation Stimulates Bacterial Capture by Filopodia, which Precedes Shigella Invasion of Epithelial Cells. *Cell Host & Microbe 9*(6), 508–519. 3, 9

[233] Roppenser, B., H. Kwon, V. Canadien, R. Xu, P. N. Devreotes, S. Grinstein, and J. H. Brumell (2013, August). Multiple Host Kinases Contribute to Akt Activation during Salmonella Infection. *PLoS ONE 8*(8), e71015–. 109, 114, 120, 124, 141

[234] Ross, A. H., D. Baltimore, and H. N. Eisen (1981, December). Phosphotyrosine-containing proteins isolated by affinity chromatography with antibodies to a synthetic hapten. *Nature 294*(5842), 654–656. 36

[235] Runau, F., L. Norris, J. Isherwood, M. Metcalfe, K. Brown, and A. Dennison (2013, February). Label-free proteomics: a potential method for identifying protein biomarkers in pancreatic cancer. *Lancet 381*, S96–.

[236] Sanada, T., M. Kim, H. Mimuro, M. Suzuki, M. Ogawa, A. Oyama, H. Ashida, T. Kobayashi, Taira Koyama, S. Nagai, Y. Shibata, J. Gohda, J.-i. Inoue, T. Mizushima, and C. Sasakawa (2012). The Shigella flexneri effector OspI deamidates UBC13 to dampen the inflammatory response. *Nature 483*(7391), 623–626. 24

[237] Sani, M., A. Allaoui, F. Fusetti, G. T. Oostergetel, W. Keegstra, and E. J. Boekema (2007). Structural organization of the needle complex of the type III secretion apparatus of Shigella flexneri. *Micron 38*(3), 291–301. 8

[238] Sansonetti, P., A. Ryter, P. Clerc, A. Maurelli, and J. Mounier (1986). Multiplication of Shigella flexneri within HeLa cells: lysis of the phagocytic vacuole and plasmid-mediated contact hemolysis. *Infection and Immunity 51*(2), 461–469. 5

[239] Sansonetti, P. J. (2006, Aug). The bacterial weaponry: lessons from Shigella. *Ann N Y Acad Sci 1072*, 307–12. 0077-8923 (Print) Journal Article Review. 2

[240] Sansonetti, P. J., J. Arondel, J. R. Cantey, M. C. Prevost, and M. Huerre (1996, Jul). Infection of rabbit Peyer's patches by Shigella flexneri: effect of adhesive or invasive bacterial phenotypes on follicle-associated epithelium. *Infect Immun 64*(7), 2752–64. 0019-9567 (Print) Journal Article. 3

[241] Sansonetti, P. J., J. Arondel, J. M. Cavaillon, and M. Huerre (1995, 8). Role of interleukin-1 in the pathogenesis of experimental shigellosis. *The Journal of Clinical Investigation 96*(2), 884–892. 3

[242] Sansonetti, P. J., J. Arondel, A. Fontaine, H. d'Hauteville, and M. L. Bernardini (1991). OmpB (osmo-regulation) and icsA (cell-to-cell spread) mutants of Shigella flexneri: vaccine candidates and probes to study the pathogenesis of shigellosis. *Vaccine 9*(6), 416–422. 13

[243] Sansonetti, P. J., J. Arondel, M. Huerre, A. Harada, and K. Matsushima (1999, Mar). Interleukin-8 controls bacterial transepithelial translocation at the cost of epithelial destruction in experimental shigellosis. *Infect Immun 67*(3), 1471–80. 0019-9567 (Print) Journal Article. 5

[244] Sansonetti, P. J., D. J. Kopecko, and S. B. Formal (1982, March). Involvement of a plasmid in the invasive ability of Shigella flexneri. *Infection and Immunity 35*(3), 852–860. 6

[245] Sansonetti, P. J., J. Mounier, M. C. Prévost, and R.-M. Mège (1994). Cadherin expression is required for the spread of Shigella flexneri between epithelial cells. *Cell 76*(5), 829 – 839. 14

[246] Sansonetti, P. J., A. Phalipon, J. Arondel, K. Thirumalai, S. Banerjee, S. Akira, K. Takeda, and A. Zychlinsky (2000). Caspase-1 Activation of IL-1beta and IL-18 Are Essential for Shigella flexneri Induced Inflammation. *Immunity 12*(5), 581 – 590. 3

[247] Santapaola, D., F. Del Chierico, A. Petrucca, S. Uzzau, M. Casalino, B. Colonna, R. Sessa, F. Berlutti, and M. Nicoletti (2006, Feb). Apyrase, the Product of the Virulence Plasmid-Encoded phoN2 (apy) Gene of Shigella flexneri, Is Necessary for Proper Unipolar IcsA Localization and for Efficient Intercellular Spread. *Journal of Bacteriology 188*(4), 1620–1627. 14

[248] Schmutz, C., E. Ahrné, C. A. Kasper, T. Tschon, I. Sorg, R. F. Dreier, A. Schmidt, and C. Arrieumerlou (2013, October). Systems-Level Overview of Host Protein Phosphorylation During Shigella flexneri Infection Revealed by Phosphoproteomics. *Molecular & Cellular Proteomics 12*(10), 2952–2968. 94, 99, 101, 110, 111, 123

[249] Schroeder, G. N. and H. Hilbi (2007, January). Cholesterol is required to trigger caspase-1 activation and macrophage apoptosis after phagosomal escape of Shigella. *Cellular Microbiology 9*(1), 265–278. 9

[250] Schroeder, G. N. and H. Hilbi (2008, Jan). Molecular pathogenesis of Shigella spp.: controlling host cell signaling, invasion, and death by type III secretion. *Clin Microbiol Rev 21*(1), 134–56. 1098-6618 (Electronic) Journal Article Research Support, Non-U.S. Gov't Review. 3, 4, 5, 6, 7, 8, 11, 12, 15, 25, 137

[251] Scully, R. and A. Xie (2013, October). Double strand break repair functions of histone H2AX. *Mutation Research/Fundamental and Molecular Mechanisms of Mutagenesis 750*(1-2), 5–14. 133

[252] Sen, R. and D. Baltimore (1986, December). Inducibility of kappa immunoglobulin enhancer-binding protein NF-kappaB by a posttranslational mechanism. *Cell 47*(6), 921–928. 22

[253] Senerovic, L., S. P. Tsunoda, C. Goosmann, V. Brinkmann, A. Zychlinsky, F. Meissner, and M. Kolbe (2012, September). Spontaneous formation of IpaB ion channels in host cell membranes reveals how Shigella induces pyroptosis in macrophages. *Cell Death Dis 3*, e384–. 3

[254] Shen, D.-K., N. Mariya, I. Martinez Argudo, and A. J. Blocker (2012). Needle length control and the secretion substrate specificity switch are only loosely coupled in the type III secretion apparatus of Shigella. *microbiology 158*, 1884–1896. 97

[255] Shiloh, Y. and Y. Ziv (2013, April). The ATM protein kinase: regulating the cellular response to genotoxic stress, and more. *Nat Rev Mol Cell Biol 14*(4), 197–210. 133

[256] Simons, K. and J. L. Sampaio (2011, October). Membrane Organization and Lipid Rafts. *Cold Spring Harbor Perspectives in Biology 3*(10), –. 9

[257] Simons, K. and D. Toomre (2000, October). Lipid rafts and signal transduction. *Nat Rev Mol Cell Biol 1*(1), 31–39. 9

[258] Skoudy, A., J. Mounier, A. Aruffo, H. Ohayon, P. Gounon, P. Sansonetti, and G. Tran Van Nhieu (2000, Feb). CD44 binds to the Shigella IpaB protein and participates in bacterial invasion of epithelial cells. *Cell Microbiol 2*(1), 19–33. 1462-5814 (Print) Journal Article. 9

[259] Sood, V. and J. H. Brickner (2014, April). Nuclear pore interactions with the genome. *Current Opinion in Genetics & Development 25*(0), 43–49. 135

[260] Stehelin, D., H. E. Varmus, J. M. Bishop, and P. K. Vogt (1976, March). DNA related to the transforming gene(s) of avian sarcoma viruses is present in normal avian DNA. *Nature 260*(5547), 170–173. 11

[261] Susan S. Taylor, Choel Kim, Dominico Vigil, Nina M. Haste, Jie Yang, Jian Wu, and Ganesh S. Anand (2005). Dynamics of signaling by PKA. *Biochimica et Biophysica Acta (BBA) - Proteins and Proteomics 1754*, 25 – 37. Inhibitors of Protein Kinases (4th International Conference, Inhibitors of Protein Kinases) and Associated Workshop: Modelling of Specific Molecular Recognition Processes (Warsaw, Poland, June 25-29, 2005).

[262] Suzuki, S., L. Franchi, Y. He, R. Muñoz Planillo, H. Mimuro, T. Suzuki, C. Sasakawa, and G. Núñez (2014, 02). Shigella Type III Secretion Protein MxiI Is Recognized by Naip2 to Induce Nlrc4 Inflammasome Activation Independently of Pkcdelta. *PLoS Pathog 10*(2), e1003926. 3

[263] Suzuki, T., H. Miki, T. Takenawa, and C. Sasakawa (1998, May 15). Neural Wiskott-Aldrich syndrome protein is implicated in the actin-based motility of Shigella flexneri. *EMBO J 17*(10), 2767–76. 0261-4189 (Print) Journal Article. 14

[264] Taneja, N. (2007). Changing Epidemiology of Shigellosis and Emergence of Ciprofloxacin-Resistant Shigellae in India. *Journal of Clinical Microbiology 45*(2), 678–679. 3

[265] Taro Kawai and Shizuo Akira (2011). Toll-like Receptors and Their Crosstalk with Other Innate Receptors in Infection and Immunity. *Immunity 34*(5), 637–650. 21

[266] Tattoli, I., M. T. Sorbara, D. J. Philpott, and S. E. Girardin (2012, December). Bacterial autophagy: The trigger, the target and the timing. *autophagy 8*(1554-8627), 1848–1850. 12

[267] Tattoli, I., M. T. Sorbara, D. Vuckovic, A. Ling, F. Soares, L. M. Carneiro, C. Yang, A. Emili, D. Philpott, and S. Girardin (2012). Amino Acid Starvation Induced by Invasive Bacterial Pathogens Triggers an Innate Host Defense Program. *Cell Host and Microbe 11*(6), 563–575. 123, 139

[268] Tcherkezian, J., M. Cargnello, Y. Romeo, E. L. Huttlin, G. Lavoie, S. P. Gygi, and P. P. Roux (2014, February). Proteomic analysis of cap-dependent translation identifies LARP1 as a key regulator of 5'TOP mRNA translation. *Genes & Development 28*(4), 357–371. 95

[269] Thingholm, T. E. and O. N. Jensen (2009). Enrichment and Characterization of Phosphopeptides by Immobilized Metal Affinity Chromatography (IMAC) and Mass Spectrometry. In M. Graauw (Ed.), *Phospho-Proteomics*, Volume 527 of *Methods in Molecular Biology*, pp. 47–56. Humana Press. 40

[270] Tobe, T., S. Nagai, N. Okada, B. Adter, M. Yoshikawa, and C. Sasakawa (1991). Temperature-regulated expression of invasion genes in Shigella flexneri is controlled through the transcriptional activation of the virB gene on the large plasmid. *Molecular Microbiology 5*(4), 887–893. 6

[271] Tobe, T., M. Yoshikawa, T. Mizuno, and C. Sasakawa (1993, October). Transcriptional control of the invasion regulatory gene virB of Shigella flexneri: activation by virF and repression by H-NS. *Journal of Bacteriology 175*(19), 6142–6149. 7

[272] Tran Van Nhieu, G., A. Ben Ze'ev, and P. Sansonetti (1997, May). Modulation of bacterial entry into epithelial cells by association between vinculin and the Shigella IpaA invasin. *EMBO J 16*(10), 2717–2729. 10

[273] Tran Van Nhieu, G., E. Caron, A. Hall, and P. J. Sansonetti (1999, Jun 15). IpaC induces actin polymerization and filopodia formation during Shigella entry into epithelial cells. *EMBO J 18*(12), 3249–62. 0261-4189 (Print) Journal Article. 10

[274] Tran Van Nhieu, G., C. Clair, R. Bruzzone, M. Mesnil, P. Sansonetti, and L. Combettes (2003, Aug). Connexin-dependent inter-cellular communication increases invasion and dissemination of Shigella in epithelial cells. *Nat Cell Biol 5*(8), 720–6. 1465-7392 (Print) Journal Article. 27

[275] Tran Van Nhieu, G. and J. Guignot (2009, December). When Shigella Tells the Cell to Hang On. *Journal of Molecular Cell Biology 1*(2), 64–65. 16

[276] Turner, S. A., S. N. Luck, H. Sakellaris, K. Rajakumar, and B. Adler (2003, February). Molecular Epidemiology of the SRL Pathogenicity Island. *Antimicrobial Agents and Chemotherapy 47*(2), 727–734. 6

[277] Ubersax, J. A. and J. E. Ferrell Jr (2007, July). Mechanisms of specificity in protein phosphorylation. *Nat Rev Mol Cell Biol 8*(7), 530–541. 35, 36

[278] Ubersax, J. A., E. L. Woodbury, P. N. Quang, M. Paraz, J. D. Blethrow, K. Shah, K. M. Shokat, and D. O. Morgan (2003, October). Targets of the cyclin-dependent kinase Cdk1. *Nature 425*(6960), 859–864. 35

[279] van der Goot, F. G., G. T. van Nhieu, A. Allaoui, P. Sansonetti, and F. Lafont (2004). Rafts Can Trigger Contact-mediated Secretion of Bacterial Effectors via a Lipid-based Mechanism. *Journal of Biological Chemistry 279*(46), 47792–47798. 9

[280] van Noort, V., J. Seebacher, S. Bader, S. Mohammed, I. Vonkova, M. J. Betts, S. Kühner, R. Kumar, T. Maier, M. O Flaherty, V. Rybin, A. Schmeisky, E. Yus, J. Stülke, L. Serrano, R. B. Russell, A. J. Heck, P. Bork, and A.-C. Gavin (2012, February). Cross-talk between phosphorylation and lysine acetylation in a genome-reduced bacterium. *Molecular Systems Biology 8*(1), –. 143

[281] Varjosalo, M., S. Keskitalo, A. Van Drogen, H. Nurkkala, A. Vichalkovski, R. Aebersold, and M. Gstaiger (2013, April). The Protein Interaction Landscape of the Human CMGC Kinase Group. *Cell Reports 3*(4), 1306–1320. 37

[282] Veenendaal, A. K. J., J. L. Hodgkinson, L. Schwarzer, D. Stabat, S. F. Zenk, and A. J. Blocker (2007). The type III secretion system needle tip complex mediates host cell sensing and translocon insertion. *Molecular Microbiology 63*(6), 1719–1730. 8, 10

[283] Wagner, S. A., P. Beli, B. T. Weinert, M. L. Nielsen, J. Cox, M. Mann, and C. Choudhary (2011, October). A Proteome-wide, Quantitative Survey of In Vivo Ubiquitylation Sites Reveals Widespread Regulatory Roles. *Molecular & Cellular Proteomics 10*(10), –. 142

[284] Wassef, J. S., D. F. Keren, and J. L. Mailloux (1989). Role of M cells in initial antigen uptake and in ulcer formation in the rabbit intestinal loop model of shigellosis. *Infection and Immunity 57*(3), 858–863. 3

[285] Watarai, M., S. Funato, and C. Sasakawa (1996). Interaction of Ipa proteins of Shigella flexneri with alpha5beta1 integrin promotes entry of the bacteria into mammalian cells. *The Journal of Experimental Medicine 183*(3), 991–999. 9, 100

[286] Welburn, J. P. I., J. A. Tucker, T. Johnson, L. Lindert, M. Morgan, A. Willis, M. E. M. Noble, and J. A. Endicott (2007, February). How Tyrosine 15 Phosphorylation Inhibits the Activity of Cyclin-dependent Kinase 2-Cyclin A. *Journal of Biological Chemistry 282*(5), 3173–3181. 33

[287] Wickramasinghe, V., J. Savill, S. Chavali, A. Jonsdottir, E. Rajendra, T. Grüner, R. Laskey, M. Babu, and A. Venkitaraman (2013, September). Human Inositol Polyphosphate Multikinase Regulates Transcript-Selective Nuclear mRNA Export to Preserve Genome Integrity. *Molecular Cell 51*(6), 737–750. 125

[288] William H. Ewing (1949). SHIGELLA NOMENCLATURE. *J. Bacteriol. 57*(6), 633–638. 5

[289] Wisniewski, J. R. and M. Mann (2012, February). Consecutive Proteolytic Digestion in an Enzyme Reactor Increases Depth of Proteomic and Phosphoproteomic Analysis. *Anal. Chem. 84*(6), 2631–2637. 39

[290] Wright, M. H., W. P. Heal, D. J. Mann, and E. W. Tate (2010). Protein myristoylation in health and disease. *Journal of Chemical Biology 3*(1), 19–35. 31

[291] Wymann, M. P. and C. Schultz (2012, September). The Chemical Biology of Phosphoinositide 3-Kinases. *ChemBioChem 13*(14), 2022–2035. 19

[292] Yang, F., J. Yang, X. Zhang, L. Chen, Y. Jiang, Y. Yan, X. Tang, J. Wang, Z. Xiong, J. Dong, Y. Xue, Y. Zhu, X. Xu, L. Sun, S. Chen, H. Nie, J. Peng, J. Xu, Y. Wang, Z. Yuan, Y. Wen, Z. Yao, Y. Shen, B. Qiang, Y. Hou, J. Yu, and Q. Jin (2005, January). Genome dynamics and diversity of Shigella species, the etiologic agents of bacillary dysentery. *Nucleic Acids Research 33*(19), 6445–6458. 6

[293] Yarbrough, M. L., Y. Li, L. N. Kinch, N. V. Grishin, H. L. Ball, and K. Orth (2009, January). AMPylation of Rho GTPases by Vibrio VopS Disrupts Effector Binding and Downstream Signaling. *Science 323*(5911), 269–272. 31

[294] Yoshida, S., Y. Handa, T. Suzuki, M. Ogawa, M. Suzuki, A. Tamai, A. Abe, E. Katayama, and C. Sasakawa (2006). Microtubule-Severing Activity of Shigella Is Pivotal for Intercellular Spreading. *Science 314*(5801), 985–989. 11

[295] Yoshida, S., E. Katayama, A. Kuwae, H. Mimuro, T. Suzuki, and C. Sasakawa (2002, June). Shigella deliver an effector protein to trigger host microtubule destabilization, which promotes Rac1 activity and efficient bacterial internalization. *EMBO J 21*(12), 2923–2935. 12

[296] Yu, Y., S.-O. Yoon, G. Poulogiannis, Q. Yang, X. M. Ma, J. Villén, N. Kubica, G. R. Hoffman, L. C. Cantley, S. P. Gygi, and J. Blenis (2011, June). Phosphoproteomic Analysis Identifies Grb10 as an mTORC1 Substrate That Negatively Regulates Insulin Signaling. *Science 332*(6035), 1322–1326. 95

[297] Zanivan, S., M. Krueger, and M. Mann (2012). In Vivo Quantitative Proteomics: The SILAC Mouse. In M. Shimaoka (Ed.), *Methods in Molecular Biology*, Volume 757, pp. 435–450–. Humana Press.

[298] Zheng, J., E. A. Trafny, D. R. Knighton, N. Xuong, S. S. Taylor, L. F. Ten Eyck, and J. M. Sowadski (1993, May). 2.2 Å refined crystal structure of the catalytic subunit of cAMP-dependent protein kinase complexed with MnATP and a peptide inhibitor. *Acta Crystallographica Section D 49*(3), 362–365.

[299] Zhu, L., G. Zhao, R. Stein, X. Zheng, W. Hu, N. Shang, X. Bu, X. Liu, J. Wang, E. Feng, B. Wang, X. Zhang, Q. Ye, P. Huang, M. Zeng, and H. Wang (2010). The Proteome of Shigella flexneri 2a 2457T Grown at 30 and 37°C. *Molecular & Cellular Proteomics 9*(6), 1209–1220. 29

[300] Zhu, Y., H. Li, C. Long, L. Hu, H. Xu, L. Liu, S. Chen, D.-C. Wang, and F. Shao (2007). Structural Insights into the Enzymatic Mechanism of the Pathogenic MAPK Phosphothreonine Lyase. *Molecular Cell 28*(5), 899 – 913. 25

[301] Zinzalla, V., D. Stracka, W. Oppliger, and M. Hall (2011, March). Activation of mTORC2 by Association with the Ribosome. *Cell 144*(5), 757–768. 140

[302] Zurawski, D. V., C. Mitsuhata, K. L. Mumy, B. A. McCormick, and A. T. Maurelli (2006, Oct). OspF and OspC1 are Shigella flexneri type III secretion system effectors that are required for postinvasion aspects of virulence. *Infect Immun 74*(10), 5964–76. 0019-9567 (Print) Journal Article Research Support, N.I.H., Extramural Research Support, Non-U.S. Gov't. 10

[303] Zurawski, D. V., K. L. Mumy, L. Badea, J. A. Prentice, E. L. Hartland, B. A. McCormick, and A. T. Maurelli (2008, Jan). The NleE/OspZ family of effector proteins is required for polymorphonuclear transepithelial migration, a characteristic shared by enteropathogenic Escherichia coli and Shigella flexneri infections. *Infect Immun 76*(1), 369–79. 1098-5522 (Electronic) Journal Article Research Support, N.I.H., Extramural Research Support, Non-U.S. Gov't. 11

[304] Zurawski, D. V., K. L. Mumy, C. S. Faherty, B. A. McCormick, and A. T. Maurelli (2009, Jan). Shigella flexneri type III secretion system effectors OspB and OspF target the nucleus to downregulate the host inflammatory response via interactions with retinoblastoma protein. *Mol Microbiol 71*(2), 350–68. 1365-2958 (Electronic) Journal Article Research Support, N.I.H., Extramural Research Support, Non-U.S. Gov't Research Support, U.S. Gov't, Non-P.H.S. 10, 24

[305] Zychlinsky, A., C. Fitting, J. M. Cavaillon, and P. J. Sansonetti (1994, Sep). Interleukin 1 is released by murine macrophages during apoptosis induced by Shigella flexneri. *J Clin Invest 94*(3), 1328–32. 0021-9738 (Print) Journal Article. 3

[306] Zychlinsky, A., K. Thirumalai, J. Arondel, J. R. Cantey, A. O. Aliprantis, and P. J. Sansonetti (1996). In vivo apoptosis in Shigella flexneri infections. *Infection and 64*(12), 5357–65. 3

Acronyms

ABM	actin-based motility
AMP	adenosinmonophosphate
APC	anaphase promoting complex
ATM	ataxia telangiectasia mutated
ATP	adenosine triphosphate
ATR	ataxia telangiectasia and Rad3 related protein
AUC	area under the curve
CARD	caspase recruitment domain
DAG	diacylglycerol
DAMP	danger-associated molecular pattern
DAP	diaminopimelic acid
DUSP	dual-specificity phosphatase
EGF	epidermal growth factor
EGFR	epidermal growth factor receptor
EHEC	enterohaemorrhagic *Escherichia coli*
EPEC	enteropathogenic *Escherichia coli*
EPK	eukaryotic protein kinases
ERK	extracellular-signal regulated kinase
FAK	focal adhesion kinase
Fic	filamentation induced by cAMP
flg22	flagellin 22 peptide
GEF	GTP exchange factor
GTP	guanosine-5'-triphosphate
icgR	intracellular growth regulator
IcsA	intracellular spread
iE-DAP	g-D-glutamyl-meso-diaminopimelic acid
IEF	isoelectric focusing
IκB	inhibitor of NF-κB
IκBα	inhibitor of NF-κB alpha
IKK	inhibitor of nuclear factor κ-B kinase
IKKγ	Inhibitor of nuclear factor κ-B kinase subunit γ
IL-18	interleukin 18

IL-1β	interleukin 1β
IL-8	interleukin-8
ILK	integrin-like kinase
IMAC	metal affinity chromatography
INF-γ	interferon γ
INPP4	inositol polyphosphate 4-phosphatase type I
Ins(1,4,5)P3	Inositol-1,4,5-trisphosphate
IPMK	inositol polyphosphate multikinase
IS	insertion sequences
iTRAQ	isobaric tags for relative and absolute quantitation
JNK	c-Jun N-terminal kinase
KLH	keyhole limpet hemocyanin
LC-MS/MS	liquid chromatography tandem mass spectrometry
LPS	lipopolysaccharide
LRR	leucine-rich repeat
MAMP	microbe-associated molecular pattern
MAPK	mitogen-activated protein kinase
m-cells	microfold cells
MDP	muramyl dipeptide
MEF	mouse embryonic fibroblasts
MOAC	metal oxide affinity chromatography
MOI	multiplicity of infection
MSK	mitogen- and stress-activated kinase
MTM	myotubularin
MTMR	myotubularin-related protein
mTOR	mammalian target of rapamycin
mTORC1	mammalian target of rapamycin complex 1
mTORC2	mammalian target of rapamycin complex 2
NF-κB	nuclear factor κB
NK	natural killer
NLR	Nod-like receptor
NLS	nuclear localization sequence
NPC	nuclear pore complex
N-WASP	Wiskott-Aldrich syndrome protein
PAI	pathogenicity islands
PAMP	pathogen-associated molecular pattern
PGN	peptidoglycan

PI(3,4)P2	phosphatidylinositol 3,4-bisphosphate
PI(3,4,5)P3	phosphatidylinositol (3,4,5)-trisphosphate
PI(3,5)P2	phosphatidylinositol 3,5-bisphosphate
PI(4,5)P2	phosphatidylinositol 4,5-bisphosphate
pI	isolectric point
PI	phosphatidylinositol
PI3K	phosphatidylinositol 3-kinase
PI3P	phosphatidylinositol 3-phosphate
PI4K	phosphatidylinositol 4-kinase
PI4P	phosphatidylinositol 4-phosphate
PI5K	phosphatidylinositol 5-kinase
PI5P	phosphatidylinositol 5-phosphate
PKA	protein kinase A
PKC	protein kinase C
PLC	phospholipase C
PLIP	PTEN-like phosphatase
PMN	polymorphonuclear cells
PRR	pattern recognition receptor
pS	phospho-serine
pT	phospho-threonine
PTEN	phosphatase and tensin homolog
PTM	post-translational modification
pY	phospho-tyrosine
RIP2	receptor-interacting serine/threonine-protein kinase 2
RLR	RIG-I like receptor
ROCK	Rho-associated protein kinase
SCX	strong cation exchange
SH2	src homology 2
SHI	*Shigella* pathogenicity islands
SHIP	phosphatidylinositol 3,4,5-trisphosphate 5-phosphatase
SILAC	stable isotope labeling in cell culture
SPI1	*Salmonella* pathogenicity island 1
SPI2	*Salmonella* pathogenicity island 2
SRL	*Shigella* resistance locus
TAK1	TGF-beta activated kinase 1
TiO_2	titanium dioxide
TLR	Toll-like receptor
TRAF6	TNF receptor-associated factor 6
TTSS	type three secretion system

Acknowledgements

I would like to express my sincere gratitude and appreciation to.....

- ... my supervisor Cécile Arrieumerlou for giving me the opportunity to do my PhD in her lab. I really appreciate her dedication towards my project and the numerous valuable inputs I obtained. I especially want to acknowledge that the door of her office was always open for discussions about data and new ideas.
- ... my committee members Prof. Christoph Dehio and Prof. Mike Hall for their interest towards my project and the scientific inputs during the committee meetings. I also want to thank Prof. Matthias Wymann for joining the committee and participation on my defense.
- ... all of the group members for the fantastic working atmosphere that was characterized by great willingness to support each other. A special thanks to Isabel Sorg and Therese Tschon for their helpful assistance during my "large-scale" experiments even if the experiment had to be repeated several times. I also want to acknowledge the IT support I obtained from Christoph Kasper for quantitative image analysis and if I faced again an apparently unsolvable excel problem (That usually could be solved within 10 minutes). I want to thank Simon Ittig for providing me his newly developed lab tool and for his heroic dedication as my "personal trainer" in the gym or outdoors, expanding my PhD also towards a physical demanding exploration. I want to give thanks to Roland Dreier for helping me during the paper revision. A special thank is also directed to Marlise Amstutz for her guidance into the world of cloning. I also want to express my gratitude to Michaela Hanisch for the handling of all administrative matters.
- ... the former group members, Veronika Reiterer as well as Hesso Farhan (even if he technically was not a group member), Sonja Weichsel, Gregory Melroe, Man Lyang Kim, Klaus Handloser and Lars Grossniklaus for all the great time we spent together.
- ... The proteomic core facility team including Alex Schmidt, Erik Ahrné and Timo Glatter for their support during the experimental setup and the numerous runs of mass spectrometry analysis. The energizing and humorous atmosphere in their lab helped to withstand also monotonous and enduring sample processing procedures.
- ... the floor managers Marina Kuhn and Roger Sauder for their support and prompt assistance if there was any technical problem.
- ... the Swiss National Science Foundation for funding.
- ... my family for the support during all those years.
- ... my brother Michael for LaTeX assistance during the course of writing the thesis.
- ... my girlfriend Corinne for encouraging and supporting me during demanding times, as well as for sharing the joy in successful moments.

List of publications

- Kasper CA, Sorg I, **Schmutz C**, Tschon T, Wischnewski H, Kim ML, Arrieumerlou C. Cell-cell propagation of NF-κB transcription factor and MAP kinase activation amplifies innate immunity against bacterial infection. *Immunity*, 33(5):804–16, 2010.

- **Schmutz C**, Erik A, Kasper CA, Tschon T, Sorg I, Dreier RF, Schmidt A, Arrieumerlou C. Systems-Level Overview of Host Protein Phosphorylation During *Shigella flexneri* Infection Revealed by Phosphoproteomics. *Molecular & Cellular Proteomics*, 12(10):2952-68, 2013.

- Ittig SJ, **Schmutz C**, Schmidt A, Arrieumerlou C. Broad cell biology applications for the delivery of heterologous proteins via bacterial type III secretion. *Manuscript in Preparation*

Curriculum vitae

Personal data

Name:	Christoph Schmutz
Date of birth:	14th of December, 1984
Place of birth:	Binningen BL
Place of citizenship:	Basel BS

Education

May 2010 - present:	PhD Thesis Thesis committee: Prof. Dr. Cécile Arrieumerlou (PI), Prof. Dr. Christoph Dehio, Prof. Dr. Mike Hall, Prof. Dr. Matthias Wymann Focal Area Infection Biology Biozentrum, University of Basel
Sep. 2008 - Feb. 2010:	Master of Science in Molecular Biology Major in Infection Biology Thesis committee: Prof. Dr. Cécile Arrieumerlou (PI), Prof. Dr. Guy Cornelis Focal Area Infection Biology Biozentrum, University of Basel
Oct. 2005 - Jul. 2008:	Bachelor of Science in Biology Major in Integrative Biology University of Basel
Aug. 2001 - Dec. 2004:	Grammar school (Gymnasium) Liestal BL Higher education entrance qualification (Matura) Main subjects biology and chemistry